The University of Sheffield
Department of Civil and Structural Engineering

Collapse of Stone Column Foundations Due to Inundation

by

Tahar Ayadat
Diplome d'Ingenieur d'Etat en Genie Civil
(University of Oran, Algeria)

Thesis Submitted to the University of Sheffield
for the degree of Doctor of Philosophy

December 1990

To my beloved parents from whom I learnt that life is a continuous struggle. To my brothers and sisters, my dear wife and my children Sara and Mahdi.

Summary

An important problem encountered by foundation engineers involves partially saturated soils which possess considerable in-situ dry strength that is largely lost when the soils become wetted. Foundation design in such soils is difficult at best. In many cases, deep foundations may be required to transmit foundation loads to suitable bearing strata below the 'collapsible' soil deposit. This research has studied the behaviour and performance of stone columns confined and not confined by geofabrics and rigid piles, as deep foundations, in collapsible soil subjected to inundation.

Laboratory tests were carried out, under controlled conditions of sand density and surcharge pressure, using six different types of foundation supports (a sand column, sand columns confined by T700, T1000, T1500 or T2000 geofabrics and a rigid pile). Each type of foundation was considered in three different lengths 250 mm, 300 mm and 410 mm. This work consisted of installing and loading 'model' foundations into a stress controlled pot containing a collapsible soil and allowing a slow rise of the water level inside it. The tests were designed to investigate the efficiency of these types of foundation supports on the improvement of the carrying capacity and on the reduction of settlement of the ground.

The reduction in vertical compression of the 'piles' was also studied analytically using an analytical approach adopted and developed from models applied to soft soils.

The experimental results are compared with analytical predictions. The comparisons show that the reduction in vertical compression of the 'pile' is governed by its stiffness and its length. These variables are of prime importance in the general performance of the 'pile'.

Contents

Acknowledgements i

Summary ii

List of Figures x

List of Tables xxi

List of Plates xxiii

Table of Convertions xxiv

Notations xxv

1 Introduction 1

1.1 General: 1

1.2 Description of the Problem: 2

1.3 Aims and Scope of the Work: 5

1.4 A Brief Survey of the Thesis: 5

2 Review of Relevant Literature **7**

2.1 Introduction: 7

2.2 Collapsible soils 7

2.2.1 General: 7

2.2.2 Type and Origin of Collapsible Soils: 8

2.2.3 Causes of the Phenomenon of Collapse: 10

2.2.4 Prediction of Collapse: 12

2.2.5 Parameters Affecting the Magnitude of Collapse: 17

2.2.6 The Effect of Soaking on Soil Structure: 17

2.2.7 Foundation Treatment Methods: 18

2.2.8 Case Histories: 24

2.3 Stone Columns 24

2.3.1 General: 24

2.3.2 Behaviour and Performance of Stone Columns in Soft Soils: . 25

2.3.3 Cases Histories: 28

2.4 Geotextiles 30

2.4.1 General: 30

2.4.2 Terram: 30

2.4.3 Some Works on the Effect of Internal/External Fabric Reinforcement on the Behaviour of Sand: 31

2.5 Conclusion: 33

3 Stone Column and Pile Background Theory **35**

3.1 Introduction: 35

3.2 The integral equation theory developed for piles: 36

3.3 Theory for Stone Columns: 41

3.4 The Analytical Model Adopted: 43

3.4.1 Types of Analysis: 45

3.4.2 Parametric Equations: 45

3.4.3 Data on Pile-Soil Parameters: 49

3.4.4 Interpretation of the Predicted Results: 50

3.5 Conclusion: 53

4 Determination of Pile-Soil Parameters Used in Test Data Evaluation **55**

4.1 General: 55

4.2 Triaxial Test Equipment and Instrumentation: 57

4.2.1 General: 57

4.2.2 The loading System: 57

4.2.3 Instrumentation: 58

4.2.4 The High Air Entry Porous Ceramic: 62

4.3 Testing Programme and Experimental procedures: 65

4.3.1 General: 65

4.3.2 Specimen Preparation: 65

4.3.3 Testing Programme: 67

4.3.4 Testing Procedure: 71

4.3.5 Data Acquisition and Evaluation: 78

4.4 Interpretation of the Results: 79

4.4.1 General: 79

4.4.2 K_0 and Consolidated Undrained Tests Performed on Collapsible Soil in the 'Dry' State (series (I)): 80

4.4.3 Consolidated Undrained Tests Performed on the Collapsible Soil in the Saturated State (series (II)): 82

4.4.4 Consolidated Undrained Tests Performed on Leighton Buzzard Sand Encapsulated and not Encapsulated in a Geofabric: . . . 83

4.4.5 Summary and Comments: 84

5 The Test Apparatus and Equipment **86**

5.1 General: 86

5.2 Test Rig: 87

5.2.1 Description: 87

5.2.2 Effect of Wall Friction: 87

5.2.3 Size Effect of the Container: 88

5.3 Surcharge Pressure System: 88

5.4 Axial Loading System: 90

5.5 Test Elements: 90

5.5.1 Construction: 90

5.5.2 Measurement of Vertical Displacement: 92

5.5.3 Measurement of Horizontal Displacement: 93

5.6 Method of Inundating the Soil Stratum: 94

5.7 Ancilliary Equipment: 95

5.7.1 Compaction Apparatus: 95

5.7.2 Centering Beam: 95

5.7.3 Extractor: 96

5.7.4 Sand Scraper: 97

5.7.5 Cleaning Equipment: 97

6 Test Programme and Experimental Procedures **98**

6.1 General: 98

6.2 Properties of the Soil: 99

6.2.1 Collapsible Soil: 99

6.2.2 Sand Forming the Sand Columns: 100

6.3 Testing Programme: 100

6.3.1 Series (I): 100

6.3.2 Series (II): 101

6.3.3 Series (III): 101

6.4 Testing Procedure: 102

6.4.1 Rig & Soil Preparation, Soil Bed Formation and Sand Column or Pile Installation: 102

6.5 Application of Surcharge Pressure: 106

6.6 Application of the Axial Load: 106

6.7 Data Acquisition and Analysis: 107

6.8 Emptying the Sand Container: 108

7 Discussion on Test Results and Comparison with Theoretical Predictions 109

7.1 Introduction: 109

7.2 Checking of the collapsibility of the artificial soil prepared: 110

7.3 The General Performance and Limitations of the Test Apparatus: . . 113

7.3.1 General Limitations of the Experimental Study: 113

7.3.2 Repeatability of Test Results: 114

7.4 Performance of Sand Columns in a Collapsible Soil: 116

7.5 Performance of Sand Columns encapsulated in 'Terram' Fabrics and Rigid Piles in Collapsible Soil: 121

7.5.1 Ultimate Carrying Capacity of 'piles': 121

7.5.2 Settlement Behaviour of the 'piles' Under Load and Inundation: 127

7.6 Comparison Between Experimental and Theoretical Results: 133

8 Conclusions and Recommendations for Future Work 137

8.1 General: 137

8.2 Main Conclusions: 138

8.3 Recommendations for Future Work: 141

References 143

Appendix A 158

Appendix B 159

Appendix C 164

Appendix D 168

Appendix E 169

List of Figures

Chapter 1

Fig. 1.1 Process of collapse of a stone column in a collapsible soil subjected to inundation caused by rise of the water table.

Chapter 2

Fig. 2.1 Typical collapsible soil structures (Clemence & Finbarr, 1981).

Fig. 2.2 Typical collapse potential tests result (Clemence & Finbarr, 1981).

Fig. 2.3 Double oedometer test results(Jennings & Knight, 1975).

Fig. 2.4 Double consolidation test and ajustments for normally consolidated soil (Jennings & Knight, 1975).

Fig. 2.5 Double consolidation test and adjustments for overconsolidated soil (Jennings & Knight, 1975).

Fig. 2.6 Typical compression curve for modified Jennings and Knight oedometer test (Houston et al., 1988).

Fig. 2.7 Various stone column arrangement showing the domain of influence of each column (Baalam & Booker, 1981).

Fig. 2.8 Loads applied on the top of the soil and the stone column (Hughes et al., 1974).

Fig. 2.9 The upper figure shows the applied stress on the column and the footing against time. The lower figure shows the vertical settlement as a percentage of the footing diameter against time (Hughes et al., 1974).

Fig. 2.10-a Vertical displacement within the column against depth (Hughes et al., 1974).

Fig. 2.10-b Radial displacement at the edge of the column/initial column radius against depth (Hughes et al., 1974).

Fig. 2.11 Properties and specification of 'Terram' (Parts I and II) (ICI, 1977).

Fig. 2.12 Internally/externally fabric reinforced below grade foundations (Gray, 1982).

Chapter 3

Fig. 3.1 Stresses associated with pile (Poulos et al., 1968).

Fig. 3.2-a Values of downdrag reduction factor N_R. ($K_s tan\phi'_a = 0.20$) (Poulos et al., 1980).

Fig. 3.2-b Values of downdrag reduction factor N_R. ($K_s tan\phi'_a = 0.40$) (Poulos et al., 1980).

Fig. 3.3-a Downdrag reduction factor N_T -one-way drainage (Poulos et al., 1980).

Fig. 3.3-b Downdrag reduction factor N_T -two-way drainage (Poulos et al., 1980).

Fig. 3.4 Rate of development of downdrag force -one-way drainage. (Poulos et al., 1980).

Fig. 3.5 Rate of development of downdrag force -two-way drainage. (Poulos et al., 1980).

Fig. 3.6-a Value of deflection reduction factor Q_R. ($K_s tan\phi'_a = 0.20$) (Poulos et al., 1980).

Fig. 3.6-b Values of deflection reduction factor Q_R. ($K_s tan\phi'_a = 0.40$) (Poulos et al., 1980).

Fig. 3.7-a Deflection reduction factor Q_T one-way drainage (Poulos et al., 1980).

Fig. 3.7-b Deflection reduction factor Q_T two-way drainage (Poulos et al., 1980).

Fig. 3.8-a Degree of pile settlement vs. time -one-way drainage (Poulos et al., 1980).

Fig. 3.8-b Degree of pile settlement vs. time factor two-way drainage. (Poulos et al., 1980).

Fig. 3.9 Influence factors for final downdrag at pile tip -elastic analysis. (Poulos et al., 1980).

Fig. 3.10 Elastic solutions for top deflection of pile. (Poulos et al., 1980).

Fig. 3.11 Comparisons with pile tests of Bjerrum et al. (1969) at Sorenya (Poulos et al., 1975).

Fig. 3.12 Comparison with pile tests of Walker and Darvall (1973) (Poulos et al., 1975)
Fig. 3.13 Comparison of elastic theories and field observations (Greenwood et al., 1984).
Fig. 3.14 Concept of the unit cell (Priebe, 1976).
Fig. 3.15 Principle of 'pile' settlement in a collapsible soil subjected to inundation.
Fig. 3.16 Assumption of soil settlement variation with depth.
Fig. 3.17 Forces acting on the wall of a cylinder subjected to an internal pressure ΔP.
Fig. 3.18 Reduction in vertical compression as a function of 'pile'-stiffness. (for L = 250mm and an applied load = 20% P_u)
Fig. 3.19 Reduction in vertical compression as a function of 'pile'-stiffness. (for L = 300 mm and an applied load = 20% P_u)
Fig. 3.20 Reduction in vertical compression as a function of 'pile'-stiffness. (for L = 410 mm and an applied load = 20% P_u)
Fig. 3.21 Reduction in vertical compression as a function of 'pile'-stiffness. (for L = 250 mm and an applied load = 50% P_u)
Fig. 3.22 Reduction in vertical compression as a function of 'pile'-stiffness. (for L = 300 mm and an applied load = 50% P_u)
Fig. 3.23 Reduction in vertical compression as a function of 'pile'-stiffness. (for L = 410 mm and an applied load = 50% P_u)
Fig. 3.24 Reduction in vertical compression as a function of 'pile'-stiffness. (for L = 250 mm and an applied load = 80% P_u)
Fig. 3.25 Reduction in vertical compression as a function of 'pile'-stiffness. (for L = 300 mm and an applied load = 80% P_u)
Fig. 3.26 Reduction in vertical compression as a function of 'pile'-stiffness. (for L = 410 mm and an applied load = 80% P_u)
Fig. 3.27 Reduction in vertical compression as a function of 'pile'-length for an applied load = 20% P_u (slip analysis).
Fig. 3.28 Reduction in vertical compression as a function of 'pile'-length for

an applied load = 50% P_u (slip analysis).

Fig. 3.29 Reduction in vertical compression as a function of 'pile'-length for an applied load = 80% P_u (slip analysis).

Fig. 3.30 Reduction in vertical compression as a function of 'pile'-length for an applied load = 20% P_u (elastic analysis).

Fig. 3.31 Reduction in vertical compression as a function of 'pile'-length for an applied load = 50% P_u (elastic analysis).

Fig. 3.32 Reduction in vertical compression as a function of 'pile'-length for an applied load = 80% P_u (elastic analysis).

Chapter 4

Fig. 4.1 Sources of error in external strain measurement (Jardine et al., 1984).

Fig. 4.2 Derivation of Young's modulus using repeated loading cycles. (Head, 1982)

Fig. 4.3 The general arrangement of the triaxial loading system.

Fig. 4.4 Schematic cross-section of the volume change unit.

Fig. 4.5 The lateral strain indicator.

Fig. 4.6 Details of the split mould.

Fig. 4.7 Details of the top cap holder.

Fig. 4.8 The compaction hammer used to compact the Leighton buzzard sand in the triaxial cell.

Fig. 4.9 Schematic diagram of testing programme.

Fig. 4.10 Undrained K_0-tests on samples of CS compacted at 4% moisture content.

Fig. 4.11-a Stress-strain behaviour of 'dry' samples of CS (cell pressure = 54 KPa).

Fig. 4.11-b Pore pressure plotted against strain.

Fig. 4.11-c Relationship between volume change and strain.

Fig. 4.12-a Stress-strain behaviour of the saturated CS under three different cell pressure (55, 115 and 155 KPa).

Fig. 4.12-b Mohr's rupture diagram.

Fig. 4.13 Stress-strain behaviour of the saturated CS under a cell pressure = 48 KPa.

Fig. 4.14 Stress-starin behaviour of saturated LBS specimens under three different cell pressure.

Fig. 4.15 Stress-strain behaviour of saturated LBS specimens confined by T700 under three different cell pressure.

Fig. 4.16 Stress-strain behaviour of saturated LBS specimens confined by T1000 under three different cell pressure.

Fig. 4.17 Stress-strain behaviour of saturated LBS specimens confined by T1500 under three different cell pressure.

Fig. 4.18 Stress-strain behaviour of saturated LBS specimens confined by T2000 under three different cell pressure.

Fig. 4.19 Stress-strain behaviour of saturated LBS specimens confined and not confined by 'Terram' (cell pressure = 40 KPa).

Fig. 4.20 Stress-strain behaviour of saturated LBS specimens confined and not confined by 'Terram' (cell pressure = 80 KPa).

Fig. 4.21 Stress-strain behaviour of saturated LBS specimens confined and not confined by 'Terram' (cell pressure = 120 KPa).

Fig. 4.22 Elastic modulus of specimens of LBS confined by different geofabrics against the confining pressure.

Chapter 5

Fig. 5.1 Cross-section of the apparatus.

Fig. 5.2 Setting up of the LVDT's on the top of the container.

Fig. 5.3 Calibration graphs for LVDT's.

Fig. 5.4 Horizontal sand movement gauges.

Fig. 5.5 Arrangement of the movement gauges on the wall of the container.

Fig. 5.6 The system used to inundate the soil stratum.

Fig. 5.7 The compaction apparatus used to compact the collapsible soil in the container.
Fig. 5.8 The compaction hammer used to perform the sand column.
Fig. 5.9 The centering beam.
Fig. 5.10-a The top circular plate of the extractor.
Fig. 5.10-b The bottom crown of the extractor.
Fig. 5.11 The sand scraper.

Chapter 6

Fig. 6.1 Particle size distribution of the collapsible soil.
Fig. 6.2 The compaction curve obtained in determining the optimum moisture content.
Fig. 6.3 Particle size distribution of Leighton Buzzard sand.
Fig. 6.4 Schematic diagram of testing programme.

Chapter 7

Fig. 7.1 Collapse potential test result.
Fig. 7.2 Test result of the Rowe cell.
Fig. 7.3-a Test repeatability (I).
Fig. 7.3-b Test repeatability (II).
Fig. 7.4 Load-displacement relationship for the collapsible soil and the stone columns as foundation supports.
Fig. 7.5 Settlement curves for the collapsible soil and the stone columns after full inundation under a working load = 30% P_u.
Fig 7.6 Settlement curves for the collapsible soil and the stone columns after partial inundation under a working load = 30% P_u.

Fig. 7.7 Relationship between soil/column settlements.

Fig. 7.8 Process of settlement of a non-collapsible fill, around a stone column, due to inundation.

Fig. 7.9-a Load-displacement relationship for sand columns encapsulated and not encapsulated in a geofabric and a rigid pile of length, L = 250 mm.

Fig. 7.9-b Load-displacement relationship for stone columns encapsulated and not encapsulated in a geofabric and a rigid pile of length, L = 300 mm.

Fig. 7.9-c Load-displacement relationship for sand columns encapsulated and not encapsulated in a geofabric and a rigid pile of length, L = 410 mm

Fig. 7.10 Chin's plots for sand columns not encapsulated in a geofabric.

Fig. 7.11 Chin's plots for sand columns encapsulated in T700.

Fig. 7.12 Chin's plots for sand columns encapsulated in T1000.

Fig. 7.13 Chin's plots for sand columns encapsulated in T1500.

Fig. 7.14 Chin's plots for sand columns encapsulated in T2000.

Fig. 7.15 Chin's plots for rigid piles.

Fig. 7.16 Effect of 'pile'-stiffness on bearing capacity ratio.

Fig. 7.17 Load-displacement relationship for sand columns not confined by a geo -fabric.

Fig. 7.18 Load-displacement relationship for sand columns confined by T700.

Fig. 7.19 Load-displacement relationship for sand columns confined by T1000.

Fig. 7.20 Load-displacement relationship for sand columns confined by T1500.

Fig. 7.21 Load-displacement relationship for sand columns confined by T2000.

Fig 7.22 Load-displacement relationship for rigid piles.

Fig 7.23-a Settlement curves for the different foundation supports, of length L = 250 mm, after full inundation under an applied load = 20% P_u.

Fig 7.23-b Settlement curves for the different foundation supports, of length L = 250 mm, after full inundation under an applied load = 50% P_u.

Fig. 7.23-c Settlement curves for the different foundation supports, of length L = 250 mm, after full inundation under an applied load = 80% P_u.

Fig. 7.24-a Settlement curves for the different foundation supports, of length L = 300 mm, after full inundation under an applied load = 20% P_u.

Fig. 7.24-b Settlement curves for the different foundation supports, of length L = 300 mm, after full inundation under an applied Load = 50% P_u.

Fig. 7.24-c Settlement curves for the different foundation supports, of length L = 300 mm, after full inundation under an applied load = 80% P_u.

Fig. 7.25-a Settlement curves for the different foundation supports, of length L = 410 mm, after full inundation under an applied load = 20% P_u.

Fig. 7.25-b Settlement curves for the different foundation supports, of length L = 410 mm, after full inundation under an applied load = 50% P_u.

Fig. 7.25-c Settlement curves for the different foundation supports, of length L = 410 mm, after full inundation under an applied load = 80% P_u.

Fig 7.26-a Reduction in vertical compression as a function of 'pile'-stiffness. (for L = 250 mm and an applied load = 20% P_u)

Fig 7.26-b Reduction in vertical compression as a function of 'pile'-stiffness. (for L = 250 mm and an applied load = 50% P_u)

Fig. 7.26-c Reduction in vertical compression as a function of 'pile'-stiffness. (for L = 250 mm and an applied load = 80% P_u)

Fig. 7.27-a Reduction in vertical compression as a function of 'pile'-stiffness. (for L = 300 mm and an applied load = 20% P_u)

Fig. 7.27-b Reduction in vertical compression as a function of 'pile'-stiffness. (for L = 300 mm and an applied load = 50% P_u)

Fig. 7.27-c Reduction in vertical compression as a function of 'pile'-stiffness. (for L = 300 mm and an applied load = 80% P_u)

Fig. 7.28-a Reduction in vertical compression as a function of 'pile'-stiffness. (for L = 410 mm and an applied load = 20% P_u)

Fig. 7.28-b Reduction in vertical compression as a function of 'pile'-stiffness. (for L = 410 mm and an applied load = 50% P_u)

Fig. 7.28-c Reduction in vertical compression as a function of 'pile'-stiffness.

(for L = 410 mm and an applied load = 80% P_u)

Fig. 7.29-a Settlement curves for sand columns not confined by a geofabric after full inundation under an applied load = 20% P_u.

Fig. 7.29-b Settlement curves for sand columns not confined by a geofabric after full inundation under an applied load = 50% P_u.

Fig. 7.29-c Settlement curves for sand columns not confined by a geofabric after full inundation under an applied load = 80% P_u.

Fig. 7.30-a Settlement curves for sand columns confined by T700, after full inundation under an applied load = 20% P_u.

Fig. 7.30-b Settlement curves for sand columns confined by T700, after full inundation under an applied load = 50% P_u.

Fig. 7.30-c Settlement curves for sand columns confined by T700, after full inundation under an applied load = 80% P_u.

Fig. 7.31-a settlement curves for sand columns confined by T1000, after full inundation under an applied load = 20% P_u.

Fig. 7.31-b Settlement curves for sand columns confined by T1000, after full inundation under an applied load = 50% P_u.

Fig. 7.31-c Settlement curves for sand columns confined by T1000, after full inundation under an applied load = 80% P_u.

Fig. 7.32-a Settlement curves for sand columns confined by T1500, after full inundation under an applied load = 20% P_u.

Fig. 7.32-b Settlement curves for sand columns confined by T1500, after full inundation under an applied load = 50% P_u.

Fig. 7.32-c Settlement curves for sand columns confined by T1500, after full inundation under an applied load = 80% P_u.

Fig. 7.33-a Settlement curves for sand columns confined by T2000 after full inundation under an applied load = 20% P_u.

Fig. 7.33-b Settlement curves for sand columns confined by T2000 after full inundation under an applied load = 50% P_u.

Fig. 7.33-c Settlement curves for sand columns confined by T2000 after full inundation under an applied load = 80% P_u.

Fig. 7.34-a Settlement curves for rigid piles after full inundation under an applied load = 20% P_u.

Fig. 7.34-b Settlement curves for rigid piles after full inundation under an applied load = 50% P_u.

Fig. 7.34-c Settlement curves for rigid piles after full inundation under an applied load = 80% P_u.

Fig. 7.35 Reduction in vertical compression as a function of 'pile'-length for the diffe -rent types under an applied load = 20% P_u.

Fig. 7.36 Reduction in vertical compression as a function of 'pile'-length for the diffe -rent types under an applied load = 50% P_u.

Fig. 7.37 Reduction in vertical compression as a function of 'pile'-length for the diffe -rent types under an applied load = 80% P_u

Fig. 7.38-a Comparison of experimental and theoretical reduction in vertical compress -ion curves as a function of 'pile'-stiffness (for L = 250 mm & an applied load = 20% P_u).

Fig. 7.38-b Comparison of experimental and theoretical reduction in vertical compress -ion curves as a function of 'pile'-stiffness (for L = 250 mm & an applied load = 50% P_u).

Fig. 7.38-c Comparison of experimental and theoretical reduction in vertical compress -ion curves as a function of 'pile'-stiffness (for L = 250 mm & an applied load = 80% P_u).

Fig. 7.39-a Comparison of experimental and theoretical reduction in vertical compress -ion curves as a function of 'pile'-stiffness (for L = 300 mm & an applied load = 20% P_u).

Fig. 7.39-b Comparison of experimental and theoretical reduction in vertical compress -ion curves as a function of 'pile'-stiffness (for L = 300 mm & an applied load = 50% P_u).

Fig. 7.39-c Comparison of experimental and theoretical reduction in vertical compress -ion curves as a function of 'pile'-stiffness (for L = 300 mm & an applied load = 80% P_u).

Fig. 7.40-a Comparison of experimental and theoretical reduction in vertical compress -ion curves as a function of 'pile'-stiffness (for L = 410 mm & an applied load = 20% P_u).

Fig. 7.40-b Comparison of experimental and theoretical reduction in vertical compress -ion curves as a function of 'pile'-stiffness (for L = 410 mm & an applied load = 50% P_u).

Fig. 7.40-c Comparison of experimental and theoretical reduction in vertical compress -ion curves as a function of 'pile'-stiffness (for L = 410 mm & an applied load = 80% P_u).

Fig. 7.41 Comparison of experimental and theoretical reduction in vertical compress -ion curves as a function of 'pile'-length for the different types under an appl -ied load = 20%

Fig. 7.42 Comparison of experimental and theoretical reduction in vertical compress -ion curves as a function of 'pile'-length for the different types under an appl -ied load = 50%

Fig. 7.43 Comparison of experimental and theoretical reduction in vertical compress -ion curves as a function of 'pile'-length for the different types under an appl -ied load = 80%

List of Tables

Chapter 2

Table 2.1 Collapse potential values (Jennings & Knight, 1975).

Table 2.2 Methods of treating collapsible foundation soils (Bara, 1976).

Table 2.3 Typical examples indicating their problems and remedial measures.

Chapter 3

Table 3.1 'Pile'-soil parameters used in test data evaluation.

Chapter 4

Table 4.1 Calibration factors and Precision of the instruments employed in the triaxial testing.

Table 4.2 Testing programme performed for pile-soil parameters determination.

Table 4.3 'Pile'-soil parameters used in test data evaluation.

Chapter 5

Table 5.1 Material properties of the rigid pile.

Table 5.2 Characteristics of the LVDT's used to measure the vertical displacements.

Table 5.3 Characteristics of the LVDT's used to measure the horizontal displacements.

Chapter 6

Table 6.1 Results of some empirical criteria.

Table 6.2 Main testing programme.

Chapter 7

Table 7.1 Characteristics of the tests performed in the Rowe cell.

Table 7.2 Chacteristics of preliminary tests.

Table 7.3 Characteristics of tests performed to investigate the performance of sand columns in a collapsible soil.

Table 7.4 Load carrying capacity for all the 'piles'.

List of Plates

Chapter 4

Plate 4.1 The transducer mounted in the lateral strain indicator.

Plate 4.2 Kenwood mixer and the small container.

Chapter 5

Plate 5.1 Overall view of the apparatus.

Plate 5.2 Pressure cylinders for surcharge pressure system.

Plate 5.3 The pressure plate and the convoluted rubber membrane.

Plate 5.4 A lever arm.

Plate 5.5 The extractor.

Chapter 6

Plate 6.1 The scoop.

Plate 6.2 The wall-mounted pressure gauge.

Plate 6.3 Placement of dead weights on the hanger.

Plate 6.4 Data logging system.

Table of Conversions

Quantity	Unit	S.I.
Length	foot	0.3048 m
	inch	25.4 mm
Area	square foot	0.0929 m^2
	square inch	645.2 mm^2
Volume	cubic yard	0.7646 m^3
	cubic foot	0.02832 m^3
	cubic inch	16.39 cm^3
	gallon	4.561
Mass	ton	1.016 Mg (1.016 tonne)
	hundredweight	50.80 kg
	pound	0.4536 kg
Density	pound per cubic foot gram-	0.01602 Mg/m^3
	me per cubic centimetre	1.0 Mg/m^3(1 tonnes/m^3)
Force	pound force	4.448 N
	ton force	9.964 kN
	kilogramme force	9.807 N
Pressure and	pound force per square inch	6.895 kN/m^2
Stress	pound force per square foot	0.04788 kN/m^2
	ton force per square foot	107.3 kN/m^2
	kilogramme force per square centimetre	98.07 kN/m^2
Modulus of	pound force per square foot	0.04788 kN/m^2
Deformation	ton force per square inch	15.44 MN/m^2
Coefficient of	square foot per year	0.0929 $m^2/year$
Consolidation	square centimetre per second	3154 $m^2/year$
Coefficient of	centimeter per second	0.01 m/s
Permeability	foot per year	0.3048 m/year
		(0.9651 × 10^{-8} m/s)
Temperature	degree Fahrenheit (^oF)	n ^oF = 0.5556 (n - 32) ^oC
	degree Centigrade (^oC)	
Angle	degree	0.01745 rad
	1 ton = 2240 pounds	N = Newton

Notations

BC:	Bearing capacity.
BCR:	Bearing capacity ratio.
$c_a^{'}$:	Pile-soil adhesion.
$c_e^{'}$:	Equivalent pile-soil adhesion.
CP:	Collapse potential.
CS:	Collapsible soil.
e:	Void ratio.
e_0:	Natural void ratio.
e_1:	Void ratio at the beginning of saturation.
E:	The Young's modulus of the material forming the cylinder of reinforcement.
E_p:	Modulus of elasticity (i.e. Young's modulus) of the granular column encapsulated encapsulated in a geofabric or the rigid pile.
E_s:	Modulus of elasticity (i.e. Young's modulus) of the soil.
Gr:	Group.
h:	Length of a segment from the 'pile' body.
H:	Thickness of the collapsing layer.
H_0:	Initial height of the sample.
H_n:	The thickness of the slice considered.
I_N:	Elastic influence factor.
I_ρ:	Settlement influence factor.
K:	Pile stiffness factor.
l_c:	Critical length of the column below which the load is not transmitted.
L:	Length of the 'pile'.
LBS:	Leighton Buzzard sand.
n:	Number of slices.
N_R:	Correction factor for cases in which full slip does not occur.
N_T:	Correction factor for effects of delayed installation.
P:	Pressure.

P_0: Total overburden pressure.

P_a: Axial force in the pile at the top of the consolidating layer.

P_c: Precompression pressure.

P_r: Lateral pressure acting on the column.

P_t: The maximum downdrag force at time t.

P_u: ultimate carrying capacity.

P_v: External vertical load on the column.

PM: Pile head movement.

P_N: Final maximum downdrag force.

P_{NFS}: Final maximum downdrag force if full pile-soil slip occurs.

q: Surcharge pressure.

q_1: Bearing capacity for the unreinforced stone column.

q_2: Bearing capacity for the reinforced stone column and the rigid pile.

Q_R: Correction factor for cases in which full slip does not occur.

Q_T: Correction factor for effects of delayed installation.

r_0: Initial radius of the column.

S_0: Settlement of the top of the collapsing layer.
or Settlement of the untreated foundation.

S_i: Settlement of the treated foundation.

S_l: Settlement of the layer situated beneath the tip of the 'pile'.

SM: Soil movement.

ST: Settlement.

T700: 'Terram' product of a density of 700 g/m^2.

T1000: 'Terram' product of a density of 1000 g/m^2.

T1500: 'Terram' product of a density of 1500 g/m^2.

T2000: 'Terram' product of a density of 2000 g/m^2.

u: Pore water pressure.

U_N: Degree of development of downdrag.

U_ρ: Degree of pile movement.

β: Settlement reduction factor.

δ_1: Elastic settlement of the pile due to the axial load (P_a).

δ_2: Settlement caused by downdrag.

δ_3: Settlement due to the lateral deformation of the compressible 'pile'.

δ_n: Axial movement of the n^{th} slice of the column.

δ_v: Axial movement of stone column.

$\delta r_0/r_0$: Radial strain in the column.

δ_{rn}/r: The radial strain for that slice.

Δ: Total and final settlement caused by inundation under an external load (P_a).

Δe_c: Change in void ratio upon wetting.

Δe_s: Change in void ratio upon loading.

ΔH_c: Reduction of height of the sample.

ΔP: Change in the pressure.

ν: Poisson ratio of the soil.

ρ: Final axial movement.

ρ_{FS}: Axial movement of pile if full pile-soil slip occurs.

ρ_t: Axial movement of the pile at any time t after installation.

σ: Total stress.

σ': Effective stress.

σ_θ: The tangential stress.

ϕ': Pile-soil friction angle.

ϕ'_a: Pile-soil friction angle.

τ_a: Final pile-soil adhesion.

ε_r: Radial strain.

Chapter 1

Introduction

1.1 General:

Collapsing soils are defined as any unsaturated soil that goes through a radical rearrangement of particles and a large loss of volume upon wetting with or without additional loading. They have been found in soils from many sources (loess, alluvial, residual, aelion subaerial, colluvial, gypsiferous silts, etc.).

In the past much attention was not given to detailed studies and investigation of soils susceptible to collapse. Also structures erected tended to be inexpensive and of small size. Besides this, water consumption patterns were quite different from those of today. With rapid advancement of civilization and increasing use of water for irrigation, industrial and domestic purposes near to structures, severe damage to a structure founded on collapsible soil may occur. Also developments in all aspects of life have resulted in the construction of modern cities and large structures in areas of collapsible soil. This fact clearly establishes the need for an in-depth study of the subject of subsidence in collapsible soils.

Most of the works that have been carried out on collapsing soils have

concentrated on the development of methods of identifying readily the soils that could collapse and determining the amount of collapse that may occur. In the field of research, progress has been continuous but not to an extent which enables a practising engineer to design his structure on these soils with a high degree of confidence, safety and economy.

Foundation design in collapsible soils is difficult at best. The results from laboratory or field tests can be used to predict the amount of settlement that can be expected. In many cases, it may be feasible to apply a pretreatment technique in order to either stabilize or cause collapse of the soil deposit prior to construction of a specific structure or facility. The amount of treatment and type depend on the depth of the collapsible soil and the support requirement for the proposed facility. A wide variety of treatment methods has been suggested. However, rising construction costs along with present day environmental considerations will undoubtedly make the stone column method, which consists of granular material compacted in long cylindrical holes, a more attractive alternative to conventional methods as time goes on.

1.2 Description of the Problem:

Stone columns occupy an important place and have a major role in ground treatment methods. They can be used in different types of soils and sites. Their costs are relatively moderate and their installation requires medium-priced equipment. Their use for more than 50 years in reinforcing soft soils has demonstrated their usefulness and make them one of the most attractive methods in improving bearing capacity and reducing settlement. However, in spite of their recommendation as a treatment method for collapsible soils by several researchers; Bara (1976), Fargher et al. (1979) and Ronan (1980), there is no published work reporting their use in such soils.

This research investigation is based on some field information which is

not published. The information refer to some works carried out to reinforce loose fill using stone columns. They showed that, when the water table rose, the loose fill collapsed and the stone columns didn't reduce the settlement and there was failure when using this method of foundation support. Based on reported results on the successful use of stone columns to reinforce soft soils and loose fills a basic question arose. Why did this happen and what were the causes?

Before answering this question, it was decided to produce a similar testing programme to that believed to apply on site using a 'model' sand column loaded in a stress controlled pot which contained a loose fill made of a collapsible soil, the water level being allowed to rise slowly inside it. The apparatus used is shown in Figure 5.1. At the end, a similar trend to that of field tests was observed and similar results were obtained with a high level of repeatability. Provided that stone columns generally fail by bulging at relatively shallow depths (typically less than 4 diameters from the top of the column, Williams (1969), Hughes et al. (1974) and Poulos et al. (1969)), the water table, in a loose fill (not collapsible), would have to rise close to ground level in order to have any significant effect on the performance of the column when loaded. It was reported that, under such circumstances, the ultimate capacity of the column could be reduced by up to 50% in the worst cases (Simpson et al. 1989). However, in this case (a collapsible fill) the capacity of the column was reduced drastically and large settlements were observed even for partial penetration and partial inundation (see section 7.4).

After the confirmation of the field results by laboratory test, a careful investigation was performed in order to answer the question posed earlier. For this purpose, an extensive and in-depth review of the literature has been done. At the end, based on some excellent works carried out on the deformation characteristics and the stress-path followed during wetting of an element of a collapsible soil, the causes of the problem were deduced. Grigorian (1967), Zur et al. (1973) and Maswoswe (1985) found that, during the inundation of an element of soil in a collapsing ground, the lateral pressure around the element decreased and a large reduction of

its volume resulted from axial as well as lateral deformations. These findings were found to be the main causes of the problem and the phenomenon encountered in collapsible loose fills reinforced by stone columns. To explain the process, Fig. 1.1 has been used. It consists of a fully penetrating stone column loaded in a collapsible soil. Fig. 1.1-a is taken as the initial state where the water table is below the top of the hard layer. Consider the section A-A where the distance between it and the hard layer is an arbitrary value d (diameter of the stone column). The small element of the stone column under this section is in equilibrium. The forces acting on it are:

1. The vertical forces acting downward due to the weight and the load of all the top bloc.

2. The reaction forces acting upward and which are due to the confining pressure around the element provided by the soil.

In Fig. 1.1-b, the water table has risen up to the section A-A. This results in a large reduction of volume of the soil and consequentely the section A-A will settle to the position of section B-B and the whole bloc above this section will move downward and will press the thin layer below it. With the decrease of the confining pressure around the small element of the column, caused by inundation, the element will deform laterally and settle by the same amount as that of the soil. The same explanation can be used for an other element of the stone column and so on. This explains how the column settles and fails in strengthening a collapsing loose fill.

By discovering the causes of the problem, another question was asked. How to deal with this problem and how to eliminate or control it? This time the answer was very simple. The elimination of the problem consisted of the prevention of the loss of the confining pressure around the stone column. According to Mc Gown et al (1977 and 1978), Gray et al. (1982) and Gorle et al. (1989), internal or external reinforcement of sand, using geotextiles, improves its mechanical properties. Either of the methods can strengthen and stiffen a column of sand significantly. From this

came the idea of using geotextiles (i.e. covering the whole length of the column by a geotextile).

Another important point was studied. The problem of collapse is a problem of settlement and it is evident that the predictive methods developed for stone columns in soft soil are no longer valid for collapsing soils, so a new predictive method has to be developed.

1.3 Aims and Scope of the Work:

The main objectives of the research work described here are:

1. To investigate the efficiency of this method (i.e. covering the column by a geotextile) on the improvement of the carrying capacity and on the reduction of the settlement of the foundation for two variables,
   (a) The length of the column, and
   (b) The stiffness of the column (i.e. the strength of the geotextile used.)
2. To help establish a predictive method for settlement of deep foundations in collapsible soils by comparing the experimental results with analytical predictions.

1.4 A Brief Survey of the Thesis:

This thesis consists of eight chapters. The following chapter, i.e. chapter 2 presents a literature review of three main topics, collapsing soils, stone columns in soft soils and sand reinforcement using geotextiles. Chapter 3 presents an analytical study of the effects of 'pile'-stiffness and 'pile'-length on the settlement behaviour of a

'pile'. Chapter 4 includes the triaxial equipment, test procedures and all the results obtained for the determination of pile-soil parameters used in test data evaluation (i.e. data used in the analytical study), while the test materials, equipment and test procedure used in the main testing programme are described in chapters 5 and 6. In chapter 7, the experimental results are discussed in detail, and compared with the analytical predictions presented in chapter 3. The conclusions that can be drawn from both the analytical and experimental studies, together with some recommendation for future research are given in chapter 8.

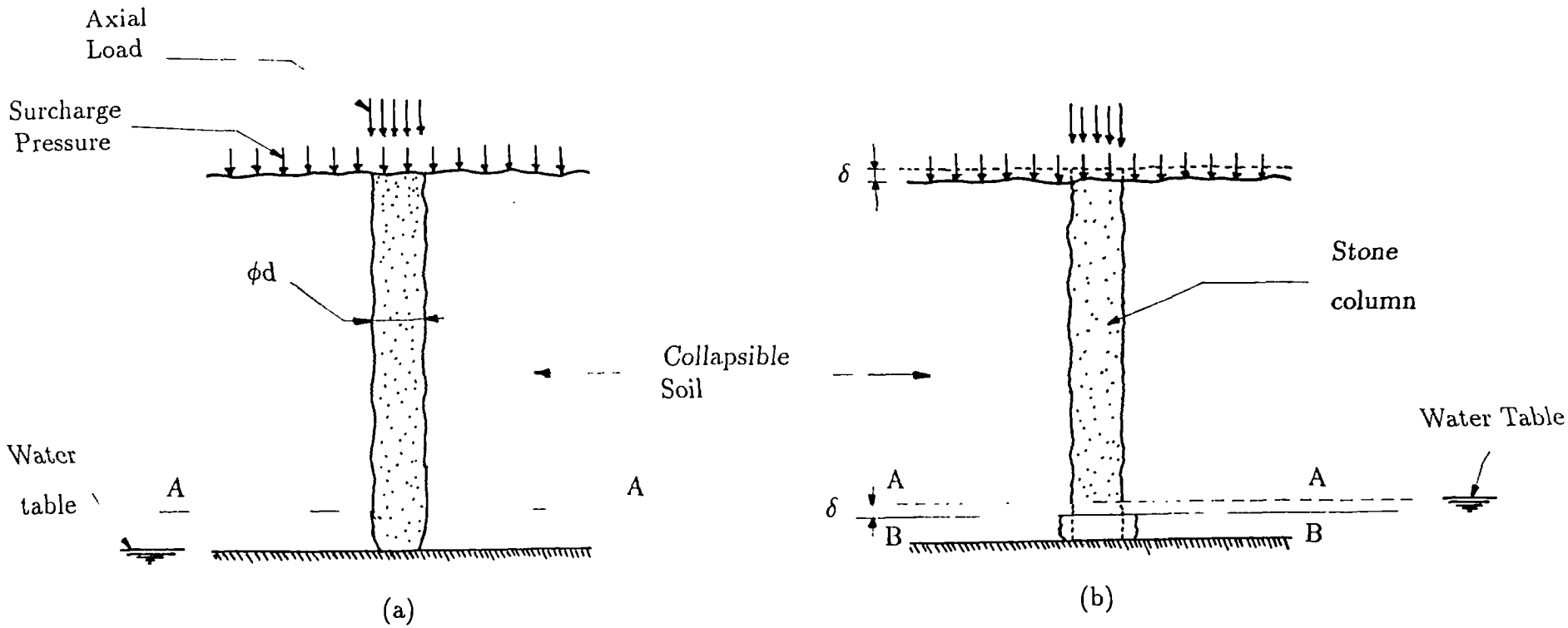

Fig. 1.1 Process of Collapse of a Stone Column in a Collapsible Soil Subjected to Inundation Caused by Rise of the Water Table

Chapter 2

Review of Relevant Literature

2.1 Introduction:

As stated in section 1.2, there is no published work reporting the use of stone columns in collapsible soils. In these circumstances and according to the objective of this investigation, literature on three main topics is reviewed. Firstly, an account is given of previous work on collapsible soils, including their origins and some case histories. Secondly, the performance and behaviour of stone columns in soft soils are reviewed. Finally, some works on the internal and/or external reinforcement of sand by geotextiles are described.

2.2 Collapsible soils:

2.2.1 General:

Much of the observations and research on collapsing soils focuses entirely on collapse in naturally deposited soils. Most of the work on the structure, mechanisms of

collapse, and laboratory methods for predicting collapse in naturally deposited soils also apply to compacted soils.

In this section, an outline is given of published work dealing with collapsing soils in both states, natural and compacted. The review is intended to cover the more important published papers, particularly in relation to the prediction of collapse and foundation treatment methods to enable construction to take place on such soils.

2.2.2 Type and Origin of Collapsible Soils:

The most extensive deposits of collapsing soil are aeolian or wind-deposited sands and silts (loess). However, in addition to these deposits, there is a wide variety of other types of deposit which have been identified as having an unstable structure. These are in alluvial flood plains, in fans and mudflows, in colluvial deposits, residual soils, volcanic tuffs and man-made fill.

2.2.2.1- Aeolian (Wind-Laid) Deposits:

These deposits consist of materials transported by wind which form dunes, loess , loessial-type deposits, aeolic beaches, and large volcanic dust deposits. They consist of cohesionless or slightly cohesive soils which may contain a clay cement binder such as the loessial soils and may have a low relative density. These deposits are characteristic of arid regions where the watertable is at great depth below the ground surface. They are formed mainly by two types of soils, aeolian silt (loess) and aeolian sand (Bowles, 1978; Clemence and Finbar, 1981).

2.2.2.2- Water-Laid Deposits:

Water-laid deposits consist primarily of loose sediments which form alluvial fans, flows and flowslides. These materials were originally deposited by flash floods or mud flows derived from small watersheds subjected to cloud-bursts at infrequent intervals. These deposits dry out and never again become saturated until the arrival of another flow. Flows consist of poorly consolidated materials that contain a considerable amount of clay.

2.2.2.3- Residual Soil Deposits:

These soils are the product of weathering, i.e., the disintegration and mechanical alteration of the components of parent rocks. The particles of residual materials may vary in size from large fragments to gravel, sand, silt, colloids and, in some cases, organic matter. The collapsible grain structure has developed as a result of leaching of soluble and colloidal material. This leaching out of the soluble and fine materials results in a high void ratio and unstable structure (Brink and Kantey, 1961; Bowles, 1978).

2.2.2.4- Other Soil Deposits:

Other soil types that exhibit collapse upon soaking include those derived from volcanic tuff, gypsum, loose sands cemented by soluble salts, dispersive clays and sodium-rich montmorillonite (Clemence and Finbarr, 1981). Man-made fills compacted dry of Proctor optimum water content also have been known to exhibit marked collapse behaviour (Barden et al, 1973; and Leonards & Altschaeffl, 1971).

2.2.3 Causes of the Phenomenon of Collapse:

In order for collapse to occur the soil must have a structure that lends itself to this action. According to Barden et al (1969), appreciable collapse of a soil requires the following three conditions to be fulfilled:

1. An open, potentially unstable, partly saturated structure;
2. A high enough value of an applied or existing stress component to develop a metastable condition;
3. A strong soil bonding or cementing agent to stabilise intergranular contacts with a reduction which, upon wetting, will produce collapse.

All cases so far studied have shown that these soils have a honeycomb structure of bulky-shaped grains with the grains held in place by some bonding material or forces (e.g. Barden & Sides, 1970; Collins & Mc Gown, 1974). The material or force must be susceptible to removal or reduction by the arrival of additional water. When support is removed, the grains are able to slide (shear) past one another moving into vacant spaces. The temporary strength of these soils is provided in a variety of ways as discussed in the following sub-sections.

2.2.3.1- Silt Bond:

In cases where the soil consists of sand with a fine silt binder, the temporary strength is due to capillary tension or is related to it, Barden et al (1969), Morgenstern & de Matos (1975), Prusza & Choudry (1979) and Ganeshan (1982).
As the soil dries below the shrinkage limit, the water remaining withdraws into the narrow spaces close to the junction of the soil grains as shown in Figure 2.1. The air water interface in these capillary size spaces places the water under tension. Thus

the excess water pressure,u, in the usual expression for effective stress,

$$\sigma' = \sigma - u$$

becomes negative and the actual effective stress becomes larger than the total stress applied by the load. This negative pore water pressure increases the apparent strength of the soil. However, the addition of water reduces the beneficial effect of the negative pore water pressure. If the soil is porous, it can then have a rapid decrease in volume upon wetting.

2.2.3.2- Clay Bond:

The majority of collapsing soils involve the action of clay particles in the bonds between the sand grains. A number of structural arrangements of the clay particles are possible depending on the history of the soil. Clays that are formed by authigenesis possibly form a parallel plate onionskin effect around the quartz particles. Gradual evaporation of the pore water can cause the clay plates to retreat with the water into the menisci at interparticle contacts. Knight (1963) and Barden et al (1973), using an electron microscope, found that under such conditions the clay grains cluster around the junctions in a random flocculated arrangement, giving a buttress type of support to the bulky grains. Gross capillary tensions can also be present in these buttresses.

2.2.3.3- Cementing Agents:

The bonding or rigidity effect in a soil that is reduced during collapse need not be due to capillary suction or clay bridges. A similar effect can be produced by chemical cementing agents such as iron oxide, calcium carbonate, or a welding at the grain contacts. These could restrain the bulky grains from rotating so that a more dense arrangement could be secured.

Whatever the physical basis of the bonding strength, all types are weakened by the addition of water, thereby allowing local shear stresses to collapse the structure. A large number of collapse mechanisms have been postulated on the basis of test data obtained from a variety of soils (Holtz and Hilf, 1961; Burland, 1965; Cox, 1970; Kane, 1973; and Maswoswe, 1985).

2.2.4 Prediction of Collapse:

The soil engineer needs to be able to identify readily the soils that could collapse and to determine the amount of collapse that may occur. In some cases he is also concerned about the time required for collapse. The tests for these factors vary from the very simple to the complex and time consuming. Some may be performed by the engineer in a field in a few minutes. Others require laboratory work with great costs associated with securing good quantitative information.
For the better evaluation of engineering properties of collapsible soils, different criteria have been adopted or established by different investigators. These criteria can be grouped under the following sub-heads:

1. Empirical methods which include:
   (a) criteria based on voids ratio relationships;
   (b) criteria based on moisture content and atterberg limits relationships;
   (c) criteria based on density and atterberg limits relationships.
2. Experimental methods which include both a qualitative as well as a quantitative approach.
3. Analytical methods.

2.2.4.1- Empirical Methods:

Northey (1969), Darwell and Bruce (1976), Bara (1976), Hassani et al. (1982) and Lutenegger et al. (1988) have reviewed these criteria. While all the criteria are certainly useful, they may be locally applicable and provide a rough indication of whether or not a particular soil may be collapsible. None of these criteria provide a direct measure of the amount of deformation that could be expected.
Additionally, many of these criteria are based on remoulded or compacted soil properties, and therefore they do not take into account any influence of natural soil fabric. A recent review of these criteria Saber(1987) indicated that in most cases no single criterion alone is accurate enough to predict collapsibility for a particular soil.

2.2.4.2- Experimental Methods:

Several experimental methods have been developed (both in the laboratory and in the field) in order to indicate the succeptibility to collapse and to determine the amount of deformation that may occur (Benites, 1967; Gibbs and Bara, 1976; Reginatto et al., 1973; El Sohby, 1989, and others). The most used and recommended methods are those based on oedometer tests.

Jennings and Knight (1975) suggested a satisfactory test using a consolidometer ring. A sample of the soil is cut to fit in the ring, and the loads are applied progressively until 200 kPa is reached. At the end of this loading, the specimen is flooded with water and left for 24 hours and the consolidometer test is then carried on to its normal maximum loading limit. The resulting curve is shown in Fig. 2.2. The collapse potential (CP) is then defined as:

$$CP = \frac{\Delta e_c}{1 + e_0}$$

where:

Δe_c: change in void ratio upon wetting; and

e_0: natural void ratio.

The collapse potential may also be defined as:

$$CP = \frac{\Delta H_c}{H_0}$$

where:

ΔH_c: reduction of the height of the sample,

H_0: initial height of the sample.

Guiding figures from their experience are summarised in Table 2.1.

Lutenegger el al. (1988), based on the work of Abelev (1948), proposed a similar procedure to that of Jennings and Knight but with a stress level of 300 kPa and a collapse potential defined as:

$$CP = \frac{\Delta e_c}{1 + e_1}$$

where:

e_1: void ratio at the beginning of saturation.

The collapse potential is not a design figure and has no particular use in judging just how much collapse will take place in a particular case. It is merely an index or guide to expectation, and tells the experienced engineer when to expect or not to expect trouble and whether there is justification for a more comprehensive investigation.

For design purposes the prediction of collapse settlement may be obtained from a test method due to Knight (1961) who used the results of the double oedometer test conducted in ordinary consolidation machines. This method is still considered the most useful method for giving a quantitative estimation of the magnitude of collapse. Two undisturbed similar samples are preferably cut by hand from block samples to fit in the consolidometer ring, and placed in a consolidometer under a 1 kPa seating load for 24 hours. At the end of the 24 h. period, one sample is inundated by flooding with water, while the other sample is kept at its natural

water content. Both samples are then left for a further 24 h. The test is then carried out in the ordinary manner, doubling the applied load each 24 h., and the results are plotted (Fig. 2.3).

The e versus log P curves obtained from the two tests do not start from the same point and the initial void ratios of the two samples after the first 24 h. of loading are not identical. The total overburden pressure P_0 is calculated and plotted. The precompression pression, P_c, is found from the soaked curve and compared with P_0.

- In the case of a normally consolidated soil:

$$\frac{P_c}{P_0} = 0.8 - 1.5$$

compression is considered to take place on the virgin curve and the natural moisture content curve is adjusted to the (e_0,P_0) point by drawing a curve parallel to the natural moisture consolidation curve, as shown in Figure 2.4. If the loading is increased by ΔP , then the unit settlement for the soil, without change of natural moisture content will be:

$$\frac{\Delta e_s}{1 + e_0}$$

If the loading remains constant and the soil increases in water content, then the unit additional settlement will be:

$$\frac{\Delta e_c}{1 + e_0}$$

- In the case of an overconsolidated soil:

$$\frac{P_0}{P_c} < 1.5$$

the adjustment of the curve largely follows the ordinary settllement computation practices. The only difference between the two cases lies in the determination of the (e_0 , P_0) point as shown in Figure 2.5.

The validity of the double oedometer test depends on the saturated (or soaked) curve, i.e., the saturated curve should be unique and independent of the applied stress path before saturation. While this is true, at a close approximation for granular soils, the uniqueness of the saturated curve has not yet been demonstrated for clay soils (Burland, 1965).

According to this difficulty, a variation of the Jennings and Knight double oedometer test was devised by Houston et al. (1988) as the laboratory method to be used to obtain the data required for the prediction of soil collapse. Their method was strongly supported by the results of a full-scale field test carried out in Northern Scottsdale, Arizona.
The modified Jennings and Knight procedure consists of running a simple oedometer test on a given soil sample and then establishing from the result the slope or shape of the inundated compression curve. Fig. 2.6 illustrates the construction of the laboratory curves used to predict the collapse strain using this method.

2.2.4.3- Theoretical Prediction:

Very limited work has been published in this matter (Ali et al., 1989; Amirsoleymani, 1989).It seems that an analytical method for predicting settlements of collapsing soil is at present difficult to develop. The most accurate prediction would be one which would involve conducting a test in the field with the actual load in place. This is, unfortunately, expensive, time consuming and only shows the effect at the area tested.

Obviously the criteria based on settlement prediction by oedometer test is more reliable than other empirical or analytical approaches as it takes into account the actual soil structure pattern which is so important for predicting the collapse.

2.2.5 Parameters Affecting the Magnitude of Collapse:

The most significant parameters governing collapse of partially saturated soils are the initial dry density, moisture content, degree of saturation and overburden pressure. The infuence of these factors on the amount of collapse was investigated by several researchers. Most of them agreed that:

1. For a given moisture content the amount of collapse increases with increasing the dry density. Whereas, for any given dry density, the magnitude of collapse decreases with increasing moisture content and there is a critical moisture content above which no collapse occurs (Holtz, 1948; Barden et al., 1969; Booth, 1975; Lefebvre et al., 1989 and Lawton, 1989).

2. At a given dry density, the overburden stress level at which the maximum amount of collapse took place varied inversely with the compaction water content (Booth, 1975; Cox, 1978; and Lawton, 1989).

3. There is a critical degree of saturation beyond which the soils do not appear to be susceptible to collapse. Mishu (1963), Booth (1975 and 1977), and Geneshan (1982) proposed a critical degree of saturation of 50 to 60%. Markin (1969) and Prusza & Choudry (1979) suggested slightly higher values, between 60 and 65%.

2.2.6 The Effect of Soaking on Soil Structure:

Russian studies (Goldshtein, 1969) have shown that there are four main types of soaking that can trigger the collapse of soils:

1. Local, shallow soaking of a random nature caused by water sources from pipelines or uncontrolled drainage of surface water from construction. Water from local soaking does not usually penetrate to great depths and there is

normally no rise in the ground-water level. In these cases, settlement occurs mainly in the upper layer of soil below the soaked zone.

2. Intense, deep, local soaking of soil caused by discharge of industrial effluents or irrigation. If the flow rate is sufficient to cause a continuous rise in the ground-water level, then the entire zone of collapsible soil may be saturated in a short time span (several months to a year). In this case, the settlement is extremely uneven and dangerous. It may include the whole thickness of the soil layer and collapse may occur either under the load from existing structures or under the weight of the soil itself.

3. Slow and relatively uniform rise of the ground-water level under the influence of water sources outside the collapsible soil area. The settlement is normally uniform and gradual.

4. Gradual slow increase of the water content of a thick layer of soil, resulting from condensation of steam or accumulation of moisture due to changes in the evaporation conditions (e.g. when the ground is covered by concrete or asphalt). The weakening of the internal cohesion of the soil is then partial. Correspondingly, the settlement is incomplete, and slowly increases with the rise in degree of saturation of the soil. Collapse may be triggered by water alone, or by soaking and loading acting together.

2.2.7 Foundation Treatment Methods:

The amount and type of treatment depends on the depth of the collapsbile soil and the support requirements for the proposed structure. Table 2.2 gives a summary by Bara (1976) of current, past and possible future treatment methods.

The simplest solution is to carry the foundations down to the depth at which the collapse phenomenon is absent or of negligible proportions. This may be

achieved by piling. If the collapsing soil layer is not too thick (less than 4 m), it is often economical and practical to remove it and replace it with a suitable soil which has been compacted to a satisfactory density. The material used for soil exchange should preferably to coarse, inorganic and should require little compactive effort. This type of foundation treatment has been used for small pumping plants, bridge footings and canal structures.

Prevention of the wetting of the foundation soil can be attempted by appropriate surface and sub-surface drainage and water proofing measures and by ensuring that all service connections to the structure are sufficiently flexible to survive settlement, or are introduced in ducts. These measures would be practicable when the structure does not cause too large a change in the water regime of the area it is built on.

However, the two suggestions above avoid actually changing the structure of the soil. This means that the problem is still there should those "by-passing" measures fail to have the desired effect. The following is a brief description of some of the methods which endeavour to change the structure of the soil and thereby eliminate or minimize the collapse danger.

2.2.7.1- Pre-collapse of the structure by driven piles:

Pre-collapse of the grain structure by the use of driven cast-in-situ piles. As the piles are driven, they displace and compact the loose soil, thus providing a more dense foundation material.

2.2.7.2- Prewetting by ponding:

This method consists of creating artificial reservoirs on the supported areas and letting the soil collapse. It is one of the earliest methods applied to these soils and is especially suitable when the collapsing layer is thick (say about 5 m.) and the use of foundation piles is expensive. This method has been used successfully by several researchers, e.g., Gibbs and Bara (1967) for the San Louis project and by Beles et al. (1969) for the foundation of a water reservoir.

However, this method has a few limitations. It is rather awkward to use in urban areas since it can cause damage to neighbouring buildings and necessitates drainage or water proofing measures which are costly. It is also very slow.

2.2.7.3- Dynamic compaction:

Dynamic compaction at ground level can be very useful when the compaction of shallow layer of collapsing soil is needed and this could be achieved successfully with or without sprinkling the soil with water. Williams et al. (1971) describe a new impact roller, a flat-sided one, which was found to cause consolidation to greater depth than vibrating or pneumatic rollers.

2.2.7.4- Deep compaction:

This method has been described and evaluated by Litrinov (1969; 1971), who apparently devised it, and by Abelev (1975). It involves first pre-cutting trenches around the area to be compacted. These trenches are 0.2 - 0.4 m. wide and 4 - 6 m. deep and isolate the area to be treated from its surrounding. Charges are then exploded in deep boreholes after having prewetted the soil. These charges have a strong hydrodynamic effect on the soil weakened by the saturation yet still prone to

further settlement, and cause an intensive compaction of the ground. Apparently, no underground hollows are formed at the locations of the explosions.

This method has the advantage of being very efficient and can be used for sites having a thick layer of collapsing soil and on which very heavy structures are to be built. It also has the advantages of being quick (eight days in one case). However, it presents the same inconvenience of the ponding method, in that the neighbouring buildings have to be protected against soaking by erecting a water proof shield between their collapsible foundations and the works, and by ensuring that all canalisation of the project are laid following the requirements in collapsing soils.

2.2.7.5- Silt slurry injection:

The silt slurry injection method was used as early as 1953 (Johnson, 1953). The idea is to inject a silt slurry into the pores of the soil, the latter being used as a filter.

The success of this method depends mainly on the ability of the soil to act as a filter (and for this, the soil must be permeable enough), and on the ability of the soil to let the water pass out under pressure. If not, the mass would remain liquid and as the injection work continued, the soil would be likely to fail. Note that this technique can be used as a pre-construction method as well as a post-construction method.

2.2.7.6- Chemical measures:

Chemical measures have been used to treat loose soils and have proven to be very effective. The Russian literature descibes extensively these procedures (Sokolovich,

1965 and 1971; Beketov et al., 1967). The methods currently employed are:

- Gaseous silicatization of sandy and loessial soils;
- Strengthning of carbonate cements by polymers; and
- Chemical strengthening of alluvial soils by clay-silicate solutions.

For a more detailed account of chemical methods, refer to Salameh (1973); Clemence et al. (1981); and Clemence (1985).

2.2.7.7- Grouting:

Since the problem of collapsing soils is essentially one of high initial void ratios, a logical procedure would be to fill these voids with a stabilizing mixture. Soil cement grouting (Mayer 1958) and chemical grouting (ASCE, 1966 and Lambe, 1962) have been successfully used to correct and stabilize buildings that have failed and to stabilize collapsing soils. It may be stated a priori that because grouting is a high cost soil treatment method and because it can only be used in situations where there is sufficient confinement to permit the needed injection pressures, the use of grouting is limited to zones of relatively small volume and to certain special problems; e.g., uncontrollable seepage, foundation underpinning. Further limitations are imposed because grouting procedures are often complex, and the results of grouting are difficult to examine and evaluate.

2.2.7.8- Pre-wetting and rolling:

For roads and runways on collapsing soils, the induction of collapse by pre-wetting and rolling is logical. Stage construction of roads may be a feasible solution in some cases. Some of the collapse may be induced under traffic before the final levelling

and wearing courses are laid.

As for the methods which are a future possibility, i.e., heat treatment, ultrasonics, electro-omosis, or chemical additives (other than lime or cement), further technological advances are necessary before they can become feasible.

For this type of problem, it is worth carrying out more detailed testing than is normally carried out and design the foundation on the basis of allowable settlement in addition to allowable bearing capacity.

Charles (1978) presented some field trials where three different ground treatment methods (pre-loading with a surcharge of fill, 'dynamic consolidation' and inundation) were used separatly on the same site. The work reported deals with the treatment and the performance of cohesive fill left by opencast ironstone mining at Snatchill experimental housing site, Corby. The backfill, which had been replaced by dragline during opencast mining, was generally significantly wet of standard proctor optimum moisture content and had an undrained shear strength of the order of 100 kN/m^2, yet due to the lack of compaction during placement it behaved as a loose unsaturated fill.

All three treatment methods had some success in compacting this cohesive fill. The inundation experiment appears to be least successful of these methods. Inundation produced least compression of the fill during treatment. The ineffectiveness of this method as a method of ground treatment, according to Charles, is probably due to the difficulty of saturating the fill by the addition of water from the ground surface. The water tends to run away down the largest voids and fissures and fails to provide a uniform treatment over the area. It may be that satisfactory inundation would only be achieved by a ground water table rising up through the fill.

Of the three treatment methods used at Snatchill only surcharge loading led to a demonstrably better performance. The superiority of this form of ground treatment was shown by the greater enforced settlement produced during the treatment. However, the economics of this form of treatment depend on the nearness of a supply of fill material.

2.2.8 Case Histories:

Most of the cases reported in the literature before 1980 were reviewed by Hassani et al. (1982). In this section, only the cases reported in the last decade are summarised in Table 2.3.

2.3 Stone Columns

2.3.1 General:

Stone columns, which consist of granular material compacted in long cylindrical holes, are used as a technique for improving the strength and consolidation characteristics of compressible soil. Unlike pile foundations they make very efficient use of the soil near the surface. They are ideal for light loads; however, but they are less effective at supporting heavy loads because they cannot transfer the applied stresses to the deeper layers of soil.

According to Hughes et al. (1974), stone columns were first used in 1830 by French military engineers to support the heavy foundations of the ironworks at the artillery Arsenal in Bayonne (Moreau et al., 1835). The Arsenal was founded on soft estuarine deposits. The columns were two metres long, 0.2 m in diameter and supported loads of 10 KN each. There were constructed by driving stakes into the

ground, withdrawing them, then back-filling the holes with crushed limestone.

Stone columns were forgotten until the 1930's when they were rediscovered as a by-product of the technique of vibroflotation for compacting granular soils. Compact granular columns were formed within the granular soil, this process according to Steuerman (1939) could more than double the bearing capacity of a site. Even so, it was not until the early 1960's that the vibroflotation technique was used to form stone columns in compressible soils (Dullage, 1969).

For treatment of cohesive soils, stone columns are placed directly beneath the loaded footings in a grid pattern using either the wet vibro replacement method or the dry vibro displacement method. Three possible regular arrangements are illustrated in Fig. 2.7. The columns may lie on the vertices of an equilateral triangle, a square or a regular hexagon (this last case is of limited practical importance). In order to reduce the complexity of the problem each domain is approximated by a circle of effective diameter d_e, the perimeter of which is shear-free, undergoes no normal displacement, and which has the same area as the actual domain (Balaam et al., 1981).

This section concentrates on the behaviour and performance of stone columns in soft soils and then briefly summarises some case histories.

2.3.2 Behaviour and Performance of Stone Columns in Soft Soils:

Hughes et al. (1974) and Schlosser (1979) stated that the granular material in the circular column is confined by radial stress just as though the column was in a triaxial apparatus. When load is applied from a spread footing, it tends to concen-

trate on the column as the stronger element of the composite. The column dilates and applies lateral stress to the surrounding clay which is resisted by passive pressure (Greenwood, 1970; Thorburn, 1975). The load capacity of the column is then controlled by the passive resistance of the soft soil and the maximum bearing capacity will rise when the ratio of the principal stresses is also a maximum depending upon the angle of friction of the column material (Greenwood, 1970; Mitchell, 1981).

Hughes et al. (1975) concluded that the behaviour of the composite soil-column depends on:

- The undrained shear strength of the soil,
- The in-situ lateral stress in the soil,
- The radial pressure/deformation characteristics of the soil,
- The angle of internal friction of the column material,
- The initial diameter of the column.

Watt et al. (1967) and Luce (1968) stated that the columns initially act as piles. As loading increases they dilate and develop passive resistance in the soft soil between the columns. At the same time the columns act as drains for the clay, thus accelerating consolidation and mobilizing additional strength in the clay. Eventually equilibrium is reached with uniform bearing through-out. According to them, the stone columns also act as shear pins against a circular arc type of foundation failure.

Hughes et al. (1974) carried out a series of model experiments at Cambridge, using radiographic techniques to determine the actual behaviour of a single column in a uniform normally consolidated clay.

The stone columns were made from Leighton Buzzard sand. The clay (Kaolin) was first one-dimensionally consolidated, then kept under a constant stress. Loads were applied to the top of the column only (Fig. 2.8). Displacements in the clay and sand were measured by taking radiographs of lead shot markers placed inside the column and the clay.

The conclusions drawn from the results of the experimental program are:

1. The model column both increased the rate and reduced the size of the settlements. Settlements were reduced by about a factor of six which is slightly higher than a factor of four reported by Moreau et al. (1835), Fig. 2.9.

2. For the particular clay and sand used in the experiment the vertical movement did not go below four column diameters (Fig. 2.10). This was supported by the elastic analysis of Mattes and Poulos (1969) but represented double the value reported by Williams (1969). It would appear for this particular case that if the length/diameter ratio is less than four then the columns would fail in end bearing before bulging.

3. Beyond this critical length the column does not contribute extra benefit in terms of enhanced ultimate load, but it helps to reduce settlement by penetrating to a firm stratum.

Several other works were carried out in order to investigate the performance of stone columns in soft soils. These works include both laboratory testing (Charles et al., 1983 and Juran et al, 1988) and field investigations (Hughes et al., 1975 and Mitchell, 1985). Even in a seismic area, its performance was evaluated (Engelhardt et al., 1975). All the works confirmed that very substantial increases of bearing capacity and reductions of settlement can be obtained from stone columns well compacted into clays.

2.3.3 Cases Histories:

There is a large number of cases where stone columns were used with success (e.g. Watt et al., 1967; Rathgeb et al., 1975; Morgenthaler et al., 1978; Vautrain, 1980; Bhandari, 1983; Romana, 1983). However, their use is not a hundred percent successful. In some cases their use without precautions ended with failure.

In this sub-section, it is considered worthy to present two cases where stone columns failed in reinforcing soft soils.

2.3.3.1- Case 1: Mc Kenna (1975):

Stone columns were used for the purpose of reducing the settlements of high embankments built on soft alluvium. They were constructed under one end of the east Brent trial embankment using the vibro-flotation replacement technique. The soft soil was 27.5 m thick, the columns were 0.9 m in diameter and 11.3 m long, and they were constructed on a triangular grid at 2.4 m centres. The embankment was built to a height of 7.9 m. The foundations were instrumented, and a comparison of the piled and unpiled ground showed that the columns had no apparent effect on the settlement performance of the embankment. As a result, stone columns were not used under the motorway embankments.

It was postulated that these columns were ineffective for two reasons:

1. The grading of the 38 mm single-size crushed limestone was too coarse to act as a filter, and as a result, the voids in the gravel backfill probably became filled with clay slurry which prevented them from acting as drains.

2. The method of construction would probably have remoulded the adjacent soft clays and damaged the natural drainage paths, so nullifying any potential drainage provided by the stone columns.

Possible reasons why the stone columns did not reduce the settlement in the upper part (12.5 m) of clayey alluvium might be that the backfill was so coarse that as the embankment load came onto the columns the crushed stone forming each column was not restrained sufficiently by the surrounding soft clay, and, as the columns expanded , the soft clay squeezed into the voids.

2.3.3.2- Case 2: Machado Filho (1987):

A field testing program was carried out in order to evaluate the behaviour of stone columns for the improvement of a soft clay foundation.

The program consisted of two test fills, 5 m high, and equally instrumented. The first was founded on untreated soft clay and the other on a triangular grid of stone columns with spacing of 2.5 m on the left side and 3.0 m on the right. Observations were made during one year from which the following main conclusions were derived:

1. The excess pore water pressure observed at the end of construction in the upper soft clay layer corresponded to 67% of the load applied, showing that there was a dissipation during the permanence of the draining layer (34 days in the embankment without columns and 105 days in the other), and the raising to 5 m (73 days in the embankment without columns and 89 in the other). Three months after construction, dissipation of 55% of the remaining pore pressures was registered. These values were equivalent in both embankments.

2. The total mean settlements observed in the embankments founded on stone columns were 3.7% lower for 3.0 m spacing and 14.6% for 2.5 m spacing, with an average of 11.2%. This difference is not significant, considering that the untreated foundation underwent the maximum load for a longer period.

According to Machado Filho, this unsatisfactory performance is attributed

principally to the wide spacing between the columns.

2.4 Geotextiles

2.4.1 General:

A geotextile is an article constructed from fibre where a fibre is defined as an individual strand of material having one dimension much larger than the other two dimensions. It is, therefore, theoretically possible to have an infinite range of textile materials. In practice, however, the term textile is generally limited to products made from materials which are commonly available in fibrous form and, in particular, those which are available relatively cheaply.
The following sub-sections introduce one kind of textiles namely 'Terram' and review some work performed on the reinforcement of sand using geotextiles.

2.4.2 Terram:

Terram is ICI fibers' trade name for its fabrics for the Civil Engineering industry. These range from lightweight, thermally bonded, non-woven, permeable materials designed for use in ground stabilization, drainage, reinforcement, and erosion control to special-purpose fabrics.

Terram is made from 67% polypropylene and 33% polyethylene. Its structural characteristics, mechanical properties, hydraulic properties and others are shown in Figs. 2.11.

Terram is resistant to all naturally occurring soil alkalis -even 10% sodium hydroxide has little effect. It has excellent resistance to all naturally occurring soil acids -(i.e. to acids of pH $>$ 2), and to general chemical attack e.g. water, oil, petrol.

Since polypropylene and polyethylene are not sources of nourishment, resistance to attack by bacteria, fungi, etc is excellent. Rats and termites will not eat the product as food.

'Terram' is generally stable over the temperature range -40°C to +100°C. In common with other thermoplastic materials strength is reduced at elevated temperatures but exposure to high temperatures for short periods is not detrimental to subsequent fabric performance (ICI, 1977).

It may be exposed to direct sunlight for short periods but as prolonged exposure leads to a gradual loss of strength (ICI, 1977), it is not recommended to leave the material uncovered for periods longer than a couple of weeks, especially in areas of high isolation (ICI, 1977).

2.4.3 Some Works on the Effect of Internal/External Fabric Reinforcement on the Behaviour of Sand:

At Strathclyde University a widely based study of the influence of various types of inclusions in soil systems has been carried out with particular consideration being given to the behaviour of soil systems incorporating fabrics and in particular ICI fibres melt-bonded Terram membranes.

McGown et al. (1977) and McGown et al. (1978) performed an experimental program in order to illustrate the fundamental principles of the influence of non-woven fabric inclusions on the behaviour of soil masses. They showed that the reinforcement generally increased the strength of the composite. More important than the strengthening was the fact that the strains to the peak strength were increased and the brittleness of the system post-peak was markedly reduced. Similar results were obtained by Gray et al. (1983).

Gray et al. (1982) investigated experimentally, using the triaxial apparatus, the stress-deformation behaviour of internally/externally reinforced sand masses. Internal reinforcement was provided by insertion of fabric layers within the sand; external, by simultaneous encapsulation in a geotextile.

The test results indicated that separated reinforcement (either internal or external) or conjunctive reinforcement of granular columns, can stiffen the column significantly.
Stress-deformation response of such a reinforced composite can be controlled to a large extent by selection and placement of fabrics with appropriate modulii and other properties.

Internally/externally reinforced granular soils show promise of being used as load bearing structural units in soft, cohesive soils. Reinforced 'earth pillars' and 'trench foundations' are possible alternatives in this regard to the vibro replacement-stone column system in such soils (Fig. 2.12).

Gorle et al. (1989) carried out a testing program which included model tests with prestressed geosynthetic and laboratory tests with granular materials either confined by a geotextile or reinforced with short fibres.

The results showed that confinement, and especially fibre reinforcement, lead to a considerable improvement of the mechanical properties, the modulus of elasticity and the shear resistance (angle of internal friction, cohesion) of these materials, capable of transforming the properties of a clean sand into those of a crushed stone layer.

2.5 Conclusion:

An important problem encountered by foundation engineers involves partially saturated soils which possess considerable in-situ dry strength that is largely lost when the soils become wetted. In the design and construction of hydraulic works, where foundation wetting is to be expected, this problem requires particular attention. Even in non-hydraulic structures the undesirable wetting of foundations may occur when the water table rises or when surface run-off is not properly removed from the structure site.

From what has been discussed in this chapter, it can be seen that most of the research that has been carried out on these soils has concentrated on the development of methods of identifying readily the soils that could collapse and determining the amount of collapse that may occur. However, very little work has been done in order to enable a practising engineer to design his structures on collapsing soils with a high degree of confidence, safety and economy.

Several foundation treatment methods for collapsible soils have been suggested and even some of them were recommended by some researchers. However, going through the history on these types of soil, only a few of them have been used.

The most popular remedial measures were ponding and piling. They were used in almost all the cases reported here and elsewhere. But their technical and financial constraints and limitations in collapsible soils urge researches to investigate the performance of other practical solutions.

The behaviour and performance of stone columns and their history in reinforcing soft soils make them a more attractive alternative to conventional methods as time goes on.

The work performed with the geotextile provides a good insight into how internal or external reinforcement of sand improves its mechanical properties. Either

of the methods can strengthen and stiffen a column of sand significantly.

In the field of research, progress is continuous, and the 12^{th} International Conference held in Rio de Janiero, where more than 20 works were discussed on collapsible soils, is another witness. But, it is quite surprising that, up to the present time, the behaviour and performance of stone columns in collapsible soil has not been investigated.

Depth of Subsoil Treatment Desired	Foundation Treatment Method
Current and Past Methods	
0 to 1.5 meters	1- Moistening and compaction (conventional, extra-heavy, impact, or vibratory Rollers)
1.5 to 10 meters	2- Overexcavation and recompaction (earth pads with or without stabilization by additives such as lime or cement) 3- Vibroflotation (free-draining soils) 4- Rock columns (vibroreplacement) 5- Displacement piles 6- Injection of silt or lime 7- Ponding or flooding (if no impervious layers exist)
over 10 meters	8- Any of the above or combinations of the above methods, where applicable 9- Ponding and infiltration wells 10- Ponding and infiltration wells with the use of explosives
Possible Future Methods	
	1- Heat treatment to solidify the soils in place 2- Ultrasonics to produce vibrations that will destroy the bonding mechanism of the metastable soil 3- Chemical additives to strengthen the bonding mechanism of the metastable soil structure, (possibly electrochemical methods of application) 4- Use of grout-like additives to fill the pore spaces before solidification

Table 2.2 **Method of Treating Collapsible Foundation Soils**

(Bara, 1976)

Type of Structure	Reference	Details of Structure	Foundation	Problems	Remedial Measures
Guyed mast	Selby (1982)	165 m high	up to 15 m of aeolian sand	following a period of heavy rain, discrepancies in guy tensions occured caused by settlement of the footing; an open crack 20 mm wide was also observed adjacent to the footing.	various solutions to the problem were considered, including grouting and piling, but it was decided to waterproof and drain the ground surface around the footing and so prevent further penetration of water. Footing deflections monitored over a period of years has shown that this solution has proved satisfactory.
Loxton high school	Selby (1982)	single-story masonry structure with strip footing	a loose calcareous silty and aeolian sand	leaking water pipe was the cause of progressive collapse of foundation soils causing cracks exceeding 25 mm in width in the masonry walls	All water pipes were subsequently relaid above ground and the structure was supported by underpinning with deep bored piles, drilled at 3 m centres to a lime stone horizon 7.5 m below surface, carring the footing beams on cantitevered brackets.
popular housing construction	Ferreira et al. (1989)	1856 units	collapsible soil from the brasilian types	laboratory and field investigations showed that the soil is susceptible to collapse by wetting.	short bored piles used as treatment failed in reducing the settlement to the required values.
San luis canal	Knodel (1981)	172 Km long and had a capacity of 370 m_3/s	soils which exhibited collapsible behaviour	32 Km of the canal passed through the collapsible soils.	ponding and compacting this area.
Water tanks	Selby (1982)		collapsible soil at Lovely, Australia	collapse upon wetting	to prevent collapse of the tanks it was decided top reload the foundation soils after flooding for 14 days. Sand drains were installed to accelerate consolidation and the fill, which was readily available on this site, was placed over a period of 3 weeks. Settlements of up to 300 mm were recorded during this process.
Blacktop road	Weston (1980)	120 Km length	40 Km of the road lies on approximately 15 m of Kalahari sand	the sand was reported as collapsible.	the following point were suggested: a heavier or different types of rollers; either apply water to the road bed or wait for rainfall; throughly rip to the full depth required to be compacted; excavate material, replace and compact in lifts of 200 to 300 mm.
Railroad bridge	Ordemir et al (1985)	2030 m long, with 2 abutment and 28 towers spaced at 70 m centers. Some towers were 65 m high.	very thick alluvial deposit and the ground water at great depth	consedering the potential settlement of the dry alluvium upon saturation.	In order to overcome the settlement problem, it was decided to design and construct the foundation on drilled peirs extending below groundwater. Drilled peirs were selected because they have many advantages in medium to very dense alluvium in which other types of piles can hardly be driven or constructed.
Bridge abutment	Delage (1989)	8 m high	compacted schist residual	following heavy rainfall, large and instantenious settlement occured which put the bridge out of service.	extensive investigations concluded that the total settlement recorded was not caused only by the water from the rainfall but also from the capillary rise since the water table was at the natural ground level.

Table 2.3 Typical examples indicating their problems and remedial measures

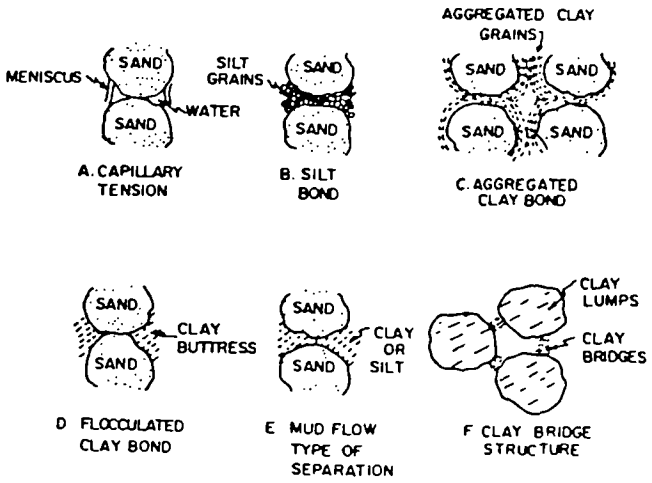

Fig. 2.1 Typical Collapsible Soil Structures (Clemence & Finbarr, 1981)

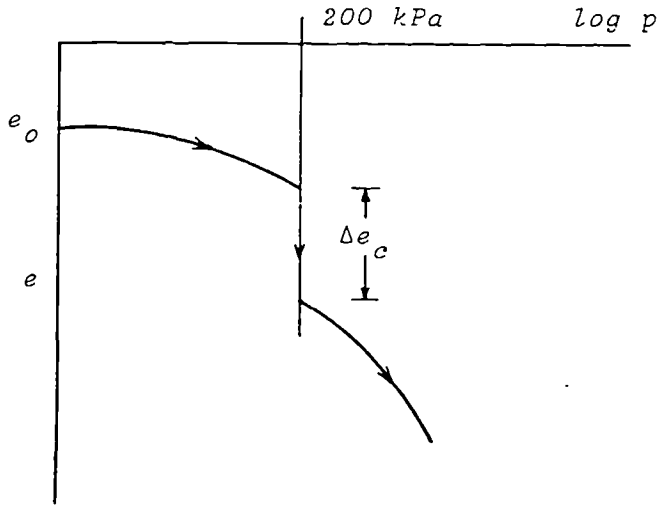

Fig. 2.2 Typical Collapse Potential Tests Result (Clemence & Finbarr, 1981)

CP	Severity of Problem
0 - 1%	No problem
1% - 5%	Moderate trouble
5% - 10%	Trouble
10% - 20%	Severe trouble
> 20%	Very severe trouble

Table 2.1 Collapse Potential Values (Jennings & Knight, 1975)

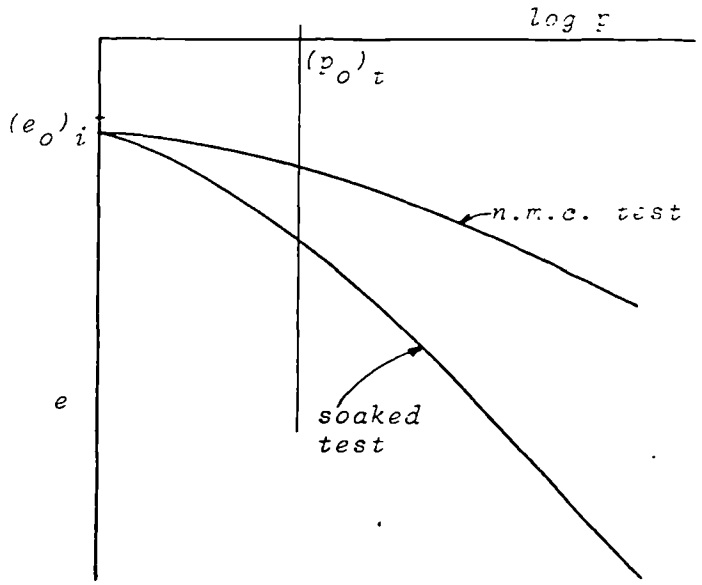

Fig. 2.3 Double Oedometer Test Results
(Jennings & Knight, 1975)

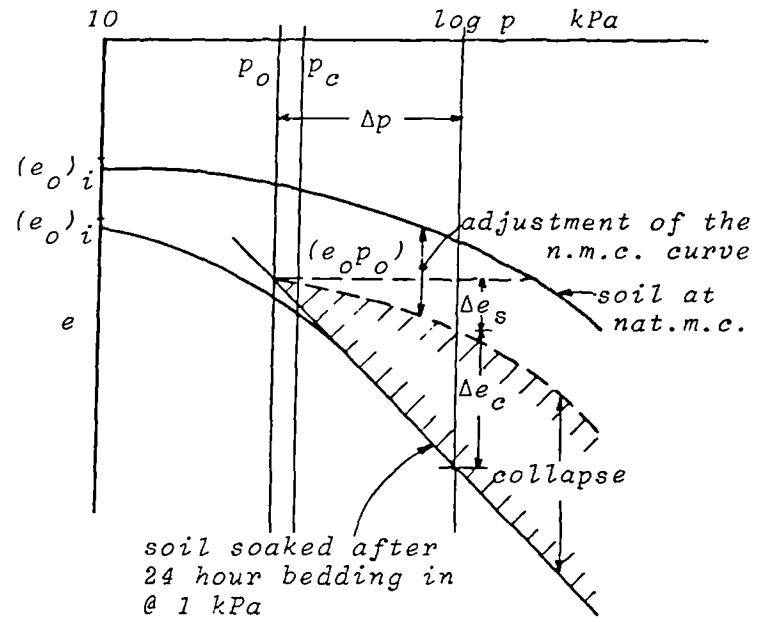

Fig. 2.4 Double Consolidation Test and Ajustments for Normally Consolidated Soil (Jennings & Knight, 1975)

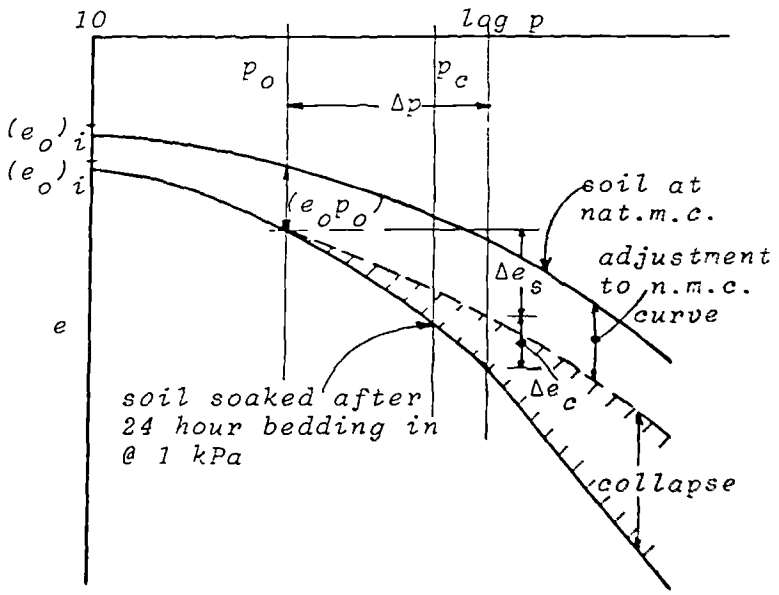

Fig. 2.5 Double Consolidation Test and Adjustments for Over-consolidated Soil (Jennings & Knight, 1975)

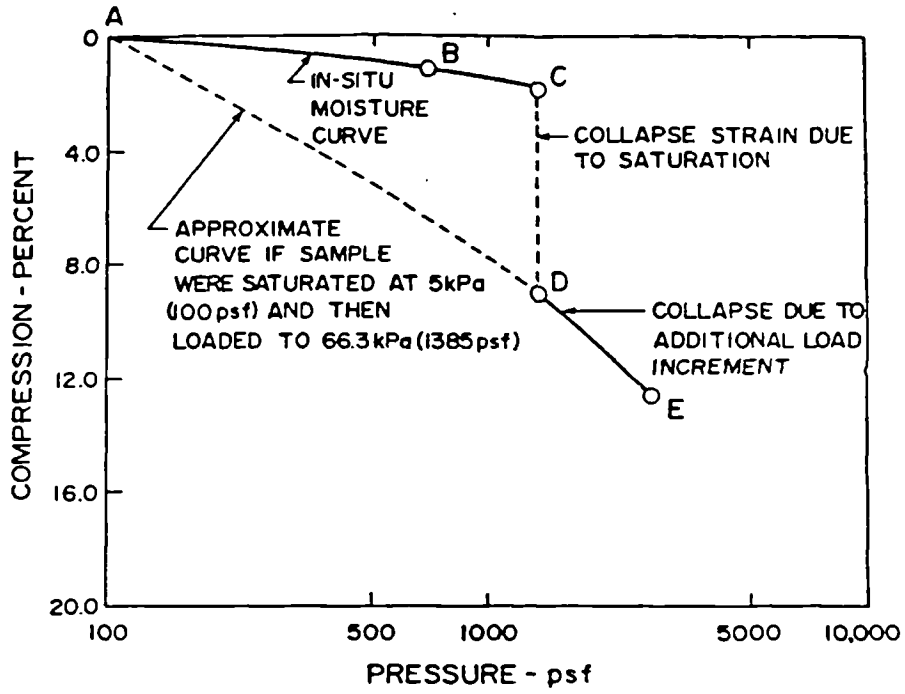

Fig. 2.6 Typical Compression Curve for Modified Jennings and Knight Oedometer Test (Houston et al., 1988)

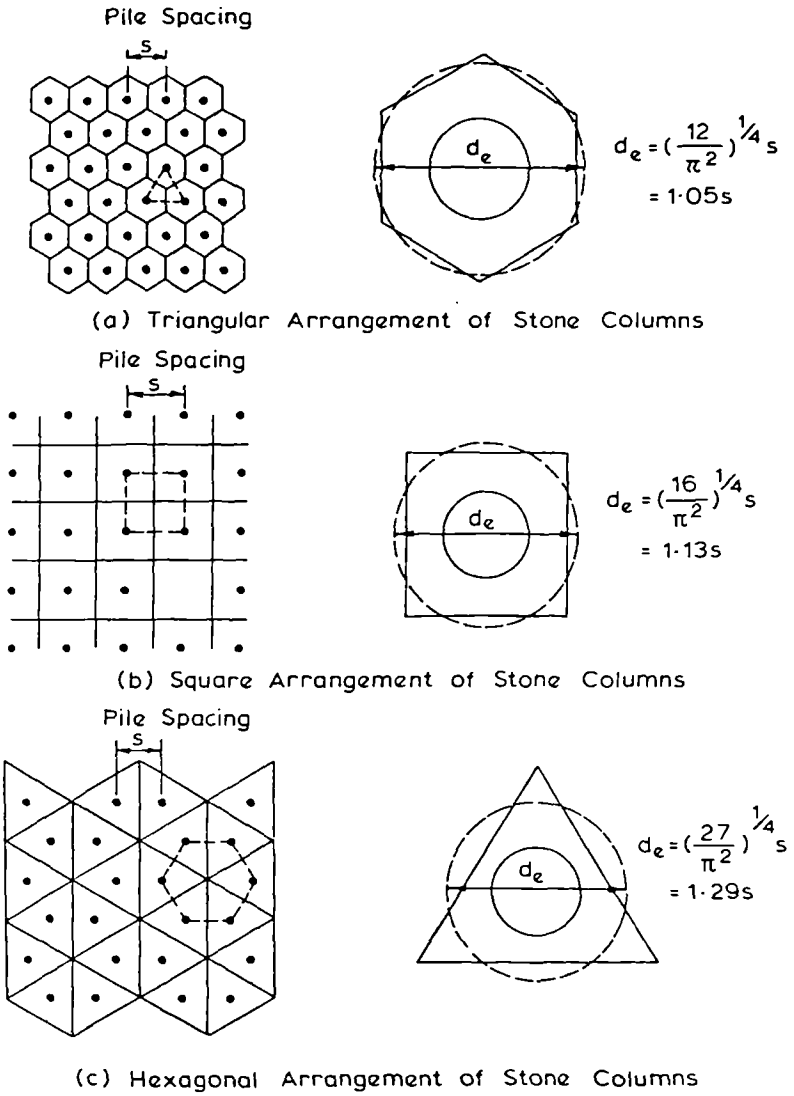

Fig. 2.7 Various Stone Column Arrangement Showing the Domain of Influence of each Column (Baalam & Booker, 1981)

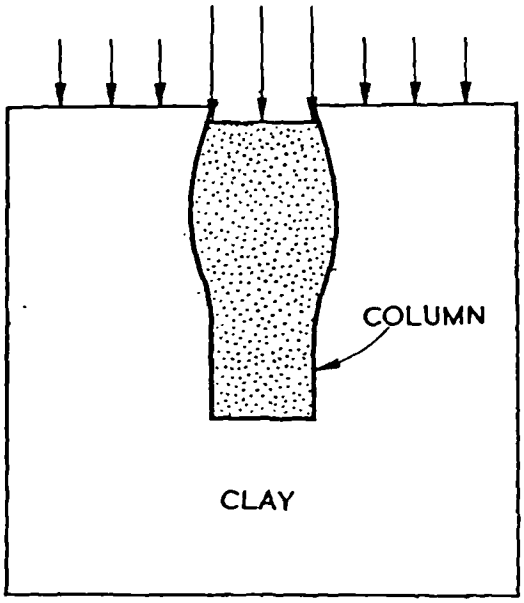

Fig. 2.8 Loads Applied on the Top of the Soil and the Stone Column (Hughes et al., 1974)

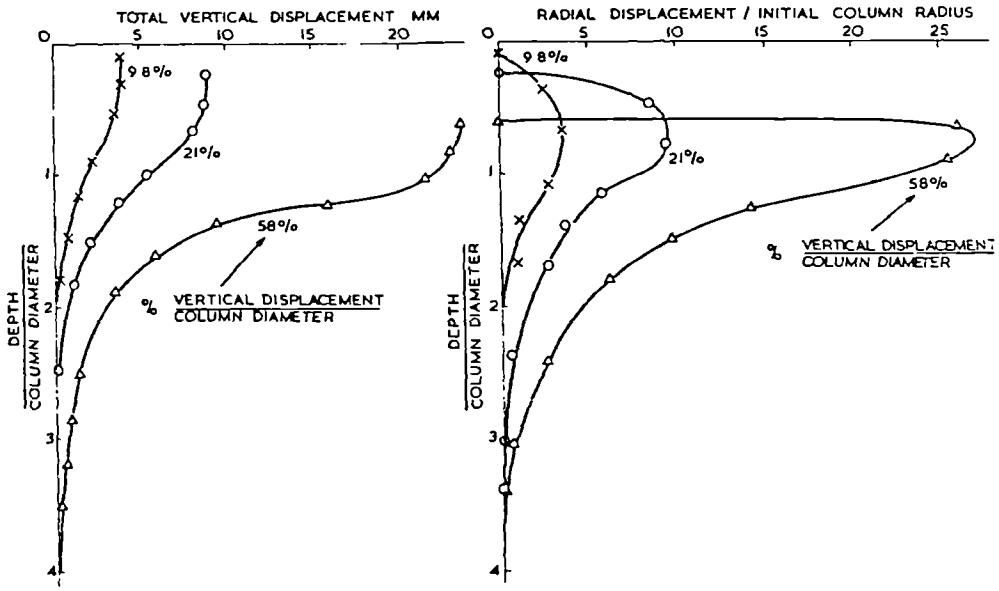

Fig. 2.10 a) Vertical Displacement within the Column against Depth
b) Radial Displacement at the Edge of the Column/Initial Column Radius against Depth (Hughes et al., 1974)

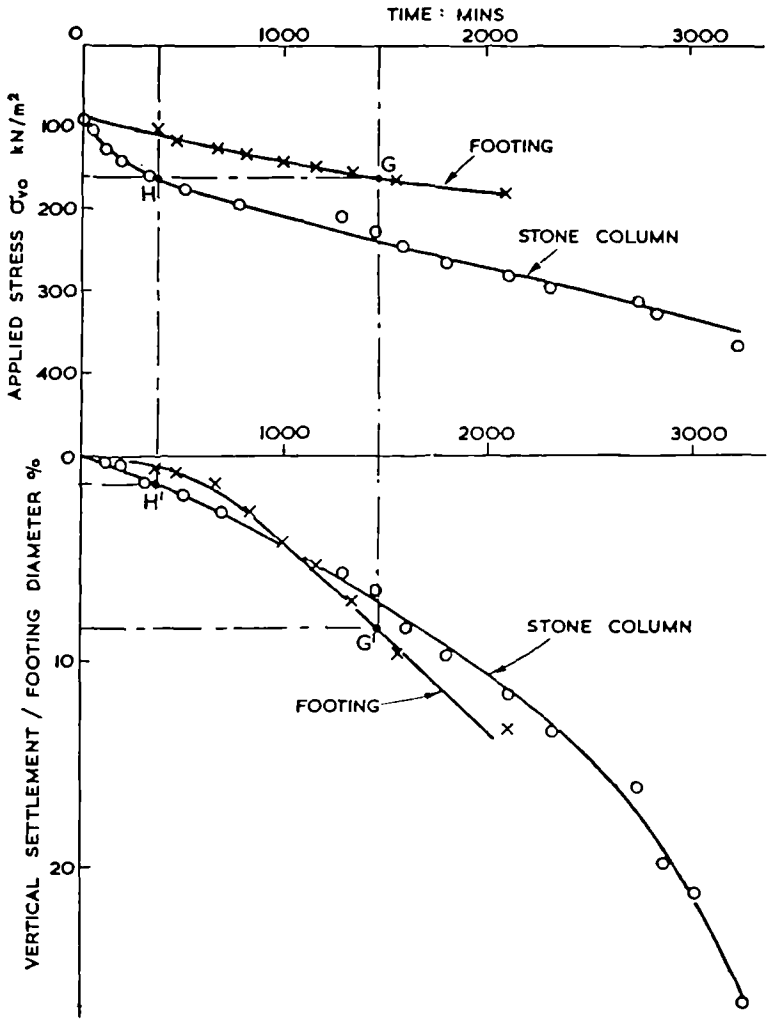

Fig. 2.9 The Upper Figure Shows the Applied Stress on the Column and the Footing Against Time. The Lower Figure Shows the Vertical Settlement as a Percentage of the Footing Diameter against Time (Hughes et al., 1974)

Structural characteristics

'Terram' Product	500	700	1000	1500	2000
Thickness mm	0.4	0.5	0.7	0.8	1.0
Fibre Diameter micron	35	35	35	35	35
Thickness in terms of fibre diameters	11	16	20	23	25
Porosity % at 250 kg/m^2	81	80	79	73	70
Porosity % at 2×10^4 kg/m^2	75	74	74	68	65
Weight variability %	<10	<10	<10	<10	<10

Mechanical properties

	'Terram' Product	500	700	1000	1500	2000
200mm Plane strain test	Tensile Strength Max load Newtons/200mm	750	1200	1700	2200	2400
	Extension at Max. load –%	35	40	45	50	55
	Load at 5% ext'n –Newtons	200	400	500	600	720
	Rupture Energy – Joules	40	70	100	160	190
25mm Grab test	Max load Newtons	400	600	850	1200	1450
	Ext'n to Max load –%	70	75	80	80	80
	Load at 5% ext'n–Newtons	70	120	160	210	250
	Tear Strength Wing – Newtons	110	190	250	310	380
Burst test	Bursting Load Newtons	50	80	110	150	200
	Distension at Burst – mm	15	15	15	15	15

Fig: 2.11 Properties and Specification of 'Terram' (Part I) (ICI, 1977)

Tensile tests

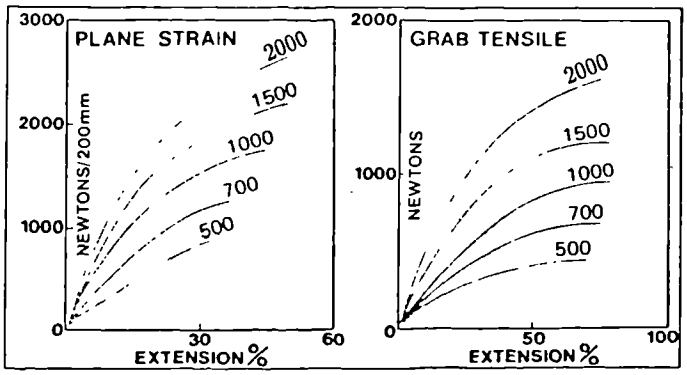

Production data

'Terram' Product	500	700	1000	1500	2000
Standard Roll Width m.	4.5 5.3	4.5/5.3	4.5/5.3	4.5/5.3	4.5/5.3
Standard Roll Length m.	200	100	100	100	100
Standard Roll Weight kg	69 84	38/63	52/100	83/128	110/160
Standard Roll Diameter mm	310	270	300	330	370
Weight category gsm.	up to 70	71/100	101/170	171/222	230/280
Composition	67% polypropylene/33% polyethylene SG=0.92				

Hydraulic properties

'Terram' Product	500	700	1000	1500	2000
Water Permeability $L/m^2/sec$ 100mm head	150	80	40	35	33
Pore size O_{90} micron	350	180	100	60	50
Pore size O_{50} micron	200	120	70	40	30
The Darcy co-efficient (k) of the 'Terram' membranes shown in this table is of the order of 0.5×10^{-3} m/sec					

Fig. 2.11 Properties and Specification of 'Terrm' (Part II) (ICI, 1977)

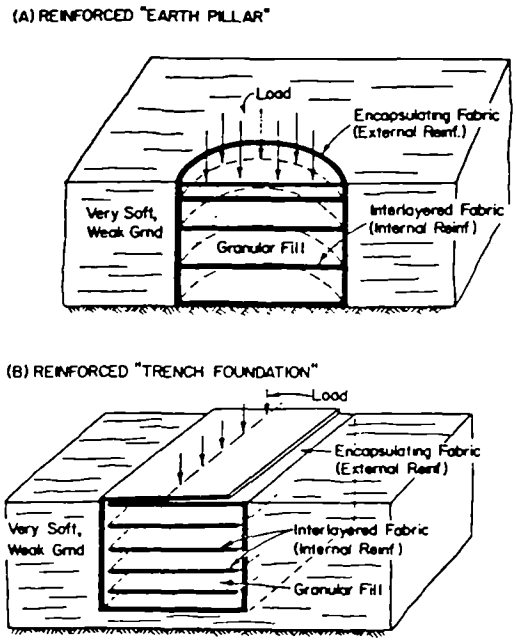

Fig. 2.12 Internally/Externally Fabric Reinforced Below Grade Foundations (Gray et al., 1982)

Chapter 3

Stone Column and Pile Background Theory

3.1 Introduction:

There are considerable data on the practical effectiveness of stone column treatment methods for soft soils from sites worldwide. Comparatively theoretical studies of the mechanisms and phenomena have been performed, in order to predict the behaviour of granular columns in certain ground conditions. In addition, several models , developed for piles, were found to be suitable for this purpose, especially those quoted by Randolph et al. (1978) as 'the integral equation method' and which are based on elastic theory.

In this chapter most of the theoretical works on granular columns are reviewed. Besides, some of the analytical models developed for piles and based on the elastic theory are summarised. The analytical model adopted and developed for this investigation is described and the predicted results are then interpreted.

3.2 The integral equation theory developed for piles:

The integral equation method was derived from fundamental compatibility concepts of the theory of elasticity. The model uses the solution for displacements due to a force in a semi-infinite elastic solid given by Mindlin (1936).

The procedure of analysis is explained with the aid of Fig.(3.1), which shows a solid pile embedded in soil to a depth L. For calculation, the pile was divided into n equal segments of length l. The interaction shear stress between the pile and soil was assumed constant over the length l and the resultant force F, was assumed to act at the midpoint of the segment. Other assumptions made depended on the case studied.

Several investigators have used this method to analyse the behaviour of single axially-loaded piles in specific cases (e.g. Seed and Reese, 1955; D'Appolonia and Romualdi, 1963; Thurman and D'Appolonia, 1965; Salas and Belzunce, 1965; Coyle and Reese, 1966). Others developed and extended this approach in order to have general application by covering a sufficient range of variables. The variables studied were:

1. The effects of the length to diameter ratio of the pile, Poisson ratio of the soil and the depth of the soil on the behaviour of a floating incompressible pile (Poulos and Davis, 1968).

2. The effect of the same factors in addition to the effects of the ratio of pile stiffnesses, on the behaviour of a floating compressible pile (Mattes and Poulos, 1969).

3. The effects of the previous factors on the behaviour of an end-bearing com-

pressible pile (Poulos and Mattes, 1969).

4. Consideration of both vertical and radial displacements (Mattes, 1969).

5. The influence of negative friction on the behaviour of a single compressible pile. Two cases were considered, the elastic case and taking account of local yield between the pile and the soil (Poulos and Mattes, 1969).

6. The rate of development of down-drag load in an impermeable pile with time (Poulos et al., 1972). The case of a permeable pile was also outlined.

Poulos and Davis (1975) critisized all the results of the foregoing solutions proposed for downdrag, for not being expressed in a form that can be applied readily to practical problems. Then they presented a series of parametric solutions for the magnitude and the rate of development of maximum downdrag force and axial movement of a pile in a consolidating soil layer subjected to surface loading. The results were expressed in terms of the downdrag force and axial movements that would occur if full pile-soil slip occurred along the pile shaft. The results were presented as follows:

(a)- Final maximum downdrag force:

The final maximum force, P_N, in a pile, generally occurs at the pile tip and may be expressed in terms of the downdrag force for full slip, as follows:

$$P_N = P_{NFS} N_R N_T + P_a \qquad (3.1)$$

in which:

P_{NFS}: final maximum downdrag force if full pile-soil slip occurs;

N_R: correction factor for cases in which full slip does not occur,

N_T: correction factor for effects of delayed installation,

P_a: axial force in the pile at the top of the consolidating layer,

The term P_{NFS} was expressed as:

$$P_{NFS} = \pi d \int_0^L \tau_a dz \qquad (3.2)$$

in which τ_a is final pile-soil adhesion. For a uniform soil layer:

$$P_{NFS} = \pi dL \left[c_a^{'} + K_s tan\phi_a^{'} \left(\frac{\gamma L}{2} + q \right) \right] \qquad (3.3)$$

and values of N_R and N_T are presented in Figures 3.2(a), 3.2(b), 3.3(a), and 3.3(b).

(b)- Rate of development of downdrag force:

The rate of development of the maximum downdrag force with time is shown in Fig. 3.4. At any time t after installation of the pile, assuming the applied axial load, P_a, has been applied previously, the maximum downdrag force, P_t, can be calculated as:

$$P_t = U_N \left(P_N - P_a \right) + P_a \qquad (3.4)$$

where:

P_N: final maximum downdrag force calculated from Eq.(3.1),

P_a: axial force in the pile at the top of the consolidating layer,

U_N: degree of development of downdrag for

$$T_V = M_{c_v} \frac{t_e}{L^2}$$

It is plotted in Fig. 3.5.

(c)- Pile movement:

The axial movement, ρ, of the pile at the level of the top of the consolidating layer can be expressed as:

$$\rho = \rho_{FS} Q_R Q_T + \frac{P_a L}{E_p A_p} \qquad (3.5)$$

in which:

ρ_{FS}: axial movement of pile if full pile-soil slip occurs,

Q_R: correction factor for cases in which full slip does not occur,

Q_T: correction factor for effects of delayed installation.

By integration of the strains in the pile, it may be shown that ρ_{FS} in a uniform soil is:

$$\rho_{FS} = \frac{2qL^2R_A}{E_p d}\left[c_a^{'} + K_s tan\phi_a^{'}\left(\frac{\gamma L}{3q} + 1\right)\right] \qquad (3.6)$$

Correction factors Q_R and Q_T are plotted in Figs 3.6 and 3.7.

The second term in Eq.(3.5) represents the movement of the pile acting as a free-standing column under the axial load. The addition of this value to the settlement due to downdrag will give the correct settlement if full slip occurs, but a slight overestimate in other cases.

(d)- Rate of development of pile movement:

As with the maximum downdrag force, the movement of the pile, ρ_t, at any time t after installation may be calculated as:

$$\rho_t = U_\rho\left(\rho - \frac{P_a L}{E_p a_p}\right) + \frac{P_a L}{E_p A_p} \qquad (3.7)$$

in which:

ρ: final movement of pile, from Eq. (3.5),

U_p: degree of pile movement, for a time factor

$$T_v = M_{c_v}\frac{t}{L^2}$$

The movement is plotted versus time factor T_v in Fig. 3.8.

Poulos et al. (1980) stated that, if fully elastic conditions are indicated, a more satisfactory prediction may be made by using the elastic solutions, in which case the values of K and ν_s may become significant.

If the soil settlement is assumed to vary linearly from S_0 at the surface to zero at the base, the elastic maximum downdrag force may be expressed approximately as follows:

$$P_N = I_N E_s S_0 L R N_T + P_a \qquad (3.8)$$

where:

I_N: elastic influence factor obtained from figures similar to those shown in Fig. 3.9.

$$R = \frac{(1-2\nu_s)(1+\nu_s)}{1-\nu_s}$$

For an uniform layer subjected to a surchage pressure q, Eq.(3.8) becomes:

$$P_N = I_N q L^2 R N_T + P_a \qquad (3.9)$$

The axial movement of the pile may be expressed approximately as follows:

$$\rho = \frac{qd}{E_p R_A} I_p Q_T + \frac{P_a L}{E_p A_p} \qquad (3.10)$$

I_p: settlement influence factor obtained from figures similar to those shown in Fig. 3.10.

When the consolidating soil layer is overlain by other layers, the settlement of the portion of the pile in these layers must be added to the calculated pile-settlement at the level of the top of the consolidating layer. If the consolidating soil layer has an initial stress p_0 acting at the top of the layer, it can be treated as having an equivalent pile-soil adhesion c'_{ae}, where:

$$c'_{ae} = c'_a + p_0 K_s tan\varphi'_a$$

c'_a, φ'_a: Pile-soil adhesion and friction angle.

K_s: Coefficient of lateral pressure, assumed to remain constant during consolidation.

It is very important to note that Poulos et al. (1975) have checked the validity of the previous series of the parametric solutions. They compared between

predicted and measured pile behaviour from different field tests (Bjerrum et al., 1969; Walker et al., 1973). Comparisons between measured and theoretical distributions of pile shortening and downdrag force are shown in Fig. 3.11 and 3.12, which reveal remarkable agreement.

The integral equation method was also used in analysing the general characteristics of the bahaviour of a pile group (e.g. Poulos, 1968; Butterfield and Banerjee, 1971; Kuwabara and Poulos, 1989).

3.3 Theory for Stone Columns:

The design of stone or compacted sand columns to reinforce soft foundation soils should enable the engineer to meet the required criteria for bearing capacity and admissible settlement under the expected working loads. Different methods have been proposed to estimate the bearing capacity and the admissible settlement of granular columns. They are ranging from empirical (Greenwood, 1970; Thorburn, 1975; Barksdale and Bachus, 1983) to sophisticated numerical solutions (Balaam et al., 1977; Morgenthaler et al. ,1978; Balaam and Poulos, 1983; Majorana et al., 1983; Mitchell, 1985; Balaam et al., 1985). However, the analytical approach is still the most popular and widely used because it has several advantages over an empirical and a purely numerical approach. One of these advantages is that, the analytic solution is relatively simple and can be calculated swiftly, to show the effect of many parameters governing the solution.

The different methods of analysis developed for granular columns can be divided into two groups:

1. Solutions based on the lateral earth pressure support,

2. Solutions based on the distribution of stresses between the soil and the column.

The more well-known models are due to Porteur (1973), Brauns (1978), Hughes and Withers (1974), Priebe (1976), Balaam et al. (1977), Balaam et al. (1981), Goughnour and Bayuk (1979), Van Impe et al. (1983), Goughnour (1983).

Greenwood et al. (1982) compared some of the foregoing analyses with field and laboratory observations in the diagram reproduced in Fig. 3.13. They concluded that the simplicity of the Hughes et al. and Priebe methods are attractive and make them most widely used.

From the forgoing considerations and based on settlement prediction, which is the purpose of the theoretical part of the present investigation, only the methods used to compute settlement for stone columns in soft soils using the last two models (i.e. Hughes et al. and Priebe models) are summarised.

Hughes and Withers (1974) proposed a summation of contributions from discrete horizontal slices of the column.

$$\delta_v = \delta_1 + \delta_2 + ... + \delta_n \qquad (3.11)$$

$$\delta_n = 2H_n \frac{\delta_{rn}}{r} \qquad (3.12)$$

where:

H_n: the thickness of soil layer considered,

δ_{rn}/r: the radial strain for that layer.

They assumed a constant volume during settlement and expansion of each slice, and no significant change in the ratio of vertical and horizontal stresses within the column. Shears on the sides of each slice reduce loading on each successive lower one, and for each slice bulging of the column is limited by the value of lateral strength of the ground. Using measured radial stress/strain curves from

the Cambridge pressuremeter it was possible to define the shape of the load settlement curve for the column. This method is still widely used because of its simplicity.

Priebe (1976) introduced an analytical solution to the problem using the concept of the unit cell. In his model, Fig. 3.14, the radial deformation of the stone column was given by:

$$\delta r_0 = \Delta P \frac{1+\nu}{E} r_0 \frac{(1-2\nu)(1-\frac{r_0^2}{a^2})}{1-2\nu+\frac{r_0^2}{a^2}} \qquad (3.13)$$

where:

ν: poisson ratio of the soil,

$$\Delta P = P_v k_{as} - P_r$$

$$k_{as} = tan^2(45^o - \frac{\phi_s}{2})$$

P_v: external vertical load on the column,

P_r: lateral pressure acting on the column.

The total settlement was defined as :

$$\delta c = 2\frac{\delta r_0}{r_0} H_0 \qquad (3.14)$$

where:

H_0: length of the column,

r_0: initial radius of column.

3.4 The Analytical Model Adopted:

An analytical solution was adopted and developed for settlement prediction, because this factor is the most predominant one in collapsing soils. The model was derived from those applied to compressible piles and stone columns in soft soils. It consists

of simple parametric equations convenient for hand calculations.

The principle of the solution is illustrated by Fig. 3.15. For convenience, the total and final settlement of a pile in a collapsible soil, caused by inundation under an applied external load P, was divided into three parts.

$$\Delta = \delta_1 + \delta_2 + \delta_3 \qquad (3.15)$$

where:

Δ: is the total and final settlement caused by inundation under an external load P.

δ_1: is the elastic settlement of the pile due to the axial load P.

δ_2: is the settlement caused by downdrag. The experience with construction and operation of large residential, social-service, and industrial building on pile foundations in collapsible soils has shown that as a result of soaking of the soils additional settlements of the structure occur. The investigations of many others (Griogoryan et al., 1975; Gupalenko et al., 1976; Klepikov et al., 1980) have demonstrated that additional settlements of the foundation take place as a result of action on them, of 'negative friction' forces. Details of downdrag are given in Appendix A .

δ_3: is the settlement due to the lateral deformation of the compressible pile.

As mentioned earlier, the settlements δ_1 and δ_2 were obtained from the analytical model of Poulos and Davis (1975) developed for compressible piles in compressible soils, whereas, δ_3 was obtained from theoretical models applied to stone columns in soft soils. It was determined, for comparaison purpose, in two ways. Firstly, by following the procedure of Hughes and Withers (1974) and secondly, by applying the approach developed by Priebe (1976). The third component of the settlement (δ_3) was not considered in the model of Poulos and Davies because con-

sideration, in their cases, of both vertical and radial displacements led to solutions which were insignificantly different from those obtained by considering vertical displacements only (Mattes, 1969).

3.4.1 Types of Analysis:

Two types of analyses have been employed. A purely elastic and a modified elastic analysis. The purely elastic approach was modified to take account of local yield or slip between the pile and the soil. Such a modification is very desirable in considering negative friction, since, the field evidence (Bjerrum et al., 1969) indicated that shaft-soil slip is very likely to occur when large soil settlements take place. In this thesis, for simplicity, the elastic analysis and the slip analysis will refer to the purely elastic and modified elastic analyses respectively.

The elastic analysis was performed for two cases. Firstly, assuming a 'dry' state (i.e. at natural moisture content) and then a saturated state. The slip analysis was restricted only to the saturated state. The dry case was not considered in the latter analysis because the results obtained from the elastic analysis confirmed that, saturation represents the worst case for settlement determination in a collapsible soil.

3.4.2 Parametric Equations:

3.4.2.1 Formulation of the settlement δ_1 and δ_2:

In the elastic analysis, the elastic settlement (δ_1) and the settlement (δ_2) due to downdrag, were obtained from equation (3.10) presented earlier. In the slip analysis, Eq. (3.5) was used to determine both components of settlement.

The displacement of the pile due to the settlement (S_l) of the layer situated beneath its tip, caused by inundation, was added. By assuming that the soil settlement varies linearly from S_0 at the surface to zero at the base (Fig.3.16), the settlement S_l was expressed as:

$$S_l = \frac{H - L}{H} S_0 \qquad (3.16)$$

where:

H: thickness of the collapsing layer,

L: length of the pile,

S_0: settlement of the top of the collapsing layer.

3.4.2.2 Formulation of the settlement δ_3:

The settlement of the granular columns due to lateral deformation, (δ_3), was determined in two ways:

Procedure 1: following the same procedure suggested by Hughes et al. (1974),

Procedure 2: applying the approach developed by Priebe (1976)

It was assumed, in both cases that :

- an uniform and a cylindrical deformation of the granular column occurred,
- a constant volume during settlement and expansion of each slice resulted,
- no significant change in the ratio of the vertical and horizontal stresses within the column.

i) Procedure 1:

By assuming an uniform and a cylindrical deformation of the column, the summation of contributions from discrete horizontal slices of the column proposed by Hughes et al and presented by Eq. (3.11) and (3.12) was re-written as:

$$\delta_v = n\delta_n$$

$$\delta_n = 2H_n\frac{\delta r_0}{r_0}$$

by putting, $H_0 = nH_n$, the vertical settlement was defined as:

$$\delta_v = 2H_0\frac{\delta r_0}{r_0}$$

where:

n: number of slices,

δ_n: settlement of the n^{th} slice,

H_n: length of the n^{th} slice,

$\delta r_0 / r_0$: radial strain in the column.

The radial strain $\delta r_0/r_0$ was estimated by assuming compatibility of lateral deformations between the column material and the cylinder fabric around it, and by considering plane strain conditions. The cylinder fabric, of thickness t and radius r_0, was subjected to an internal pressure ΔP as shown in Fig.3.17.

From equilibrium,

$$2r_0\Delta P = 2\sigma_\theta t$$

Therefore:

$$\sigma_\theta = \frac{\Delta P r_0}{t}$$

Where:

σ_θ: is the tangential stress.

But:

$$\sigma_\theta = E\varepsilon_\theta$$

so that the circumferential strain

$$\varepsilon_\theta = \frac{\Delta P r_0}{Et}$$

where, E is the Young's modulus of the material forming the cylinder.

Now

$$\varepsilon_\theta = \frac{2\pi(r_0 + \delta r_0) - 2\pi r_0}{2\pi r_0} = \frac{\delta r_0}{r_0} = \varepsilon_r$$

Hence, the radial strain is expressed as:

$$\varepsilon_r = \frac{\delta r_0}{r_0} = \frac{\Delta P r_0}{Et}$$

ii) Procedure 2:

The model developed by Priebe (1976), based on the concept of the unit cell, was used. The radial strain was given by Eq. (3.13) and the total settlement caused by radial deformation was obtained from Eq. (3.14). It is clear that both procedures are similar, the only difference is the determination of the radial strain. In procedure 2, the radial strain was taken directly from Priebe's model, whereas, in procedure 1 it was derived from compatibility in radial strains between the column material and the fabric. In the original model of Hughes et al., the radial strain was obtained by field measurement using the Cambridge pressuremeter.

3.4.2.3 General forms of the total settlement Δ:

The general forms of the total settlement are:

1- Elastic analysis using 'Poulos-modified Hughes' model:

$$\Delta = \frac{P_a L}{E_p A_p} + \frac{qd}{E_p A_p} I_\rho Q_T + 2\frac{\Delta P r_0}{Et} H_0$$

2- Elastic analysis using 'Poulos-Preibe' model:

$$\Delta = \frac{P_a L}{E_p A_p} + \frac{qd}{E_p A_p} I_\rho Q_T + 2\Delta P \frac{(1-\nu)}{E} \frac{(1-2\nu)(1-r_0^2/a^2)}{1-2\nu+r_0^2/a^2} H_0$$

3- Slip analysis using 'Poulos- modified Hughes' model:

$$\Delta = \frac{P_a L}{E_p A_p} + \frac{2qL^2 R_a}{E_p d}\left[c_a^{'} + K_s tan\phi_a^{'}\left(\frac{\gamma L}{3q}+1\right)\right] Q_R\, Q_T + 2\frac{\Delta P r_0}{Et} H_0$$

4- Slip analysis using 'Poulos-Preibe' model:

$$\Delta = \frac{P_a L}{E_p A_p} + \frac{2qL^2 R_a}{E_p d}\left[c_a^{'} + K_s tan\phi_a^{'}\left(\frac{\gamma L}{3q}+1\right)\right] Q_R\, Q_T$$
$$+2\Delta P\frac{(1-\nu)}{E}\frac{(1-2\nu)(1-r_0^2/a^2)}{1-2\nu+r_0^2/a^2} H_0$$

All the parameters were defined previously.

3.4.3 Data on Pile-Soil Parameters:

All the parameters needed for this analytical approach were estimated from the results of triaxial tests. The testing programme, equipment, testing procedures and results are described in chapter 4. A summary of these results is presented in Table 3.1. The modulii of elasticity of the different types of 'piles' (i.e. sand columns confined and not confined by geofabrics) were determined for three different confining pressures (40, 80 and 120 kPa). Details will be given in the next chapter (chapter 4).

The effects of two parameters on the behaviour of the granular columns or the piles were investigated. These parameters were:

1. The stiffness of the granular column or the pile (E_p),
2. The ratio L/d (i.e. the ratio of the length to the diameter of the granular column or the pile)

Six types of foundation support were used, a sand column, a sand column encapsulated by: T700, T1000, T1500, or T2000, and a rigid pile. Beside, three

different lengths were adopted 250 mm, 300 mm, and 410 mm. Details are given in Chapter 6.

A small computer program , using the Fortan language (see Appendix B), was written to estimate the total settlement and hence the settlement reduction factor defined as:

$$\beta = \frac{S_i}{S_0}$$

where:

S_i: settlement of the treated foundation,

S_0: settlement of the untreated foundation.

A design example is described in Appendix C which shows how the theory is used.

3.4.4 Interpretation of the Predicted Results:

The total settlement for various values of (E_p) and (L/d) was calculated for three working loads expressed as fractions of the ultimate load (20%, 50%, and 80%). The values of all the ultimate loads are given in Chapter 7. The settlement reduction factors (β) were then estimated and the influence of the two principal parameters (E_p) and(L/d) on the settlement behaviour of the piles was investigated. Only the resulting curves obtained for the different values of (E_p), determined under a cell pressure equal to 40 KPa, will be presented and discussed. The other curves, which correspond to the different values of (E_p) determined under the cell pressures 80 KPa and 120 KPa, are similar in shape and different only in the magnitude of *beta*.

3.4.4.1 Effects of Pile-Stiffness on the Settlement Behaviour:

The effects of pile-rigidity on the settlement behaviour are shown in Figs 3.18 to 3.26 where the settlements are plotted in terms of a reduction factor(β). It was found that this method of expressing the reduced settlement enabled comparisons to be made simply between prediction and measured results.

Each figure represents the reduction in vertical compression as a function of pile-stiffness. It shows the results computed, using both analyses (elastic and slip analyses), for different types of pile of a given length at a given working load.

All the results were estimated by using both approaches described previously and which differentiate only on the way of estimating the third component of settlement (δ_3). However, only those obtained by the slip analysis are plotted in these figures.

By investigating all the curves of all the figures it was concluded that the settlement of a pile decreases as its stiffness increases. For relatively small values of E_p, the reduction in settlement is remarkable as E_p increases. But for large values, the reduction is small. This may be explained by separating the three component of settlement. It was noticed that the settlement caused by lateral deformation has a great influence on the settlement behaviour of the piles. As E_p increases, the settlement caused by lateral deformation(δ_3) decreases rapidly up to a certain value. After that the piles begin to behave as relatively incompressible in respect to the soil and the effect of this part of the settlement on the total settlement is insignificant. This observation was strongly supported by the works of Poulos & Davies (1968), Mattes & Poulos (1969), Mattes (1969) in which they concluded that, for piles of high stiffness, although they may be considered as compressible in respect to the surrounding soil, the radial strains are neglected.

Another cause is the expressions given to estimate the settlement δ_1 and

δ_2. These two components of the total settlement are inversely proportional to the pile-stiffness E_p. Therefore, increasing the theoretical stiffness from $E_p = 0$ to $E_p = \infty$ results in a decrease in settlement which is characterized by two stages, of different rates, defined by the nature of the relationship settlement-stiffness (see Eq. 3.5 and Eq. 3.10).

In general, the analyses show that, for a given pile (i.e. a pile of given length and stiffness), the settlement predicted at any given working load using the elastic analysis is smaller than that computed by using the slip analysis. The difference is significant for small values of E_p but small for larger values. The main cause is the difference between the settlement caused by downdrag considered in both analyses since all the other components are similar.

Comparing the results obtained using the elastic analysis and taking the soil parameters in the 'dry' and the saturated states, it was noticed that there are slight differences between the two cases. This is mainly due to the pile parameters (i.e. modulii of elasticity) which were taken the same for both cases. They were determined for saturated conditions.

Finally, there is no significant difference between the Poulos-Hughes and Poulos-Priebe approaches and in general there is a good agreement between the results of the two approches leading to a variety of use. The establishment and the choice of the best depends on the experimental results.

3.4.4.2 Effects of the Pile-Length on the Settlement Behaviour:

In a similar manner, the effect of the pile-length on the settlement behaviour was investigated. The results of the elastic analysis using the saturated parameters and

the slip analysis using Poulos-Hughes's approach were re-plotted differently in Figs 3.27 to 3.32. These figures show the variation of the reduction factor (β) with length for any value of stiffness (E_p) and at any working load. As was expected, the settlement of the pile decreased as the length increased. The rate of decrease between the lengths 300 mm and 410 mm is more rapid than that between 250 mm and 300 mm. This was principally due to the decrease of the additional settlement (S_l) of the layer situated beneath the tip of the pile and caused by inundation. S_l is proportional to the length(see Eq. 3.16).

3.5 Conclusion:

The analytical solution adopted for this investigation was derived from models developed for compressible piles and stone columns in soft soils. It consisted of simple parametric equations convenient for hand calculations.

The total settlement was divided into three parts:

1. The elastic settlement due to load P,
2. The settlement caused by downdrag,
3. The settlement due to lateral deformation in the column.

The first two components were computed by using the Poulos and Davis (1975) model. The third component was estimated in two different ways. Firstly, by a modified Hughes et al. (1974) model and then by using the model of Priebe (1976). Both models were developed for stone columns.

The results predicted by using two different types of analysis (elastic and

considering pile-soil slip) led to the following conclusions:

1. The settlement of a 'pile' at a given working load, expressed as a fraction of the ultimate load, decreased as its stiffness (E_p) increased.

2. As the ratio (L/d) increased, the settlement of the top of the pile decreased.

3. The settlements predicted by considering pile-soil slip were larger than those computed using the elastic analysis.

General Parameters:					
q = 100 k Pa					
d = 23 mm					
$R_A = 1$					
$A_p = \pi d^2/4$					
P_a = 20%, 50% and 80% of P_u					
L = 250 mm, 300 mm and 410 mm					
ρ_d = 1.54 Mg/m^3					
Soil Deformation Parameters:					
E_s ('dry' state) = 3600 k Pa					
E_s (saturated state) = 2900 k Pa					
$\nu = 0.3$					
$\varphi_a' = 34.8°$					
$C_a' = 0$					
'Pile' Deformation Parameters E_p (k Pa):					
Confining Presure	Type of Confinement				
	LBS (alone)	T700	T1000	T1500	T2000
40 (kPa)	18980	36300	45100	55660	73060
80 (kPa)	28760	55030	68360	84370	110730
120 (kPa)	36685	70190	87185	107605	141230

Table 3.1 'Pile'-Soil Parameters used in Test Data Evaluation

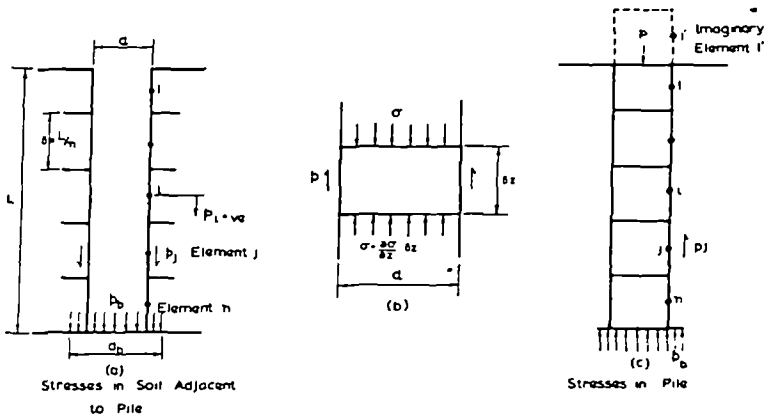

Fig. 3.1 Stresses Associated With Pile (Poulos et al., 1968)

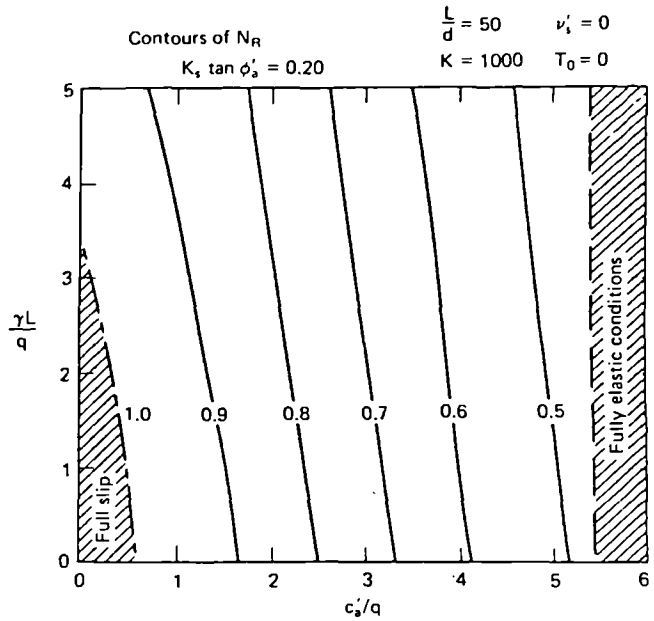

Fig. 3.2-a Values of Downdrag Reduction Factor N_R. ($K_s tan\phi'_a = 0.20$) (Poulos et al., 1980)

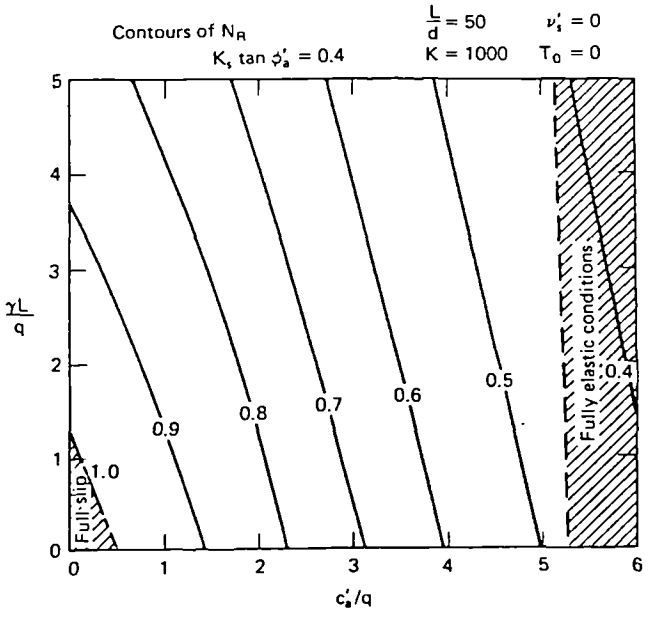

Fig. 3.2-b Values of Downdrag Reduction Factor N_R. ($K_s tan\phi'_a = 0.40$) (Poulos et al., 1980)

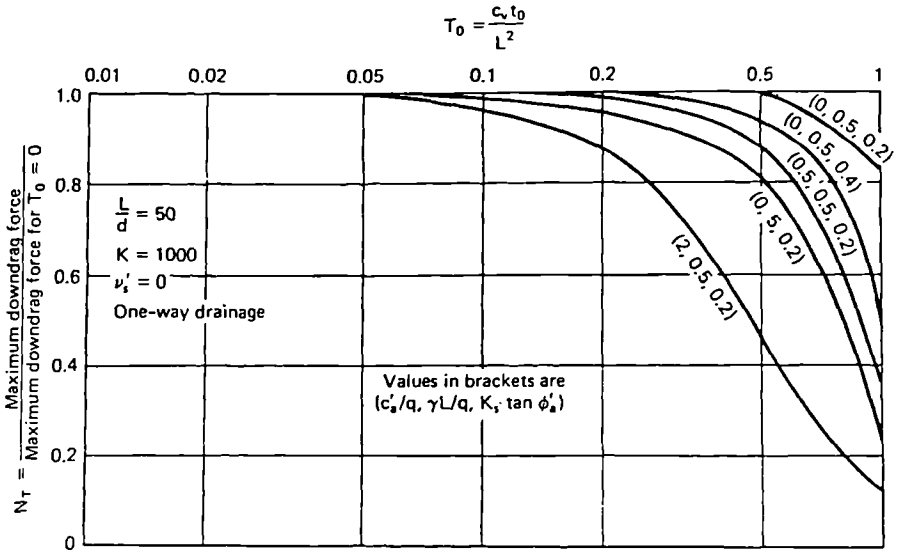

Fig. 3.3-a Downdrag Reduction Factor N_T -One-Way Drainage (Poulos et al., 1980)

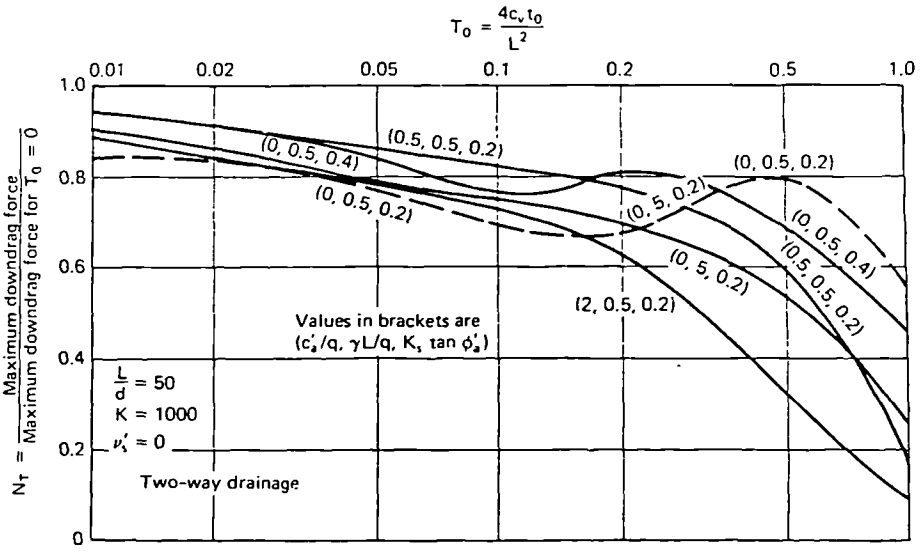

Fig. 3.3-b Downdrag Reduction Factor N_T -Two-Way Drainage (Poulos et al., 1980)

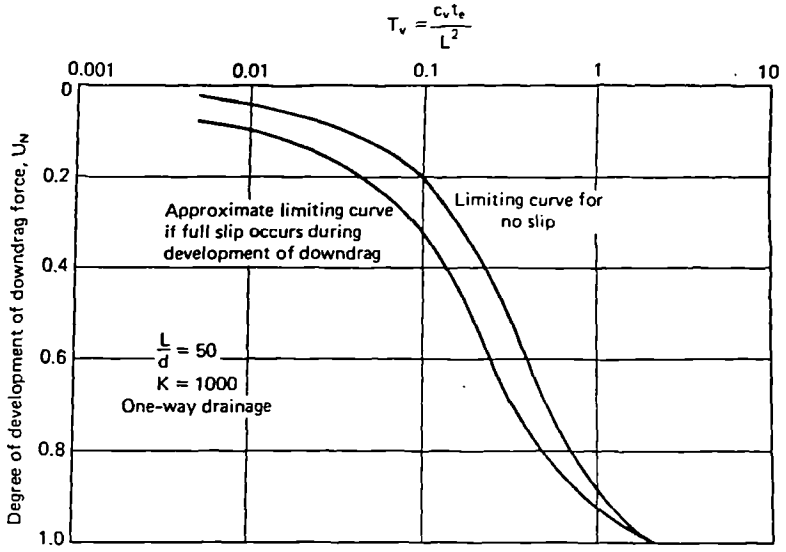

Fig. 3.4 Rate of Development of Downdrag Force -One-Way Drainage (Poulos et al., 1980)

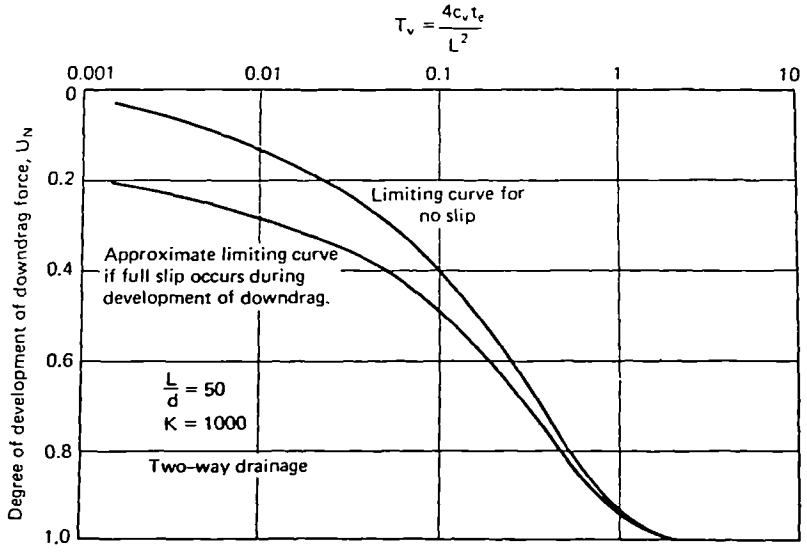

Fig. 3.5 Rate of Development of Downdrag Force -Two-Way Drainage (Poulos et al., 1980)

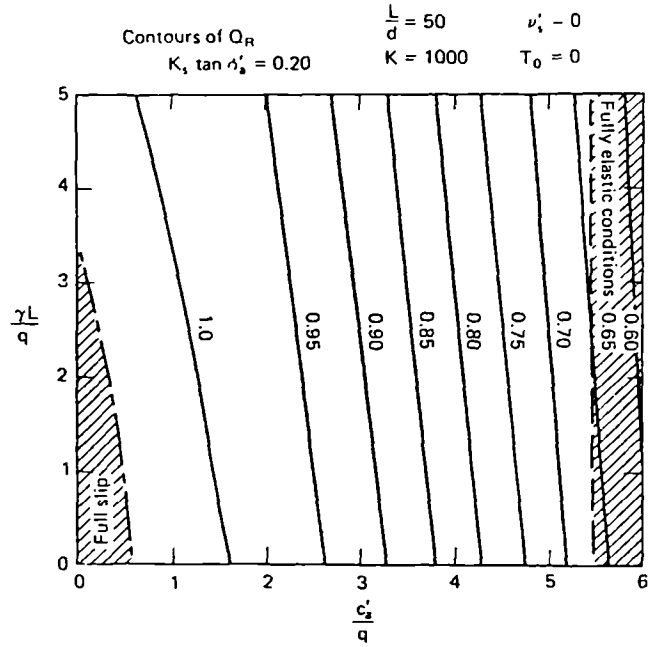

Fig. 3.6-a Value of Deflection Reduction Factor Q_R. ($K_s tan\phi'_a = 0.20$) (Poulos et al., 1980)

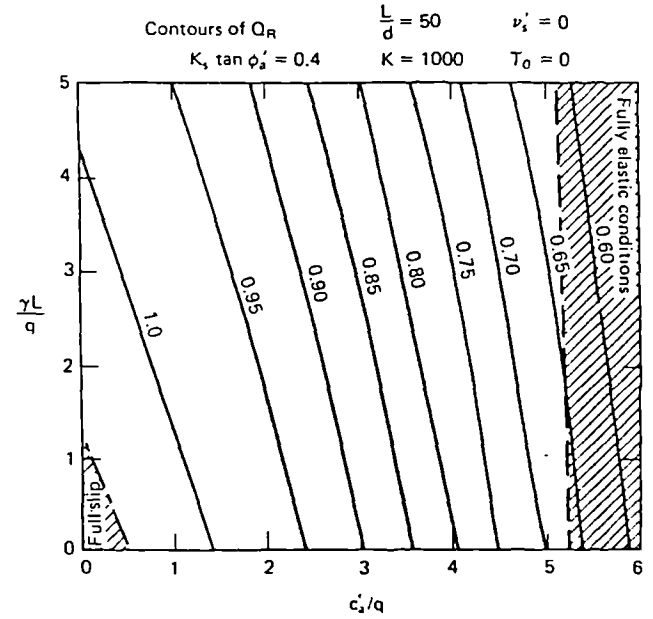

Fig. 3.6-b Values of Deflection Reduction Factor Q_R. ($K_s tan\phi'_a = 0.40$) (Poulos et al., 1980)

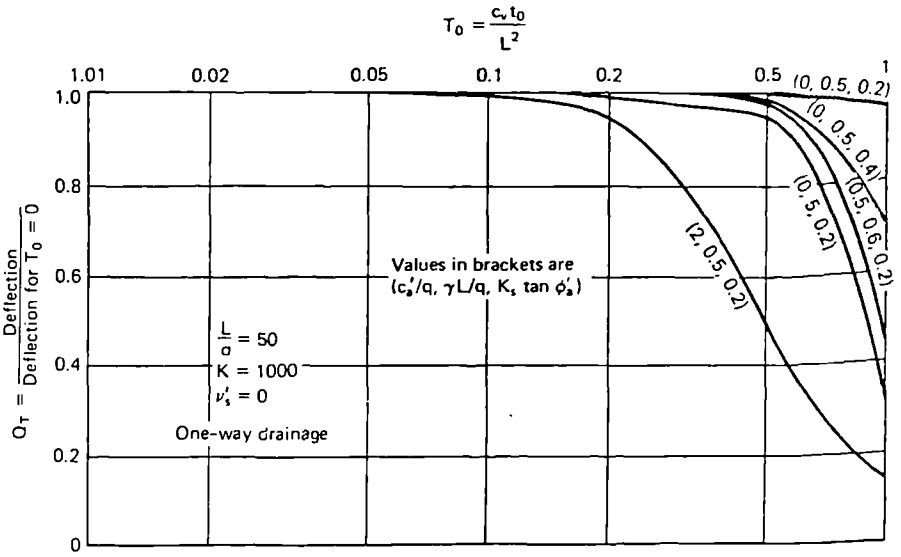

Fig. 3.7-a Deflection Reduction Factor Q_T One-Way Drainage (Poulos et al., 1980)

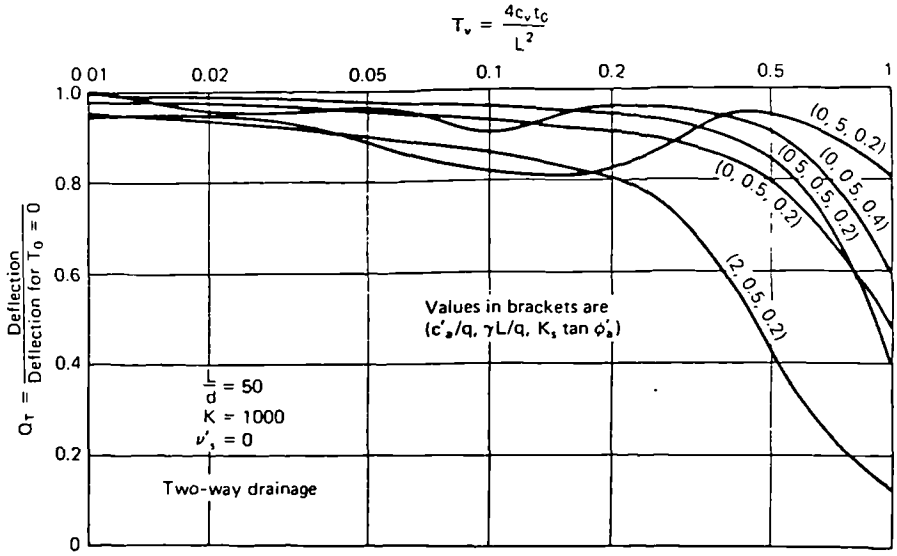

Fig. 3.7-b Deflection Reduction Factor Q_T Two-Way Drainage (Poulos et al., 1980)

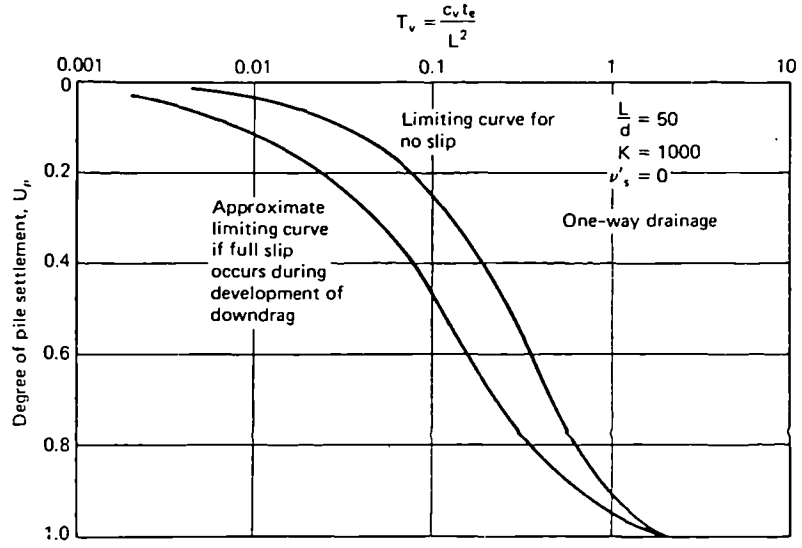

Fig. 3.8-a Degree of Pile Settlement vs. Time -One-Way Drainage (Poulos et al., 1980)

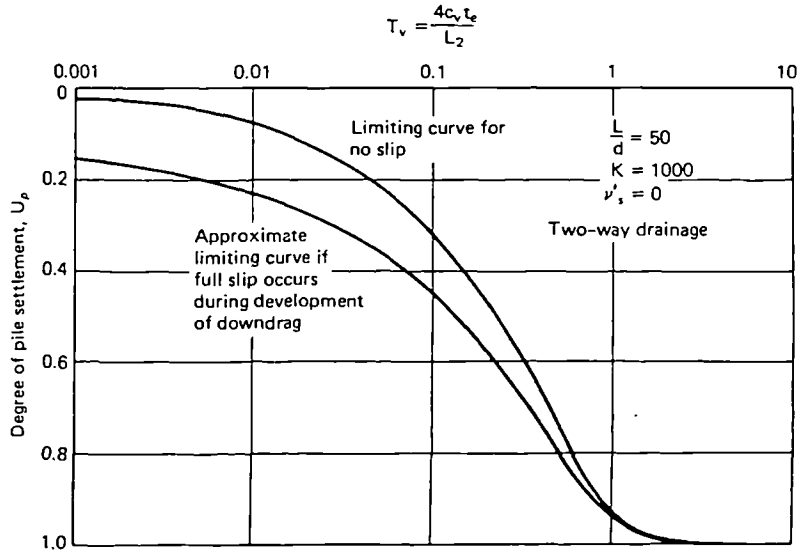

Fig. 3.8-b Degree of Pile Settlement vs. Time Factor Two-Way Drainage (Poulos et al., 1980)

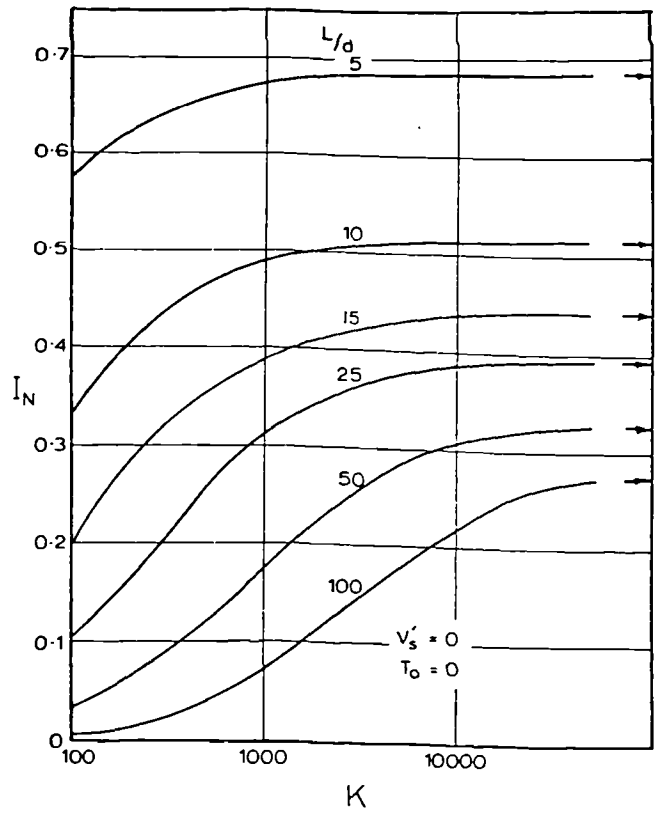

Fig. 3.9 Influence Factors for Final Downdrag at Pile Tip -Elastic Analysis (Poulos et al., 1980)

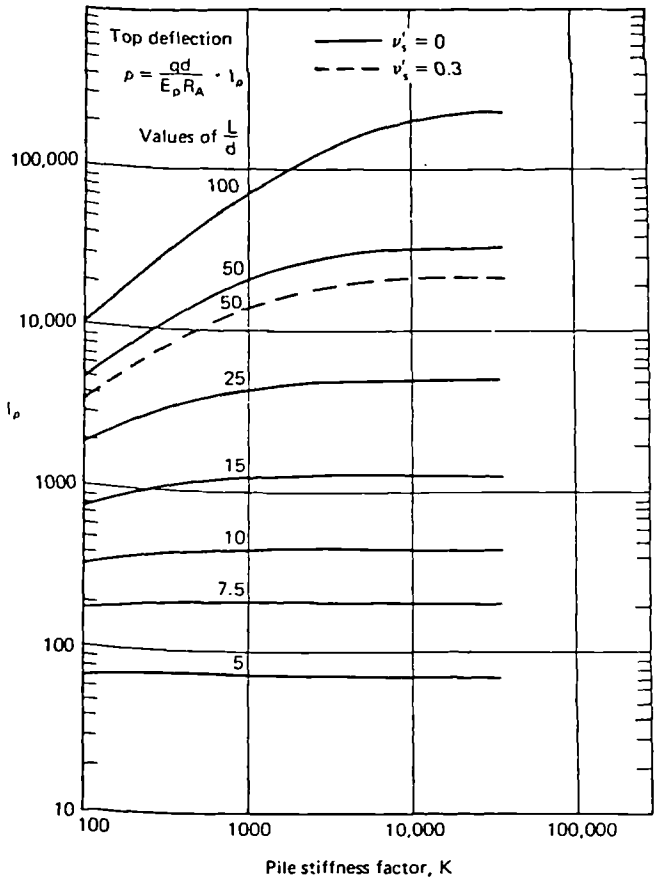

Fig. 3.10 Elastic Solutions for Top Deflection of Pile (Poulos et al., 1980)

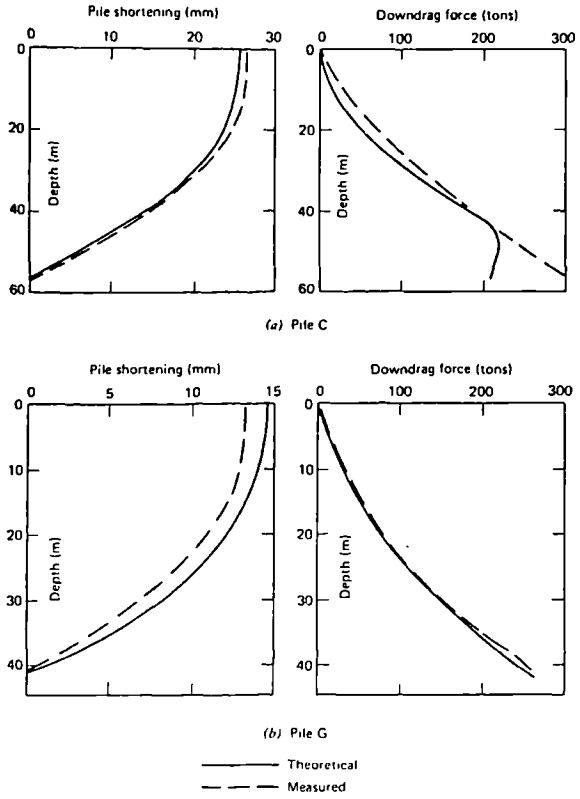

Fig. 3.11 Comparison with pile tests of Bjerrum et al. (1969) at Sorenya (Poulos et al., 1975)

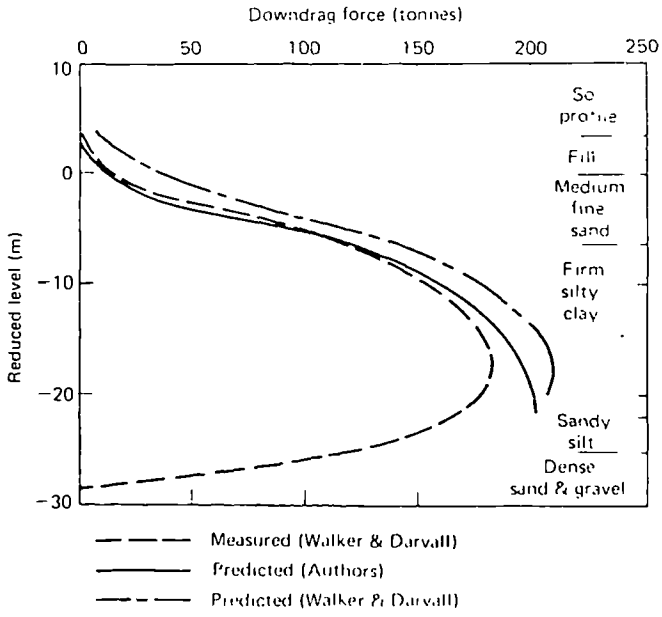

Fig. 3.12 Comparison with pile tests of Walker and Darvall (1973) (Poulos et al., 1975)

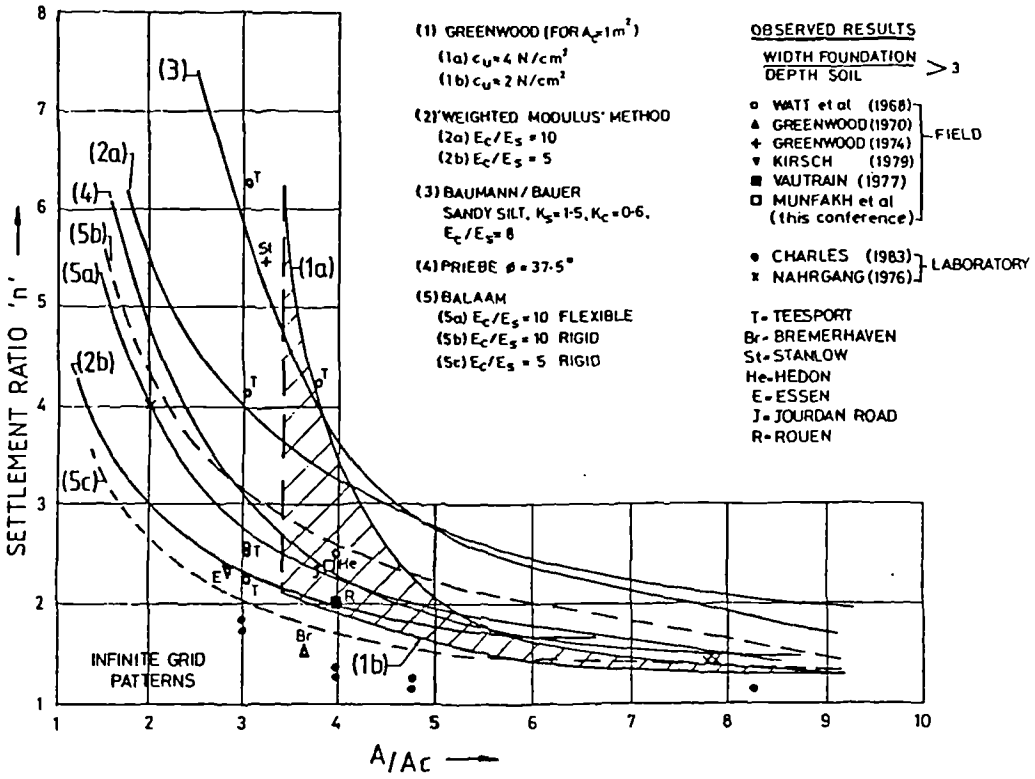

Fig. 3.13 Comparison of Elastic Theories and Field Observations (Greenwood et al., 1984)

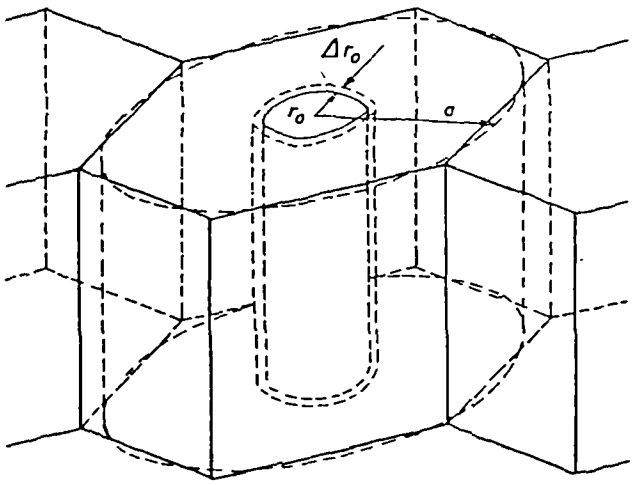

Fig. 3.14 Concept of the Unit Cell (Priebe, 1976)

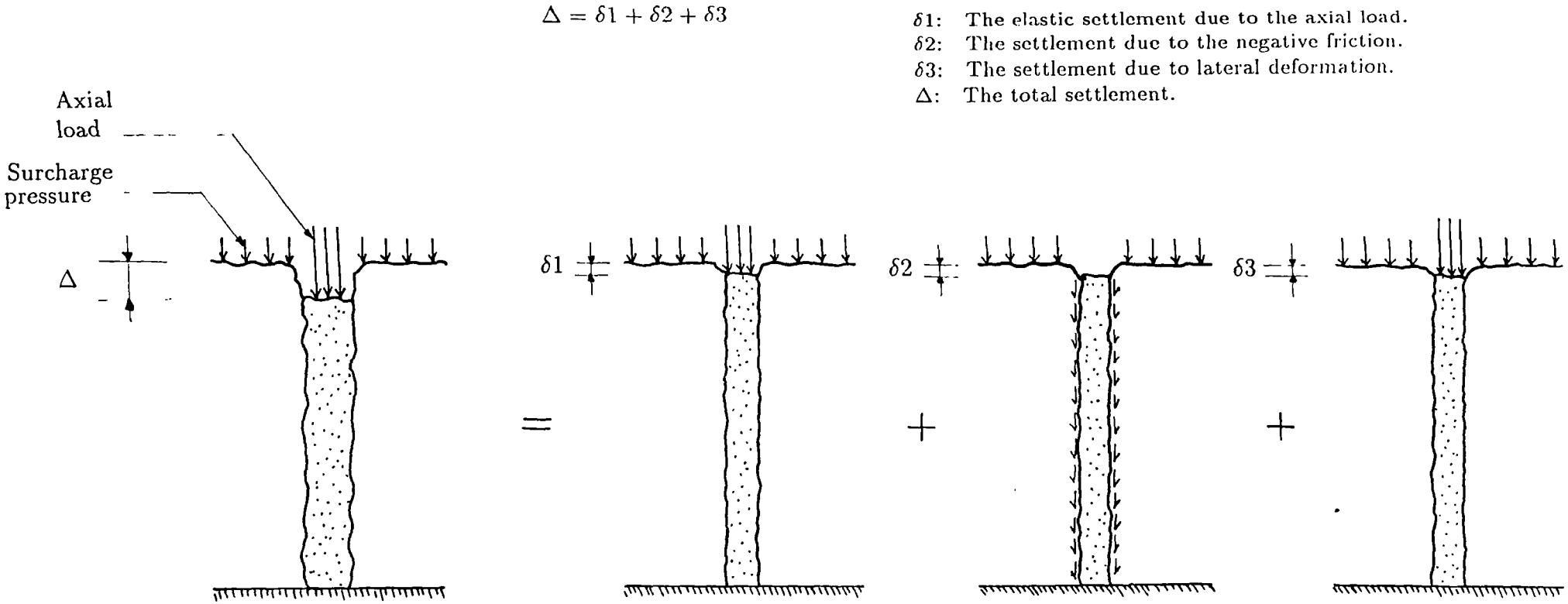

Fig. 3.15 Principle of 'Pile' Settlement in a Collapsible Soil Subjected to Inundation

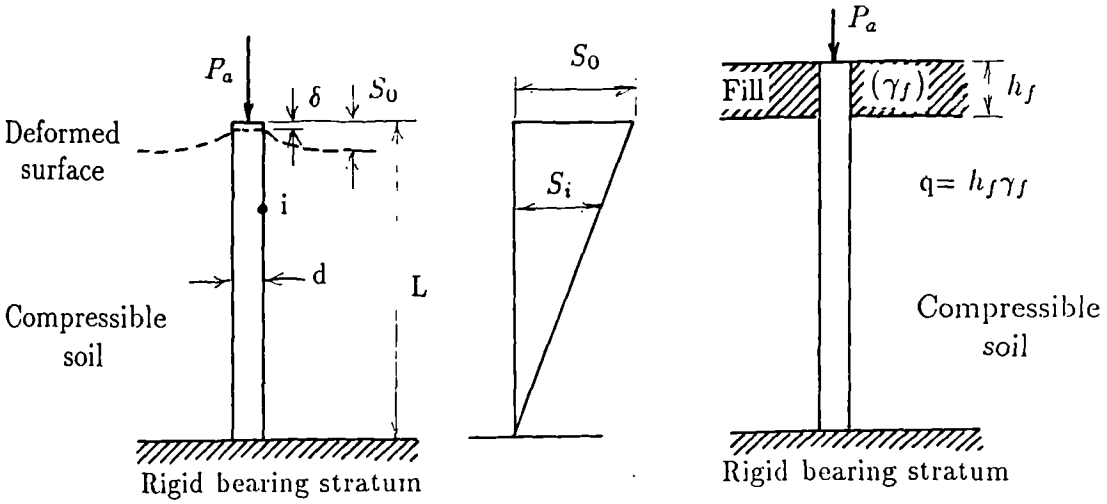

Fig. 3.16 Assumption of Soil Settlement Variation with Depth

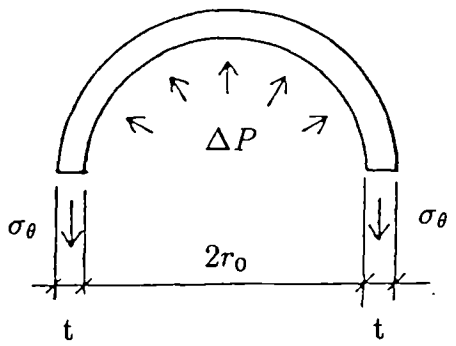

Fig. 3.17 Forces Acting on the Wall of a Cylinder Subjected to an Internal Pressure ΔP

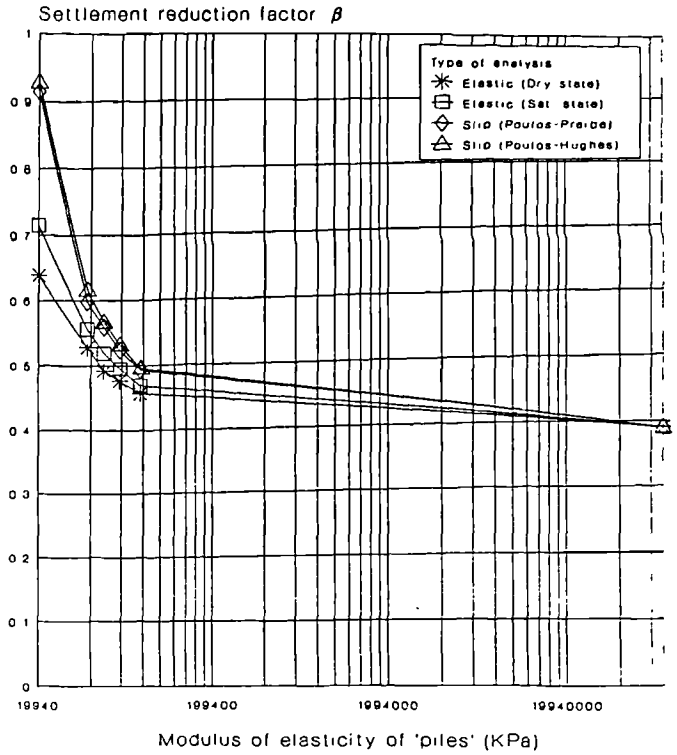

Fig. 3.18 **Reduction in vertical compression as a function of 'pile'-stiffness. (for L = 250mm and an applied load = 20% P_u)**

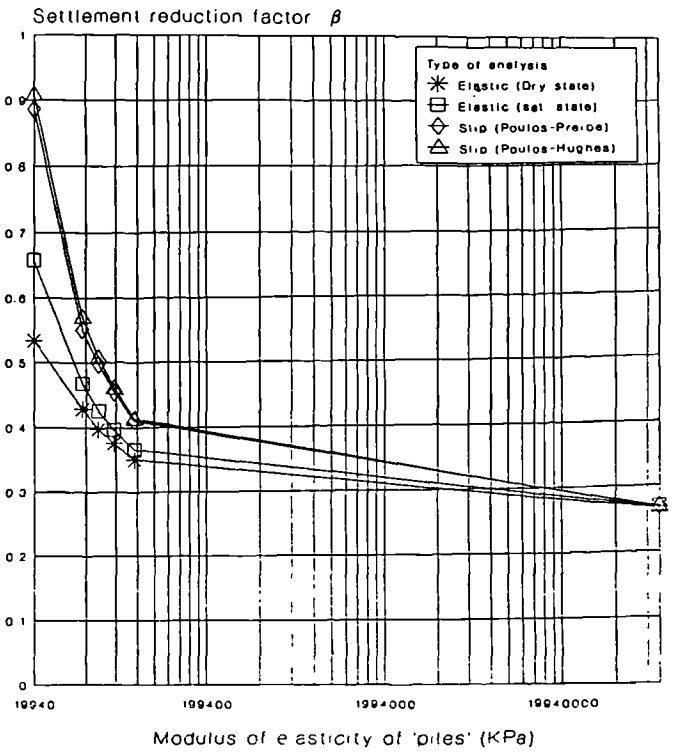

Fig. 3.19 **Reduction in vertical compression as a function of 'pile'-stiffness. (for L = 300 mm and an applied load = 20% P_u)**

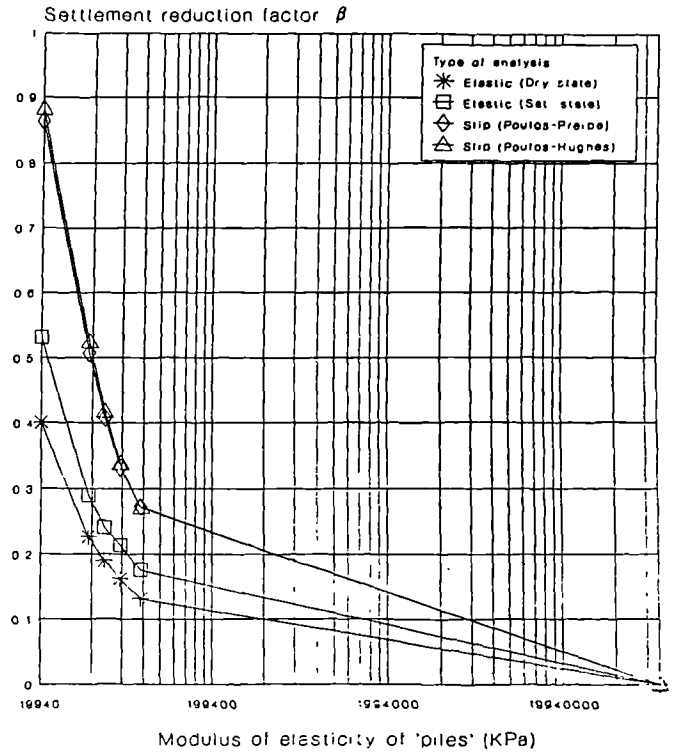

Fig. 3.20 Reduction in vertical compression as a function of 'pile'-stiffness. (for L = 410 mm and an applied load = 20% P_u)

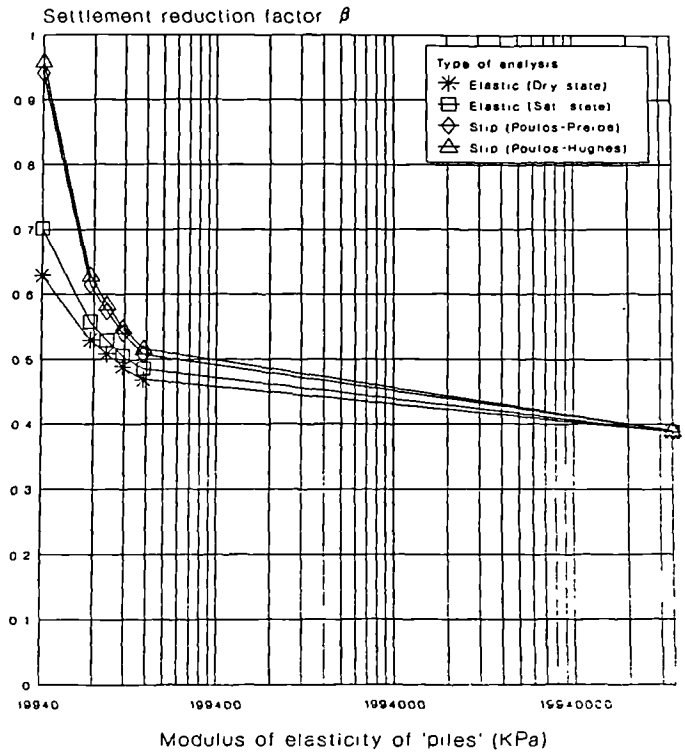

Fig. 3.21 Reduction in vertical compression as a function of 'pile'-stiffness. (for L = 250 mm and an applied load = 50% P_u)

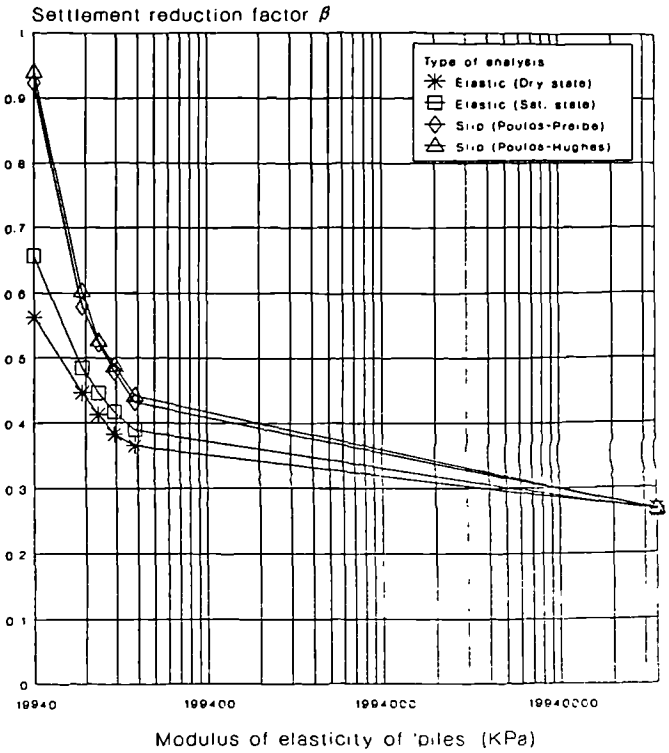

Fig. 3.22 **Reduction in vertical compression as a function of 'pile'-stiffness. (for L = 300 mm and an applied load = 50% P_u)**

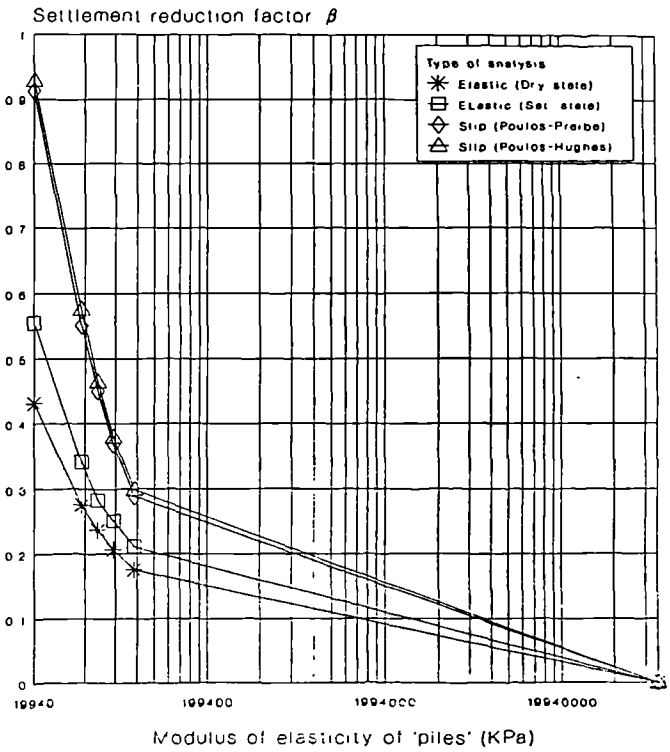

Fig. 3.23 **Reduction in vertical compression as a function of 'pile'-stiffness. (for L = 410 mm and an applied load = 50% P_u)**

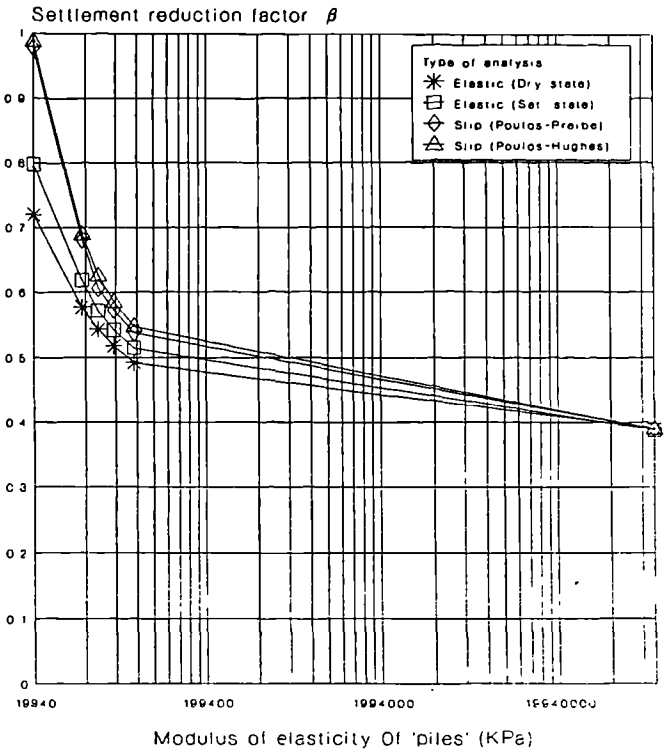

Fig. 3.24 **Reduction in vertical compression as a function of 'pile'-stiffness. (for L = 250 mm and an applied load = 80% P_u)**

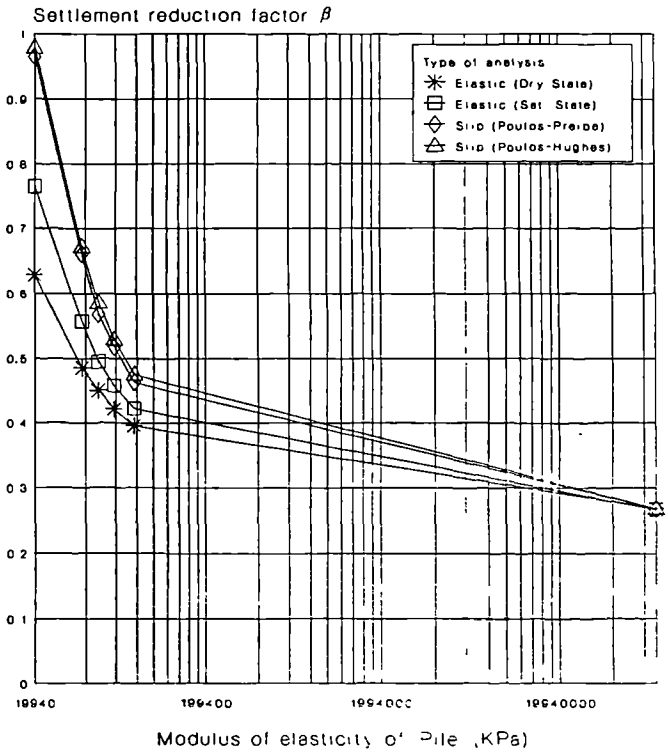

Fig. 3.25 **Reduction in vertical compression as a function of 'pile'-stiffness. (for L = 300 mm and an applied load = 80% P_u)**

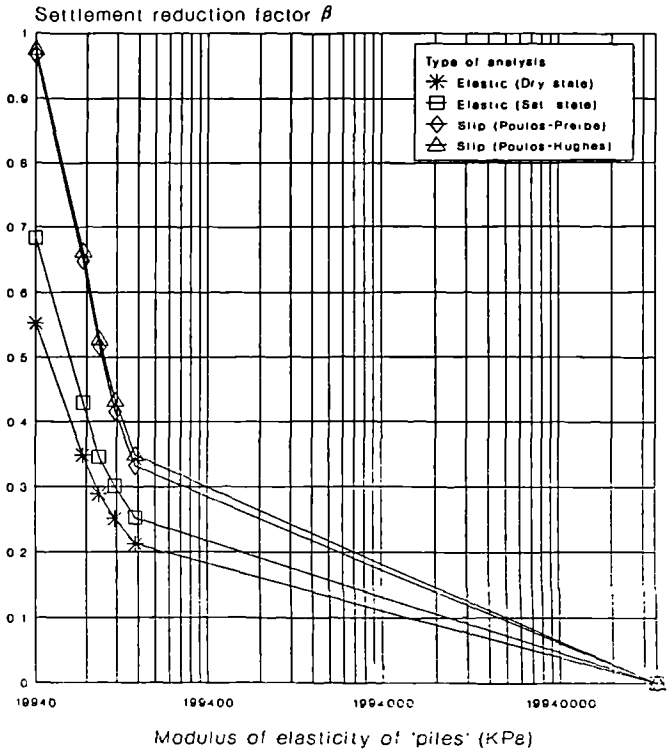

Fig. 3.26 **Reduction in vertical compression as a function of 'pile'-stiffness. (for L = 410 mm and an applied load = 80% P_u)**

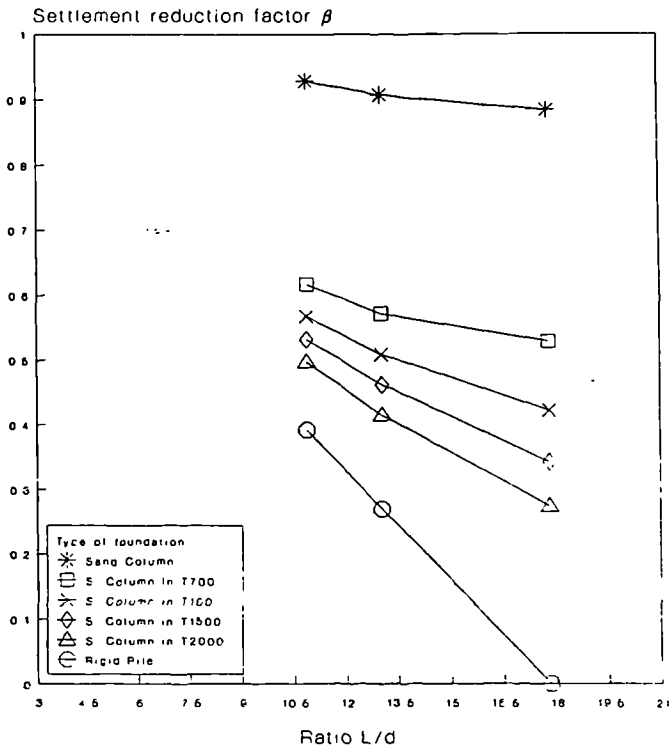

Fig. 3.27 **Reduction in vertical compression as a function of 'pile'-length for an applied load = 20% P_u (slip analysis).**

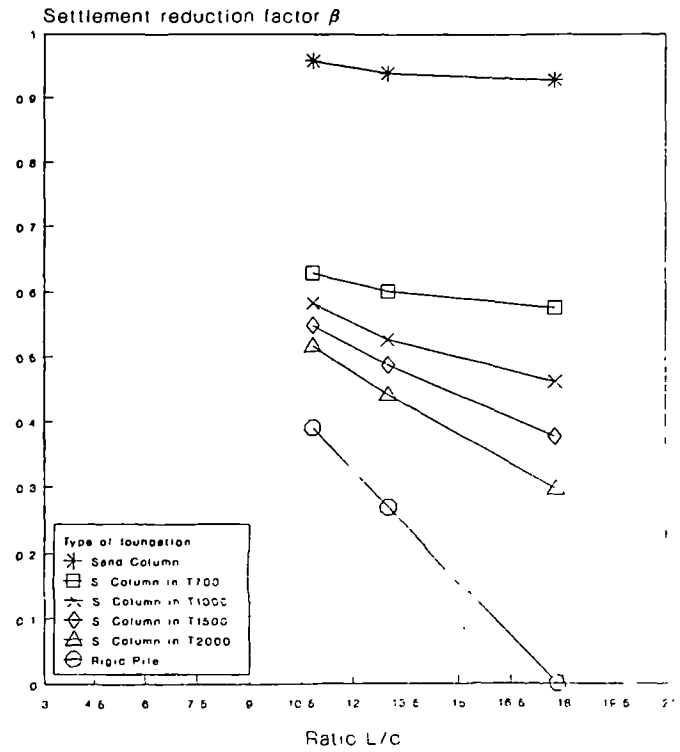

Fig. 3.28 Reduction in vertical compression as a function of 'pile'-length for an applied load = 50% P_v (slip analysis).

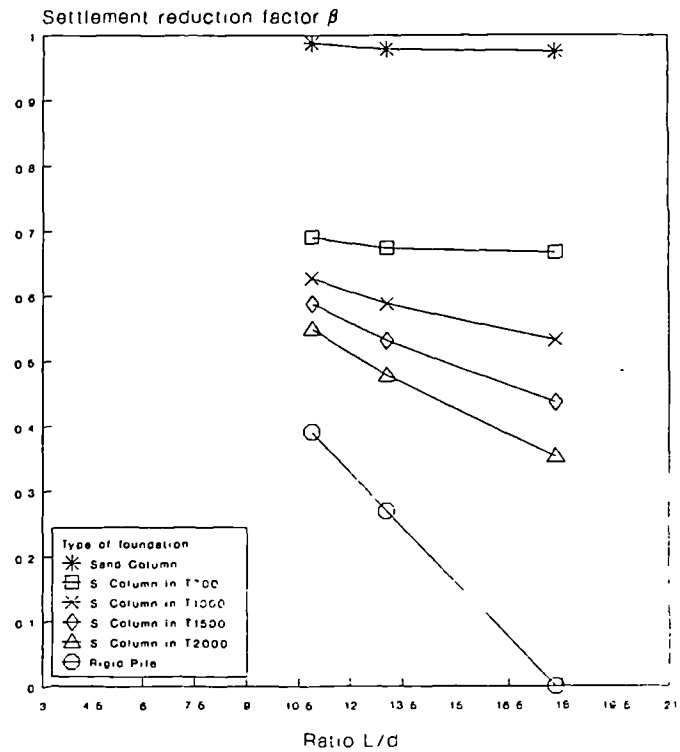

Fig. 3.29 Reduction in vertical compression as a function of 'pile'-length for an applied load = 80% P_v (slip analysis).

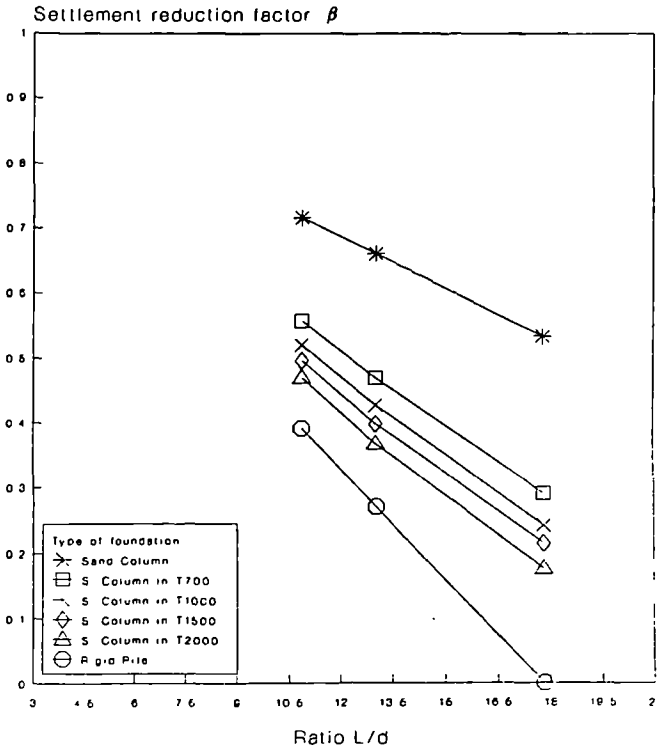

Fig. 3.30 **Reduction in vertical compression as a function of 'pile'-length for an applied load = 20% P_u (elastic analysis).**

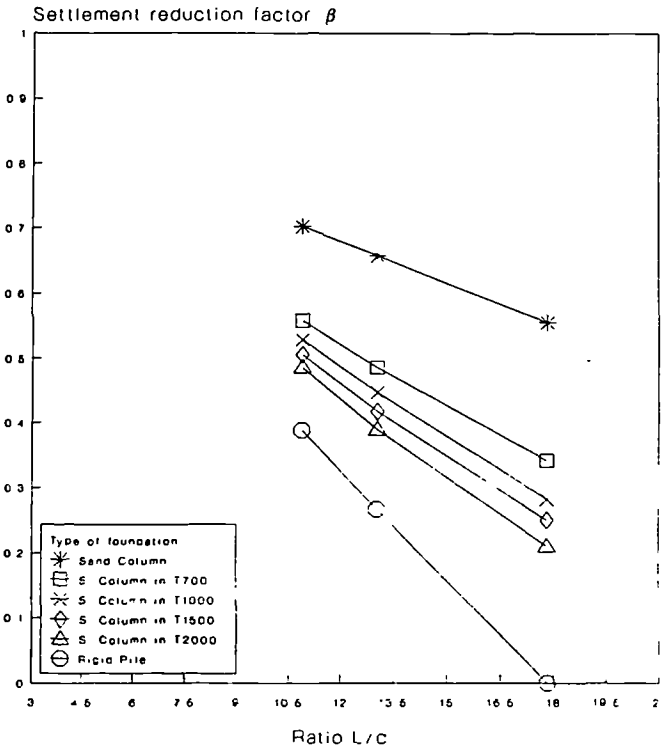

Fig. 3.31 **Reduction in vertical compression as a function of 'pile'-length for an applied load = 50% P_u (elastic analysis).**

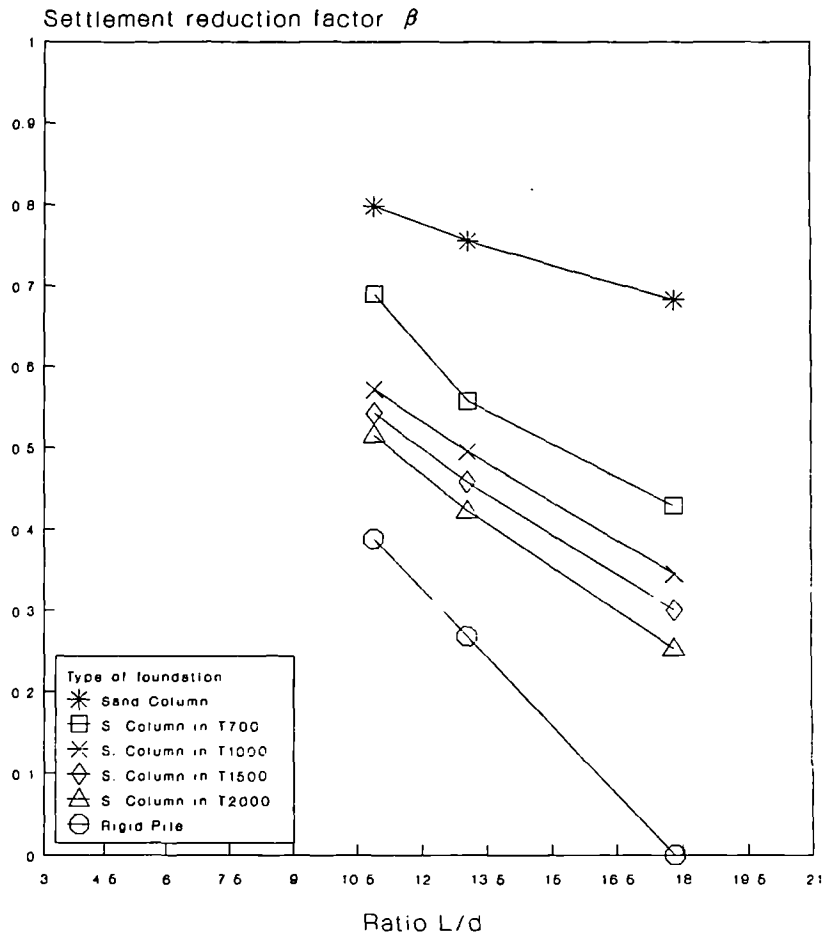

Fig. 3.32 **Reduction in vertical compression as a function of 'pile'-length for an applied load = 80% P_u (elastic analysis).**

Chapter 4

Determination of Pile-Soil Parameters Used in Test Data Evaluation

4.1 General:

The application of the theoretical solutions described in chapter 3 to practical problems generally requires knowlege of appropriate values of the soil and pile deformation parameters. Accurate determination of these parameters is difficult to achieve in routine triaxial testing. Conventionally, the determination of the axial strain of a triaxial sample is based on external measurement of displacement which includes a number of extraneous movements. The more important sources of error are illustrated in Fig. 4.1. Some of the deflexions shown in this figure may be quantified by careful calibration, but large unaccountable errors remain due to:

1. The difficulty of trimming a sample so that the end faces are perpendicular to the vertical axis of symmetry.

2. Play in the connection between the load cell and the sample top cap, and

3. The inevitable 'bedding down' at the ends of the sample, due to local surface irregularities or voids.

The importance of such errors has long been recognized and many diverse techniques have been employed in attempts to impove strain measurement. One solution has been to use a sample-mounted gauge to measure deformation locally over a certain length of the sample. Some devices of this type are submersible displacement transducers (Brown and Snaith, 1974; Royce and Brown, 1976; Yuen et al. 1978; Daramola, 1978; Brown et al., 1980 ; Costa Filho, 1980; Maswoswe, 1985); electrolevel gauges (Burland and Symes, 1982; Jardine, Symes and Burland, 1984); and the Demec strain gauges (Clayton and Khatrush, 1986).

Other techniques have been employed in attempts to improve strain measurement (e.g. X-ray and optical methods used by Roscoe et al., 1963; and Arthur et al., 1975). However, when dealing with relatively larger strains (e.g. exceeding 0.5%), the simplest improved method to reduce the effect of these errors is to apply two or three load-unload cycles to the sample during the testing stage (Head, 1982; Gorle et al., 1989). The Young's modulus is derived only from the second or subsequent loading curves (Fig. 4.2).

In the present work, the latter technique was used in order to determine the moduli of elasticity of the stone column unconfined and confined by a fabric. In this chapter, the equipment and techniques used to perform these tests are described and the results obtained are presented and discussed.

4.2 Triaxial Test Equipment and Instrumentation:

4.2.1 General:

The purpose of this section is to describe in detail the triaxial test equipment and the instrumentation used. The triaxial cell used is shown in Figure 4.3. The cell was of a conventional design, as originally described by Bishop and Henkel (1962). The back pressure and cell pressure were connected to air-water cylinders. The pressure source was compressed air connected to each cylinder via a regulator. This assembly could easily compensate for changes in the sample size during saturation and consolidation and for leakage, if any, of the cell fluid. The pressure cylinders were regularly filled with de-aired water to encourage any air remaining in the pressure lines to go into solution at high pressures. The cell had an extended loading ram fitted with an internal load cell.

4.2.2 The Loading System:

The requirements of the tests and the need for mechanical simplicity lead to the use of a controlled stress system. The equipment needed for setting up this system was first assembled by Gunawan (1978) for liquefaction testing. As discussed by Gunawan, the design of a dead weight loading device centres on three main considerations:

1. Simplicity of the loading mechanism,
2. Suitable load magnification, to avoid excessive shifting and difficult manoeuvering of heavy weights (which could cause some disturbance to the samples when the loads are applied).

3. Provision of a suitably damped load arrestor to avoid damage to the top of the cell, as well as the floor, as the load falls following collapse. On the basis of these consideration a dead weight loading system with 3:1 lever arm was designed.

Figure 4.3, shows the general arrangement of the loading system which was *designed* by Gunawan to fit onto an existing portal frame.
The maximum axial load on the specimen was estimated to be 885 kgf (8850 N) and corresponded to 295 kgf (2950 N) of applied dead load which was readily available in the form of standard weights and lead shot.
The load was transfered from the lever to the top of the cell by a hanger. The lever arm was made from duralumin alloy bar, 25 mm × 50 mm × 900 mm long, with one end supported from the column of the frame by means of a ball race bearing. Counter-weights to balance the weight of the lever arm, the hanger, and the container for weights, totalling about 25 kg, were applied via a flexible steel cable passing over two pulleys. The effect of the torque reduction was investigated by Gunawan (1978) and was considered negligible.

The load arresting system considered was a 50 mm thich pad of rubber foam resting on top of a wooden base.

4.2.3 Instrumentation:

A summary of the instrumentation; together with the results of calibration and estimated precisions is given in Table 4.1. The calibration factors were kept the same through the investigation, because it involved only a few months of testing.

4.1.3.1 Load cell:

The load cell employed for load measurements was an Imperial College type. The principles of its design has been described by El-Ruwayih (1975).
The load cell had a capacity of 27 kN and it was calibrated under dead weight. Three calibration runs involving loading and unloading under an increment of 10 kg were made. The results were analysed using a computer programme based on the least squares line fitting method. Finally, an average calibration factor was calculated.

4.1.3.2 Displacement Transducer:

To measure the vertical displacement of the triaxial samples, a linear variable differential transformer (LVDT) of a range of 50 mm was used. This was supplied by Novatech measurements Ltd, East Sussex, England.
The calibration data were collected and analysed in much the same way as that of the load cell.
A vernier calibrator with a resolution of 0.002 mm/division was used to record the reading of each 1 mm increment.

4.1.3.3 Pressure Transducers:

The pressure transducers employed were manufactured by Druck Ltd, Leicester, England. They were used to measure the cell pressure and the pore water pressure. Their description and capability of detecting rapid changes in pore pressure which take place during a rapid settlement, were discussed by Hassona (1986).
The calibration was carried out by subjecting the transducers to hydrostatic pressure in the triaxial cell. The pressure was increased in 50 kN/m^2 steps up to the maximum pressure the transducer was expected to experience (600 kN/m^2).

4.1.3.4 Automatic Volume Change Unit:

The automatic volume change units available are those developed at Imperial College of a capacity of 100 cm^3 each. However, an arrangement which enables a reversing valve to be provided for instant reversal of flow through the unit was considered. The reversing valve is to be used when the limit of travel is approached.

The automatic volume change unit is shown in Figure 4.4. It consists of a hollow brass cylinder containing bellofram rolling seals at the top and bottom attached to a 'floating' frictionless piston. The movement of the piston caused by the water flowing into or out of the top chamber, sealed by one bellofram, being measured by a displacement transducer mounted on the outside of the cylinder. An equal amount of fluid is transferred to or from the lower chamber.

Before being calibrated, the transducer was subjected to the maximum pressure and the piston was allowed to move over its full range for few times to ensure that the bellofram seals were properly seated. Air was removed from the device through the bleed valve.

The calibration was carried out under a pressure of about 300 kN/m^2. The movement of the piston of the volume change transducer was controlled by maintaining a difference of 10 kN/m^2 between the two pressure controllers. Readings of piston displacement were taken for each 5 cm^3 volume of water passed through the device.

To obtain a precise calibration, pressure/volume controllers manufactured by Geotechnical Digital System Ltd., Egham, Surrey, England, were used. These controllers are capable of measuring changes in volume with a resolution of 1.0 mm^3. Each end of the volume change device was connected to a controller.

4.1.3.5 The Lateral Strain Indicator:

The lateral strain indicator used is illustrated in Figure 4.5. The relative movement of two curved perspex pads which bear lightly on the surface of the sample was magnified by a linear variable differential transformer mounted on the opposite side of a spring-loaded hinge.

The transducer used is shown in Plate 4.1. It is an AC-LVDT manufactured by Sangamo, Sussex with a sensitivity of 76 mV/V/mm.

To transform its signal to a DC signal, the LVDT was mounted to a D7 signal conditioning module, manufactured by RDP Electronics Ltd, Wolverhampton which was connected to a volt-meter and a digital converter.

The calibration of this transducer was carried out using the same equipment and technique as that used for the displacement transducer. Displacement increments of 0.5 mm were applied up to a maximum displacement of 10 mm. The tolerance was taken to be 0.005 mm.

4.1.3.6 Data Acquisition System:

The use of a microcomputer based data acquisition system is becoming common in Geotechnical laboratories, e.g. Atkinson et al (1985). One of its advantages is recording automatically the changes in the dimensions of the sample, the pore water pressure, axial loads, volume changes, etc. This is achieved by connecting the output leads of the measuring devices to the scanner unit of a data logging (acquisition) system.

4.1.3.6.1 The Apple IIe computer:

In the present work the apple IIe microcomputer had connected to it an IEEE-488 standard interface card. Suitable programs have been developed by the technical

staff at the University of Sheffield to control the logging sequence and an additional hardware (i.e. a real-time clock) was interfaced to the microcomputer which can be used to control the rate of scanning.

4.1.3.6.2 Analogue to Digital Converter:

The output from electrical transducers (usually in the form of an electrical analogue e.g. millivolts) cannot usually be connected directly to the micro as most require input in digital form. For this reason, an analogue to digital converter manufactured by M.C. Computers Ltd. Newbury, Berkshire, England (refer. MCCL 2014) was employed. It is a 16 channels unit and is interfaced to the computer via the IEEE-488 interface card. Each of the imput channels can be programmed for an individual gain setting.

4.1.3.6.3 The Amplifier:

A 16 channel amplifier was designed for use with the AI13 unit described above, to permit a variety of transducers to be used (with different sensitivities and energisation voltages) and to increase to ease of resolution of the measurements. Without this amplifier it was found that there was interference between the signals produced by transducers of differing types. The results of the investigations carried out by previous users and the technical staff indicated that the presence of the amplifier in the system does not introduce a significant time lag into the signals and that the whole system can cope with the rapidity of changes.

4.2.4 The High Air Entry Porous Ceramic:

Materials used as porous elements for pore water measurement for unsaturated samples should poccess the following characteristics (Bishop, 1960; Blight, 1961):

1. adequate mechanical strength to support direct loading when set into loading plates.

2. A high air entry value and uniform pore size.

3. Reasonably high permeability and porosity.

Maswoswe (1985), after encountering some problems in using an Aerox colloton grade VI high air entry stone with an air entry value of 210 kPa found that for such particular compacted samples with low degrees of saturation, ceramics with an air entry value of 500 kPa are suitable. Fortunately these ceramics with such air entry value were available in the laboratory. They were supplied by Soilmoisture Equipment Corp., of Santa Barbara, U.S.A. in large diameter and 7.5 mm thickness. For the cell, a suitable size disc (38 mm diameter by 7.5 mm thickness) was cut from the larger 'original' using a cutting shoe.

The plane surfaces of the porous ceramic disc were ground flat and parallel before it was sealed into the pedestal using an epoxy resin, according to previous practice. Epoxy resin is fairly easy to handle, gives a good bond to both metal and ceramic and when set, is quite rigid and impermeable.

To obtain a stiff pore water pressure measuring system it is critically important to ensure that the ceramic and all connecting tubes are throughly de-aired. The most efficient method of de-airing both porous ceramic and measuring systems is by solution of the air in de-aired water under pressure. Hence, the cell was filled with de-aired water and put under the highest pressure available (700 kPa). Most of the air was then removed from the porous ceramic and the measuring system by flushing through with de-aired water from the cell under a high flow gradient to atmospheric pressure.

When no more air would emerge using this method, the valve leading to atmosphere was closed and the pressure in the system allowed to build up to the

pressure in the cell. The system was usually left under pressure for about three days for a freshly installed ceramic disc. This increased the likelihood of all the air within the system going into solution.

The system was then flushed through again to remove water containing the dissolved air for at least 24 hours. The pressure supply to the cell was then shut off and the cell pressure allowed to dissipate to zero by flow through the ceramic and out to the atmosphere. The cell pressure was then increased again to 700 kPa and this time flushing was to a back pressure of (400 kPa) for about 2 days. The cell pressure and the back pressure supply were then shut off and the cell pressure again allowed to dissipate to zero. This method of de-airing the pore water pressure measuring system for a freshly mounted ceramic disc was invariably found to be satisfactory. The completeness of the de-airing had to be evaluated in some way. This check was conducted by using the response test. The method involved increasing the cell pressure by 50 kPa each time and monotoring the time taken by the pressure transducer to give the corresponding reading on the screen of the data logger. The system and the porous ceramic were considered de-aired for an interval of time of less than 5 seconds.

Three ceramics were changed after carrying out this simple test because of sealing problems.

It was found necessary to de-air the apparatus after every test but this only took 24 hours to accomplish compared to a week for a freshly mounted ceramic disc. This regular de-airing was necessary because even through no gaseous air could pass through the porous element, there was always a high concentration and pressure gradient between the air and the de-aired water on the other side of the porous element in solution. If the pore water pressure was subsequently decreased, this air would reappear as bubbles which would rapidly expand if the pore water pressure dropped very much below atmospheric pressure. For this reason, the pore air pressure within the samples was always set to such a value that the pore water

pressure would never drop below atmospheric pressure during a test.

4.3 Testing Programme and Experimental procedures:

4.3.1 General:

As stated earlier, the objective of this section was to determine the deformation characteristics (mainly the elastic modulii) of:

1. The collapsible soil in both conditions, of natural moisture content and in a saturated state.
2. The sand column unconfined or encapsulated in a geofabric under different cell pressures.

This section explains the general procedure followed in performing these tests and particular attention is paid to the question of specimen preparation.

4.3.2 Specimen Preparation:

4.3.2.1 Specimen of Collapsible Soil:

To prepare compacted samples of the collapsing soil used for triaxial testing, the soil was compacted inside a rubber membrane supported by a split mould. The mould is illustrated in Figure 4.6. Unusually thick rubber membranes were used to reduce the membrane penetration error. The rubber membranes had previously been subjected to an internal air pressure and dipped into water to permit the

detection of faults or holes. The soil was mixed with 4% by weight of de-aired water before compaction using a small mixer (Kenwood type), Plate 4.2. Compaction was performed by applying the static weight of a 30 mm diameter perpex tube 20 times on the surface of each layer from a height of 10 mm. In order to control the thickness of each compacted layer, a small marked container shown in Plate 4.2 was used to keep the amount of soil used for each layer approximately constant. The distribution of tamper applications was kept the same every time. Tamping started at the perimeter of the surface, with an overlap between every two applications, and then moved towards the centre. The weight of the tamper was 500 g, so as to obtain the desired density. During sample formation, the container of the mixer which carried the material was covered by a plastic bag, in order to eliminate evaporation. Despite this precaution, a decrease of the water content of the soil of about 0.2% was noticed. However, the results of previous works on sand (Gunawan, 1978 and Castro, 1969), indicate that for low water contents between 3 and 4%, the relative density achieved is practically constant, when using this type of compaction.

After compaction, the surface of the sample was levelled off with a knife edge. The top cap, which was fixed to a special holder shown in Figure 4.7, was lowered gently over the top of the sample and the rubber membrane rolled around it. The top holder was designed to reduce the possibility of disturbing the top part of the sample while rolling the membrane and placing the O- rings around the top cap. Any un-used material was oven-dried and weighed so that the exact amount of soil in the specimen was known.

The top and bottom ends of the membrane were sealed to the platens by means of four O-rings and were throughly cleaned and polished at the start of each test. Silicon grease was also used between the rubber membrane and the platens to inhibit leakage of the cell fluid past the O-rings.

A vacuum of an intensity of 25 kPa was applied for 20 seconds to the interior of the specimen and the mould was removed carefully. The diameter of the

detection of faults or holes. The soil was mixed with 4% by weight of de-aired water before compaction using a small mixer (Kenwood type), Plate 4.2. Compaction was performed by applying the static weight of a 30 mm diameter perpex tube 20 times on the surface of each layer from a height of 10 mm. In order to control the thickness of each compacted layer, a small marked container shown in Plate 4.2 was used to keep the amount of soil used for each layer approximately constant. The distribution of tamper applications was kept the same every time. Tamping started at the perimeter of the surface, with an overlap between every two applications, and then moved towards the centre. The weight of the tamper was 500 g, so as to obtain the desired density. During sample formation, the container of the mixer which carried the material was covered by a plastic bag, in order to eliminate evaporation. Despite this precaution, a decrease of the water content of the soil of about 0.2% was noticed. However, the results of previous works on sand (Gunawan, 1978 and Castro, 1969), indicate that for low water contents between 3 and 4%, the relative density achieved is practically constant, when using this type of compaction.

After compaction, the surface of the sample was levelled off with a knife edge. The top cap, which was fixed to a special holder shown in Figure 4.7, was lowered gently over the top of the sample and the rubber membrane rolled around it. The top holder was designed to reduce the possibility of disturbing the top part of the sample while rolling the membrane and placing the O- rings around the top cap. Any un-used material was oven-dried and weighed so that the exact amount of soil in the specimen was known.

The top and bottom ends of the membrane were sealed to the platens by means of four O-rings and were throughly cleaned and polished at the start of each test. Silicon grease was also used between the rubber membrane and the platens to inhibit leakage of the cell fluid past the O-rings.

A vacuum of an intensity of 25 kPa was applied for 20 seconds to the interior of the specimen and the mould was removed carefully. The diameter of the

specimen was measured with a micrometer at 10 locations; the height was determined by measuring the distance between the top and bottom plattens at 5 locations. Corrections to the diameter measurements were made by deducing the thickness of the rubber membrane. The vacuum pump was disconnected by closing a valve and any membrane leakage could then be detected by a rapid reduction of vacuum, as recorded by the pore pressure transducer.

4.3.2.2 Specimen of Leighton Buzzard Sand Forming the Sand Column:

The same procedure was used to prepare specimens of Leighton Buzzard sand. The only differences were:

- After stretching the rubber membrane around the mould, a geofabric of a cylindrical form was inserted inside the mould. The cylindrical geofabric, which was prepared in the same way as that described in Chapter 5, had the right diameter so that no space was left between it and the rubber membrane and can be easily entered into the mould. The height of the cylinder was equated to the space between the base pedestal and the mould top.
- Compaction was performed by the hammer shown schematically in Fig. 4.8. The required relative density was obtained by applying the dead weight (B) 15 times on the base (A), which covered the whole surface of the specimen, for each layer prepared from a height of 20 mm. The mass of the dead weight was 2 kg.

4.3.3 Testing Programme:

The testing programme consisted of the following series:

1- Series I: Tests on collapsible soil in a 'dry' condition.

2- Series II: Tests on collapsible soil in a saturated condition.

3- Series III: Tests on Leighton Buzzard sand encapsulated and not encapsulated by a geofabric.

4.3.3.1 Series (I):

The purpose of this series was to determine the *'coefficient of earth pressure at rest'*, denoted by K_0 and the elastic modulus of the collapsible soil in the 'dry' state (i.e at the natural moisture content). The series was divided into two groups:
group 1: consisted of three similar K_0 tests.
group 2: composed of only two similar consolidated undrained tests.

4.3.3.2 Series (II):

The purpose of this series was to determine:

1. The characteristics of the collapsible soil, in the saturated state, that are related to shear strength and hence to calculate the coefficient of earth pressure at rest.
2. To determine the modulus of elasticity of the collapsible soil in the saturated state.

The series was divided into two groups:
group 3: consisted of three consolidated undrained tests under different cell pressures.
group 4: composed of only two similar consolidated undrained tests.

These two series 1 and 2 were performed in order to determine mainly the modulii of elasticity of the soil at natural moisture content and saturated states

respectively. In the meantime the results were used to check the repeatability of the testing equipment.

4.3.3.3 Series (III):

This series consisted of tests carried out on Leighton Buzzard sand, which formed the sand column, not encapsulated and encapsulated in T700, T1000, T1500, and T2000 in order to determine the modulus of elasticity of the composite. The series was divided into five groups composed of 3 tests each. Each group corresponded to a single type under three different cell pressures of 40, 80, and 120 kPa. All the tests were carried out under cycling loading. Three different cell pressures were considered in order to have different series of predicted curves which will facilitate the comparison between measured and theoretical results.

4.3.4 Testing Procedure:

4.3.4.1 Series (I), Group (1):

The cell's top was removed, a small membrane placed around the pedestal and de-aired water added to keep the fine porous stone from drying out. At this stage, the 5 bar ceramic stone in the cell's pedestal would already have been throughly de-aired, as described in Section 4.2.4.

As it was important that once the sample had been prepared it be installed into the triaxial cell as quickly as possible (so as to minimize any drying out of the sample and to avoid the cavitation phenomenon), it was necessary to prepare in advance the equipment needed. Once all this had been done, the sample was prepared as described in Section 4.3.2. The water-filled membrane around the pedestal was then removed and excess water wiped off the fine porous stone with a damp cloth. The sides of the pedestal were then lightly greased with silicone grease

so as to lessen the chance of leakage past the O-rings.

The sample was then placed inside a rubber membrane placed around the pedestal and supported by a mould. Two O-rings were used to secure the membrane to the bottom pedestal. The top cap, which had an air supply inlet and a small changeable plastic filter with low air entry, was lightly greased along its sides, before being placed on the sample. With the aid of a split ring, two more O-rings secured the membrane to the top cap. The plastic filter was used as a porous element for the distribution of pore air pressure. Air must be able to pass freely through its pores, and if it does not actualy repel water, it should absorb a negligible amount. The plastic disc filter used for these tests was the same as that used by Hassona (1986).

The next stage was to place very carefully the lateral strain indicator in position at the mid-hight of the sample. It was extremely important that the pads of the strain indicator be as smooth and horizontal as possible to minimize error in radial measurements. Fortunately, the compacted samples turned out to be very good right cylinders with parallel ends.

As the sample volume change was obtained by measuring the amount of water going into the cell, it was important that very little air be trapped within the cell. Hence, the rubber membrane was set flush with the base of the pedestal and any excess membrane cut off at the top instead of rolling it down over the top 'O' rings.

The cell top was carefully replaced making sure that the load cell had initially been fully retracted to avoid accidentally axially stressing the sample. The cell was then filled with de-aired water. Once the cell was full, it was important to remember to close the water supply at source and not the cell vent to avoid prematurely pressurizing the sample with the de-aired water supply.

Once the cell had been filled with de-aired water, initial readings of all the instruments were taken. Thereafter, an equal air (into the sample) and cell

pressure were applied to the sample with the aid of an air-water interface. This was in order to artificially raise the negative pore pressure of the sample into the positive range without any compression occurring. This 'axis translation technique' was first adopted by Hilf (1956) who observed that when air pressure was applied within a sample, the change in pore water pressure for all practical purposes was equal to the change in pore air pressure. A cell and air pressure of about 365 kPa was generally found adequate to bring the pore water pressure to a positive value of around 70 kPa. The air pressure was applied very, very slowly into the sample in order to avoid the problem of pushing out the membrane from the sample and thus disturbing the strain indicator.

Having attained the required level of air pressure, the cell pressure was then increased slightly so as to make it about 3 kPa greater than the air pressure within the sample. This small pressure was used in order to let both pads of the strain indicator and membrane bed in properly. The cell pressure was then left on for about 48 hours. The reason for this was to enable the sample's pore water pressure to reach equilibrium and readings were taken every hour.

After this period, the axial transducer was placed in position and the deviator stress was applied to the sample at a constant rate of 3 kg per hour and the cell pressure was changed manually to maintain zero lateral strain. During this initial period, the sample was stiff and there was hardly any change in cell pressure. However, as soon as the sample started to yield, i.e. as soon as cell pressure started to increase steadily and much more rapidly, the rate of change of deviator stress was reduced to half of the previous rate.

Pore air pressure was kept constant throughout and provided the testing rate was slow enough, the measured undrained pore water pressure could be regarded as being reliable.

The test was stopped when the maximum deviator stress had been at-

tained. The sample was then removed as quickly as possible, weighed and then dried for the determination of dry weight which was used to calculate the water content.

The test was repeated three times in order to check the repeatability of the testing equipment.

4.3.4.2 Series (I), Group (2):

Sample preparation and assembly of the apparatus were basically as described for the K_0 tests. However, there were a few differences which will be described below.

Once all the equipment needed including a volume change unit had been prepared, the sample was prepared as described in Section 4.3.2 and then quickly jacketed. Note that a volume change unit for measuring the amount of water going into the cell was required. As the sample volume change was obtained by measuring the amount of water going into the cell, it was important that very little air be trapped within the cell. Hence, the rubber membrane was set flush with the base of the pedestal and any excess membrane cut off at the top instead of rolling it down over the top 'O' rings.

Once the cell top was carefully replaced and the cell had been filled with de-aired water as described for the K_0 tests, initial readings of all the instruments were taken. An equal air (into the sample) and cell pressure was applied with the aid of an air-water interface. The air and cell pressure were taken up to a very high value (600 kPa). The cell was left with that high cell pressure for about three days to let any air that might be trapped dissolve and for most of the perpex creep to occur. This procedure was proved by Maswowe (1984) after carrying out an experimental investigation in order to devise a technique for accurately determining the total volume change of the sample during shear.

After that period, by just looking into the cell, it was always found that

any air bubbles which had initially been trapped within the cell had dissolved. The air pressure was then reduced till the desired value (546 kPa) and constant water content consolidation allowed till there was no significant variation in pore water pressure. The water going in or out of the cell was also monitored.

Once consolidation was completed, constant water content shearing with pore water pressure measurement was carried at a constant rate of deviator stress. The sample was sheared to an axial strain of at least 15%.

4.3.4.3 Series (II):

Five isotropic consolidation tests at four different cell pressures (two tests were produced under the same cell pressure) followed by undrained compression tests with measurement of pore pressure were performed.

The samples were prepared as described in Section 4.3.2 and the mounting procedure was basically the same as for series 1 . A point worth mentioning is that the fine porous stone in the steel cell's pedestal was removed and changed by another porous plastic disc (with low air-entry) from the same material used for distributing the air pressure in series 1. This change was performed in order to reduce the time required to obtain complete saturation. The high air entry ceramic was not needed since the specimens were all saturated.

Saturation was usually achieved by applying sufficient back pressure to cause the pore air to dissolve completely in the surrounding pore water.

Previous publications have presented theoretical analysis to define the minimum amount of back pressure required for full saturation (Hilf, 1948; Lowe and Johnson, 1960; Black and Lee, 1973; Fredlund, 1976; and Rad & Clough, 1984). Two trends emerged from these analytical works. First, as would be expected, higher back pressures were required to obtain complete saturation as the initial degree of

saturation decreased. Second, for a given degree of saturation, a lower back pressure was required to obtain complete saturation if an initial vacuum was applied to the specimen.

A vacuum pressure was used during the present section of work to improve saturation and to lower the amount of back pressure required to saturate the specimen. A back pressure of about 400 kPa was sufficient to saturate the soil sample.

Once the sample had been prepared and the cell assembled and filled with de-aired water a negative pressure of 25 kPa was applied to the sample interior by the vacuum pump. Then an initial cell pressure of 25 kPa was applied. The connecting leads, particularly the back pressure lines, were flushed through with de-aired water before connecting them to the cell. The back pressure valve was then opened and de-aired water was allowed to flow into the specimen until the vacuum was reduced to zero. This was followed by the incremental increase of the cell pressure and the back pressure, a difference of 10 kPa being maintained at all times between the two, until saturation was achieved. Finally, the cell pressure was increased up to the desired confining pressure with the back pressure valve closed. This enabled a check on the final degree of saturation of the specimen to be carried out by calculation of the pore pressure parameter B ($B = \Delta u/\Delta\sigma_3$ where Δu is change in pore water pressure and $\Delta\sigma_3$ is change in cell pressure). When the value of B approaches unity, full saturation may be assumed and reliable measurements of pore water pressure can be expected. Only those specimens with B in the range 0.95 to 1.0 were considered acceptable. It was found that a back pressure of about 400 kPa was usually required to saturate the specimens.

After the consolidation phase, undrained compression tests were carried out under stress-controlled conditions.

4.3.4.4 Series (III):

The following procedure in general terms applied to all tests included in this series.

After sample preparation as described in Section 4.3.2, the cell was assembled and filled with de-aired water. The sample was then saturated by following the same procedure applied to tests of series (II). The negative pressure was increased to 50 kPa and the back pressure valve was then opened to allow de-aired water to flow into the specimen until the vaccum was reduced to zero. The process of saturation was continued by raising the cell pressure and the back pressure incrementally so as to keep the difference the same as that of the previous stage. To save time, these increments were applied simultaneously and the degree of saturation was only checked in the final stages (back pressure approaching 300 kPa).

After saturation, the specimen was consolidated and following that it was sheared under undrained conditions. During shearing, three stages of unloading and loading were applied to the sample. The range of stress over which the modulus of elasticity was determined and the magnitude of the deviator stress at either the lower or upper limits of the range of stress were chosen from the works of Makhlouf & Stewart (1965) and Karst et al. (1965). From tests carried out on Ottawa sand, they concluded that:

1. For different ranges of deviator stress that are reduced to the same minimum deviator stress value, the modulus of elasticity (E) will be, for all practical purposes, constant after the inelastic deformations have been eliminated;

2. For different ranges of deviator stress that have the same upper limit, E will be less for the larger ranges of stress and will increase in value as the range of deviator stress decreases;

3. For identical ranges of deviator stress, E will increase as the magnitude of the lower limits of the range of stress increases.

Studies made to investigate the effect of the rate of loading during which the development of pore water pressure and hence strength could be affected by creep (Bjerrum et al., 1958, Bishop et al., 1960 and Richardson & Whithman, 1963) established that the measured soil strength increases with increasing rates of loading. In clays this effect may be attributable to an uneven pore water pressure distribution as well as to creep. However, in sand, because the equalisation of pore water pressure takes place very quickly, creep must be mainly responsible.

Hassona (1986) found that, by testing similar materials, a standard loading rate of 6 kg/min. reduced the differential effects of creep to an acceptable level. This rate was adopted for this series.

4.3.5 Data Acquisition and Evaluation:

A computer program, used by previous researchers on 'liquifaction studies', was set up to take readings from the instrumentation at the end of each increment of load. The test data of the saturated samples were processed by the same computer programs, whereas, for the 'dry' samples, a hand calculation was performed.

The deviator stress during undrained shear to failure was calculated using the assumption of a right cylinder. Yung (1987) indicated that this assumption is unlikely to introduce an error of more than 5% into the values of the stresses of the specimen. The deviator stress was obtained from the load cell readings. No correction was applied to it for membrane penetration for the following reasons:-

1. The diameters of the specimens were large enough to reduce the influence of membrane penetration (Baldi & Nova, 1984)

2. For the collapsible soil, which was in loose state and contained a considerable amount of fine particles, the use of rubber membranes (0.4 mm thick) was proved good enough to reduce the membrane penetration to an acceptable

level (Lade & Harnandez, 1977; Molenkamp and Luger, 1981).

3. For the Leighton Buzzard sand, the use of a geofabric to encapsulate the sample completely eliminated the effect of the rubber membrane penetration

Strain and pore water pressure were computed from transducer measurements during each test.

4.4 Interpretation of the Results:

4.4.1 General:

In this section, the experimental results of all the successful tests carried out in the triaxial cell on the collapsible soil and the Leighton Buzzard sand are presented. The section is sub-divided into:

1. Results of K_0 and consolidated undrained tests performed on the collapsible soil in the dry state (series (I)).
2. Results of consolidated undrained tests performed on the collapsible soil in the saturated state (series (II)).
3. Results of consolidated undrained tests performed on Leighton Buzzard sand encapsulated and not encapsulated in a geofabric (series (III)).

Where necessary, brief comments are made on the results and the testing procedure. The section is then concluded with a summary.

The main objective of this part of the research programme was the determination of the modulii of elasticity of the collapsible soil and the sand columns used in the analytical solution.

At a first glance, the main objective might be thought straightforward. In practice, it turned out that very sophisticated triaxial testing was required. However, this triaxial cell is not available in the laboratory, and its design is time consuming and break down in the equipment was frequently encountered. In addition, the length of the testing programme and the slow rate of testing for some tests implies that there was ample time for things to go wrong. Because of this, the testing equipment was kept as simple as possible.

4.4.2 K_0 and Consolidated Undrained Tests Performed on Collapsible Soil in the 'Dry' State (series (I)):

The tests of this series were carried out in order to determine the elastic modulus of the collapsible soil at its natural moisture content state and under the field conditions (i.e. conditions applied to the soil in the large container). These tests were performed in two stages which were imposed by the capability of the testing equipment. Firstly, the determination of the coefficient of earth pressure at rest K_{0d} (i.e. the horizontal stresses acting on an element of soil for any given overburden) and then the stress-strain relationship from which the modulus of elasticity was deduced.

The term K_0 is used in this thesis to identify any test phase carried out under radial stress conditions with zero horizontal strain. K_{0d} for the 'dry' state was defined by :

$$K_{0d} = \frac{\sigma_h - u_a}{\sigma_v - u_a}$$

where:

σ_h: total horizontal stress,

σ_v: total vertical stress,

u_a: pore air pressure.

This definition was used by Fredlund (1976). However, Kane (1972) had

simply taken K_{0d} as:

$$K_{0d} = \frac{\sigma_h}{\sigma_v}$$

In an investigation of this nature, the repeatability of each individual test is significant. For the first stage, a total of 3 K_0 tests were performed under the same conditions. The material, apparatus and the procedure followed are described in Section 4.3.2 and Section 4.3.4. The results are presented in Fig. 4.10 where the term $(\sigma_h - u_a)$ was plotted against $(\sigma_v - u_a)$. An average value of $K_{0d} = 0.54$ was deduced. The maximum error made in adopting this value was computed with not less than 95% confidence. The possible cause for this value being slightly greater than those reported for the sand in a loose state was that the soil was slightly overconsolidated during sample preparation due to the compaction technique and mainly due to the suction which characterises an unsaturated soil.

For the second stage, which consisted of 2 identical shearing tests up to failure, the specimens were initially consolidated at constant water content with pore water pressure measurement. This phase was held at least 24 hours prior to commencing compression. Constant water content consolidation was preferred to consolidation with drainage because pore water pressure equalisation within the sample is relatively quick when the former method is adopted. This is because no significant pore water flow is involved, just a re-arrangement of pore water menisci (Yoshimi & Osterberg, 1963; Barden, 1974).

The confining cell pressure applied to the specimen was 54 kPa. This value was deduced from the K_{0d} test and using an overburden pressure of 100 kPa applied to all the tests of the main testing programme.

The results obtained are presented in Figs. 4.11-a to 4.11-c. Normally all the results of the shearing tests were plotted three dimensionally in terms of shear stress and $(u_a - u_w)$ against void ratio (or axial strain). However, it is often more convenient to plot the results two-dimensionally in terms of the variable of interest

against void ratio (or axial strain). This makes the data easier to interpret.

Fig. 4.11-a shows the stress-strain relationship. It can be seen that the material was brittle. The shearing resistance of the specimens increased up to an axial strain of about 3.0% when they started yielding. This is typical of most loose sands.

In order to compare stress-strain curves of 'dry' and saturated states, and consequently material stiffnesses, it was convenient to use some simple stiffness indicators. For the purpose of the present work secant Young's modulii were chosen. The points, at which the modulii were computed, were arbitrarily selected and corresponded to axial strains of 0.5% and 2%. The elastic modulus derived using this method was E_d = 3600 kPa.

Fig. 4.11 b shows the variation of $(u_w - u_a)$ during shearing with the axial strain. Provided that the air pressure was kept constant during testing, it can be seen that the pore water pressure increased during shearing. This increase was rapid up to the yielding point.

4.4.3 Consolidated Undrained Tests Performed on the Collapsible Soil in the Saturated State (series (II)):

The determination of the elastic modulus of the collapsible soil at the saturated state was also realised in two stages. Stage 2 was similar to that of series (I), whereas in stage 1, the direct measurement of the coefficient of earth pressure at rest (K_{0s}) was not possible due to the disturbance of the lateral strain indicator during saturation. Therefore, Jaky's formula

$$K_{0s} = 1 - sin\phi' \qquad (4.1)$$

was used for its determination, since following collapse on wetting, the soil becomes normally consolidated (Maswowe, 1985).

In order to determine the shear strength characteristics of the material used for K_{0s} computation, three consolidated undrained tests on identical specimens were carried out under three different net confining pressures of 55, 115 and 155 kPa.

The results are shown in Fig. 4.12-a. It is clear that the material changed its behaviour from brittle (Fig. 4.11-a) to plastic with remarkably well-expressed lateral bulging. In addition, a large reduction in strength was noticed by comparing the stress-strain relationship of both states under an applied net confining pressure of 55 kPa.

The Mohr's rupture diagram was plotted in term of effective stresses in Fig. 4.12-b From which a values of $c' = 0$ and $\phi' = 34.8^o$ was computed. These values are typical to most loose sands sheared undrained.

The coefficient of earth pressure at rest K_{0s} was computed from equation (4.1). It was found that $K_{0s} = 0.43$. This value was smaller than that measured for the 'dry' state. This fact concluded that, during collapse the lateral pressure of a typical element of soil in the ground decreased.

The results, shown in Fig. 4.13, confirmed that during collapse by wetting the shear strength of the material is reduced. Consequently, the stiffness of the material is also reduced. The secant modulus determined between the strain of 0.5% and 2% dropped to a value of $E_s = 2900$ kPa.

4.4.4 Consolidated Undrained Tests Performed on Leighton Buzzard Sand Encapsulated and not Encapsulated in a Geofabric (series (III)):

The material used in these tests was Leighton Buzzard sand which formed the sand columns in the main testing programme. The tests were performed using the apparatus and procedure which were described in Section 4.3.2 and Section 4.3.4. All

tests were carried out on dense specimens. The specimens preparation was described in Sub-Section 4.3.2.2. A total of 15 tests, divided into 5 different groups, were performed on specimens prepared at the same relative density. Each group consisted of three tests on identical specimens consolidated under three different cell pressure (40, 80, 120 kPa). The specimens of each group were encapsulated by one of the following geofabrics, T700, T1000, T1500, and T2000. The specimens of one group were tested without encapsulation. After the consolidation stage, the specimens were sheared up to an arbitrary value of deviator stress where three cycles of unloading and loading were performed. The final stage of loading was carried out up to failure or a higher deviator stress. The choice of the limits and the interval of the cycles were discussed in Sub-Section 4.3.4.4.
The results are presented in three forms:

(1)- Figs 4.14 to 4.18 show the effect of the confining pressure on the stiffnesses of specimens encapsulated by the same geofabric. It is clear that the modulii of elasticity increase with increase in the confining pressure.

(2)- Figs 4.19 to 4.21 show the effect of confining the specimens by different geofabrics under the same cell pressure. For a given specimen, the vertical stresses at failure and the elasticity modulii increase with the tensile strength of the geotextile.

(3)- Fig. 4.22 groups both effects. It can be seen that the modulus of elasticity of sand encapsulated by a geofabric definitely is a function of confining pressure.

The modulii of elasticity of all the specimens derived from the second loading curves are summarized in Table 4.3. All the values were obtained from considering the secant modulii.

The angle of internal friction of LBS measured by standard triaxial tests, at a relative density of 85%, was $\phi' = 41°$.

4.4.5 Summary and Comments:

External measurement of strain has led to widespread debate in recent years as to the true magnitude of initial stiffness and the influence of bedding errors. The errors mainly result from tilting of the sample, bedding at the end plattens and the effects of compliance in the apparatus. Some of the causes such as the compliance of the apparatus can be calibrated for. However, errors such as those due to the non-perpendicularity of the connection between load cell and sample top cap, and bedding down at the ends of the sample due to local surface irregularities are extremely difficult to eliminate.

In the present work the modulii of elasticity of the collapsible soil were not directly used in the analytical solution. They were required to calculate the stiffness factors K in the 'dry' and saturated states for the elastic analysis only. These factors, defined as $K = E_p/E_s$, were used to determine the settlement influence factors I_ρ from the appropriate graphs. The error made in computing the stiffness factors doesn't affect significantly the corresponding values of (I_ρ). In addition, a careful sample preparation was performed and a special sample top cap was provided in order to eliminate the play in the connection between it and the load cell. Because of this the conventional determination of the stress-strain relationship for the collapsible soil in both states was accepted.

The modulii of elasticity of Leighton Buzzard sand confined by the different geofabrics (i.e. the sand columns) were used directly into the parametric solutions described in Chapter 3.

Because of the sand grading (coarse) and the presence of the geofabrics, the determination of the modulus of deformation using conventional tests leads, to some extent, to underestimated values. For this reason an impoved method using cyclic loading was used to reduce the errors based upon the external measurement of strain.

All the results obtained in this part of study are summarised in Table 4.3.

Transducer Type	Calibration Factor	Precision
Axial LVDT	69.7 mV/mm	0.09 mm
Radial LVDT	876 mV/mm	0.005 mm
Pressure Transducers		
N^o. 117287	4.19 mV/kPa	0.38 kPa
N^o. 117288	4.20 mV/kPa	0.38 kPa
Load Cell	4.785 mV/Kg	2.0 N
Volume Change Unit	45.283 mV/cm^3	0.25 cm^3

Table 4.1 **Calibration Factors and Precision of the Instruments Employed in the Triaxial Testing**

'Pile' Deformation Parameters:						
Type of Confinement	Test Code Name	E_p (kPa)	Test Code Name	E_p (kPa)	Test Code Name	E_p (kPa)
Soil Alone (LBS)	CUB1	18980	CUB2	28760	CUB3	36685
T700	CUB4	36300	CUB5	55030	CUB6	70190
T1000	CUB7	45100	CUB8	68360	CUB9	87185
T1500	CUB10	55660	CUB11	84370	CUB12	107605
T2000	CUB13	73060	CUB14	110730	CUB15	141230
Soil Deformation Parameters:						
'Dry' state: $E_s = 3600$ kPa						
Saturated state: $E_s = 2900$ kPa						

Table 4.3 **'Pile'-Soil Parameters used in Test Data Evaluation**

Table 4.2 Testing Programme

Series (I):

Test N^o	Test Code Name	Soil Conditions	Net Confining Pressure (kPa)	Group N^o
1	KD1			
2	KD2	m.c.= 4%		Gr (1)
3	KD3	$\rho_d = 1.54$ Mg/m^3		
4	CUD1	m.c = 4%	54	
5	CUD2	$\rho_d = 1.54$ Mg/m^3	54	Gr (2)

Series (II):

Test N^o	Test Code Name	Soil Conditions	Net Confining Pressure (kPa)	Group N^o
6	CUS1		55	
7	CUS2		115	Gr (3)
8	CUS3	saturated	155	
9	CUS4	$\rho_d = 1.54$ Mg/m^3	48	
10	CUS5		48	Gr (4)

Series (III):

Test N^o	Test Code Name	Net Confining Pressure (kPa)	Type of Confinement	Group N^o
11	CUB1	40	None	
12	CUB2	80	None	Gr (5)
13	CUB3	120	None	
14	CUB4	40	T700	
15	CUB5	80	T700	Gr (6)
16	CUB6	120	T700	
17	CUB7	40	T1000	
18	CUB8	80	T1000	Gr (7)
19	CUB9	120	T1000	
20	CUB10	40	T1500	
21	CUB11	80	T1500	Gr (8)
22	CUB12	120	T1500	
23	CUB13	40	T2000	
24	CUB14	80	T2000	Gr (9)
25	CUB15	120	T2000	

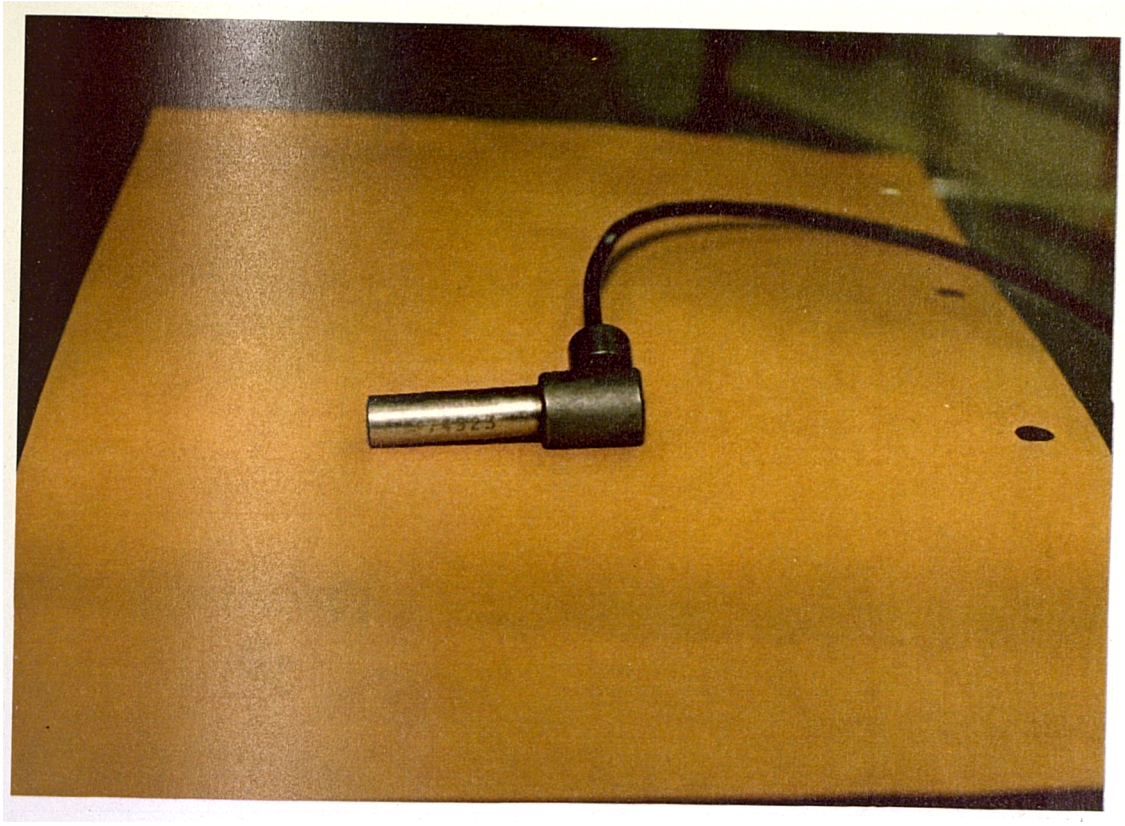

Plate 4.1 The Transducer Mounted in the Lateral Strain Indicator

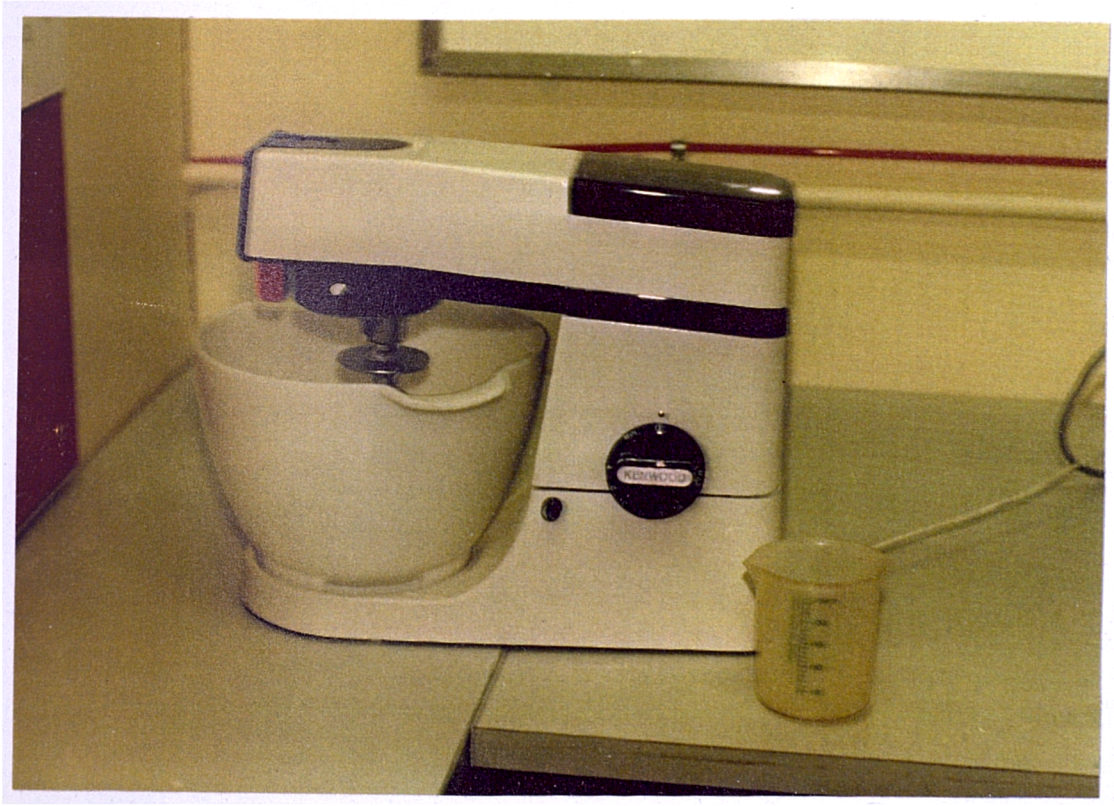

Plate 4.2 Kenwood Mixer and the Small Container

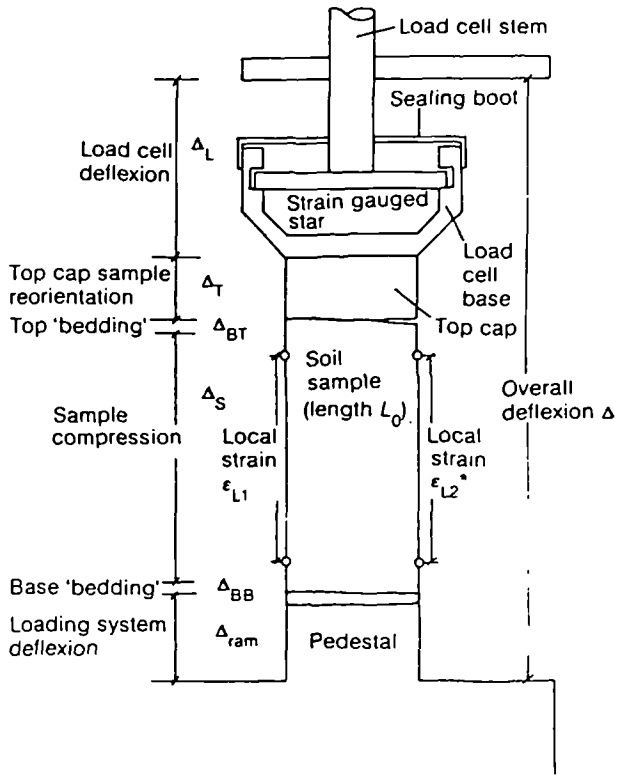

Fig. 4.1 Sources of Error in External Strain Measurement (Jardine et al., 1984)

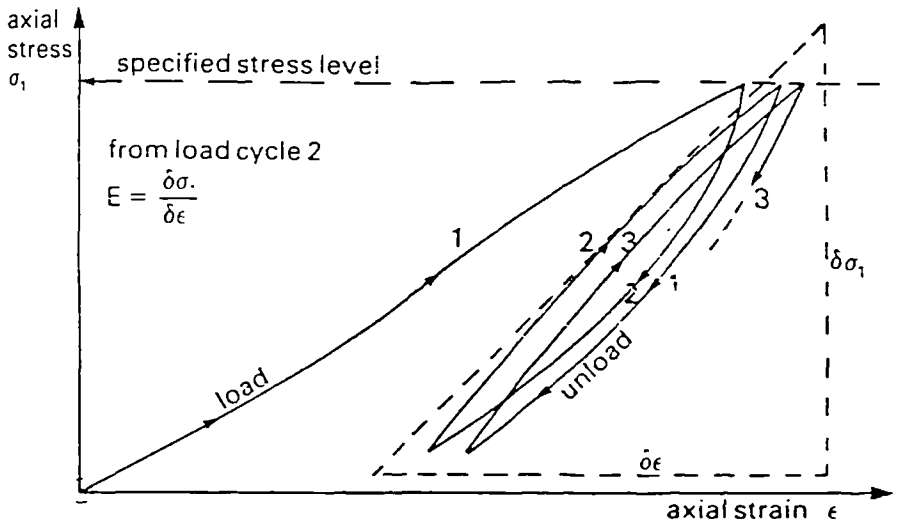

Fig. 4.2 Derivation of Young's Modulus using Repeated Loading Cycles (Head, 1982)

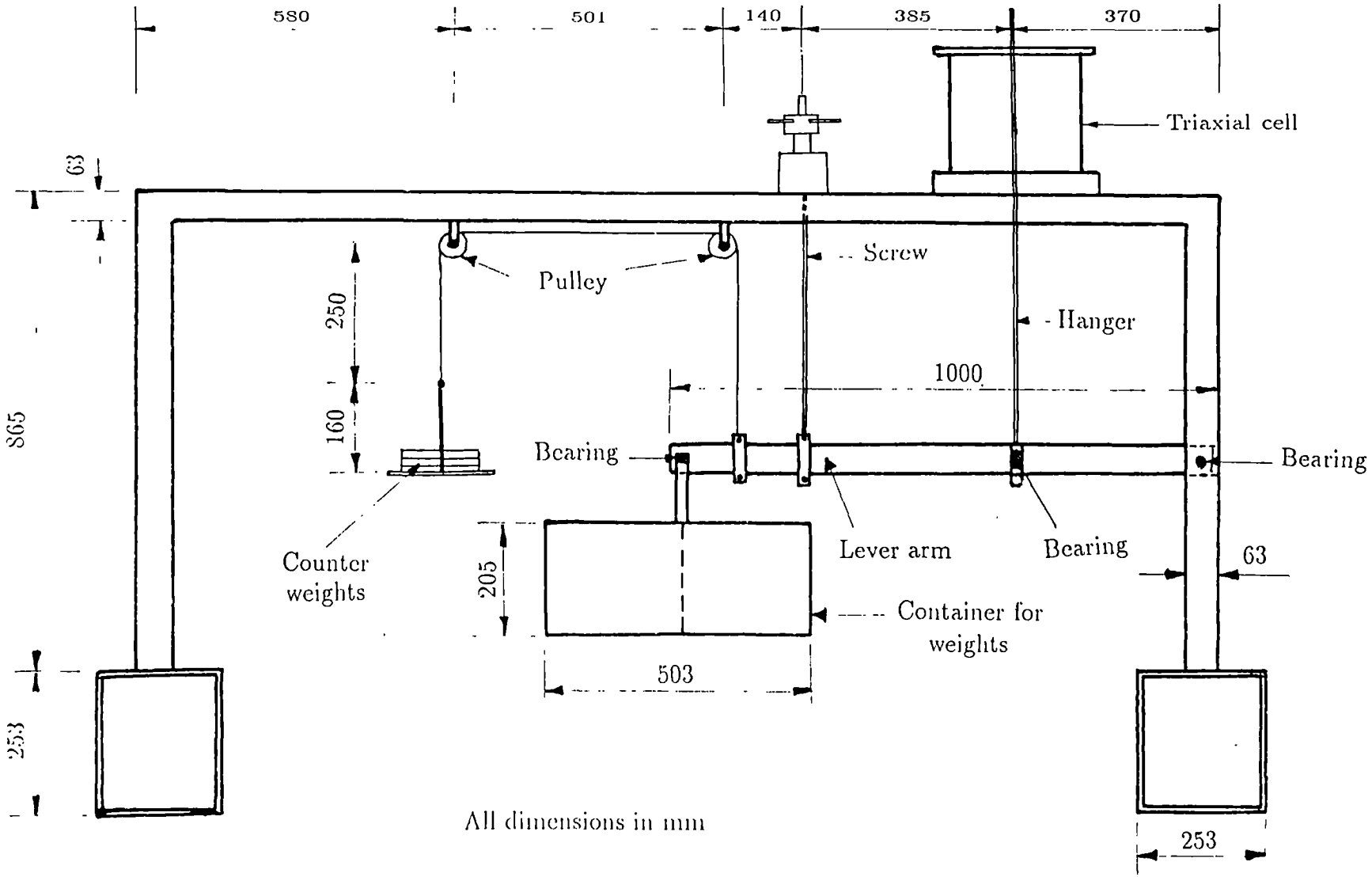

Fig. 4.3 The General Arrangement of the Triaxial Loading System

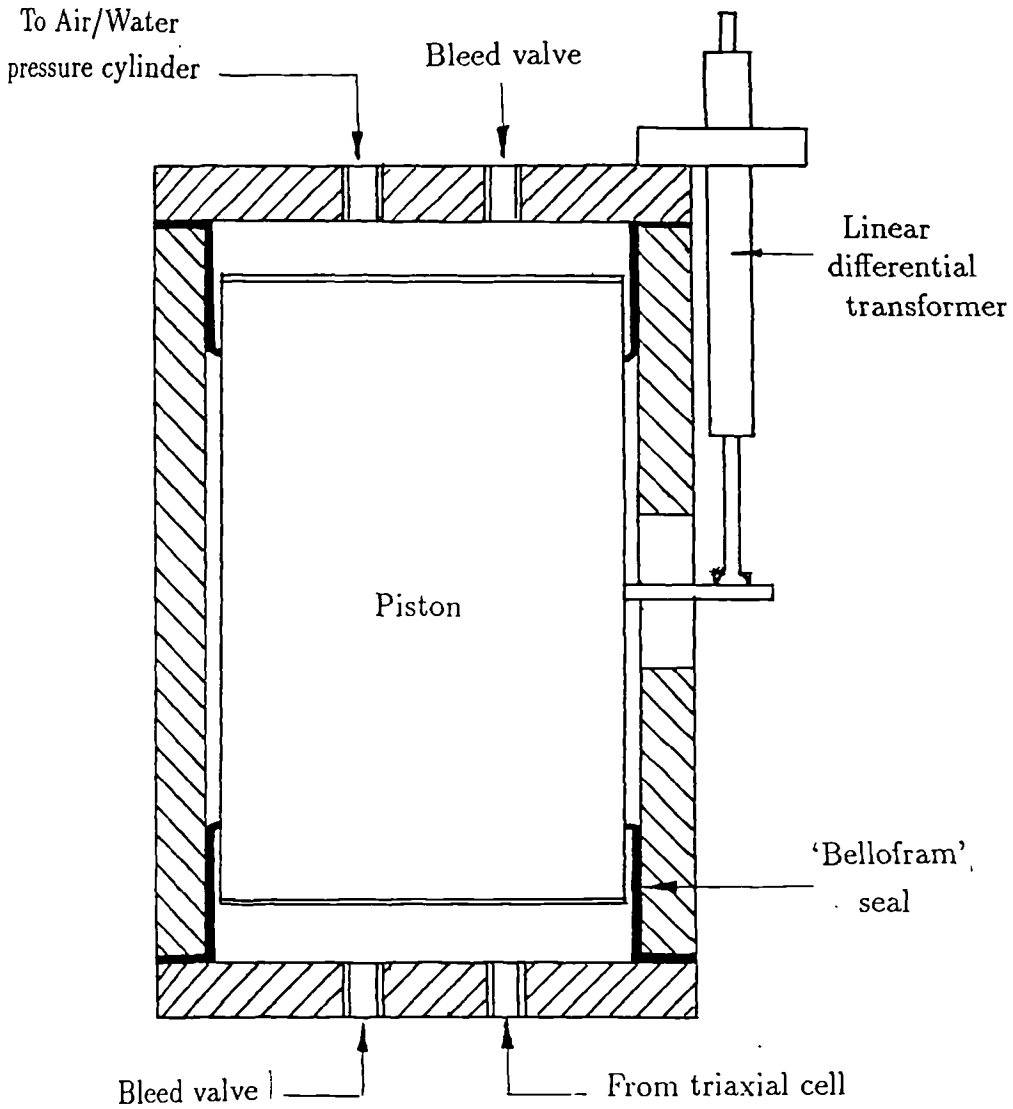

Fig. 4.4 Schematic Cross-Section of the Volume Change Unit

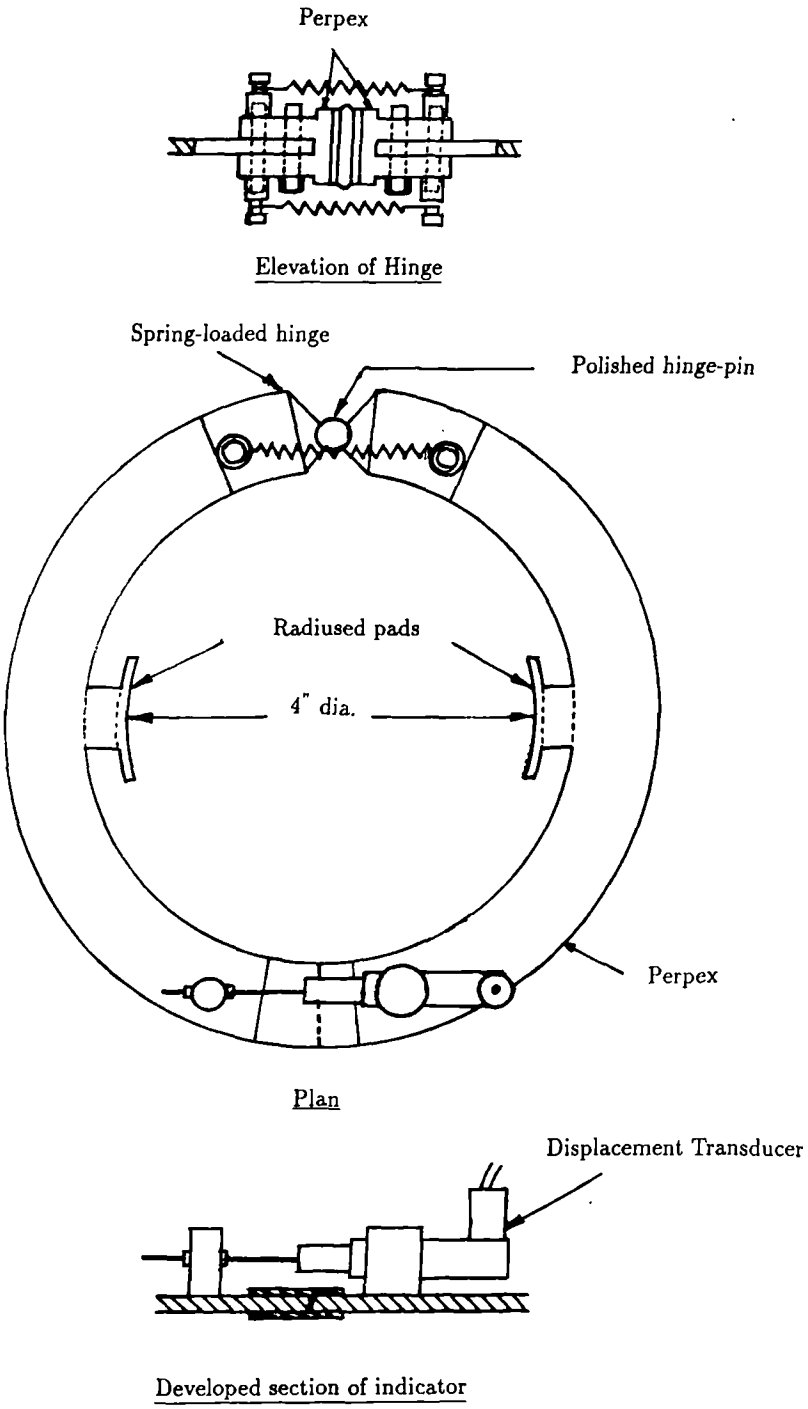

Fig. 4.5 The Lateral Strain Indicator

All dimensions in mm

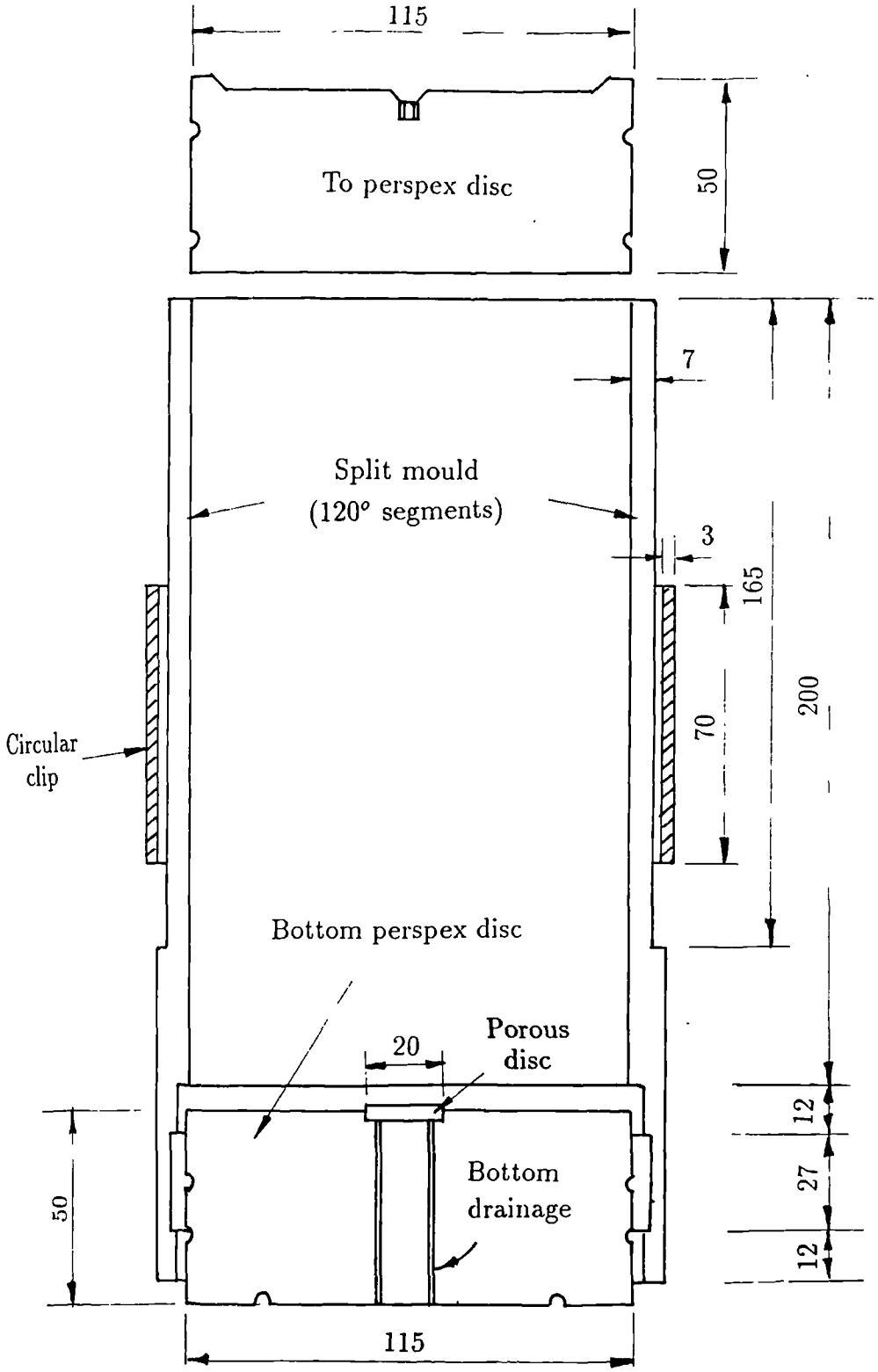

Fig. 4.6 Details of the Split Mould

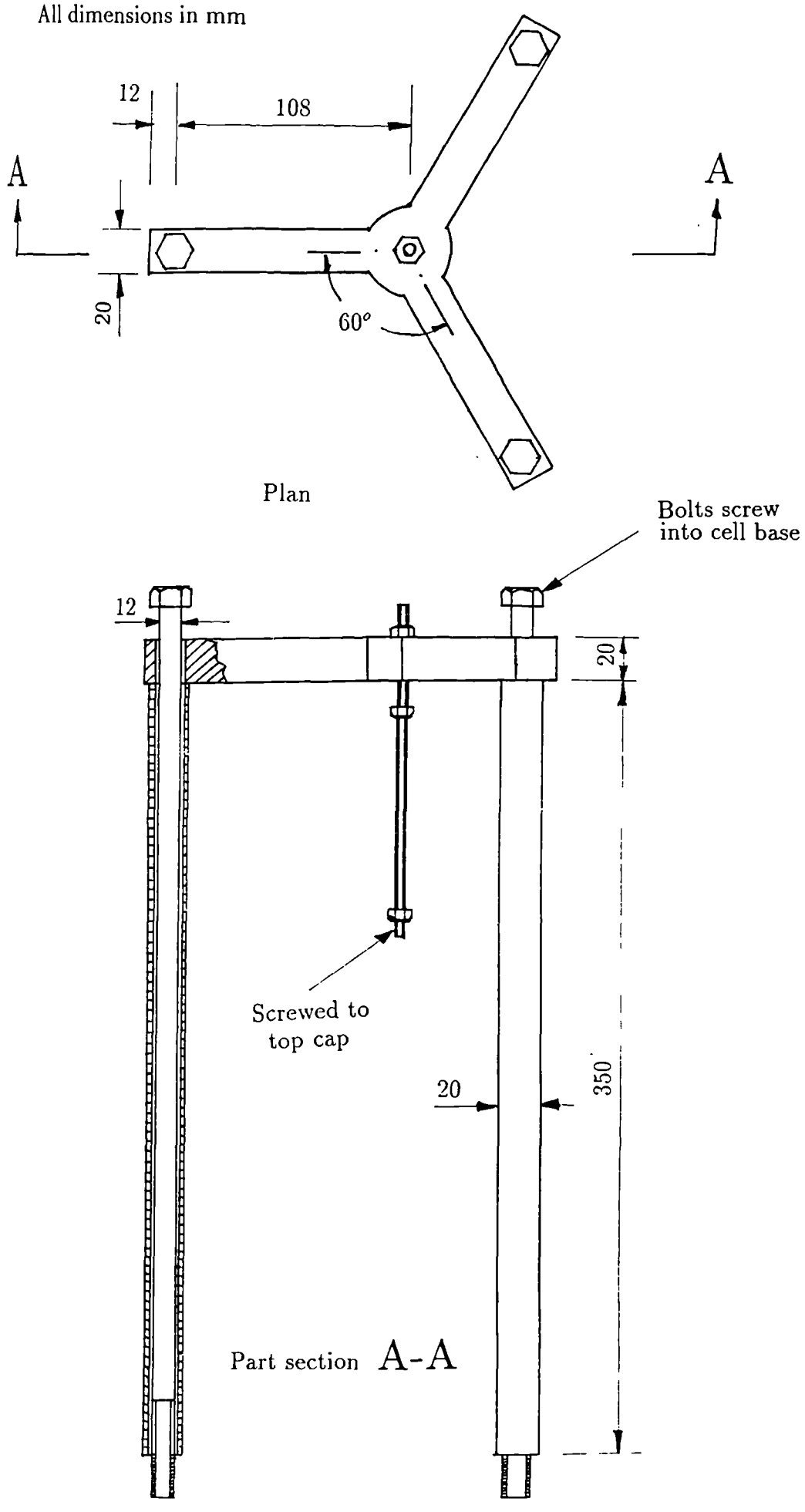

Fig. 4.7 **Details of the Top Cap Holder**

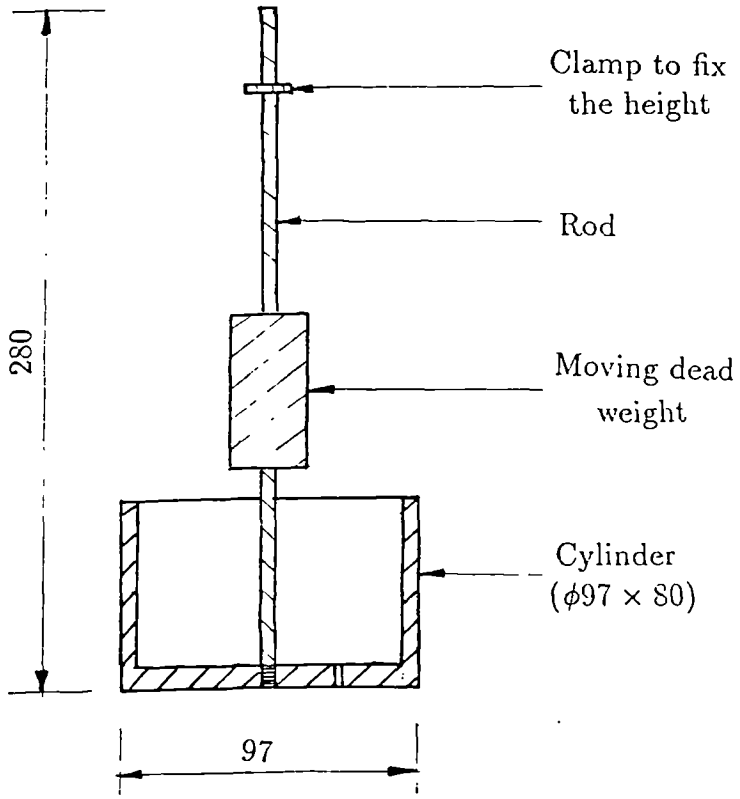

Fig. 4.8 The Compaction Hammer used to Compact the Leighton Buzzard Sand in the Triaxial Cell

Fig. 4.9 Schematic Diagram of Testing Programme

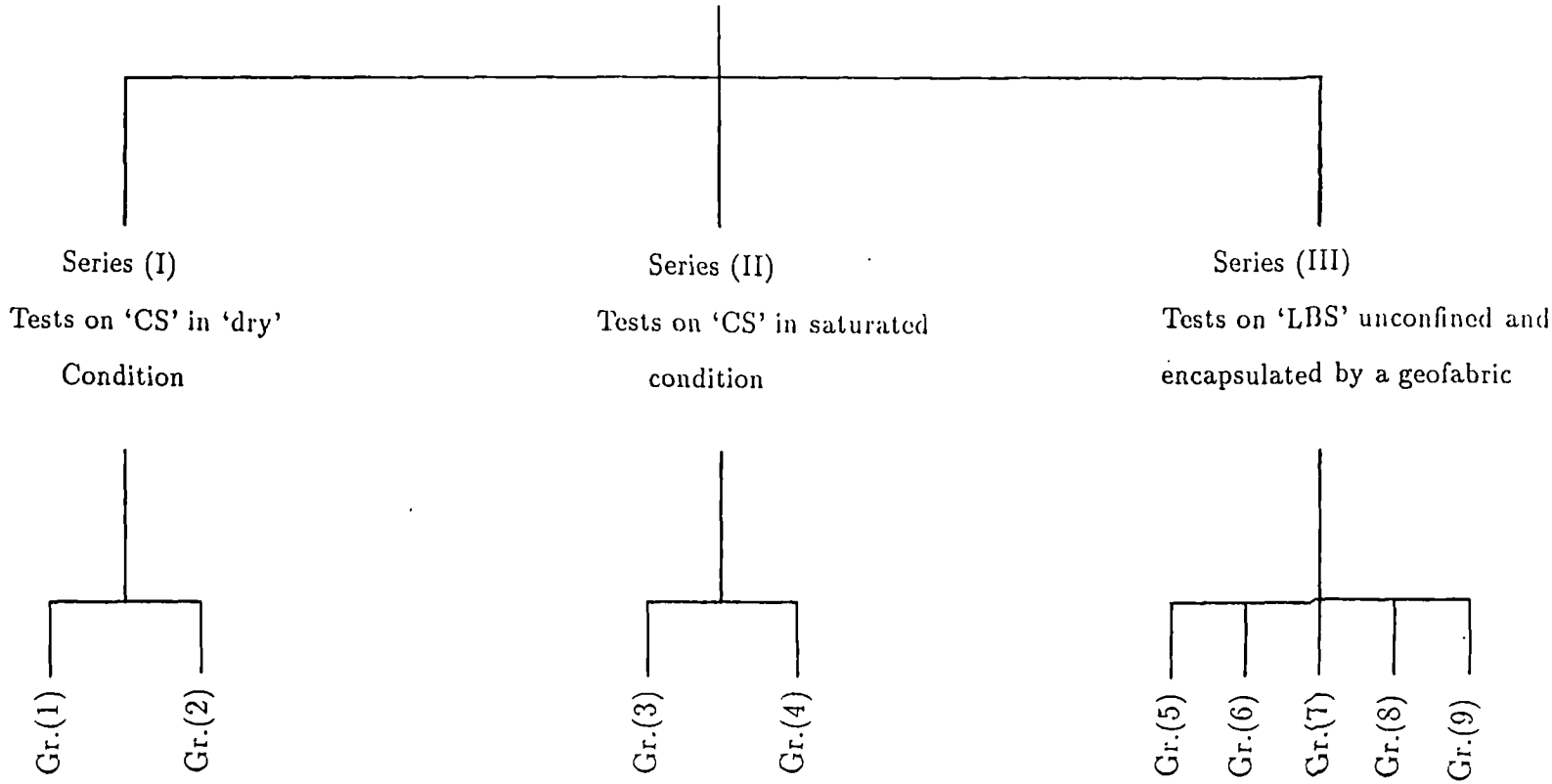

Notation
CS: Collapsible soil
LBS: Leighton Buzzard sand

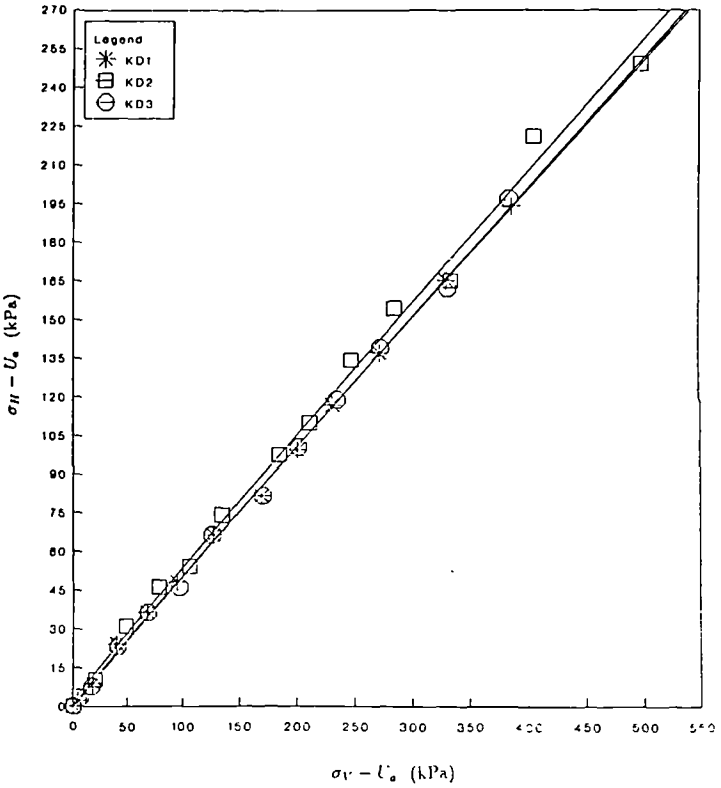

Fig. 4.10 Undrained K_0-tests on samples of CS compacted at 4% moisture content.

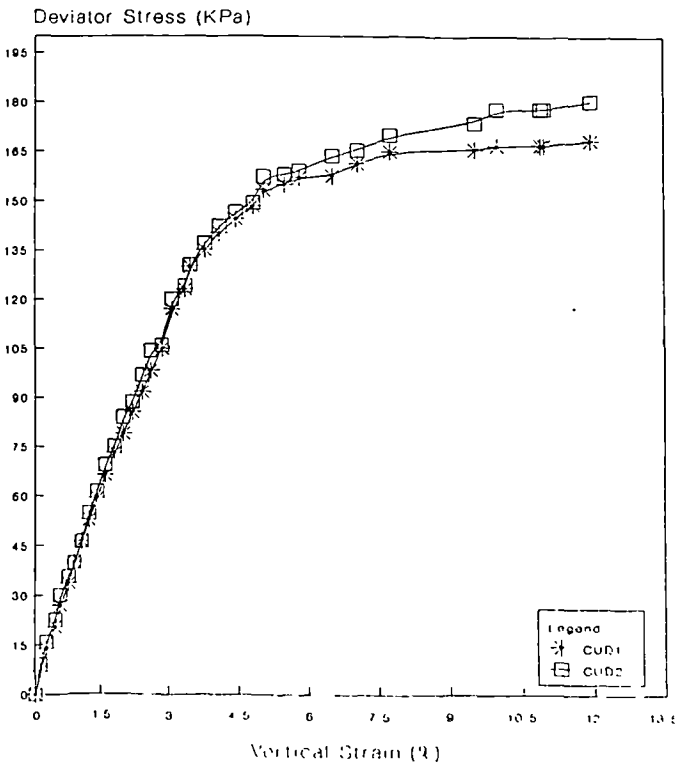

Fig. 4.11-a Stress-strain behaviour of 'dry' samples of CS (cell pressure = 54 KPa).

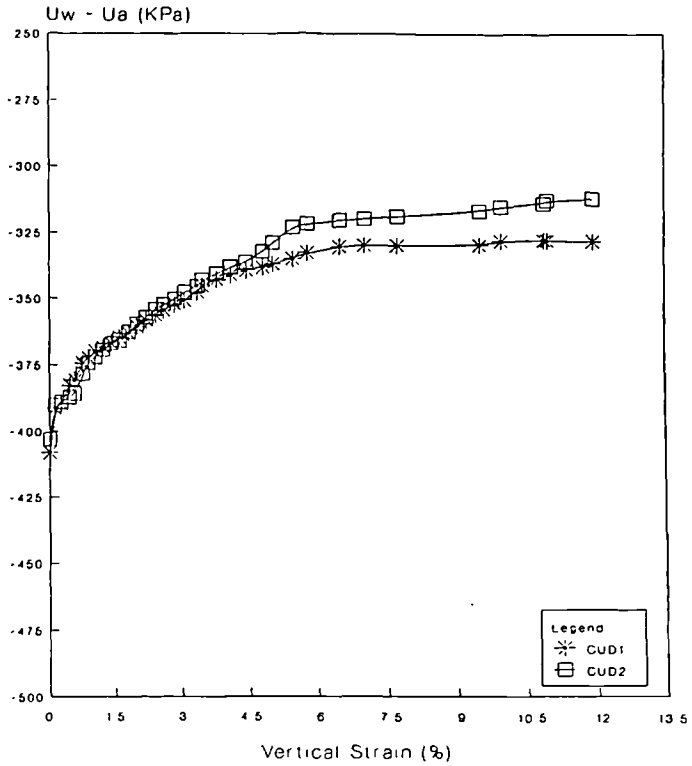

Fig. 4.11-b Pore pressure plotted against strain.

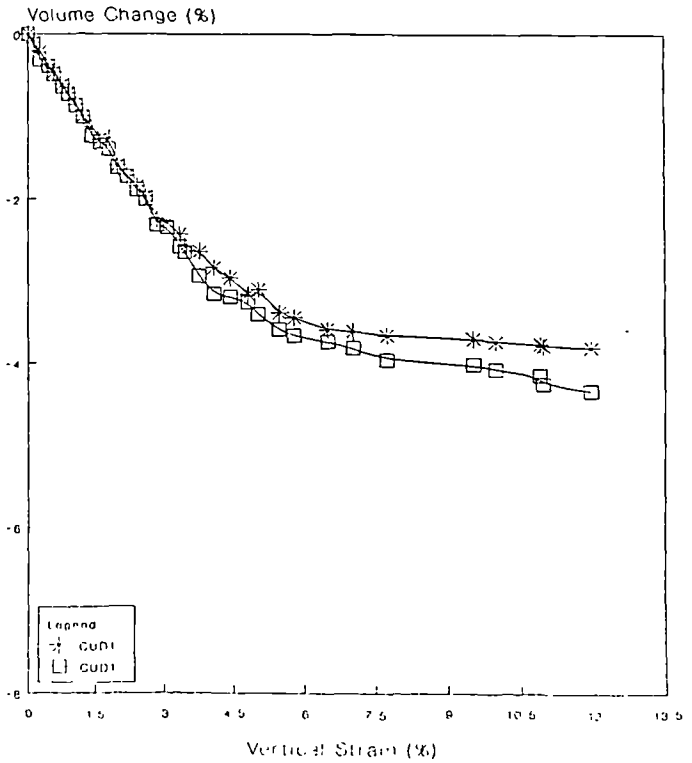

Fig. 4.11-c Relationship between volume change and strain.

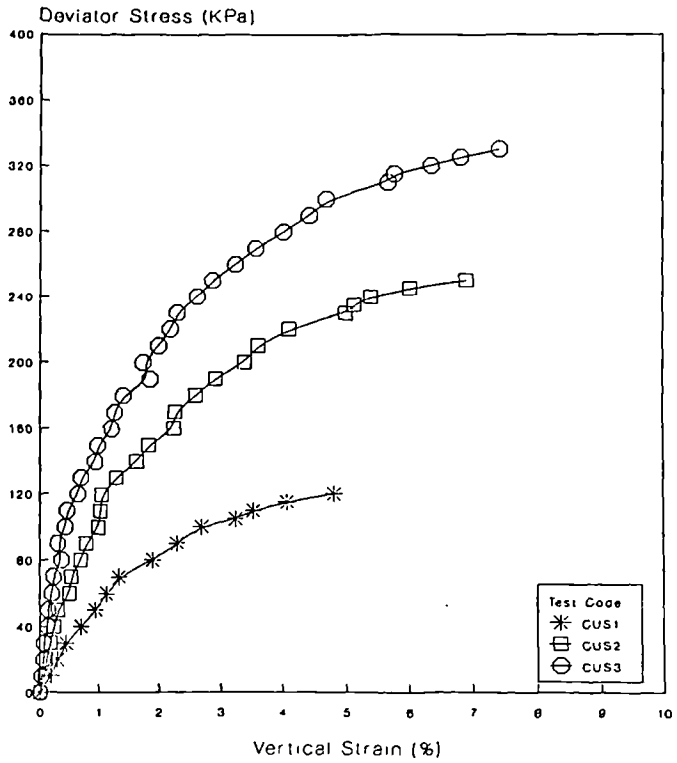

Fig. 4.12 **Stress-strain behaviour of the saturated CS under three different cell pressure (55, 115 and 155 KPa).**

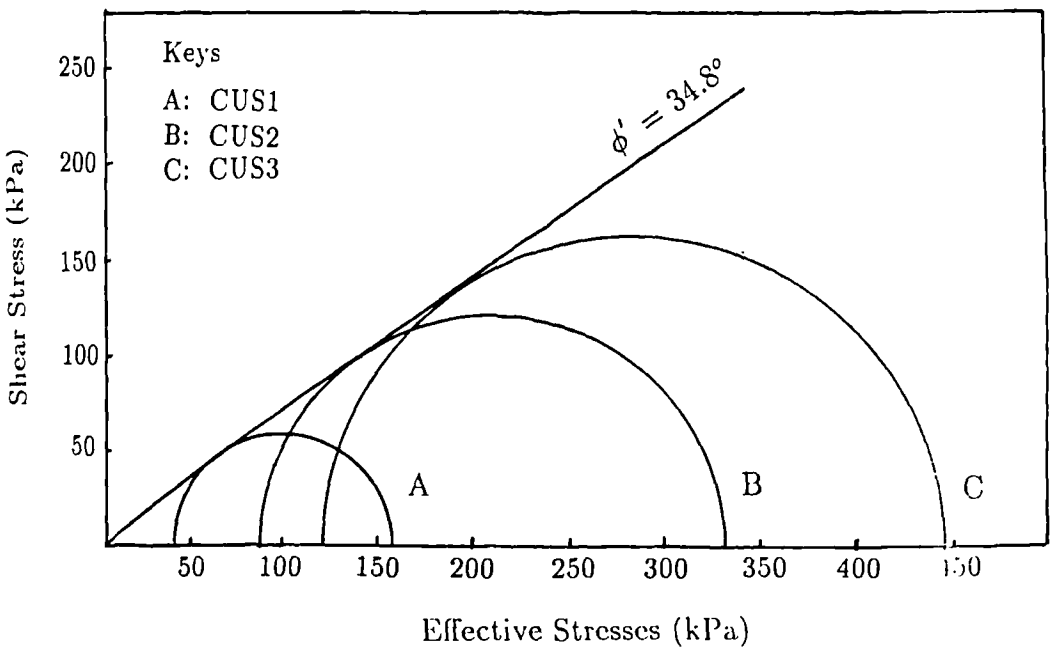

Fig. 4.12-b Mohr's rupture diagram

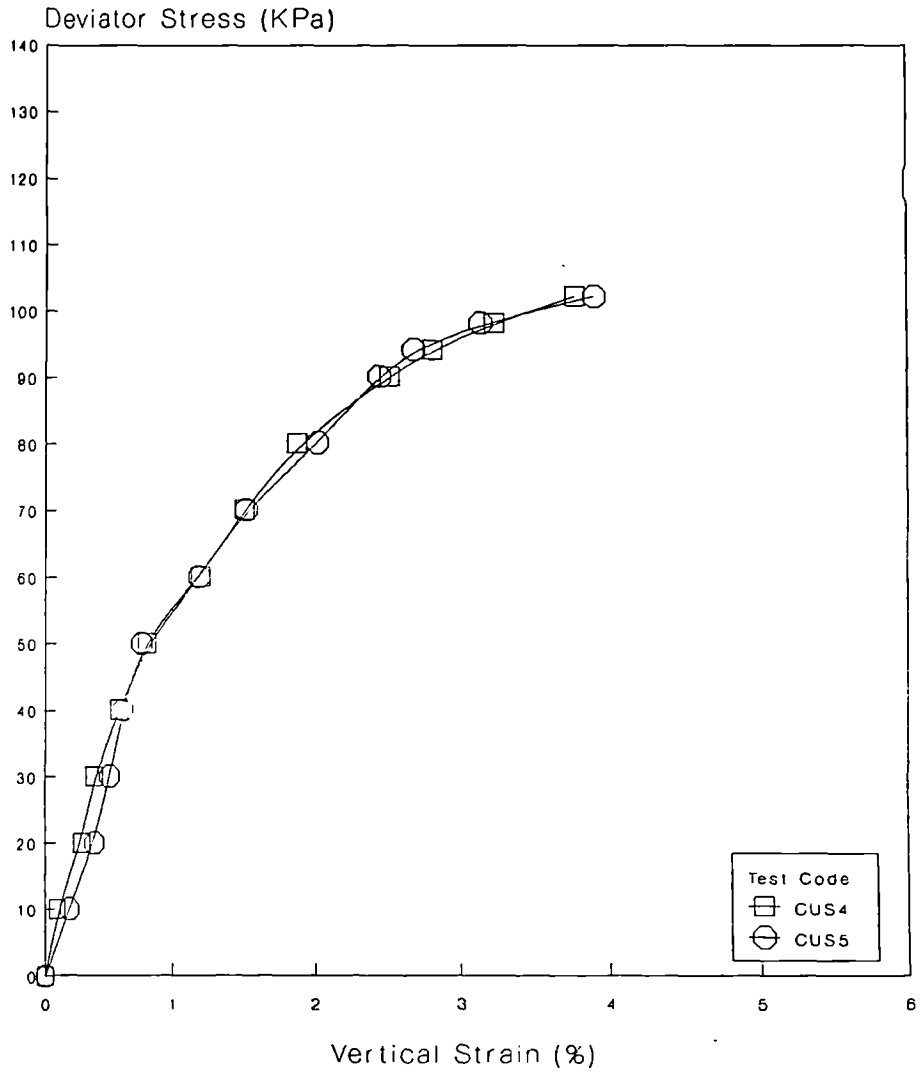

Fig. 4.13 **Stress-strain behaviour of the saturated CS under a cell pressure equal to 48 KPa.**

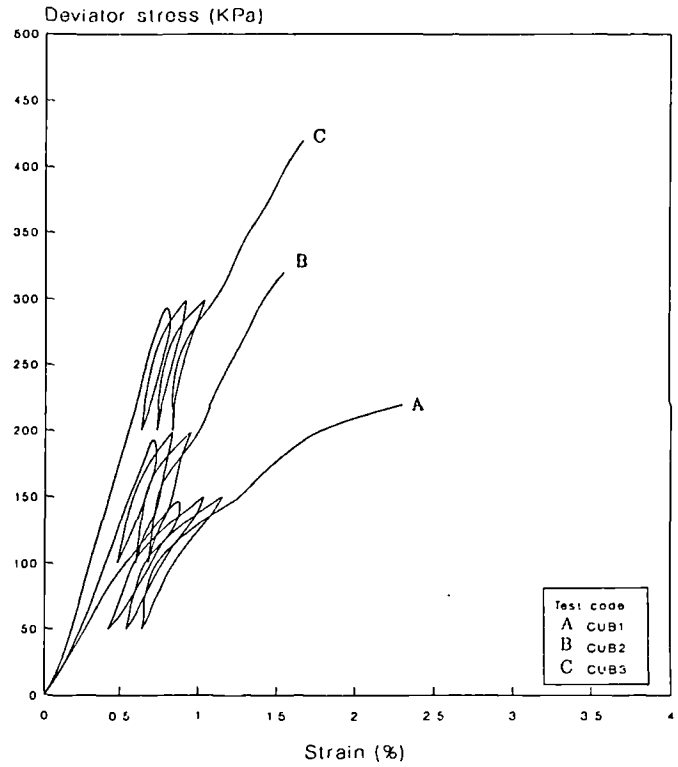

Fig. 4.14 **Stress-strain behaviour of saturated LBS specimens under three different cell pressures.**

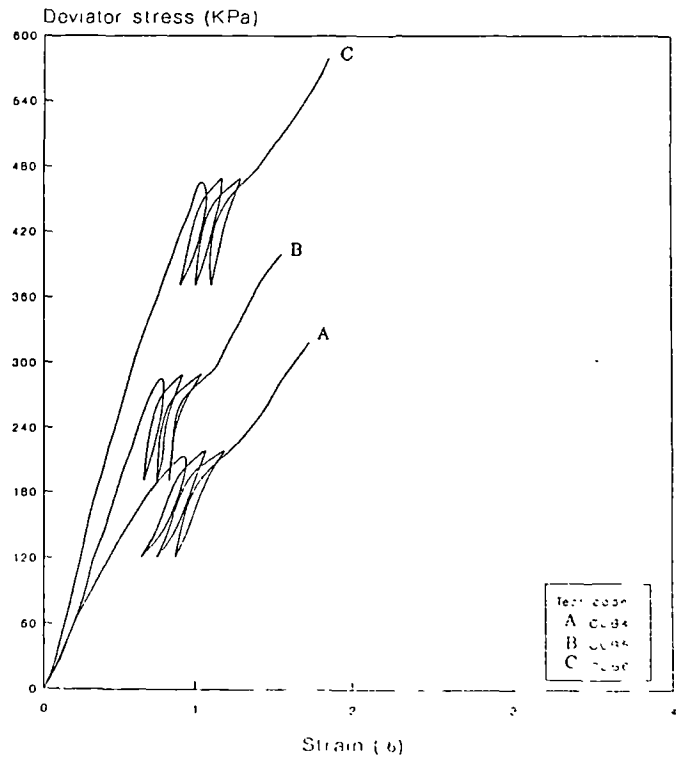

Fig. 4.15 **Stress-strain behaviour of saturated LBS specimens confined by T700 under three different cell pressures.**

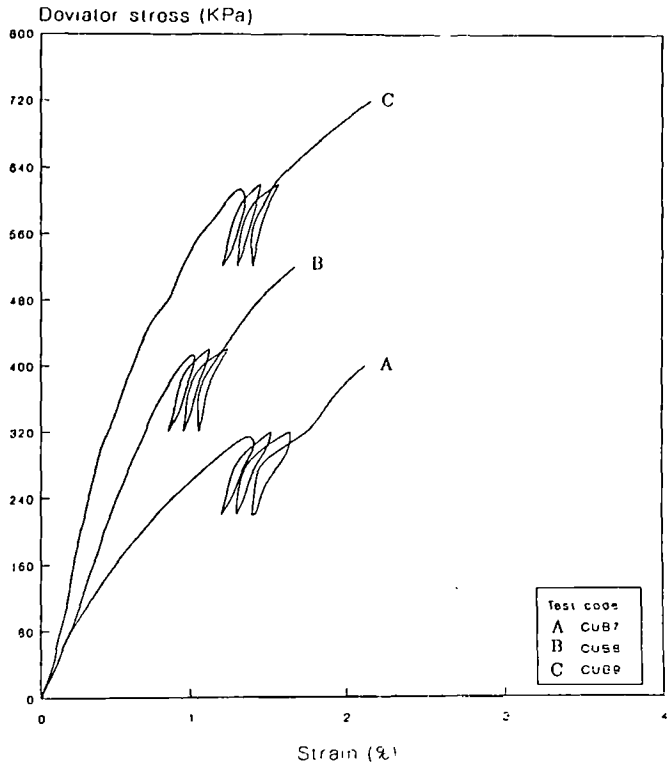

Fig. 4.16 Stress-strain behaviour of saturated LBS specimens confined by T1000 under three different cell pressures.

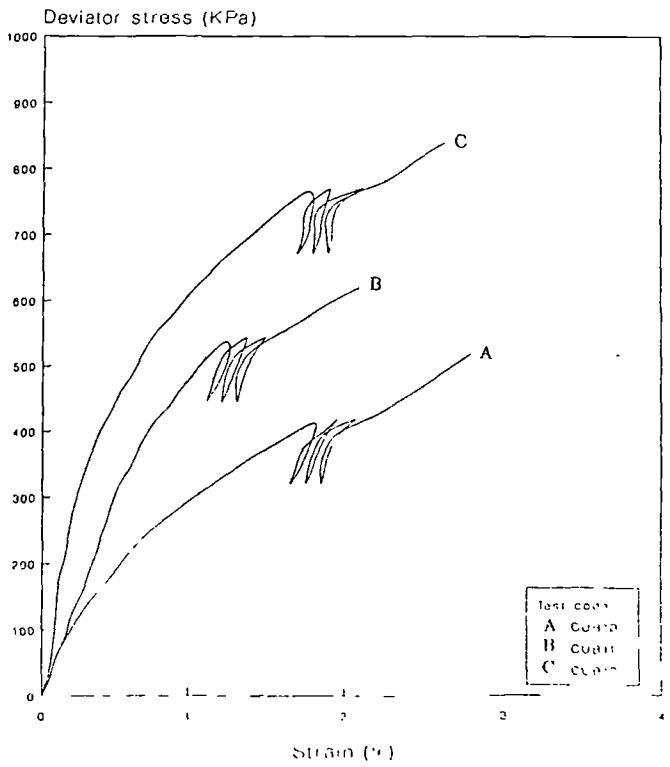

Fig. 4.17 Stress-strain behaviour of saturated LBS specimens confined by T1500 under three different cell pressures.

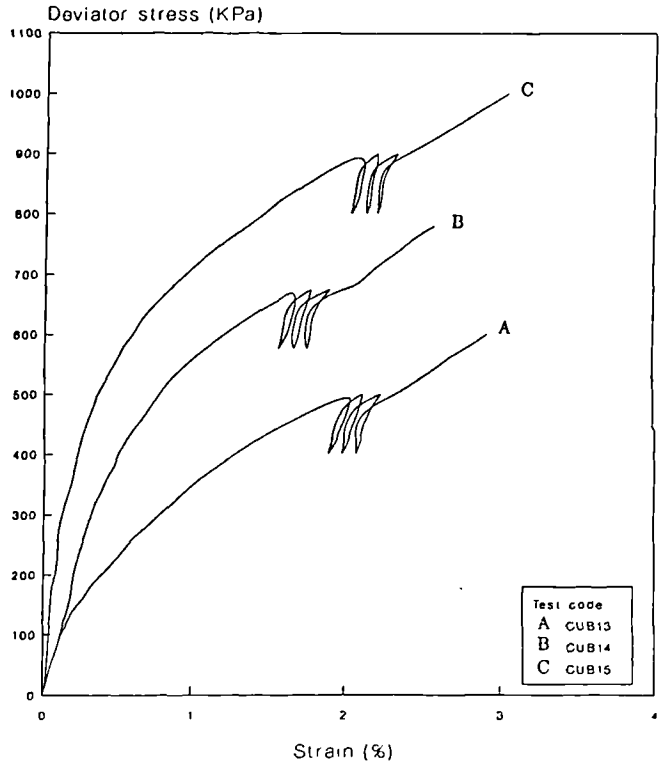

Fig. 4.18 **Stress-strain behaviour of saturated LBS specimens confined by T2000 under three different cell pressures.**

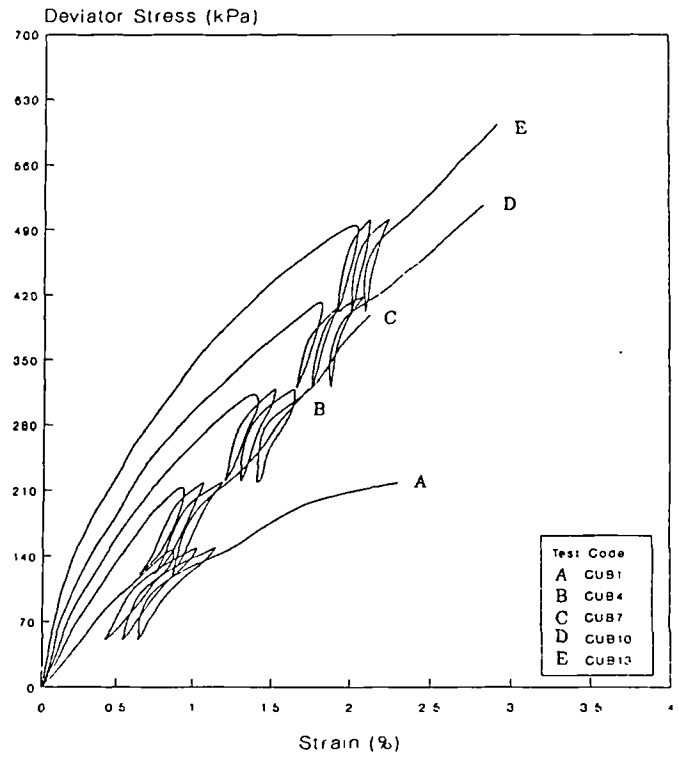

Fig. 4.19 **Stress-strain behaviour of saturated LBS specimens confined and not confined by 'Terram' (cell pressure = 40 KPa).**

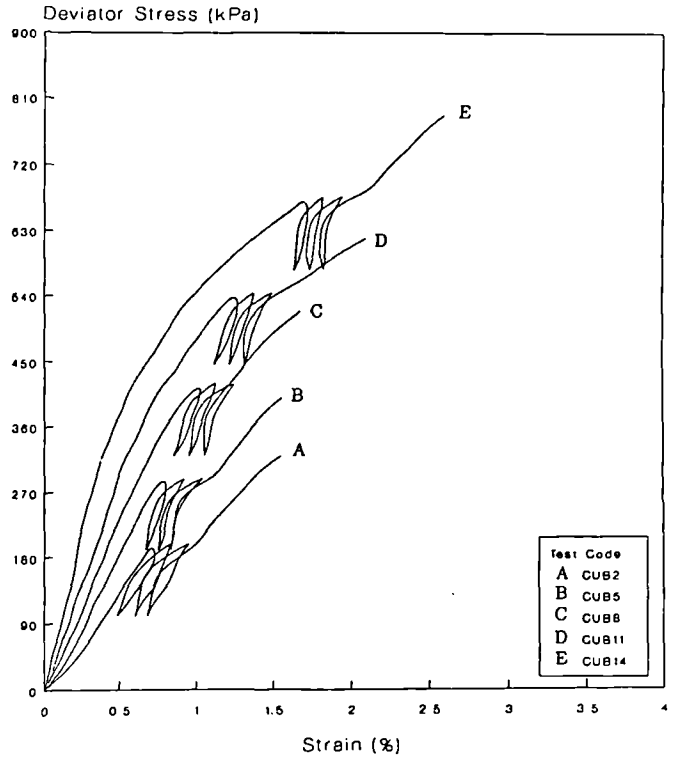

Fig. 4.20 **Stress-strain behaviour of saturated LBS specimens confined and not confined by 'Terram' (cell pressure = 80 KPa).**

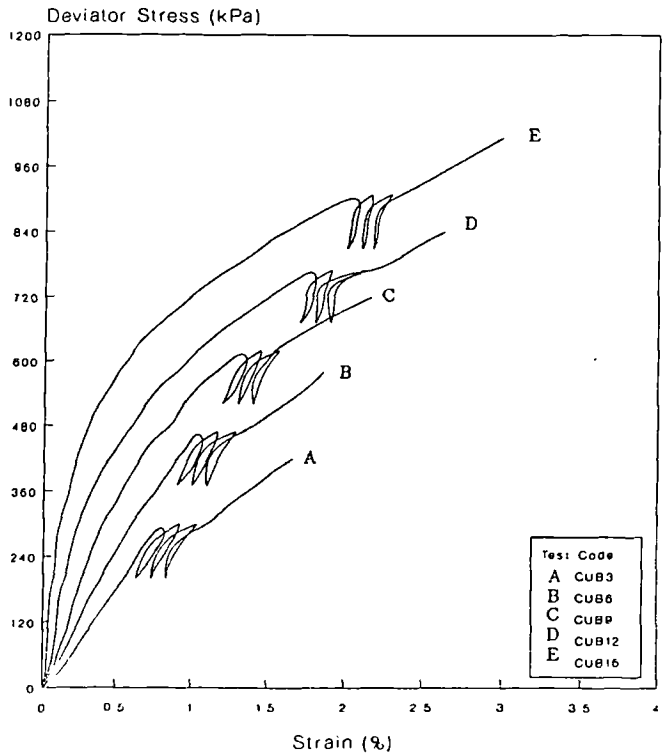

Fig. 4.21 **Stress-strain behaviour of saturated LBS specimens confined and not confined by 'Terram' (cell pressure = 120 KPa).**

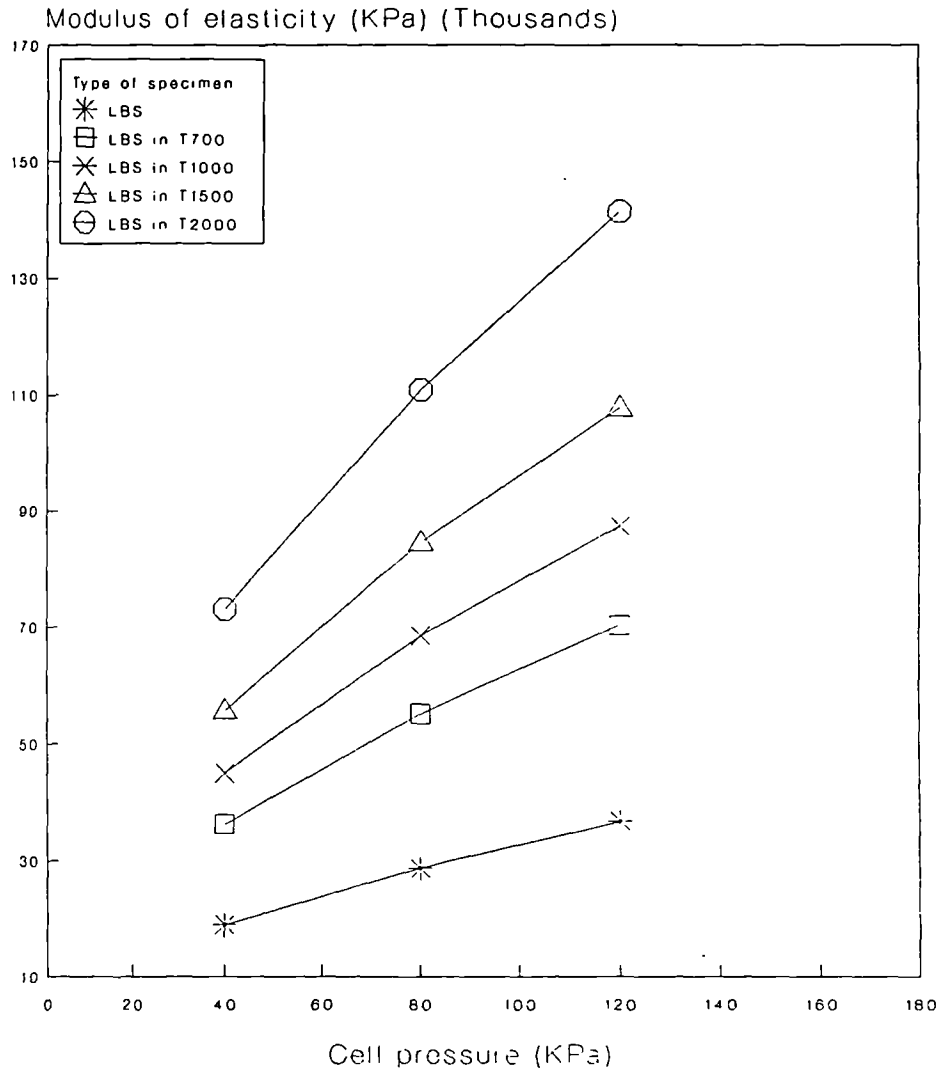

Fig. 4.22 **Elastic modulus of specimens of LBS confined by different geofabrics against the confining pressure.**

Chapter 5

The Test Apparatus and Equipment

5.1 General:

A detailed description of the apparatus and the instrumentation used in this investigation to study the performance of sand columns confined or not confined by a geofabric and rigid piles in collapsible soil is presented in this chapter. The size of test was limited to some extent by the availability of the test rig used by earlier workers for a different type of research (to study the behaviour of expanded anchors).

Two identical sets of apparatus were built for this investigation. A cross-section and an overall view of the apparatus is shown in Fig. 5.1 and Plate 5.1 respectively. The sand column or the rigid pile was installed in a collapsible soil at 4% moisture content placed under controlled conditions in a cylindrical steel container. Static loads were applied by means of a loading system using a lever arm. Overburden pressure was simulated by applying a surcharge pressure on the soil surface whereby the stress condition of the sand could be controlled.

5.2 Test Rig:

5.2.1 Description:

The test rig, as illustrated in Fig. 5.1, consists of a cylindrical steel container of 390 mm inside diameter, 520 mm deep and 17.5 mm wall thickness, closed at the bottom end by a circular steel plate 25 mm thick and bolted to the bottom flange of the cylinder. Another 25 mm thick circular plate served as a lid on the top end of the cylinder with a circular 40 mm diameter hole in the centre. This lid was provided with facilities for application of a surcharge pressure. The whole container was welded to a rigid steel frame of 55 mm × 55 mm angle sections to serve as a wide stable base to the rig.

In order to allow sufficient space for the pressure plate, the container was filled with soil up to a height of 410 mm only. The container diameter was 17 times the pile or stone column diameter. The clearance between the pile base and the container bottom was variable.

5.2.2 Effect of Wall Friction:

Up to the present time most laboratory studies on foundations involve using a container to hold the soil. An inherent drawback of the container is the development of friction between the soil and the container wall. In general this has the effect of reducing the average horizontal stress in the soil. Wall friction can be reduced to negligible proportions, if horizontal soil movement at the container walls can be tolerated. This is achieved by lining the container wall with a rubber membrane and applying a thin layer of lubricant between the wall and the membrane. The membrane is then held in place by suction.

In the present investigation wall friction was reduced to some extent by

polishing the internal wall surface and applying a very thin layer of silicone grease on it.

An experimental investigations carried out by Potyondy (1961) and Chan (1976) showed that the beneficial effect of the lubricant is clear. Chan concluded that the effect of not applying the lubricant was to reduce the compressive ultimate bearing capacity of a test pile by 41%.

5.2.3 Size Effect of the Container:

The size of the soil container can have a direct effect on the observed pile behaviour, because at the boundaries of the soil mass, the stress-strain response of the container walls is not the same as that of the soil. Therefore, ideally, the size of the container should be such that the change of stresses at the boundaries are negligible.

According to Banerjee (1970) piles do interact even beyond 8 diameter distance. Based on this, the diameter of the sand columns and the piles were chosen so that this problem was overcome.

5.3 Surcharge Pressure System:

An air/water pressure system was used to produce a surcharge pressure on the soil surface. This system consisted of an airtight pressure cylinder, Plate 5.2, which was connected to an air compressor through an adjustable pressure regulator to keep a certain amount of constant pressure in the cylinder. It was also connected through a hard rubber tube to one of two klinger valves fitted on the top lid of the soil container. The pressure cylinder can also be used to fill the pressure chamber with water prior to each test.

The pressure chamber, as shown in Fig. 5.1, is the space formed between

the pressure plate and the top lid of the soil container. The pressure plate, Plate 5.3 , consisted of a 6 mm thick aluminium plate, 385 mm in diameter bolted firmly to a perspex plate with the same diameter, 25 mm thick at the rim and dished to zero thickness near the centre. Both plates had a 40 mm central hole. A 40 mm diameter, 160 mm high stainless steel tube with a flange at one end (with a groove in which an 'O' ring was fitted) was bolted to the steel plate (on the perpex plate side) such that it trapped a convoluted rubber membrane, Plate (5.3). The convolution allowed the extension of the membrane as the soil sample decreased in volume.

The membrane was manufactured in the laboratory fulfilling the following considerations:

- The thickness of the rubber membrane must be such that it is impermeable to pressurised water.
- Must have a low resistance to expansion.
- Must be capable of transmitting the applied pressure directly to the soil sample.

The details of manufacturing process are given in Appendix (D).

This rubber membrane passes smoothly over an 'O' ring placed in a groove cut on the top flange of the soil container. The seal prevented any leakage of water from the pressure chamber to the soil.

The pressure chamber in this system can withstand pressures up to 400 kN/m^2 without leakage.

The purpose of the surcharge pressure on the sand surface was to create a certain effective depth of the pile length apart from stabilizing the tests by increasing the pile's ultimate bearing capacity and reducing the size of the experimental errors. A surcharge pressure of 100 kN/m^2 on the soil surface was found adequate to achieve

the objectives mentioned.

5.4 Axial Loading System:

A lever was used to apply the compressive static loads. The lever arm, with a ratio of 6:1, as shown in Plate 5.4, rested on a thrust bearing placed on a pivot mounted on the top plate of the container. The function of the thrust bearing was for re-levelling of the lever during the test. At each point of loading or support along the lever, there were ball races to reduce friction. Load hangers were provided at both ends of the lever arm to apply the compressive force to the sand column.

The compressive force was transmitted to the top of the column by a circular plate of the same diameter as the column, which was fixed to a 12 mm diameter threaded cylindrical rod. The rod was bolted to the lever arm at the loading point where there was a clamp to hold the rod in position during levelling of the lever arm.

5.5 Test Elements:

5.5.1 Construction:

Three different types of foundation support were used during this investigation, sand columns without confinement, sand columns confined by 'Terram' with four different strengths (T700, T1000, T1500, and T2000) and rigid piles. Each type had an external diameter of 23.0 mm and embedded lengths of 250 mm, 300 mm and 410 mm.

5.5.1.1 Sand Columns Without Confinement:

The sand columns were formed inside the soil using aluminium tubes of 23.0 mm inside diameter. The thickness of the wall of the tubes was 0.56 mm. It was chosen under the condition that there was no disturbance of the column during the withdrawal of the tube. The tubes were cut and machined to the desired length with an extra length of 80 mm left at the top of each tube without machining and which had two symmetric holes of 5 mm diameter each. This arrangement was made in order to facilitate the clamping of the tubes to the centring beam during the column formation and to the extractor during the withdrawal. The centring beam and the extractor are described hereinafter.

5.5.1.2 Sand Columns Confined by 'Terram':

A rectangular piece of Terram with a specific strength was cut to form the geofabric tube which confined the sand column. The length of the piece was 50 mm greater than the desired length of the sand column. This extra length was used to accommodate the compaction hammer during the formation of the column head. It was removed at the end using scissors. The width of the piece was 4 mm greater than the perimeter of the sand column. This was left in order to be used as a joining bond.

The geofabric tube was made by gluing this 4 mm bond along the whole length with the other end of the piece. The glued joint was pressed tightly between two aluminium plates of 500 mm length, 20 mm width, and 5 mm thickness, for more than two hours to get the glue to penetrate well into the fabric structure. The pressure was provided by three clamps. At the end of the operation the clamps and the plates were removed and the resulting piece was shaped around a metallic tube of approximately 23.0 mm external diameter, for 24 hours.

The glue used was Bostik clear. It was recommended by ICI for its practical effectiveness.

5.5.1.3 Rigid Piles:

The piles were fabricated from tube of high strength aluminium alloy. The characteristics of the aluminium are shown in Table 5.1.

Each pile consisted of two tubular sections, which were:

- The pile main body, which was close ended, was carefully machined so that at the end it was very smooth.
- The pile head, 80 mm long, 25 mm diameter, which served as a hanging element of the pile in the centring beam during soil bed formation.

This head was provided with a 12 mm diameter threaded cylindrical rod, welded to its top, which served as an element of transmisson of the axial compressive force from the loading point of the lever arm to the pile head. The pile was manufactured as a whole body.

5.5.2 Measurement of Vertical Displacement:

Two different types of linear variable differential transformer 'LVDT' with an energising power supply of 5 V and 10 V, were used to measure the movement of the pile top and the soil respectively. The setting of these LVDT's is shown in Fig. 5.2.

The LVDT's used for monitoring the pile head movement (P.M.), were of type DC-LVDT-D2/100A supplied by RDP-Electronics Ltd., with a maximum travel of 50 mm and having the characteristics shown in Table 5.2.

The LVDT's used for measuring the settlement of the soil (S.M.) were of the type DC-LVDT supplied by RDP-Electronics Ltd., with a maximum travel of 100 mm. Table 5.2 summarizes some of their characteristics.

The calibration graphs of these LVDT's with a supply voltage of 5 V and 10 V are shown in Fig. 5.3.

5.5.3 Measurement of Horizontal Displacement:

An attempt was made to measure the horizontal movements within the soil mass due to the expansion of the sand column by using 8 horizontal sand movement gauges shown in Fig. 5.4. These gauges were similar to those developed by Carr (1970).

The horizontal movement gauge comprised a conductor tube 2 mm in diameter, a moving rod of 1.5 mm in diameter and a moving footing attached to the moving rod. The conductor tube was fixed to the wall of the container by a guide screw. The horizontal movement gauges were installed at right angles to each other (4 at each side) at the positions shown in Fig. 5.5. The gauges were placed in the sand mass at the required positions during soil bed formation. The displacement of the moving rods due to sand column expansion were measured using LVDT's.

These LVDT's were of the type 8FLP10A supplied by RDP-Electronics Ltd., with a maximum travel of 10 mm and having the characteristics shown in Table 5.3.

Unfortunately no horizontal displacements were monitored during the tests. On the contrary, during the preliminary tests it was noticed that, instead of having the rods moving in the outside direction of the container, they were going inside it. At the end of the tests and after removing the soil, it was found that all the rods were deformed and inclined instead of remaining horizontal. This phenomenon was repeated at anytime when the horizontal movement gauges were used, and this

confirmed that, this technique is not suitable for this kind of soil when inundation from the bottom causes significant soil collapse.

Another study was carried out in order to use the instrumentation system developed by Selig et al (1970) for measuring horizontal soil strain. The technique was called the radial strain method and it was first used in this department by Eid (1978) for measuring the radial deformations from cavity expansion in clays.

The strain gage system consists of two basic components, a pair of embedded sensors and an external instrument package. The sensors consist of two disc-shaped coils which are placed in the soil in parallel and coaxial alignments.

Again this technique was not used, since the strain behaviour of the collapsible soil during inundation made it impossible to keep the disk-shaped coils parallel and coaxial.

Other methods were proposed, but because of their costs, they were abandoned.

5.6 Method of Inundating the Soil Stratum:

The system used to inundate the soil stratum consisted of two cylindrical plastic tanks mounted vertically on a wooden board. The longest tank (tank A), of 1000 mm height and 75 mm diameter, was connected to a hole of 30 mm diameter at the bottom centre of each container. It was placed approximately 50 mm higher than the base of the containers in order to keep the movement of the water very slow. The other tank (tank B), of 800 mm height and 250 mm diameter, was placed a little higher than the tank A (about 50 mm), and was connected to a tap from the bottom. Both tanks were connected to each other from the bottom. All the

connections were made through rubber tubes and were controlled by small taps. The level of the water was controlled by small burettes attached to the tanks (Fig. 5.6).

5.7 Ancilliary Equipment:

5.7.1 Compaction Apparatus:

a) The compaction apparatus depicted in Fig. 5.7 was designed for compacting the collapsible soil in the container. It consisted of a 150 mm diameter aluminium plate of 8 mm thickness, which was screwed to one end of a 400 mm solid rod, and a 2 kg dead mass which slides freely along the rod.

b) The compaction of the sand column was performed by using a special hammer. The hammer was composed of two parts. During compaction, one part was kept immovable and the other in motion. The immovable part consisted of a small cylinder made of brass of 35 mm in height, which was screwed to one end of a 800 mm solid rod of 6 mm diameter. The cylinder of brass had approximately the same diameter as the column. The other part consisted of a dead mass fixed to the top end of a 560 mm brass tube of 12 mm inside diameter. The tube and the mass, which weighted 500 g, could slide freely along the rod (Fig. 5.8).

5.7.2 Centering Beam:

A centering beam, of 550 length, 38 mm width and 6 mm thickness (Fig. 5.9), was used to hold the tube, which formed the sand column, in the centre of the container. This plate was provided in the centre with a circular hole of 25 mm diameter around which, a small cylindrical tube of 50 mm height, 6 mm thickness and the same

diameter as the hole, was welded. The tube was provided by a screw which served as a clamp.

5.7.3 Extractor:

An extractor, shown in plate 5.5, was used to pull out the tube forming the sand column after finishing the compaction of each layer. It comprised two parts:

1- The extracting part:

This part had the shape of a 'T' and formed the mobile part of the extractor. The vertical element was a 12 mm diameter threaded rod provided at its end by a special instrument which served as the clamping part and made so that it prevented any revolution of the tube during pulling out. The principle of its functioning is similar to that of a ball race. This element was bolted at the other end to a rectangular plate of moderate size to serve as a handle which facilitated the revolution of the extracting rod.

2- The Guiding Parts:

They consisted of a circular plate and a crown, of 8 mm thickness, bolted to the top and bottom ends of four treaded rods, of 12 mm diameter and 450 mm height, respectively. The circular plate, which is shown in Fig. 5.10-a, had in its centre a small tube threaded on the inside. The role of the tube was to hold and guide the 'T' element. The bottom crown, shown in Fig.5.10-b, was fixed to 4 plates of 225 mm length, 38 mm width and 10 mm thickness. These plates served as a base for the extractor by which it can stand on the top of the container.

5.7.4 Sand Scraper:

A sand scraper, shown in Fig. 5.11, was used to level the sand surface under the surcharge plate without touching the sand column or pile shaft or disturbing the initial setting.

5.7.5 Cleaning Equipment:

The following equipment was used for cleaning the soil container before each test:

1. Steel wire brush: Used to brush the walls of the container to remove grease 'soaked' soil particles clinging to the walls.

2. Mop: this is made of a long aluminium tube around the end of which sponge layers were wrapped. When the container's walls were rubbed with this it removed fine soil particles and silicone grease from the container's walls.

3. Grease applier: consisted of a rectangular piece of wood to which a sponge was nailed, the wooden piece was connected to an extended aluminium tube handle. Silicone grease was placed on the sponge and hence applied to the container's walls.

High Strength Aluminium Tube	1.6% Copper
Contains:	2.5% Magnesium
	0.23% Cromium
	5.6% Zinc
	90.07% Aluminium
Ultimate Compressive Strength	572 N/mm^2
Weight	0.032 gm/mm length
Young's Modulus (E_p)	70000 N/mm^2

Table 5.1 Material Properties of the Rigid Pile

LVDT Type	Linear Range	Calibration Factor (mm/mV)	Maximum Energising Power Supply	Average Sensitivity (V/mm)
P.M.	100 mm	1.009 $\times 10^{-2}$	15 V	0.15
S.M.	50 mm	1.034 $\times 10^{-2}$	10 V	-

Table 5.2 **Characteristics of the LVDT's used to Measure the Vertical Displacement**

LVDT Type	Linear Range	Tolerance	Maximum Energising Power Supply	Weight
8FLP10A	12 mm	$\pm$ 1.0%	10 V	5 g.

Table 5.3 **Characteristics of the LVDT's used to Measure the Horizontal Displacement**

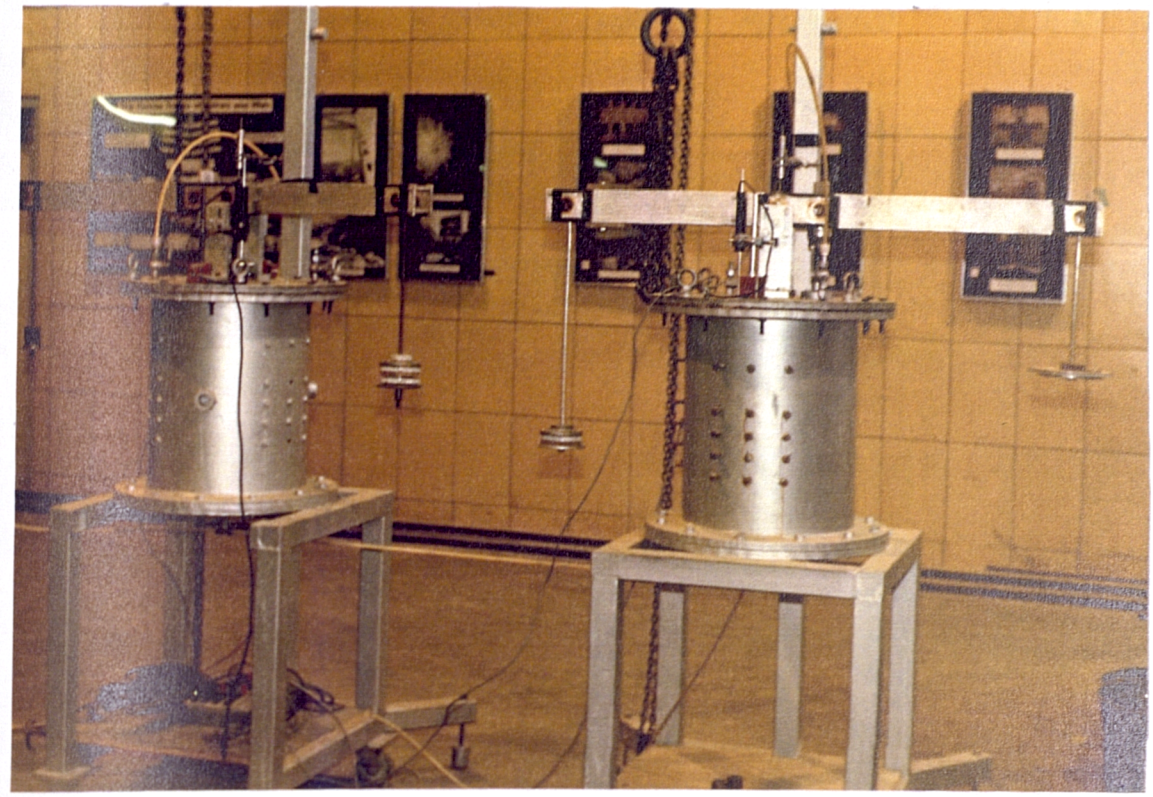

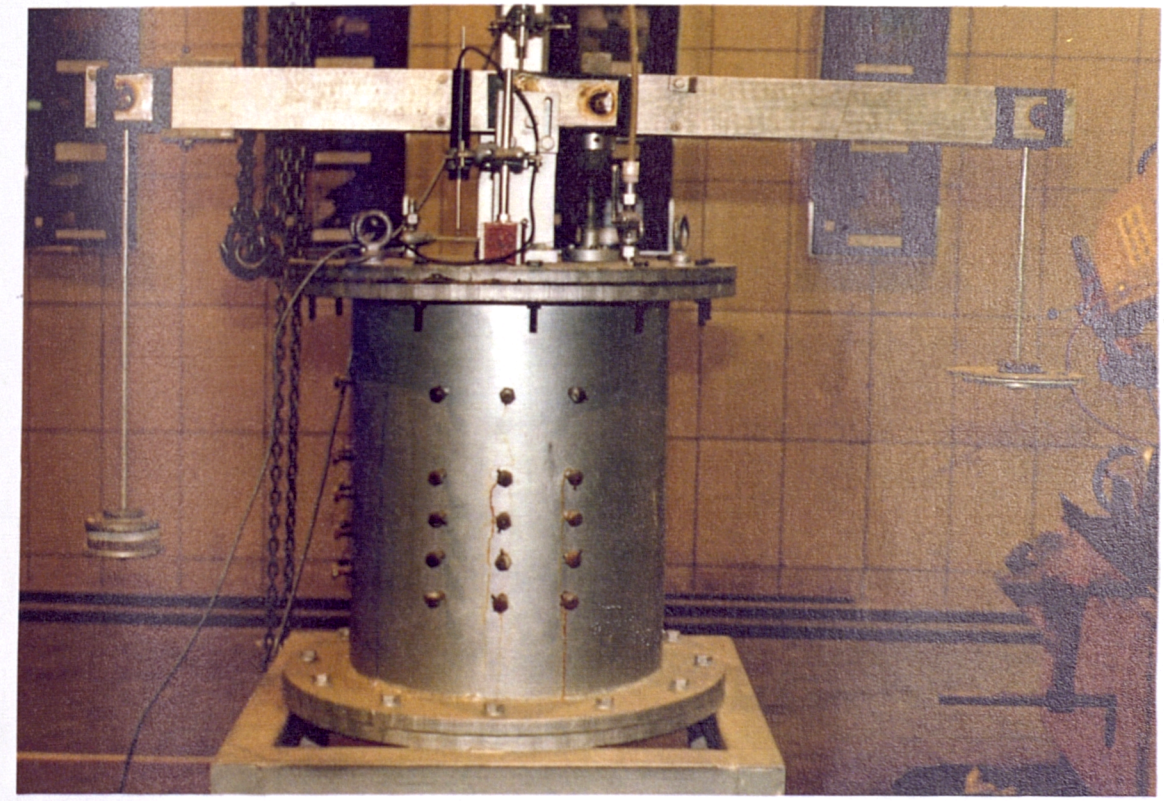

Plate 5.1 Overall View of the Apparatus

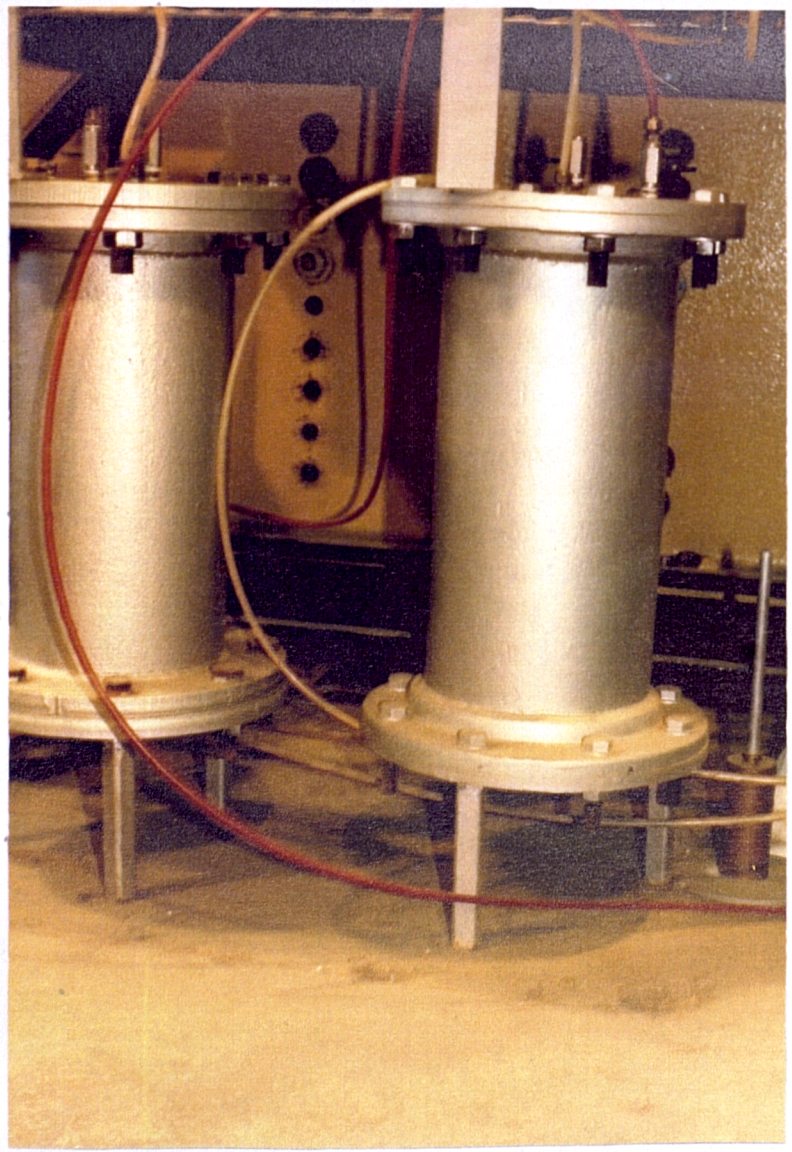

Plate 5.2 Pressure Cylinders for Surcharge Pressure System

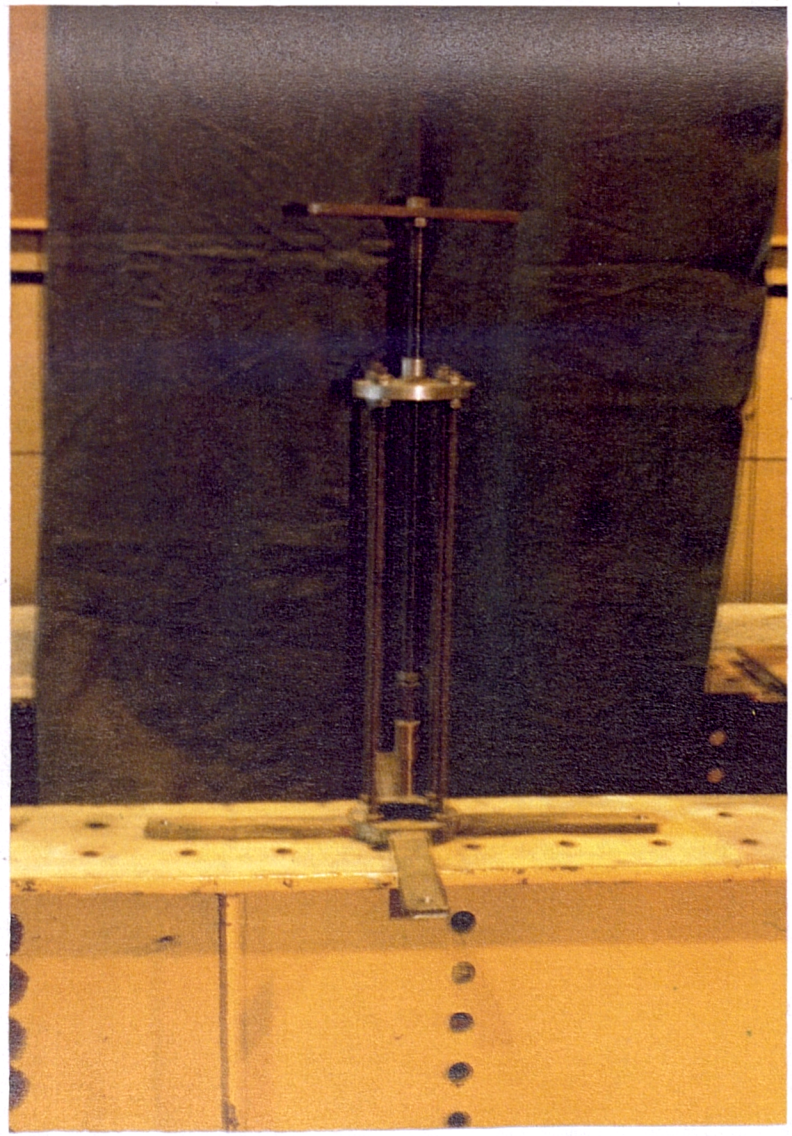

Plate 5.5 The Extractor

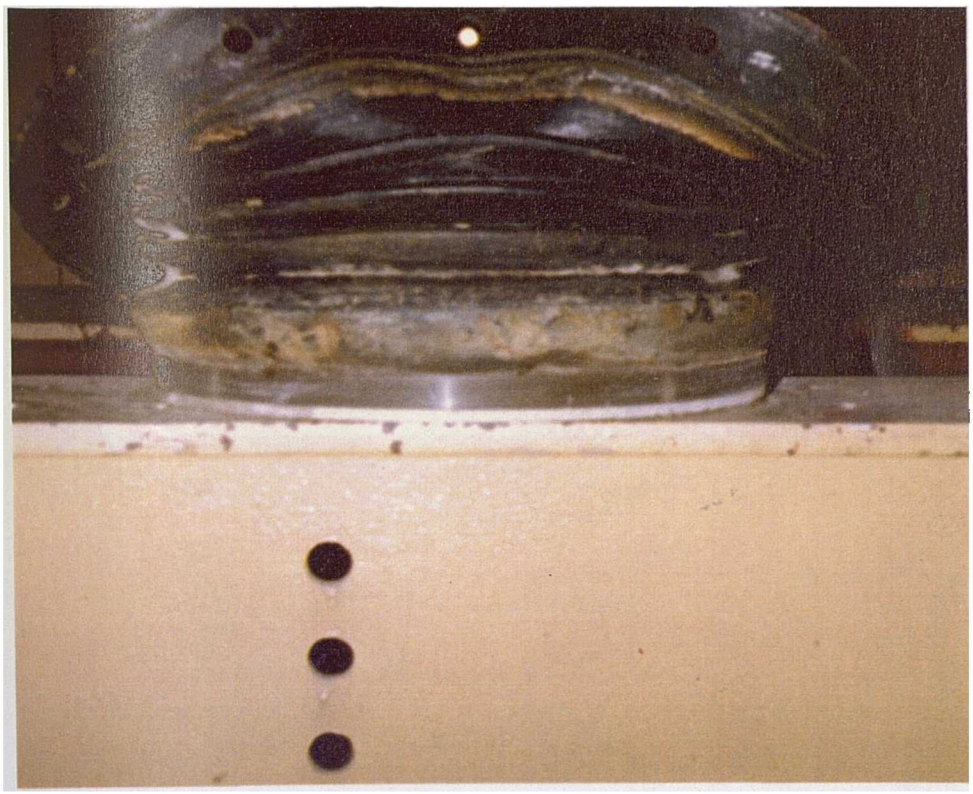

Plate 5.3 The Pressure Plate and the Convoluted Rubber Membrane

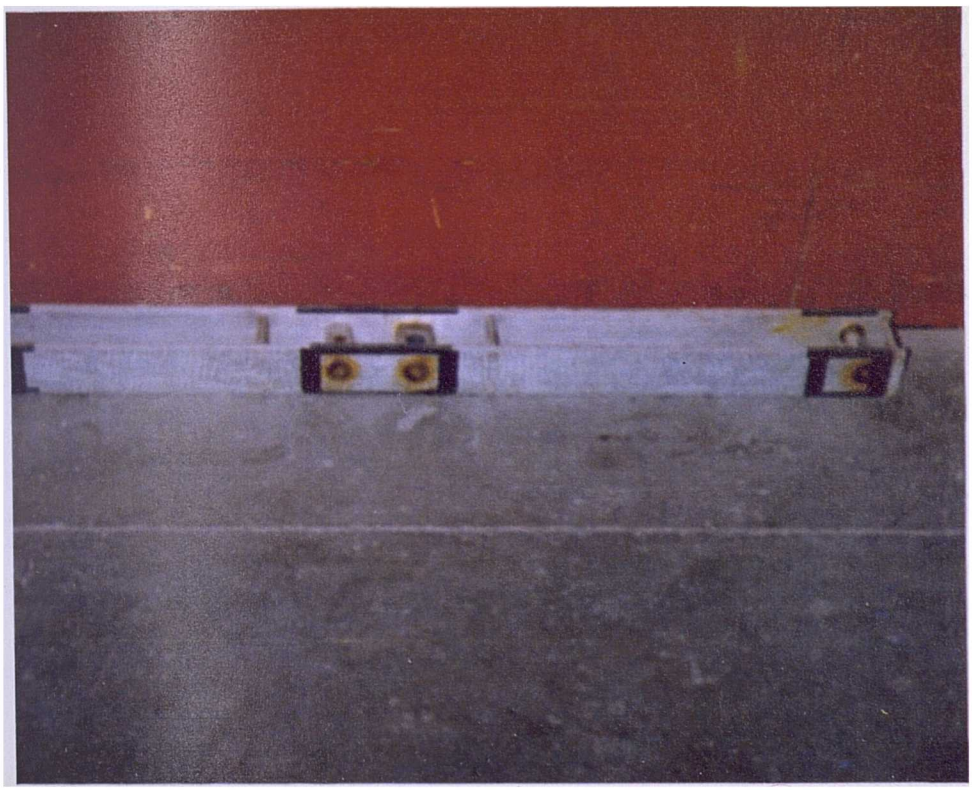

Plate 5.4 A Lever Arm

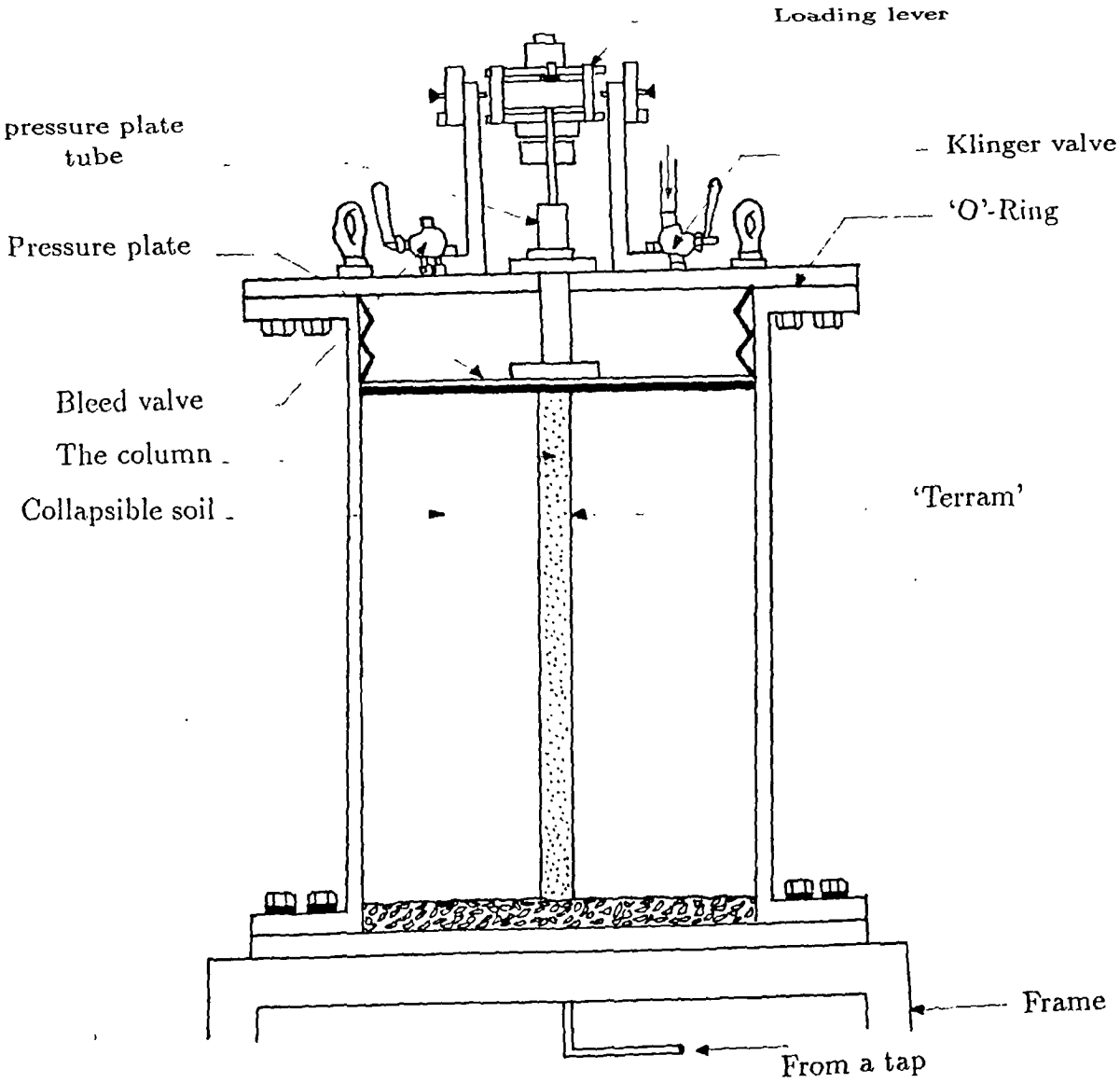

Fig. 5.1 Cross-Section of the Apparatus

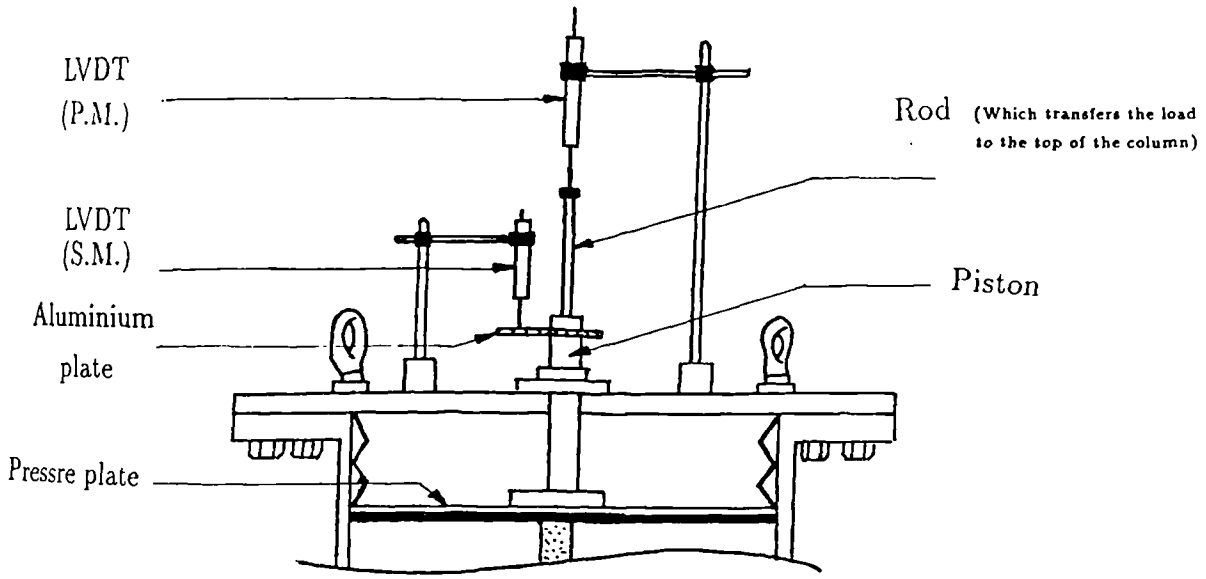

Fig. 5.2 Setting up of the LVDT's on the Top of the container

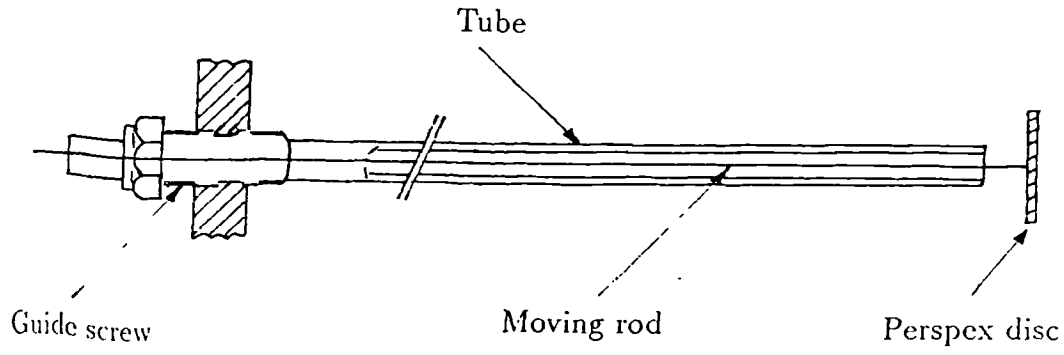

Fig. 5.4 Horizontal Sand Movement Gauges

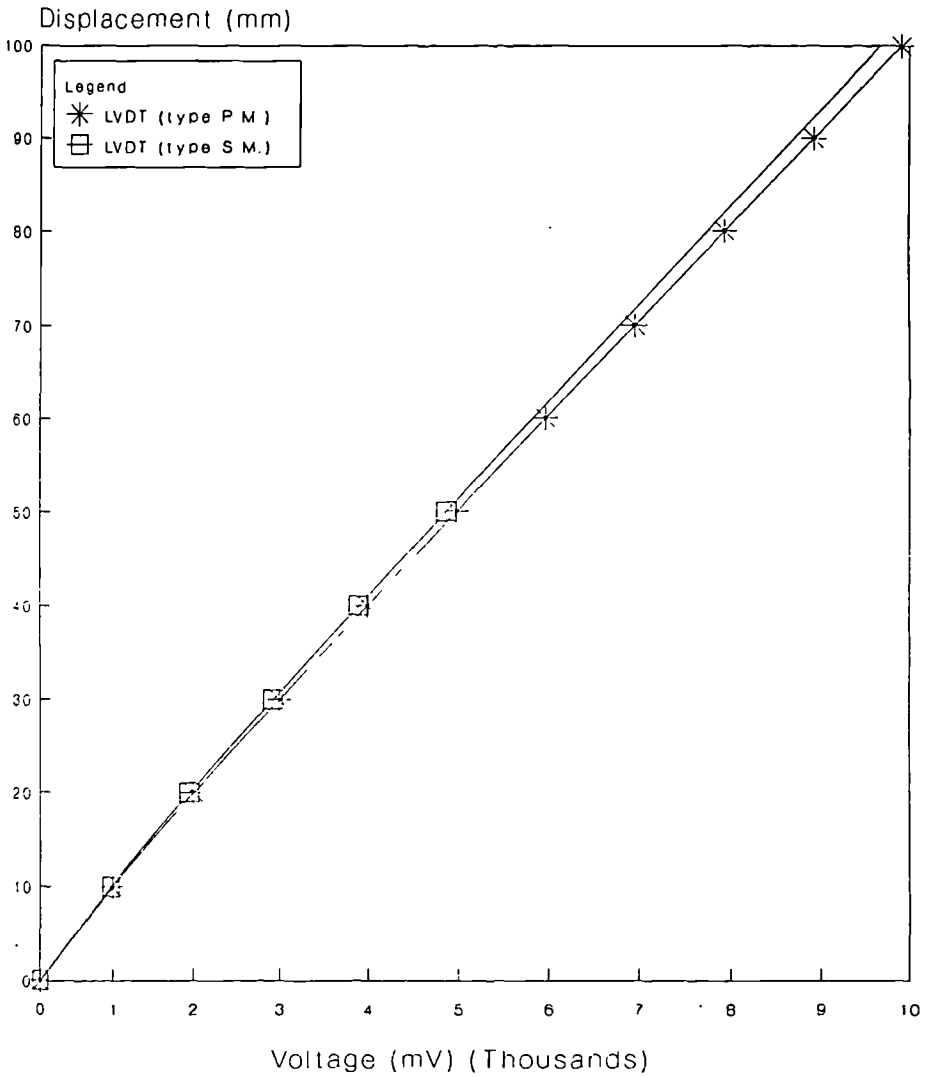

Fig. 5.3 Calibration graphs for LVDT's.

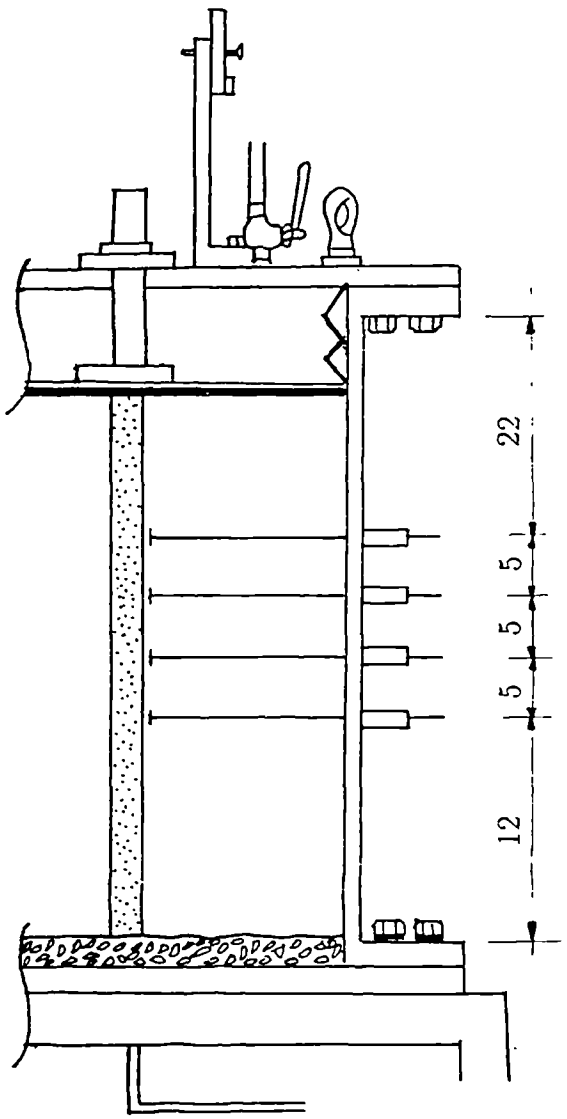

Fig. 5.5 Arrangement of the Movement Gauges on the Wall of the Container

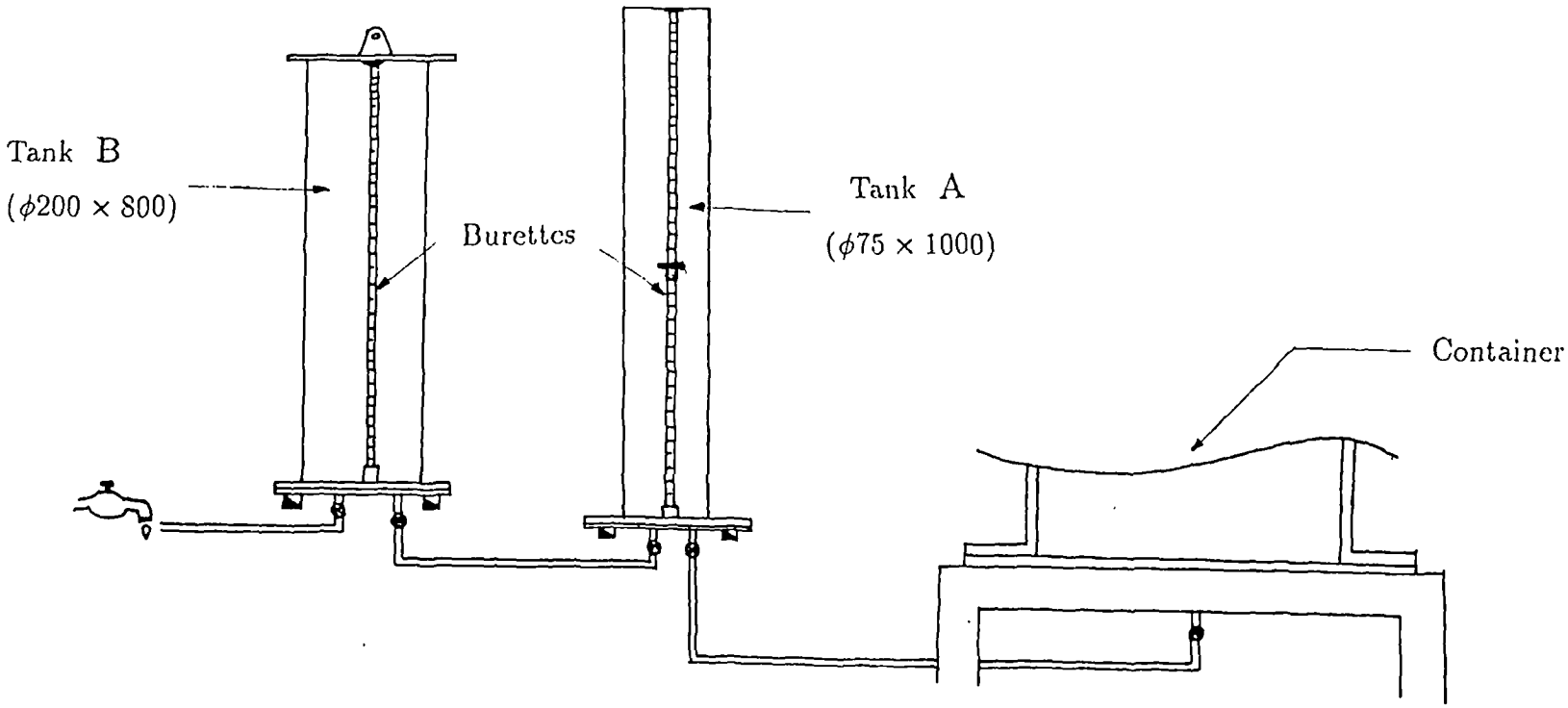

Fig. 5.6 The System used to Inundate the Soil stratum

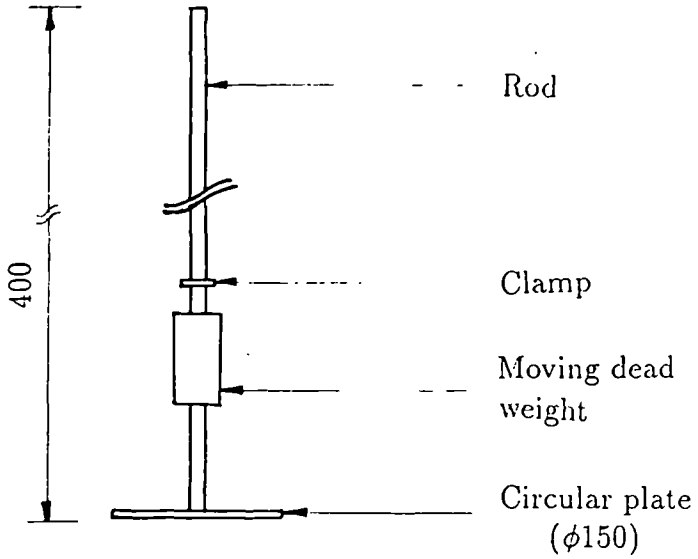

Fig. 5.7 The Compaction Apparatus used to Compact the Collapsible Soil in the Container

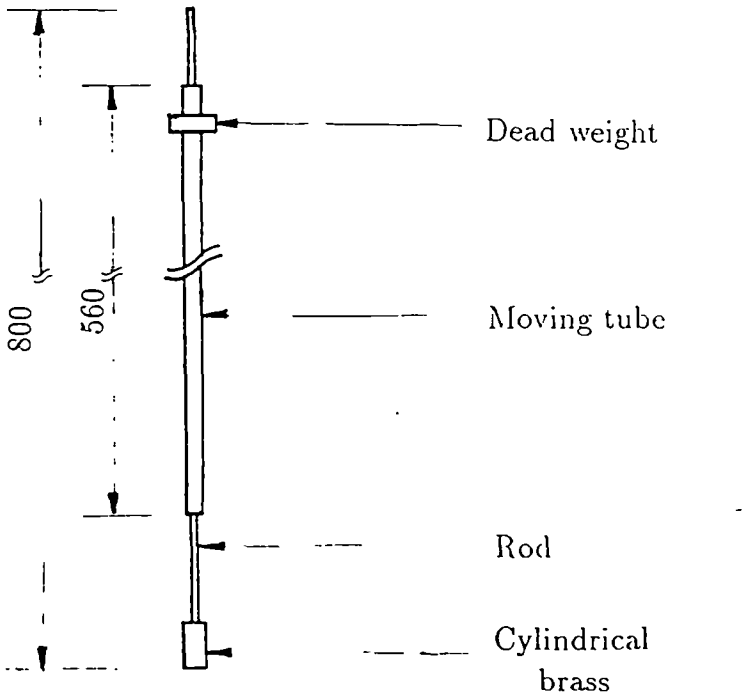

Fig. 5.8 The Compaction Hammer used to form the Sand Column

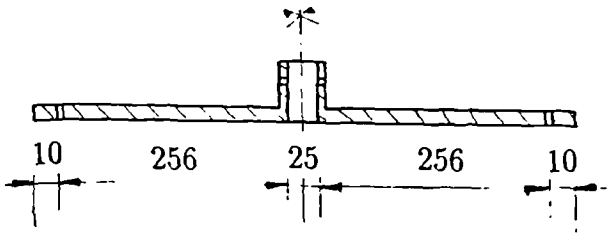

Fig. 5.9 The Centering Beam

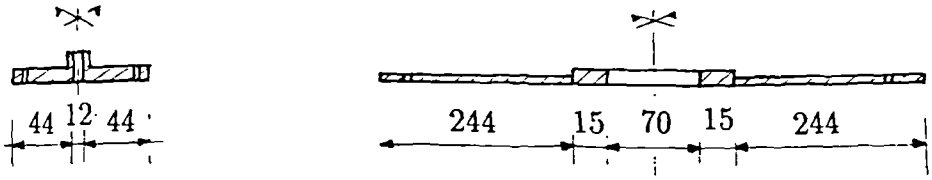

Fig. 5.10-a The Top Circular Plate of the extractor
-b The Bottom Crown of the Extractor

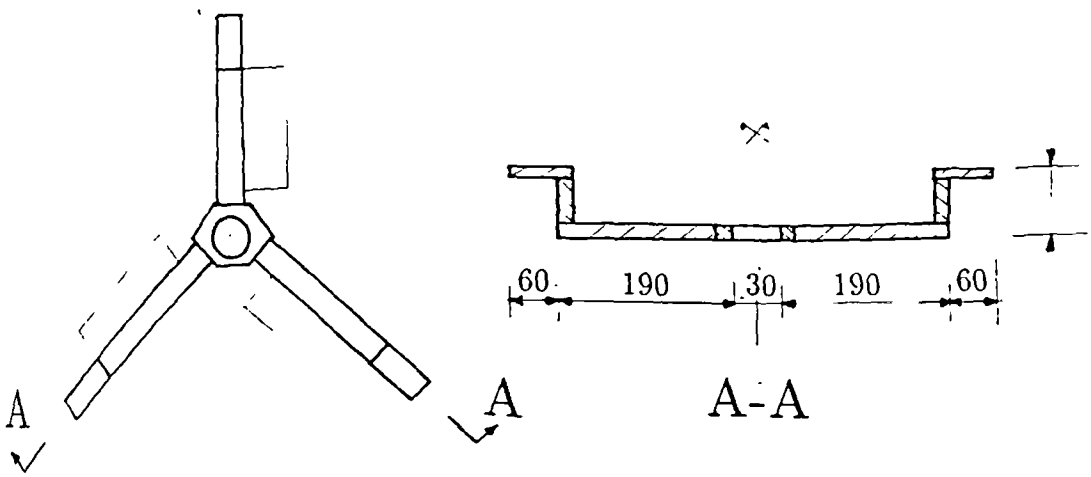

Fig. 5.11 The Sand Scraper

Chapter 6

Test Programme and Experimental Procedures

6.1 General:

In this chapter details of the testing programme, test preparation and technique are outlined along with an insight into the properties of the collapsible soil and the sand forming the 'pile' used in this investigation.

Tests on a single sand column encapsulated or not encapsulated in a 'Terram' fabric and a rigid pile were carried out to study the effects of different stiffnesses and lengths of 'pile' on its bearing capacity, settlement and general performance after inundation.

Six different stiffnesses of 'pile' were adopted with three different lengths for each type. The 'piles' employed were, a sand column without encapsulation, a sand column confined by 'Terram' fabric of the types, T700, T1000, T1500, and T2000, and a rigid pile. The lengths chosen were, 250 mm, 300 mm and 410 mm (for the case of full penetration).

6.2 Properties of the Soil:

6.2.1 Collapsible Soil:

The soil used was a gap graded soil. It was composed of three components which were locally available; 78% of concrete sand, 10% of Leighton Buzzard sand less than 90 microns, size, and 12% of speswhite kaolin clay.

Based on laboratory analyses (sieving and sedimentation) and on the results of previous researches on kaolin in this department (Rice, 1975 and Eid, 1978) the particles size distribution curve is presented in Fig. 6.1. The soil consisted of 80% sand; 5% silt and 10% clay).

The specific gravity of particles was 2.65. The optimum moisture content, which was obtained by standard proctor compaction method, was 9% (Fig. 6.2). The moisture content of the soil was 4%. It was chosen on the dry side of optimum. Maximum and minimum dry densities were 2.02 Mg/m^3 and 1.37 Mg/m^3, which corresponded to minimum and maximum void ratios of 0.30 and 0.93 respectively. The liquid limit and plastic limit were 20% and 13.5% respectively. The angle of internal friction measured by standard triaxial tests (at dry density of 1.54 Mg/m^3) was 31^o.

The usual raining methods used to obtain uniform beds of sand in similar containers were excluded for two reasons. Firstly, the soil was not dry and the slow pouring of the soil from a certain height reduces its moisture content. Secondly, Bieganousky and Marcuson (1976) have stated that only medium dense specimens can be formed using this method. This doesn't agree with the relative density of the soil bed constructed for this work. The compaction method adopted is described in Sub-Section 4.7.1.

The working dry density was 1.54 Mg/m^3. It was determined by applying

the principle of the relative density beside some of the criteria suggested for collapse identification which were based on dry density and other parameters relationships. Table 6.1 summarises some of these values.

6.2.2 Sand Forming the Sand Columns:

The sand used was a coarse uniformly graded sand, Fig 6.3. Its grading was located between 1.18 mm and 2.36 mm sizes. It was locally available in bags and didn't need to be washed. Its maximum and minimum dry densities, found by Kolbuszewski's (1948) method, were 1.98 Mg/m^3 and 1.45 Mg/m^3, which corresponded to minimum and maximum void ratios of 0.34 and 0.82 respectively. The angle of internal friction measured by standard triaxial tests was 41^o.

6.3 Testing Programme:

The testing programme can be split into the following series:

1. Series I: Tests of checking and proving,
2. Series II: Tests on 'piles' in the 'dry' condition,
3. Series III: Tests on 'piles' in the inundated soil.

6.3.1 Series (I):

The purposes of this series were:

- To check the collapsibility of the soil prepared.

- To determine the height of the capillary rise in the soil mass inside the container.
- To check the repeatability of the testing procedure.
- To investigate the performance of a sand column in a collapsible soil during and after inundation.

6.3.2 Series (II):

This series consisted of tests carried out on sand columns encapsulated in none, T700, T1000, T1500, and T2000 reinforcement and rigid piles in order to determine their bearing capacity. The series was divided into three groups composed of 6 tests each. Each group corresponded to a single pile depth of embedment. The pile depths were 250 mm, 300 mm, and 410 mm. All the tests were carried out at a surcharge pressure of 100 KN/m^2 with a soil density of 1.54 Mg/m^3 and a moisture content of 4%.

6.3.3 Series (III):

The purpose of this series was to determine the settlements of all types of foundation support mentioned in series (II) and the soil around it after inundation. The inundation for each single type was performed under three different working loads. The loads adopted were 20%, 50% and 80% of the ultimate bearing capacity.

Details of the different tests in series (II) and (III) are shown in Fig. 6.4 and in Table 6.2. Series (III) consisted of three sub-series. Each sub-series, which corresponded to a single working load, was divided in its turn into three groups similar to those of series (II).

Code names were given to each test to clarify the conditions and the

number of that test in a given series. The letters appearing in the code name have the following meaning:

BC: bearing capacity

ST: settlement

Gr: Group

Pu: ultimate load

6.4 Testing Procedure:

The following procedure in general terms applied to all tests included in series (II) and (III) and groups (c) and (d) of series (I) mentioned in section (6.3) apart from some basic differences which will be mentioned, wherever it is found to be necessary.

6.4.1 Rig & Soil Preparation, Soil Bed Formation and Sand Column or Pile Installation:

6.4.1.1 Rig Preparation:

At the beginning of each test the rig was cleaned by the use of a steel wire brush and the cleaning equipment mentioned in sub-section (5.7.5). The debris of grease-soaked sand particles were vacuumed from the bottom of the sand container. Silicon grease was smeared on the container's wall in a thin layer to reduce wall effects, wall friction and ensure the uniform distribution of the surcharge pressure throughout the depth of the container.

6.4.1.2 Soil Preparation:

To set up one test, about 75 kg of dry soil composed of the right amounts of dry concrete sand, Leighton Buzzard sand (less than 90 microns) and Koalin clay, were prepared. The procedure for the preparation was simple and reproducible. The required amounts of the aforementioned three components were weighed, then mixed in a big mixer of a capacity of 100 kg. About 3.0 kg of water was added to the mixture which was remixed to obtain a collapsible soil at 4% moisture content. The soil was quickly removed from the mixer and placed in a plastic bin. The top of the plastic bin was covered, first, by a plastic sheet then by its cover. This precaution was made to prevent the loss of the water content. The bin was carried from the mixing room to the testing rig by a trolley.

This operation was repeated at the beginning of each test because all the soils tested were thrown away after use to avoid contamination.

6.4.1.3 Soil Bed Formation:

The soil filling process consisted of the following steps:

1- The hole situated at the bottom centre of the container, which was made for the purpose of inundation, was closed by a plastic disc filter of 4 mm thickness. The plastic filter prevented the blockage of the hole with aggregates.

2- A thin uniform layer of clean aggregates of 30 mm thickness was placed at the bottom of the container. This layer, which was well compacted, has the role of distributing the water uniformly through the whole base of the soil mass during inundation.

3- Depending on the nature of the test, one of the three following instruments, a thin aluminium tube (column former), a solid rod encapsulated in the desired Terram

fabric or a rigid pile, was installed vertically in the centre of the container using the centring plate. The vertical position of the instrument was controlled by a spirit level.

4- The soil, which was prepared and stored in a plastic bin, was placed with great care in the container using the scoop shown in Plate 6.1. The scoop, during the entire soil filling, was always kept a few millimetres above the soil surface. The soil was modestly compacted in thin layers, of 80 mm thickness each, to fill the space between the column former or the pile body and the container wall. To keep good control on the uniformity of layers heights, the inside walls of the container were divided into 5 equal portions by a marker.

The compaction was performed by using the equipment described in section (5.7). It was found from density trial tests that a height of fall of 50 mm produced a density of 1.54 Mg/m^3 (i.e. a relative density of 28%) provided that the position of the edges of the compacting instrument base did not exceed a few millimetres from the previous position. The compaction for each layer started by compacting the soil near the walls of the container and then the soil around the column former or the pile body. This process was repeated 3 times for each layer.

The soil filling and compation were performed with great care to avoid disturbances of the pile until the top of the container was reached.

6.4.1.4 Sand Column or Pile Instllation:

6.4.1.4.1 Sand column not confined by a geofabric:

The thin aluminium tube, which was positioned in the centre of the container during soil filling, was used to form the sand column. The tube was filled by the right amount of Leighton Buzzard sand to give a layer of about 40 mm after compaction. The required amount was determined from density trial tests and was measured by using a small graduated plastic container. The compaction was performed by using

the equipment described in section (5.7). It was found that a relative density of 85% corresponded to 35 blows with 200 mm height of fall. This process was repeated (n) times depending on the column length (e.g. n= 10 for fully penetrating). After compacting each layer, the tube was pulled by approximately 40 mm, using the extractor. At the end of the n^{th} layer, the column former and the extractor were taken away, then the centering and guide beam were carefully removed and the soil surface was levelled by a hand rotating scraper which also provided a suitable space for the pressure plate.

6.4.1.4.2 Sand Column Encapsulated in a 'Terram' Fabric:

The same process of installation, as described previously , was followed for this case but with a few differences which are summarised in the following points:

1. The column former was not used.
2. The extractor was used, only once, to pull out the solid rod which maintained the fabric tube in the centre of the container and kept its shape cylindrical during soil filling.

The compaction was performed in layers inside the cylindrical fabric tube up to its top.

6.4.1.4.3 Rigid Pile:

The installation process of the rigid pile was very simple. It consisted of hanging the pile in the centre of the container, prior to soil filling, using the centering beam. After soil placement, the beam was carefully removed and the soil surface was levelled. It is worthy of note that the pile was cleaned at the beginning and the end of each test using a dry piece of cloth.

In the preliminary tests, in which attempts were made to measure the horizontal movements of the soil, the horizontal movement gauges were placed at the required positions during the sand filling.

Care was taken to position these gauges at the correct distances, and to ensure that they were horizontal and radial.

6.5 Application of Surcharge Pressure:

The pressure plate was carefully placed on the soil surface so that the pile shaft passed through its central tube. After cleaning and smearing the outside surface of the central tube by silicone grease, the upper lid of the container was lifted by the overhead crane and gently positioned on top of the container and firmly bolted to it. To begin applying the surcharge pressure, the pressure cylinder was connected to one of two klinger valves provided on the container's upper lid which was connected to the pressure chamber as shown in Fig. 5.1, leaving the other one to serve as a bleeding valve. After filling the chamber with water the bleeding valve was closed and the chamber pressure was increased slowly to the required level. This was to give the surcharge pressure some time to propagate throughout the whole soil body. The increase in surcharge pressure was monitored on a wall-mounted pressure gauge (Plate 6.2). All the tests were carried out under a surcharge pressure of 100 KN/m^2.

6.6 Application of the Axial Load:

After installing the loading system, described in section (5.4), and checking that it was level, the threaded rod fixed to the pile head or the footing element, was clamped carefully in position. Great care had to be exercised to bring the footing element in contact with the sand column head and exactly in its centre. Two LVDT's were set up, as shown in Fig. 5.2, to measure the vertical displacements of the pile and the soil. Just before starting the test a set of readings of the LVDT's was taken. These readings were considered as zero readings. The application of the axial load was then started by placing dead weights on the hanger plate as shown in Plate 6.3.

Tests in this investigation were carried out using a controlled stress type of test (constant increment of load). In tests of series (II) the load was applied in increments up to failure. The increments were reduced as failure was approached. At each increment reading of pile displacement was taken when the pile movement had substantially ceased. In tests of series (III) the load was applied in increments up to the working load and then the process of inundation was started by allowing water to enter the container from the bottom. During this operation readings of pile and soil movements were taken at convenient intervals. At the end of the inundation, when the soil settlement had stopped, the loading process continued up to a certain load.

In any type of load test, after the pile had moved over a certain amount, it was necessary to adjust the lever to its original position. This operation should be performed with as little disturbance to the pile as possible. The re-levelling was executed by first lowering the lower collar on the pivot column. Then the upper collar was rotated slowly to tilt the lever to the desired position. The provision of the thrust bearing was to facilitate this operation.

6.7 Data Acquisition and Analysis:

The use of electrical transducers in this study enabled automatic recordings of the soil and pile settlements. This was achieved by connecting the output leads of the measuring devices to a scanner unit of the data logging system shown in Plate 6.4.

The data obtained as an output from the data logger were used for calculating the following information:

1. Pile top settlement,

2. Soil vertical displacement.

6.8 Emptying the Sand Container:

At the end of each test the axial loading system was dismantled, the pressurised surcharge water was drained by syphoning it from the pressure chamber and the upper lid of the container was unbolted and taken aside to remove the pressure plate. This was followed, in the case of rigid piles, by locking the pile head by the clamp described in sub-section (5.7.2) to ensure no damage of the pile during soil emptying. The container was emptied of the soil by the aid of a hand scoop and placed in a metallic bin for later disposal. The soil was not re-used for the reason mentioned in sub-section (5.4.1), and in addition to that, Bragg et al.(1980) using a soil with approximately similar ingredients as the soil used in this investigation, found that the strength of the soil increased by increasing the cycles of wetting and drying.

Following the complete removal of the soil the internal surface of the container walls was cleaned from the greasy soil particles and the container was again ready for the next text.

Table 6.2 Testing programme

Series (II):

Test N^o	Test code name	Length of pile (mm)	Type of confinement	Group N^o
1	BC1	250	None	
2	BC2	250	T700	
3	BC3	250	T1000	
4	BC4	250	T1500	Gr(1)
5	BC5	250	T2000	
6	BC6	250	Rigid pile	
7	BC7	300	None	
8	BC8	300	T700	
9	BC9	300	T1000	
10	BC10	300	T1500	Gr (2)
11	BC11	300	T2000	
12	BC12	300	Rigid pile	
13	BC13	410	None	
14	BC14	410	T700	
15	BC15	410	T1000	
16	BC16	410	T1500	Gr (3)
17	BC17	410	T2000	
18	BC18	410	Rigid pile	

Series (III):

sub-series 1: working load = 20% Pu

Test N^o	Test code name	Length of pile (mm)	Type of confinement	Group N^o
19	ST1	250	None	
20	ST2	250	T700	
21	ST3	250	T1000	
22	ST4	250	T1500	Gr (4)
23	ST5	250	T2000	
24	ST6	250	Rigid pile	
25	ST7	300	None	
26	ST8	300	T700	
27	ST9	300	T1000	
28	ST10	300	T1500	Gr (5)
29	ST11	300	T2000	
30	ST12	300	Rigid pile	
31	ST13	410	None	
32	ST14	410	T700	
33	ST15	410	T1000	
34	ST16	410	T1500	Gr (6)
35	ST17	410	T2000	
36	ST18	410	Rigid pile	

Series (III):

sub-series 2: working load= 50% Pu

Test N^o	Test code name	Length of pile (mm)	Type of confinement	Group N^o
37	ST19	250	None	
38	ST20	250	T700	
39	ST21	250	T1000	
40	ST22	250	T1500	Gr (7)
41	ST23	250	T2000	
42	ST24	250	Rigid pile	
43	ST25	300	None	
44	ST26	300	T700	
45	ST27	300	T1000	
46	ST28	300	T1500	Gr (8)
47	ST29	300	T2000	
48	ST30	300	Rigid pile	
49	ST31	410	None	
50	ST32	410	T700	
51	ST33	410	T1000	
52	ST34	410	T1500	Gr (9)
53	ST35	410	T2000	
54	ST36	410	Rigid pile	

Series (III):

sub-series 3: working load= 80% Pu

Tests N^o	Test code name	Length of pile (mm)	Type of confinement	Group N^o
55	ST37	250	None	
56	ST38	250	T700	
57	ST39	250	T1000	
58	ST40	250	T1500	Gr (10)
59	ST41	250	T2000	
60	ST42	250	Rigid pile	
61	ST43	300	None	
62	ST44	300	T700	
63	ST45	300	T1000	
64	ST46	300	T1500	Gr (11)
65	ST47	300	T2000	
66	ST48	300	Rigid pile	
67	ST49	410	None	
68	ST50	410	T700	
69	ST51	410	T1000	
70	ST52	410	T1500	Gr (12)
71	ST53	410	T2000	
72	ST54	410	Rigid pile	

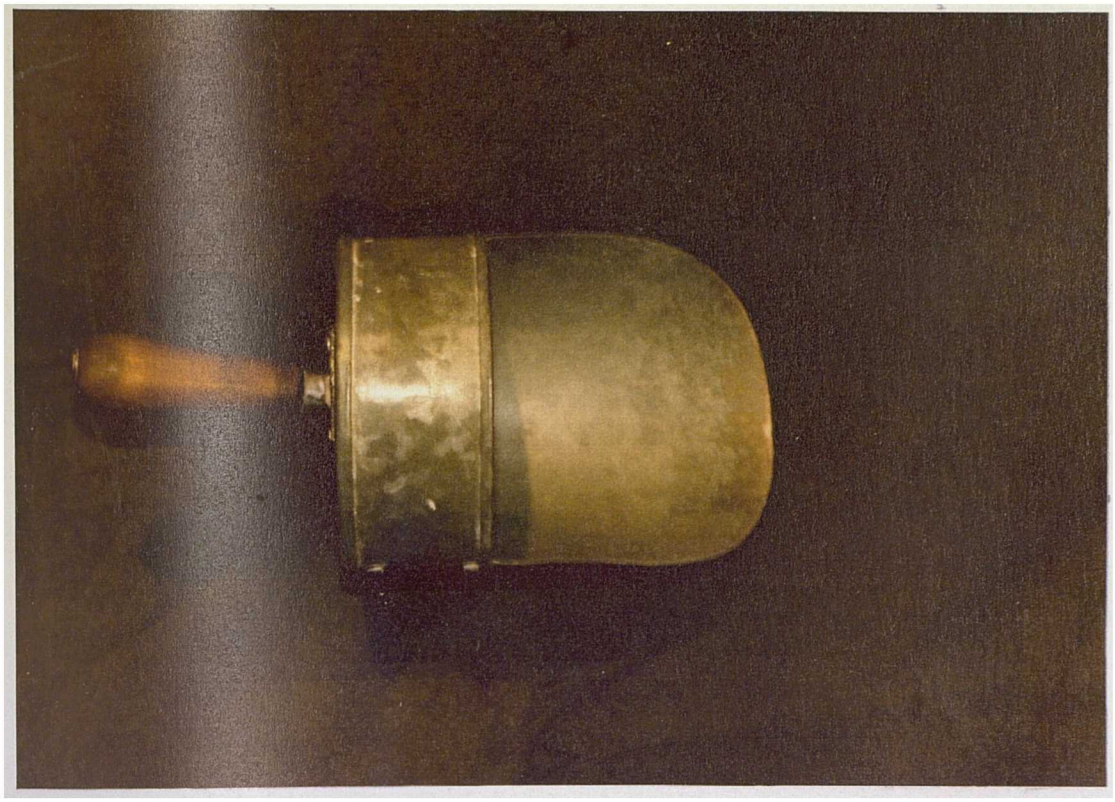

Plate 6.1 The Scoop

Plate 6.4 Data Logging System

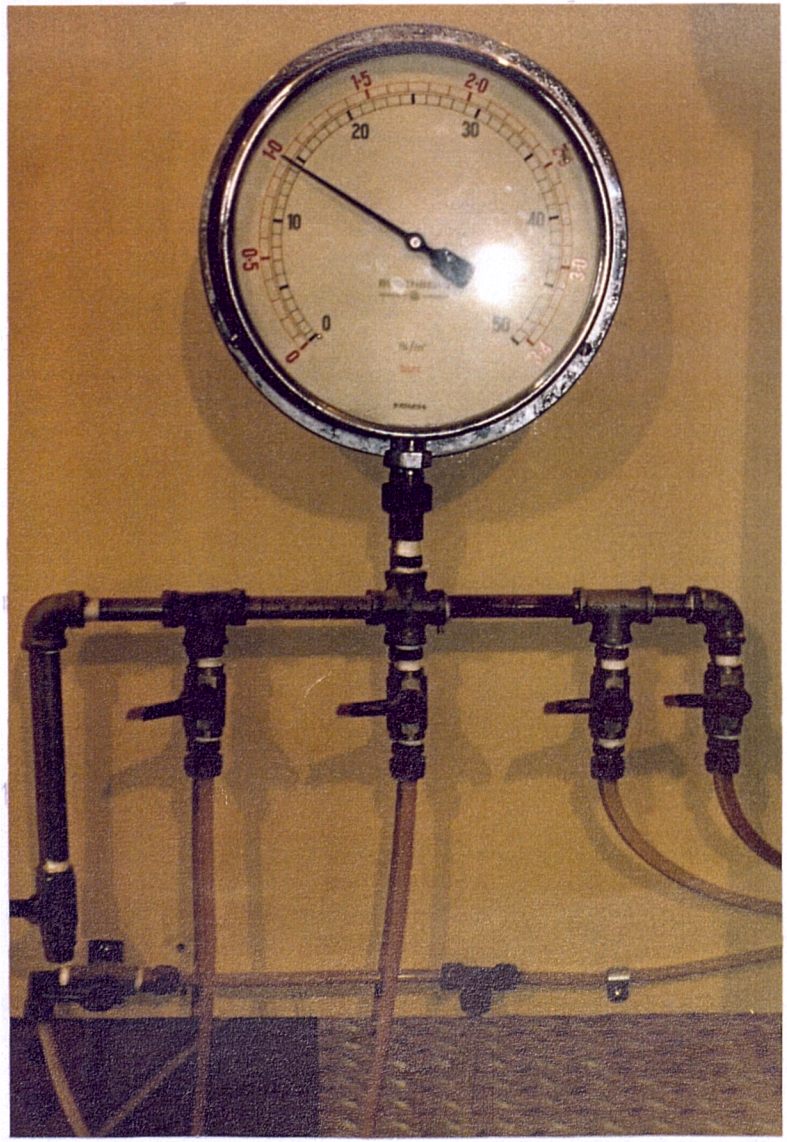

Plate 6.2 The Wall-Mounted Pressure Gauge

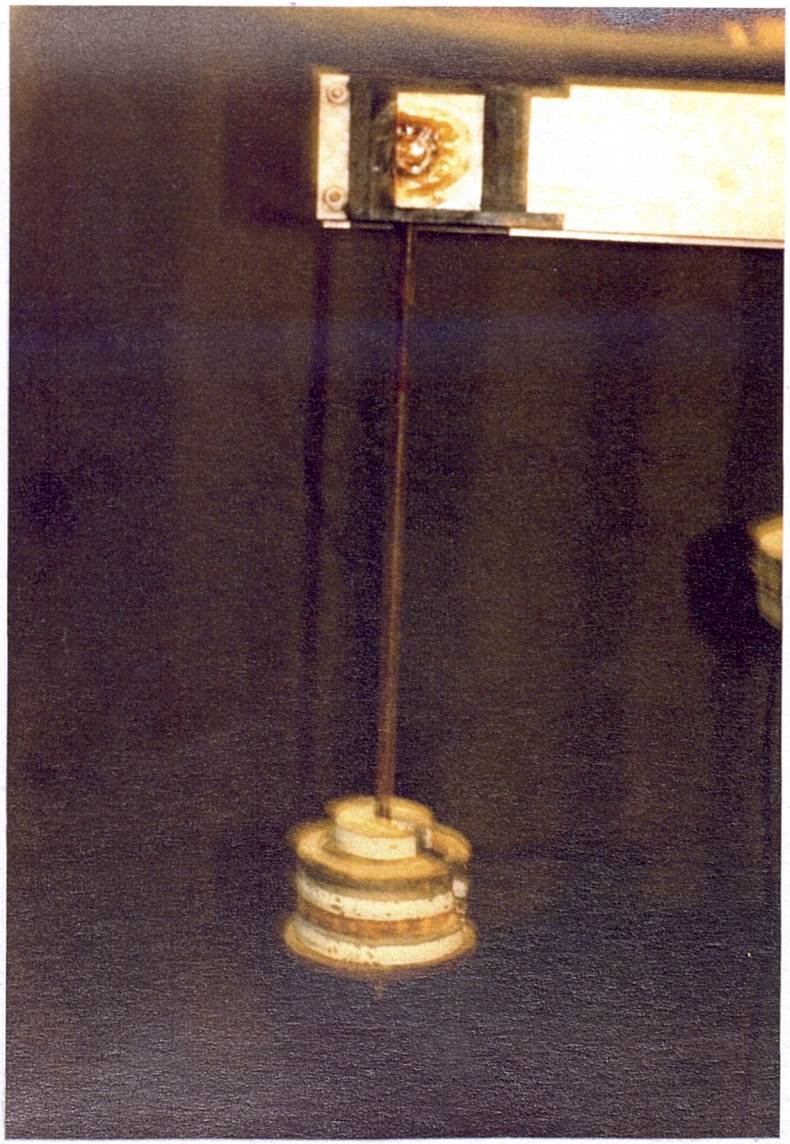

Plate 6.3 Placement of Dead Weights on the Hanger

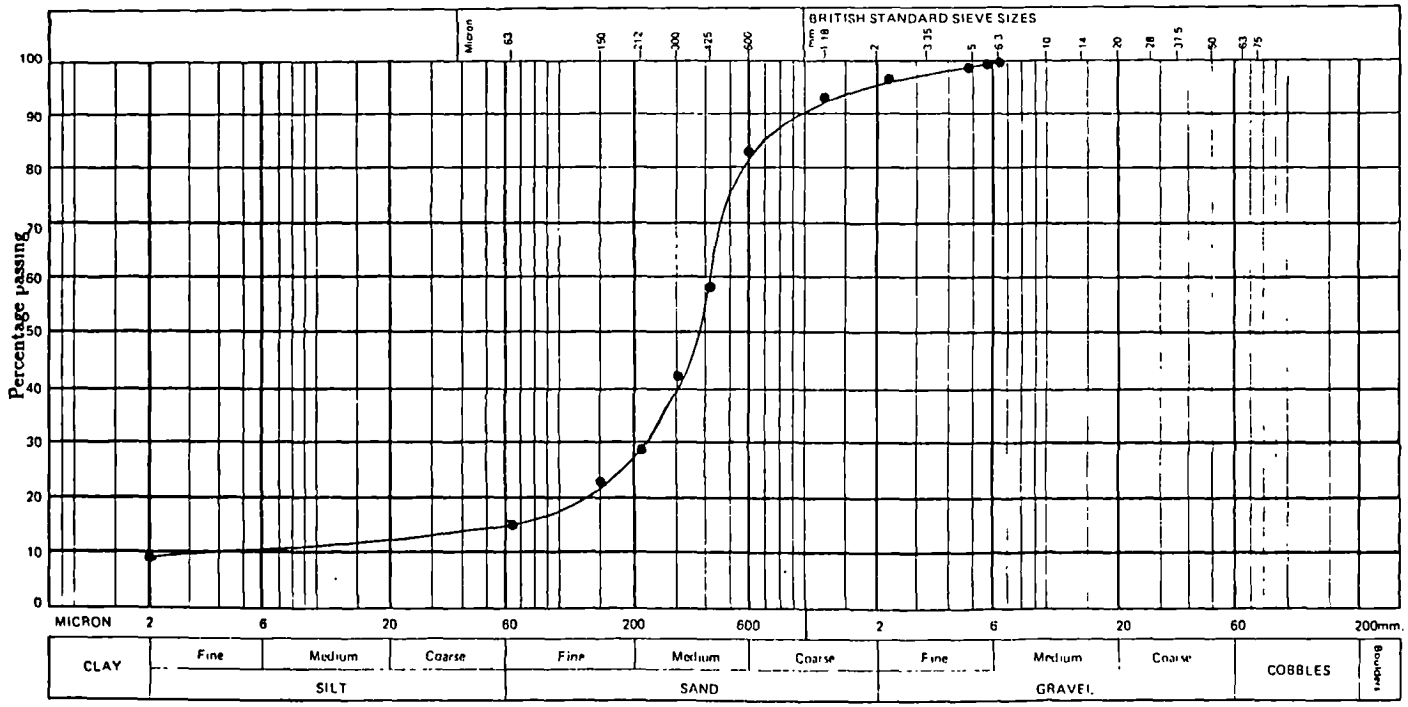

Fig. 6.1 Particle Size Distribution of the Collapsible Soil

Methods Applied	Relatif Density of 28%	Empirical Methods			
		Desinov (1951)	New Soviet Building (1967)	Priklonskij (1952)	Feda (1966)
γ_d (g/cm^3)	1.54	< 1.73	< 1.9	< 1.835	< 1.76

Table 6.1 Results of Some Empirical Criteria

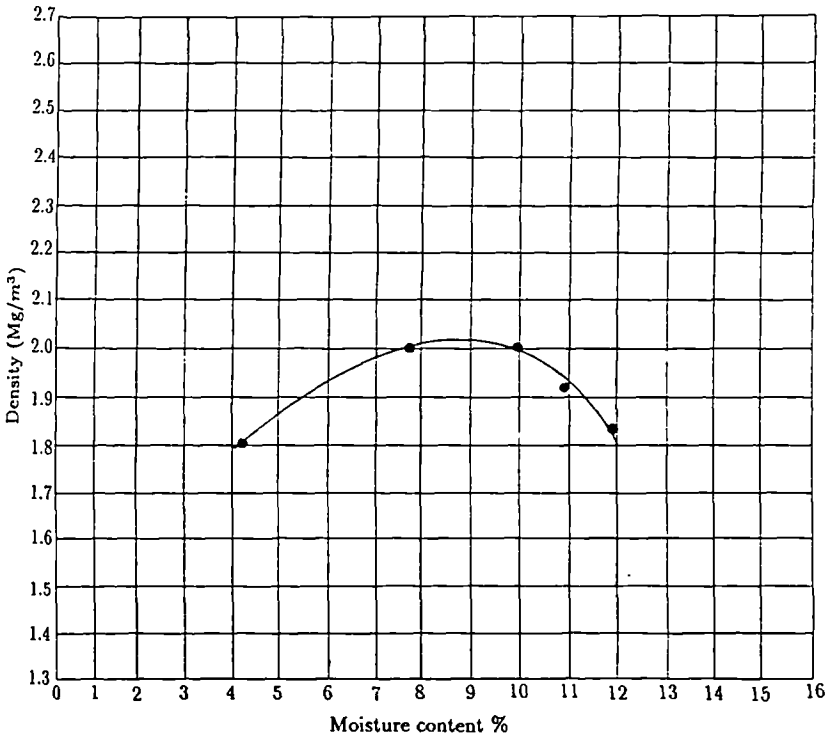

Fig. 6.2 The Compaction Curve Obtained in Determining the Optimum Moisture content

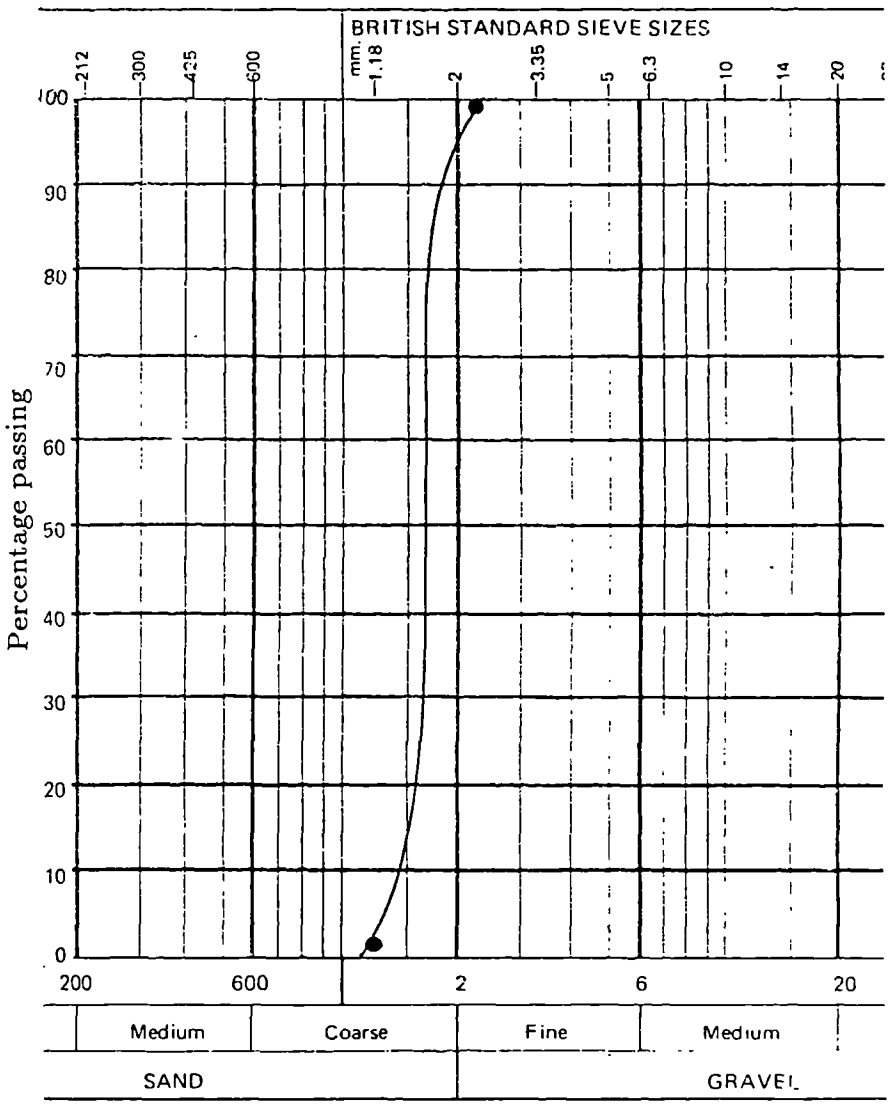

Fig. 6.3 Particle Size Distribution of Leighton Buzzard Sand

Fig. 6.4 Schematic Diagram of Testing Programme

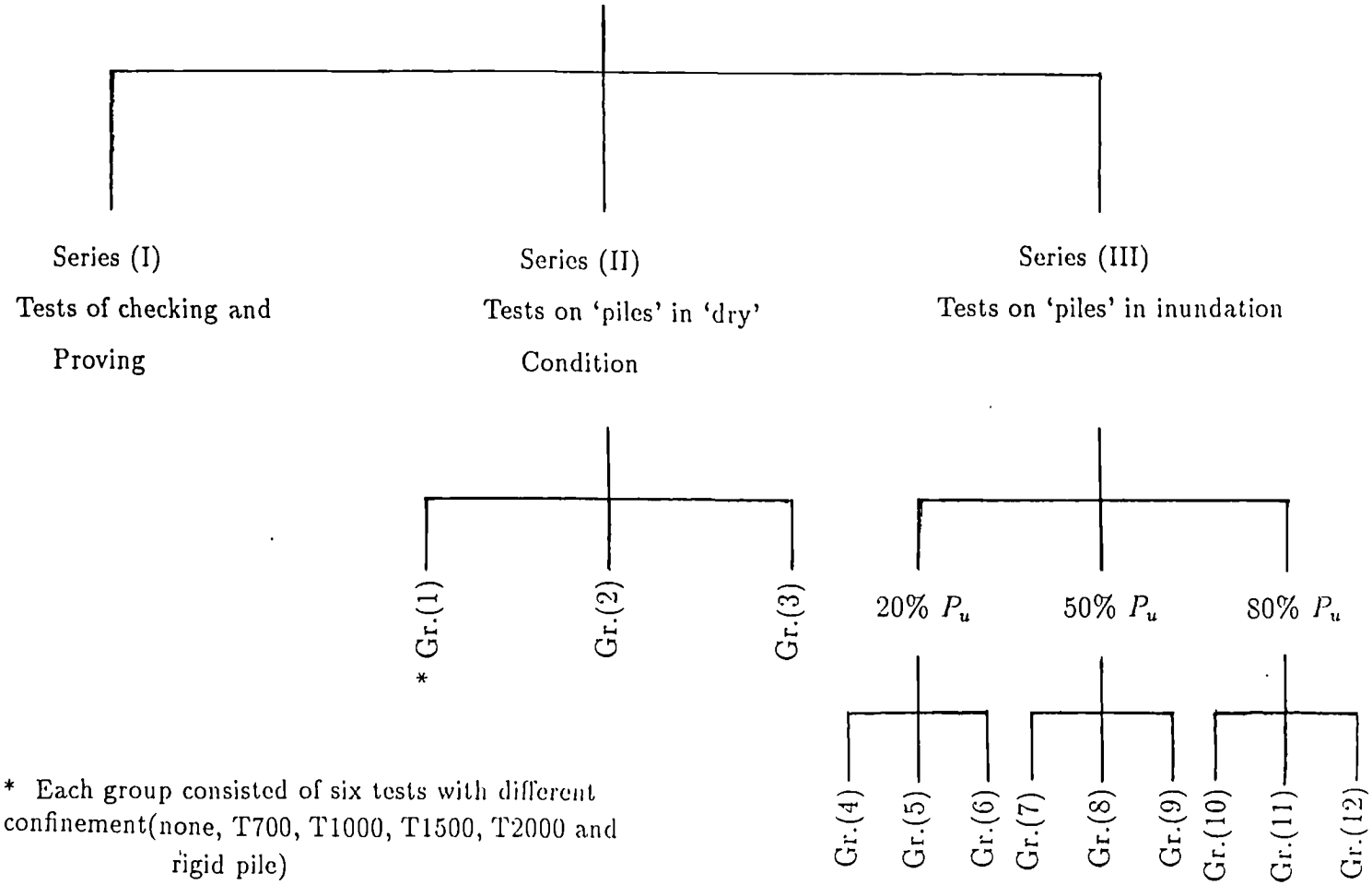

* Each group consisted of six tests with different confinement(none, T700, T1000, T1500, T2000 and rigid pile)

Chapter 7

Discussion on Test Results and Comparison with Theoretical Predictions

7.1 Introduction:

In this chapter, the tests performed to check the collapsibility of the soil prepared are first presented. Then the general performance and limitations of the test apparatus and measuring devices are reviewed and all the significant results obtained from tests from the main experimental programme presented in chapter 6 are discussed in detail. The test results are studied in relation to each other and to the behaviour of a stone column not confined by a geofabric. They are also compared with the predicted results using the analytical solutions described in chapter 3.

7.2 Checking of the collapsibility of the artificial soil prepared:

After the preparation of the artificial soil and the determination of its mechanical and physical properties presented in sub-section 6.2.1, it was decided to check its collapsibility and to examine whether it represented most of the characteristics of a collapsible soil and fullfilled all the requirements and criteria suggested for these types of soil. For this purpose 6 tests were carried out in two different test equipments. They were performed before the preliminary tests and even before the assembly of the test apparatus.

The first two (identical) tests were designed to check the collapsibility of the soil (i.e. the determination of its collapse potential). The specimens tested had a moisture content of 4% and a dry density of 1.54 Mg/m^3. They were placed in an oedometer apparatus of 76 mm diameter and 19 mm thickness. The procedure followed for testing was that suggested by Jennings and Knight (1975) and which was presented in sub-section 2.2.4. An ordinary consolidometer test at natural water content was conducted, the load being progressively increased to 200 kPa. At the end of this loading the specimen was flooded with water, left for 24 hours and the consolidometer test was then carried on to its normal maximum loading limit. The results obtained were similar to each other and the resulting curve is shown in Fig.7.1. It is clear that, due to inundation, the void ratio of the specimen was reduced from approximately $e_1 = 0.5$ to $e_2 = 0.28$ under a constant load of 200 kPa. The collapse potential defined as:

$$CP = \frac{\Delta e_c}{1 + e_0}$$

where:

Δe_c: change in void ratios $(e_2 - e_1)$

e_0: initial void ratio

was calculated and then compared to the guiding figures suggested by Jennings and

Knight from their experience and which are given in Table 2.1. It was found that CP was equal to 13% which would conclude, according to the criteria given in Table 2.1, that the construction on such soil would result in severe trouble.

Another point which is considered worthy to note is the rate of collapse. Most of the collapse was sudden and only about 20% of the total collapse occurred slowly. This implies that for this soil, which consist of sand with a fine silt and clay binder, a large portion of the temporary strength was due to capillary tension which is readily removed by the addition of water. The delayed portion of collapse was caused by the impermeability of the clay bridges existing between the soil grains in an open structure. This observation is strongly supported by the mechanisms of collapse postulated by Morgenstern & de Mattos, 1975; Ganeshan, 1982; Knight, 1961 and Booth, 1975.

The other 4 tests were planned to examine whether the artificial soil (declared as collapsible) exhibited the same characteristics of most of the reported collapsing soils. The aim of these tests was to verify whether by changing the dry density and the moisture content of the soil, the collapse potential changed in the same manner as that reported in sub-section 2.2.5.

All the tests were carried out in a Rowe cell of 250 mm diameter under similar conditions. For a detailed description of the cell see Rowe & Barden (1966). The specimens, of 75 mm thickness, were inundated from the bottom centre of the cell through a plastic filter of 250 mm diameter and 5 mm thickness. The inundation was controlled by a burette mounted vertically beside the cell so that the distance between the cell top and the water head did not exceed a few centimetres (50 mm).

The general characteristics of these tests are summarised in Table 7.1. Tests 1 and 2 were designed to investigate the effect of the initial dry density on the collapse potential, whereas tests 3 and 4 give a measure of the effect of the natural

moisture content on the magnitude of collapse. The resulting curves obtained are shown in Fig.7.2. The collapse potential values computed from the results of tests 1, 2, 3 and 4 were 13.7%, 13.24%, 13.09% and 12.55% respectively. It was noted that, for a moisture content of 4%, the collapse potential decreased by 3.35% between tests 1 and 2 and by 1.13% between tests 2 and 3. Also, for an initial dry density of 1.516 Mg/m^3, the magnitude of collapse was found to decrease by 4.12% (between tests 3 and 4). By investigating these curves it was deduced that, for a given moisture content, the collapse potential increased with increasing the dry density. Also, for any given dry density, the magnitude of collapse decreased with increasing moisture content. This finding is in agreement with Barden et al., 1969; Lovell et al., 1975; Lefebvre et al., 1989 and Lawton, 1989.

Form these findings it was concluded that the artificial soil prepared was definitely collapsible, excluded from being exceptional (i.e. exhibited a general behaviour) and was suitable for the main testing programme.

7.3 The General Performance and Limitations of the Test Apparatus:

7.3.1 General Limitations of the Experimental Study:

Much time was spent on the development and modification of the testing rig, instrumentation, ancilliary equipment, 'pile' installation, testing procedure and technique (all described in Chapters 5 and 6). This was perhaps one of the most important aspects of this work resulting in an apparatus capable of performing all the duties required for the present investigation. Nevertheless, this apparatus has also resulted in some limitations and sensitivities, some of which are listed below:

1. The diameter of the rig, limited the maximum diameter of 'pile' that could be employed to 23 mm, in order to avoid wall effects.

2. The nature of the 'piles' (stone columns confined or not by a geofabric) did not permit the installation of any instrumentation on the 'pile' bodies.

3. The collapsible soil used was loose and composed of three components (sand, silt and clay) in given proportions. Other densities and proportions of 'soil' are possible. Also other types of soil are possible.

4. In some tests, due to their sensitivity and the very small displacements which resulted, the inconsistencies which occurred in the displacement measurements therefore were not surprising.

5. Although the laboratory specimens were prepared under carefully controlled conditions to remove the effects of variability in a natural soil, a definite but acceptable amount of scatter was observed (less than 5%). This was not surprising bearing in mind the sensitive test preparations, such as; 'pile' installation, soil bed formation around the 'pile', installing the surcharge plate and rig lid, applying the surcharge and positioning the loading shaft.

6. It is thought that the sand depositing technique is the main contributor to the scatter in the data acquired, which is usual for soil deposits prepared under laboratory conditions (Boghosian, 1984).

In spite of the above limitations and sensitivities, the experiments performed have provided useful information on the performance of sand columns, confined or unconfined by a geofabric, in inundated collapsible soil and justification of this general statement is given in the following sections.

7.3.2 Repeatability of Test Results:

After the preparation of the collapsible soil and the assembly of the apparatus, some preliminary tests were undertaken in order to gain some familiarity with the procedure followed in setting up and carrying out the tests and to ensure the repeatability of the tests.

Two types of tests were performed:

- Type (1): Tests to determine the bearing capacity of a sand column not confined by a geofabric, of length 410 mm, in a 'dry' soil condition.
- Type (2): Tests on a similar sand column loaded up to a working load of 40% of its bearing capacity and then inundating the surrounding soil.

Each type consisted of three identical tests, two of them were carried out in the same container (container N^o1), whereas the other one was performed in a different container (container N^o2). The procedure followed during the testing operation was described in section 6.4.

Table 7.2 summarises some of the characteristics and conditions applied to these tests. All the tests were performed under a surcharge pressure of 100 kPa which generated an appropriate stress level similar to that under field-scale conditions. At the same time this led to an increase in the carrying capacity of the pile which, in turn, kept experimental errors to an acceptable level (El-Hadid, 1988).

The application of the axial load on the head of the 'pile' was carried out at least half an hour after the application of the surcharge pressure. This interval of time was adopted from the results of an investigation carried out by Boghosian (1984) to assess the time of recovery of the base load cell of the pile.

The results of these tests are plotted in Fig. 7.3-a and Fig. 7.3-b. As

expected, the tests of type (1) were less repeatable because of the very small displacements which occurred with these tests. Hence, these tests were chosen for a repeatability check. Test C2 was designed to repeat test C1 in the same test container and the other, test C3, to repeat the same test in the second container. The resulting curves for the three tests are given in Figure 7.3-a. It will be noted that these curves are very close to one another concluding that there was good repeatability in these tests.

The repeatability is defined by BS812 (1984) as:

$$r_1 = 2.8\sqrt{V_r}$$

where:

V_r: repeatability variance

r_1: value of repeatability below which the absolute difference between two single test results may be expected to lie with a probability of 95%.

Referring to Fig. 7.3-a it is seen that, at the applied load of 132 N, the displacements of the top of the sand column for tests C1, C2 and C3 are 2.47 mm, 2.54 mm and 2.62 mm respectively. The repeatability variance is $V_r = 1.47 \times 10^{-2}$ therefore, $r_1 = 0.34$. The maximum absolute difference value between C1 and C3 is 0.15 which is smaller than the previous repeatability value. In addition, the ultimate capacities deduced from tests C1 and C3, using Chin's plot, are 206 (N) and 213 (N) (a difference of 3.4%). Consequently, it may be concluded that the test apparatus gives repeatable and reproducible results under the same conditions.

7.4 Performance of Sand Columns in a Collapsible Soil:

In this section, the tests carried out to investigate the performance of sand columns in a collapsible soil subjected to inundation are discussed. These tests formed the basis

of this investigation and represented the starting point from which this research has been developed. They consisted of 9 tests performed in the large containers straight after the preliminary tests.

They may be divided into 3 groups of 3 tests each. Each group consisted of one type of test performed on three different foundation supports (soil alone, a sand column fully penetrating of 410 mm length and a sand column partially penetrating of 250 mm length).

These groups are:

- group (1): Tests for bearing capacity (P_u) determination in the 'dry' condition.
- group (2): Tests for the determination of the settlement of the three different foundation supports caused by full inundation under a working load of 30% P_u.
- group (3): Tests for the determination of the settlements of the different foundation supports caused by partial inundation under a working load of 30% P_u.

The general characteristics of the tests are summarised in Table 7.3. The first tests performed were BSA, B1, FSA and F1. The procedure and technique followed during the testing operation were described in chapter 6. The resulting curves for tests BSA and B1 are shown in Fig. 7.4 and for tests FSA and F1 in Fig 7.5. It was noted from the latter figure that, the foundation 'model' on the soil alone settled by an amount of 53 mm and with the presence of the sand column fully penetrating it settled by an amount of 52 mm. It was quite clear that when the specimen was inundated with the reinforcing sand column in-situ there was no reduction (or very slight) in settlement due to the presence of the sand column. The bearing capacity, which was improved in the 'dry' state due to the presence of the sand column (see Fig.7.4), was reduced drastically due to full inundation (Fig. 7.5).

Before drawing any conclusions, it was decided to carry out more tests with different foundation supports and different types of inundation. Provided that the stone columns generally failed by bulging at relatively shallow depths (typically less than 4 diameters from the top of the column), the next stage was designed to investigate the effects of partial inundation and partial penetration of the sand column on the settlement behaviour of the foundation 'model'. Partial inundation is difficult to carry out, but it was performed by inundating the lower part of the ground around the column. This operation was controlled by the quantity of water allowed to enter the container each time. The quantity used was 2 litres measured by a burette mounted on one of the tanks and used to cause inundation as described in section 5.6.

In this stage, five tests were performed namely B2, F2, PSA, P1, and P2. The procedure followed was similar to that used for the previous tests. The only difference was that during partial inundation, the quantity of water was controlled. The results of tests B2 and F2 are plotted, for comparaison purposes, in Fig.7.4 and Fig.7.5 respectively, whereas, the results of tests PSA, P1 and P2 are plotted in Fig.7.6 to show the effect of partial inundation on the settlement behaviour of the foundation 'model'. An examination of the resulting curves shown in these figures, confirmed that the similar trends were being observed. All the different foundation supports (soil alone, sand columns partially and fully penetrating) settled by approximately the same amount of around 53 mm for full inundation and around 18 mm for partial inundation. Therefore even for partial inundation and partial penetration, large settlements were observed which resulted in a catastrophic reduction in the bearing capacity of the sand columns. In a loose fill, the water table would have to rise close to ground level in order to have any significant effect. It was reported that, under such circumstances the ultimate capacity of the column could be reduced by up to 50% in the worst case (Simpson et al., 1989).

To understand the mechanism of collapse of the sand columns during inundation (i.e. to find out where the sand columns collapse), several techniques

were considered to establish the pattern of vertical displacement within the column and radial displacements at the edge of the column against depth. However, as stated in sub-section 5.5.3, none of these methods has been used because of the damage or disturbance caused to the instruments during collapse of the soil. In these circumstances, the establishement of the behaviour of the sand column during collapse was limited only to a comparaison between the settlement of the column and the soil around it at any time during inundation. For this purpose, for the tests F1, F2, P1 and P2, readings of the settlement of the column and the soil around it, during the process of inundation, were taken at equal intervals of time. The results obtained from these measurement are plotted in Fig.7.7, where the column settlements represent the abscissa and the soil settlements represent the coordinate.

This figure shows that the settlement of the column and the soil around it was approximately uniform and equal at any time during inundation even for partial inundation and for partial penetration. The fitting curves for these results made approximately an angle $\alpha = 45^{\circ}$ with the abscissa axe.

From this result it was concluded that stone columns have failed in strengthening a loose fill which exhibits a collapse bahaviour when subjected to inundation or partial inundation. The causes of this phenomenon were discussed in chapter 1. It is very important here to specify that the findings reported by Simpson et al.(1989) should be applied only to loose fills which are not collapsible. The differences between the behaviour of a sand column in a collapsible fill and a column in non-collapsible fill resulted mainly from the differences in the behaviour of a typical element of soil in the vicinity of the sand column during inundation. Quite clearly, in both cases, there is a change in volume, a change in stiffness and also a change in stress state. However, the magnitude of these changes are quite different. A change in volume of a collapsible specimen is much larger than that of non-collapsible one. Also, the lateral deformation resulting from the change in volume of a collapsible specimen is remarkably different from that of a non-collapsible soil. Grigorian (1967) found that, for specimens of loess of diameter (d), height (h)

and a ratio of h/d equal 2, the lateral deformation exceeded the vertical one by a factor of 5 to 17 under all-around pressures. However, for non-collapsible specimens and in the absence of any reported work, the elastic theory, which is applicable in this case, gives equal vertical and lateral strains after the deformation of the specimens under conditions of no volume change. These considerations alone can explain the differences in the behaviour of stone columns. The inundation of a non-collapsible fill around a stone column and below its critical length l_c has a negligible effect on its settlement behaviour because the volume change of a typical element of soil in the vicinity of the column is very small and the changes of stresses in the column caused by wetting are negligible (Fig. 7.8). The water must reach the critical length in order to have any significant effect. This is because the lateral stresses in the column at that part are larger and any change in the passive pressure may lead to the appearence of additional stresses in the surrounding soil and caused its deformation to a limited extend depending on the type of the soil. In the case of a collapsible fill this is different. Even below the critical length, the large change in volume of an element of soil in the vicinity of the column, which resulted from large vertical and lateral strains, caused the downward movement of all the mass of soil situated above the element. Consequentely, the element of soil and the small portion of the column beside it will undergo additional vertical stresses and this will increase the volume change of the element and also the lateral stresses in the small portion of the column. The small portion of the column will then deform laterally and the deformation will be easily accommodated by the soil.

7.5 Performance of Sand Columns encapsulated in 'Terram' Fabrics and Rigid Piles in Collapsible Soil:

The need to reinforce the sand columns by a geofabric was discussed in detail in section 1.2. With the achievement of the tests discussed in the previous sections and reported as series (I) in section 6.3, it was decided to investigate the efficiency of this method (covering the column by a geofabric) on the improvement of the carrying capacity and the reduction of the settlement of a foundation support. For this purpose two series of tests were designed (series (II) and (III)).

7.5.1 Ultimate Carrying Capacity of 'piles':

This series of tests was performed to demonstrate the effects of the introduction of a geofabric reinforcement to the sand column and the resulting increase of the stiffness of the foundation support on its carrying capacity. The effects of the 'pile' length were also considered.

For all these tests Chin's stability plot (1972) was used to determine the ultimate carrying capacity of the piles. This method assumes that the load-displacement curve of the pile when the load approaches the failure load is of a hyperbolic form, and the plot of ratio of displacement of the pile(Δ) to the load applied on its top (P) against an abscissa of the displacement of the pile (Δ) is linear. The inverse slope of this line would therefore give the ultimate value of the pile top load (more details are given in the following sub-section).

7.5.1.1 Effects of 'Pile'-Rigidity on Bearing Capacity:

The load-displacement characteristics of 'piles' obtained from tests BC1, BC2, BC3, BC4, BC5 and BC6, corresponding to a sand without confinement, a sand column confined by T700, T1000, T1500 or T2000 and a rigid pile (group 1 of the testing programme), are presented in Fig.7.9-a. The resulting curve obtained from test BSA, and discussed in section 7.4, is also included. In comparison it seems that, with the exception of the rigid pile (BC6), there is no significant difference in the general trend of these curves apart from the decreasing rate of the displacement for a given load with the increase of 'pile' rigidity as the pile approaches its ultimate load. For the test BC6 (rigid pile), the top load increased fairly linearly with pile settlement to about 80% of its ultimate load, beyond which the pile exhibited relatively larger amounts of settlement for small increments of top load. It is clear that the increase of the strength of the geotextile resulted in a better performance of these 'piles' under load. A glance at the initial parts of these graphs indicates that the increase in geotextile's strength resulted in an increase in the 'linearity' of these parts, indicating an increase in the skin friction along the pile shaft.

Since no distinct indication of failure could be observed from these graphs, Chin's stability method was used to predict the ultimate carrying load of these 'piles' (shown in Figs 7.10 to 7.15). In a manner similar to Kondner's (1963) pioneering work on soils, Chin suggested that the top load of a pile versus the top settlement could be expressed by a hyperbola of the form:

$$P = \frac{\Delta}{m\Delta + b}$$

where:

P: is the pile top load.

Δ: is the pile top displacement.

and the asymptote $P_u = 1/m$ where b is a constant.

Hence a plot of Δ/P versus Δ is a straight line whose slope (m) is equal to $1/P_u$. This method can also be used to diagnose the pile's structural condition beneath

the soil surface (Chin, 1978). For structurally sound and perfect piles the stability plot should produce one solid straight line without any breakage. For a pile in which both end bearing and friction loads are dominant, the successive straight lines of the stability plot should have an increasing slope. If the inverse slope of one straight line is less than that of previous one a plastic collapse in the pile shaft is indicated. However, Chin's hyperbolic assumptions of the load-displacement relationship is not an exact fit to the experimental data over the entire range of the test, but it was only intended to be a reasonable representation of the data over a large range of the displacement parameter (Kondner, 1963). Therefore, it is possible to arrive at a false Chin's ultimate value for the carrying capacity of the pile.

An earlier attempt was made to take the failure as the load which causes a pile head settlement of 10% of the pile diameter (Poulos, 1982). However, the loads resulted by this consideration and which correspond to 2.3 mm displacement, were very small and didn't give any indication of failure. It was therefore considered not applicable to use this criterion.

As expected, Chin's stability plots for the tests BC1, BC2, BC3, BC4, and BC5, consisted of successive straight lines, which is the characteristic of Chin's plot, but with slight difference in their slopes . Because of the slight difference between the slopes of the successive lines, it was considered that the stability plot for each test followed a straight line from the beginning of the test (Figs 7.10 to 7.14). However, as can be seen from Fig.7.15, for the test BC6 (rigid pile) the plot started with a horizontal line up to a region where the full mobilization of shaft friction was considered to have occurred. Then it followed an inclined straight line up to the end of the test. The inverse slope of this part of the plot produced the ultimate carrying capacity (P_u) of the pile. The reason for this behaviour was that the initial portion of the original load-displacement graph of the pile, being fairly straight, did not follow the assumption of the hyperbolic form put forward by Chin (1972) to estimate the ultimate carrying capacity of the pile. It is noteworthy that, if the initial portion of the original load-displacement curve is linear, the initial part

of the hyperbolic plot (Chin's plot) will be horizontal (Kondner, 1963) which was the case for this pile.

In Table 7.4 the ultimate deduced carrying capacities (P_u) of 'piles' in tests BC1, BC2, BC3, BC4, BC5 and BC6 are given. It is clear that the ultimate carrying capacities of these 'piles' increased with increase in their rigidity. In comparison with test BC1, a considerable increase was found in the ultimate carrying capacities of 'piles' in all the other tests (with a minimum of 21.7% for a sand column covered by T700). But it is worthy to note that, the rate of increase of the carrying capacities between the tests BC2, BC3 and BC4 is small compared to that of test BC5 and BC6.

It is clear that the reinforced stone column concept is a better alternative to the stone column alone. In the latter method a combined system of compacted, granular columns in a matrix of native soil supports a vertical load which is transmitted through a rigid footing. The load is transferred and concentrated initially on the compacted granular cylinders or 'stone columns'. The cylinders tend to dilate under this increased load and exert a lateral stress on the native, surrounding soil; but this lateral stress (and dilation) is resisted by passive earth pressure. This interaction is repeated until a state of equilibrium is reached. The rigidity and load carrying capacity of the columns depends largely upon the amount of lateral restraint or confining stress that can be mobilised in the surrounding soil.

In the reinforced sand column concept, lateral restraint comes not only from the surrounding soil but also from the encapsulating fabric. The increase in confining stress induced by the fabric may equal or exceed the restraint provided by earth pressure from the surrounding soil. The fabric inhibits the development of internal tensile strains in the soil and develops tensile stresses. The composite soil-fabric system will develop overall smaller deformations for any particular load or larger load carrying capacity at any given deformations than the soil alone. How-

ever, it is worthy to note that the imposed fabric deformations are far less than their rupture deformations. Therefore, up to and beyond the deformations at which peak stresses in the soil are mobilized, the benefit of the mobilized tensile stress in the extensible fabrics will be available at deformations beyond the peak stresses in the soil. The fabrics are likely still to be mobilizing additional tensile stresses depending upon the shape of their load-deformation curve even if the soil is losing strength. Thus the reinforced sand column system may or may not exhibit some overall reduction in load carrying capacity at deformations beyond those at which the peak stresses in the soil are mobilized, but in either case the system strength is greater than for soil alone (McGown et al., 1978). This consideration introduces an other limitation to Chin's stability plot. In the latter method, the bearing capacity of a reinforced sand column is determined from the corresponding load-displacement curve which is obtained by loading the 'pile' up to a certain vertical strain. This strain is far less than the strain of failure of the composite and may be smaller than the strain at which peak stresses in the soil (which compose the column) are mobilized. Undoubtely this will lead to an overestimation of the bearing capacity in the case of an overall reduction in load at deformations beyond those which correspond to the peak stresses in the soil.

It is evident therefore that, as the ultimate carrying capacities of these 'piles' were increasing with increase in their rigidity the corresponding displacements of the 'piles' were also increasing. These displacements are much higher than those of the rigid pile (Fig. 7.9). This is in agreement with McGown et al. (1978) and Tumay et al. (1979). This is considered to be one of the practical disadvantages of the behaviour of reinforced sand columns. Athough the columns showed satisfactory capacity to withstand the design loads, they experienced settlements greater than those for the nominally rigid pile tested under the same conditions. Provided that the fabric of the reinforcement has the capacity to undergo high elongation and to continue mobilizing tensile resistance at relatively high strains, it is very important

to consider the mechanical properties of the fabric on the bearing capacity design (i.e. bearing capacity computation) of the composite sand column encapsulated in a geofabric.

Another distinct feature of the load-diaplacement behaviour of these tests, which can be observed in Fig.7.9-a, is that as the stiffness of the 'pile' increased the load/settlement curves tended to become steeper compared with a sand column without confinement. Accordingly, the behaviour of the 'pile' was gradually transformed from a load-displacement trend of a friction pile to that of a bearing pile in which larger amounts of settlements were needed to mobilize the total bearing load.

The results obtained from the tests of group 2 and 3 (series (II)) are presented in Fig.7.9-b and 7.9-c respectively. The ultimate carrying capacities of all the tests included in these two groups (obtained by Chin's method) are summarised in Table 7.4. The same explanations and features observed for group 1 were also noted for groups 2 and 3. It was concluded that the method of reinforcing the sand columns by a geofabric did improve their bearing capacities.

To show clearly the effect of reinforcing the sand columns by geofabrics of different strength on their bearing capacity, the term bearing capacity ratio (BCR) was established. It is defined as:

$$BCR = \frac{q_2}{q_1}$$

where:

q_2: the bearing capacity for the reinforced stone column and the rigid pile.

q_1: the bearing capacity for the unreinforced stone column.

The variation of BCR with 'pile'-stiffness is shown in Fig. 7.16. The resulting curves clearly indicate that the bearing capacity of the sand column can be significantly increased by increasing the strength of the reinforcing material.

7.5.1.2 Effects of 'Pile'-Length on bearing capacity:

As mentioned earlier, each type of 'pile' was considered in three lengths (two cases of partial penetration 250 mm and 300 mm and one fully penetrating 410 mm). To examine the effects of these lengths on the carrying capacity behaviour of each type, all the results of groups 1, 2 and 3 (discussed previously) were re-plotted differently in six figures (Figs 7.17 to 7.22). With the exception of Fig.7.22, all the figures are similar to each other and show an increase of the bearing capacity of the 'piles' as the length increases. This agreed well with the findings of Vesic (1967) and Poulos (1982). The increase is higher between the lengths 300 mm and 410 mm than that between 250 mm and 300 mm. This may be explained by the difference in lengths.It was deduced that, when the length of a 'pile' of this type increases, the settlement which corresponds to a given working load decreased. Therefore, it is practically more convenient to carry the sand columns confined or unconfined by a geofabric down to a rigid stratum.

7.5.2 Settlement Behaviour of the 'piles' Under Load and Inundation:

In this section, the settlement behaviour caused by inundation under an external axial load, in a collapsible soil, for the different types of foundation support will be examined. Each type will be studied under three different working loads (20%, 50% and 80% of P_u). All the tests performed for this purpose are summarised in Table 6.2. The equipment and techniques used in performing these tests were described in chapters 5 and 6. The results obtained from these tests will be discussed in terms of the effects of the 'pile' rigidity and 'pile'-length (or the ratio of the length to the diameter of the 'pile' L/d) on the 'pile' behaviour after full inundation.

7.5.2.1 Effects of 'Pile'-Rigidity on the Settlement Behaviour:

To examine the effects of 'pile'-stiffness on its settlement behaviour caused by an external axial load and by inundation of the collapsible soil around it, all the results are plotted in 9 figures (Figs 7.23-a to 7.25-c). Each figure represents the settlement curves of one group. For convenience, these figures were divided into 3 groups. Each group, which consists of 3 figures, corresponds to a given length. Each figure represented the settlement curves of all the types of 'piles' under a given working load.

Starting with group 1 (Figs 7.23-a to 7.23-c) which corresponded to the length 250 mm, it is confirmed, by comparing the resulting curves of tests SAF20, SAF50 and SAF80 with ST1, ST19 and ST37 respectively, that the sand column without confinement did not reduce the settlement of the foundation 'model' caused by inundation particularly with light loads. It is also clear from these figures that the introduction of the geotextile reinforcement to the sand column has contributed to the reduction of settlement. This reduction increased with increase in the stiffness of the 'pile'. Obviously, the largest reduction was obtained with the rigid pile. It was found that the settlement of the foundation 'model' resting on a rigid pile under a working load of 20% P_u was 23.0 mm compared to about 53 mm for a sand column without *confinement*.

Another noticeable feature of these curves is the settlement recorded when using the first type of reinforcement (i.e. the fabric T700). It was noticed that the settlement dropped from 53 mm to about 37 mm. This is mainly due to the large difference between the stiffness of the sand column without confinement and the sand column confined by the geofabric T700. The rate of increase was then reduced with the subsequent reinforcement and this agreed well with the rate of increase in the mechanical properties of the reinforcing fabrics.

As expected, the method of reinforcing a sand column with a geofabric

is more effective at supporting light loads than heavy loads. But in general, this method did reduce the settlement of a foundation 'model' caused by inundation of the surrounding collapsible soil. The reduction increased by increasing the 'pile'-rigidity.

By investigating the results of group 1 it was noted that partial penetration represented the critical situation of all types of deep foundation. For this reason, another case of partial penetration was considered. It consisted of the length 300 mm. Similar tests to those of 250 mm pile length were performed. The results are plotted in Figs 7.24-a to 7.24-c and were classified as group 2.

The resulting curves for these tests follow the general trend of giving higher settlement reduction with increasing 'pile'-stiffness. Once again, it is shown that the use of a sand column without confinement in a collapsible soil, which at some stage in its future could be subjected to inundation or partial inundation, is quite wrong.

To complete the testing programme another series of tests was designed. The series consisted of investigating what might happen after inundation to the different types of foundation supports which were fully penetrating (410 mm). The tests were also performed at three different working loads (20%, 50% and 80% of P_u). The results, classified as group 3, are plotted in Figs 7.25-a to 7.25-c. The curves confirmed that the reduction of settlement is a function of 'pile' stiffness. The settlement definitely decreased with increase of the rigidity of the 'pile'.

Fig.7.25-c shows that the settlement was reduced to around 2.5 mm for the rigid pile. But the more important feature is the settlement reduction of the foundation 'model' resting on a sand column confined by the fabric T2000. It was reduced by about 36 mm (from about 53 mm to around 17 mm). For the other types, the general trend observed in Figs 7.23-a to 7.24-c (groups 1 and 2) was also observed here. It appears that a fully penetrating foundation is the more reli-

able and convenient solution to the problem of settlement of a collapsible soil caused by inundation. This topic will be discussed in some detail in the next subsub-section.

The present investigation on the settlement behaviour of the reinforced sand columns and rigid piles under axial load in a collapsible soil subjected to inundation is limited. It consists of a comparaison between the settlements recorded and the settlement reductions calculated for the different types of foundation support. However, it is very interesting to examine how these reductions are arrived at? Undoubtely this will necessitate the installation of appropriate instrumentation in the 'piles' bodies. But, as discussed in sub-section 7.3.1, this was not possible. In the absence of any instrumentation an attempt was made in order to explain how the increase of the pile rigidity, provided to some 'piles' by the covering geotextile, decreased the settlement. Similarly to that discussed in chapter 3 the settlement of the 'pile' may be divided into three components, the elastic settlement due to load, the settlement caused by downdrag and the settlement caused by lateral deformation. Under a given working load, the increase of pile-stiffness resulted in:

1. A decrease in the elastic settlement (Poulos et al., 1980; Bjerrum et al., 1969 and Darvall, 1973).
2. An increase of the settlement caused by downdrag (Poulos et al., 1980)
3. A decrease in the settlement caused by lateral deformation (Gray et al., 1982 and Gorle et al., 1989)

The total settlement, which is the sum of the three components, always decreases when the pile-stiffness increases. Therefore, provided that the settlement caused by downdrag is larger than the elastic settlement (Poulos et al., 1980) it is evident that the settlement caused by lateral deformation is the predominant one in this kind of foundation support. In addition, it is noted that this component of settlement decreases rapidly with increase of pile-stiffness. This is another confirmation that

the collapse of a stone column in a collapsible soil is caused by loss of confinement around the column.

To show more clearly the effects of 'pile' rigidity on settlement behaviour of the different types of foundation supports and to facilitate comparison between predicted and measured results, all the results were re-plotted in Figs 7.26-a to 7.28-c which represent the variation of the settlement reduction factor (β) as a function of the modulii of elasticity of the 'piles'. The settlement reduction factor (β) was defined in chapter 3 as:

$$\beta = \frac{S_i}{S_0}$$

where:

S_i: settlement of the treated foundation

S_0: settlement of the untreated foundation

All the figures agree well showing that:

1. There is no doubt about the failure of sand columns not confined by a geofabric in strengthening a loose fill which exhibit a collapse behaviour during inundation.

2. There is a reduction of settlement which increases on increasing the stiffness of the 'piles'. For some 'piles' the increase in stiffnesses was caused by the different strengths of the reinforcing geofabric.

3. The use of sand columns encapsulated in a geofabric as deep foundations is more efficient for small loads. For working loads of 20% P_u and a fully penetrating sand column encapsulated in T2000, it was found that $\beta = 0.32$. Accordingly, for this case the magnitude of collapse defined as:

$$CP = \frac{\Delta H}{H_0}$$

where:

ΔH: settlement of the foundation 'model'

H_0: thickness of the collapsing layer.

was dropped from 13% for the soil alone to about 4% for the sand column encapsulated in a fabric T2000. According to Jennings and Knight (1975) this finding means that the reinforcement has changed the situation from exhibiting severe trouble for the soil alone, as foundation support, to only moderate trouble for a foundation consisting of sand column encapsulated in a T2000 fabric (see Table 2.1).

7.5.2.2 Effects of 'Pile'-Length on settlement behaviour:

To study the effects of 'pile' length on the settlement behaviour of the different types of foundation supports under external axial load and subjected to inundation, all the results obtained from the tests of series (III) (Table 6.2) were plotted in Figs 7.29-a to 7.34-c. Each figure represents one type of foundation support, of 3 different lengths, under a given working load.

With the exception of Figs 7.29-a, 7.29-b and 7.29-c, all the figures show that the total settlement of the foundation 'model' due to the external load and inundation decreased on increasing the length of the 'pile'. The decrease obtained by increasing the length from 300 mm to 410 mm is bigger than that between 250 mm and 300 mm. This trend may be simply explained by the existence of a collapsible layer beneath the tip of the partially penetrating 'pile'. The additional settlement of the 'pile' caused by the collapse of this layer decreases with increasing length. Therefore, although the increase of the length of the 'pile' increases its contact with the surrounding soil and hence the additional settlement caused by downdrag (Tomlinson, 1969 and Zeevaert, 1978), it seems that the settlement caused by the collapse of the layer situated beneath the tip of the 'pile' is the more predominant and has a greater influence on the total settlement recorded. Accordingly, as mentioned in the previous sub-section, in collapsible soils the foundation must be carried to a

depth where the collapse is negligible or doesn't exist.

For latter comparison with predicted results all the data from the previous figures were re-plotted as shown in Figs 7.35 to 7.37. These figures present the variation of the settlement reduction factor (β) as a function of L/d (the ratio of the length to the 'pile' diameter). The resulting curves clearly show that increase of the length of any type of 'pile' (except sand columns without confinement) did decrease the settlement of the foundation 'model' caused by inundation when under an external axial load.

7.6 Comparison Between Experimental and Theoretical Results:

A comparison was made between the measured and the predicted settlement of the top of a 'pile' caused by inundation when under an external axial load, i.e., between the results discussed in sub-sections 7.5.2 and 3.4.4. The experimental settlement reduction curves have been given in two forms. The first form (form 1), which corresponded to the reduction in vertical compression as a function of 'pile'-stiffness, the data are plotted in Figures 7.26-a to 7.28-c. The second form (form 2) are presented in Figs 7.35 to 7.37 and were designed to show the reduction in vertical compression as a function of 'pile'-length. Apart from the sand columns without confinement, which are the exceptions to the general trend as discussed in the previous section, the curves of both forms clearly show that the increase of 'pile'-stiffness and 'pile'-length reduces the settlement to an acceptable extent for the more rigid and longest 'piles'. The theoretical simulated settlement reduction curves have also been given in two forms (form 1 and 2). The curves which belong to form 1 were presented in Figs 3.16 to 3.24 and those of form 2 in Figs 3.25 to 3.30. By comparing these predictions with the experimental results it was deduced that the analytical solution to the problem of settlement in collapsible soils subjected to

inundation is far from being elastic. Therefore all the theoretical curves obtained by considering an elastic solution were rejected. For further comparison only the theoretical curves obtained by employing a slip solution will be considered. For this purpose all the experimental curves of Figs 7.26-a to7.28-c and the corresponding theoretical curves of the slip solution of Figs 3.16 to 3.24 were grouped in Figs 7.38-a to 7.40-c. A similar method of presentation was adopted for the experimental and theoretical curves of form 2. All the figures of this form are grouped in Figs 7.41 to 7.43. This method of presentation was found convenient for comparison purposes.

These figures (Figs 7.38-a to 7.40-c and Figs 7.41 to 7.43) reveal a remarkable degree of agreement between the shape of the experimental and theoretical curves of settlement reduction. The only point of disagreement is that the theory predicts a smaller settlement. The difference between the predicted and the measured settlement reductions increases with increase in the working load and decreases with increase in the 'pile'-length. This disagreement may be attributed to the following factors:

1. For partial penetration it was assumed that the soil settlement varied linearly from S_0 at the surface to zero at the base. However, the field evidence (Ferreira et al., 1987 and Charles, 1978) shows that the settlement of a collapsible layer caused by inundation varies in a hyperbolic form with depth. Therefore, the additional settlement caused by the collapse of the layer situated beneath the tip of the partially penetrating 'pile' in the latter consideration is larger than that obtained by assuming a linear variation of settlement with depth.

2. For full penetration the theory assumed that the bearing stratum is rigid whereas, in reality, the compressibility of the bearing stratum may allow a considerable movement of the 'pile'.

3. The assumption of having constant E_s and E_p with depth is conservative. It was found by Poulos et al. (1980) that downdrag forces and pile movement

decreased (typically by 10 to 25 %) as compared with the case of linearly-varying E_s and E_p.

4. The third component of settlement (δ_3) was estimated by assuming compatibility of lateral deformations between the column material and the cylinder fabric around it. The deformation of the cylinder fabric was considered to follow Hooke's law. However, the stress-strain behaviour of the material used showed that this approach underestimated the value of (δ_3).

In conclusion, although the agreement between measured and predicted results is good and may be better if consideration is taken of the previous mentioned points, it seems very difficult to draw a final conclusion about the theoretical solution proposed to predict what might happen. This difficulty is due to the following factors:

1. The limitations of the theory imposed by the determination of the pile-soil paramaters. The conventional types of triaxial tests have been found to underestimate the values of the modulii of elasticity (E_s) and (E_p) of the soil and the 'pile' respectively (Bromham & Styles, 1971 and Mattes, 1972). The suitability of the deformation parameters derived (in this investigation) from triaxial tests for settlement analysis should be further investigated. Possibilities of other, more appropriate forms of laboratory testing were reviewed in section 4.1.

2. The lack of published full-scale test data on stone columns reinforced by geofabrics and rigid piles in collapsible soils subjected to inundation.

However, it is definitely confirmed that, to predict the settlement of the top of a 'pile' under an axial load in a collapsible soil subjected to inumndation, the local yield or slip between the 'pile' and the soil must be taken into account. It is also noteworthy that there is no significant difference in the determination of the settlement caused by lateral deformation (δ_3) using the Priebe approach or by the modified Hughes

method. It seems that the latter method slightly reduced the difference between the measured and predicted results. Therefore it is recommended to use the modified Hughes method for the computation of δ_3 during the estimation of the total settlement of the top of a 'pile' in a collapsible soil as given by equation 3.15.

Table 7.1 Characteristics of the Tests Performed in the Rowe Cell (series I):

Test Code $N°$	Moisture Content (%)	Dry Density (Mg/m^3)	Void Ratio
1	4	1.468	0.805
2	4	1.502	0.764
3	4	1.516	0.748
4	5.2	1.516	0.748

Table 7.2 Characteristics of Preliminary Tests (series I):

Test $N°$	Test Code $N°$	Type of 'Pile'	Length of 'Pile' (mm)	Tests's Type	Container $N°$
1	C1	sand	410	1	1
2	C2	column	410	1	1
3	C3	not confined	410	1	2
4	S1	by a	410	2	1
5	S2	geofabric	410	2	1
6	S3		410	2	2

Table 7.3 Characteristics of Tests Performed (series I):

Test $N°$	Test Code Name	Length of 'Pile'	Inundation	Group	Type of Foundation
1	BSA		No		soil alone
2	B1	410	No	Gr (1)	sand column
3	B2	250	No		sand column
4	FSA		Full		soil alone
5	F1	410	Full	Gr (2)	sand column
6	F2	250	Full		sand column
7	PSA		Partial		soil alone
8	P1	410	Partial	Gr (3)	sand column
9	P2	250	Partial		sand column

Type of Foundation	Test Code Name	P_u (N) Chin's Method	Test Code Name	P_u (N) Chin's Method	Test Code Name	P_u (N) Chin's Method
Sand Column	BC1	189.6	BC7	195.2	BC13	205
S. Column Confined by T700	BC2	230.8	BC8	251	BC14	272
S. Column Confined by T1000	BC3	240	BC9	259	BC15	282
S. Column Confined by T1500	BC4	255	BC10	273	BC16	294
S. Column Confined by T2000	BC5	300	BC11	317	BC17	340
Rigid Pile	BC6	388	BC12	417	BC18	507

Table 7.4 Load Carrying Capacity for all the 'Piles'

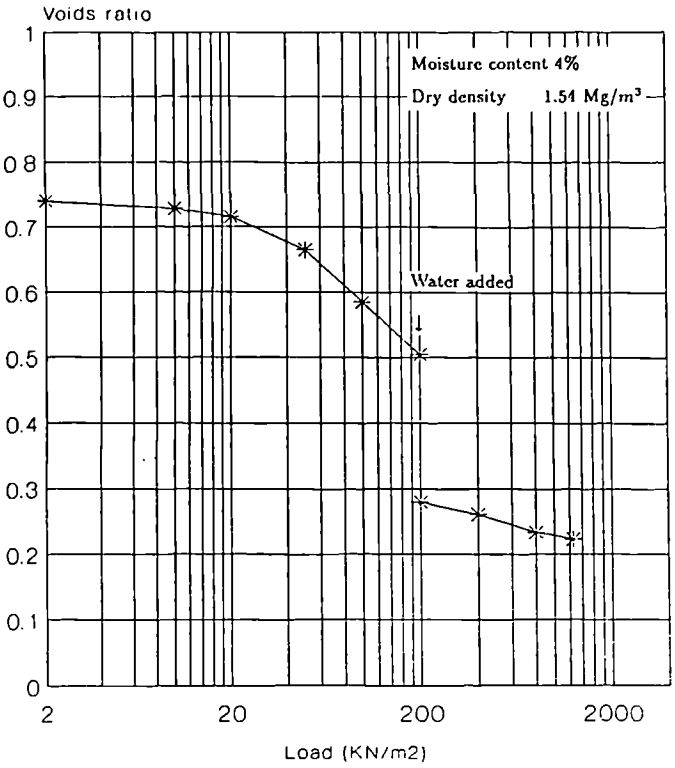

Fig. 7.1 Collapse potential test result.

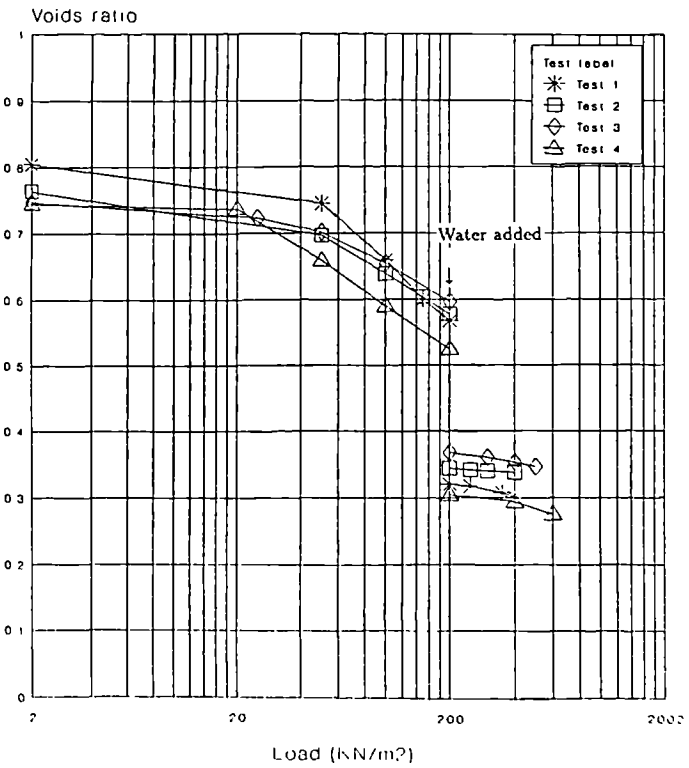

Fig. 7.2 Test result of the Rowe cell.

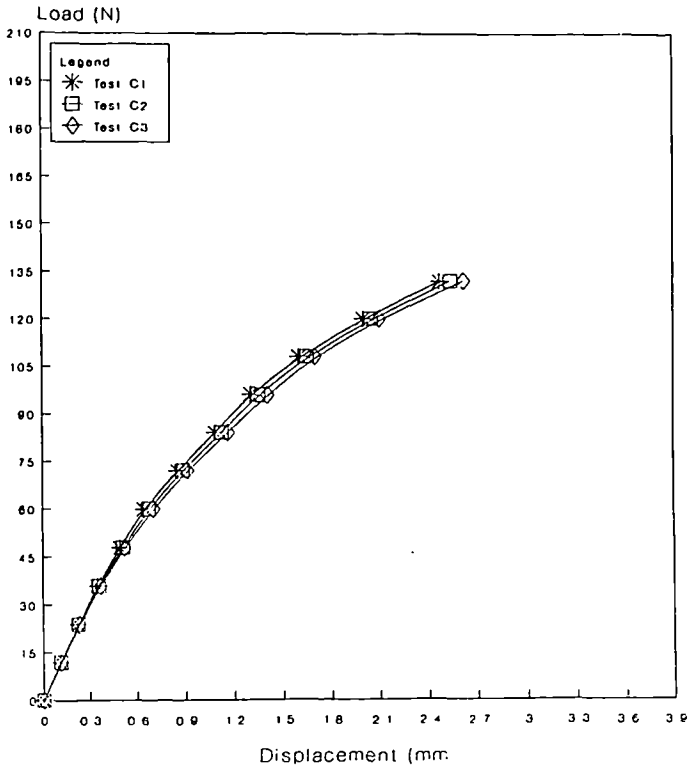

Fig. 7.3-a Test repeatability (I).

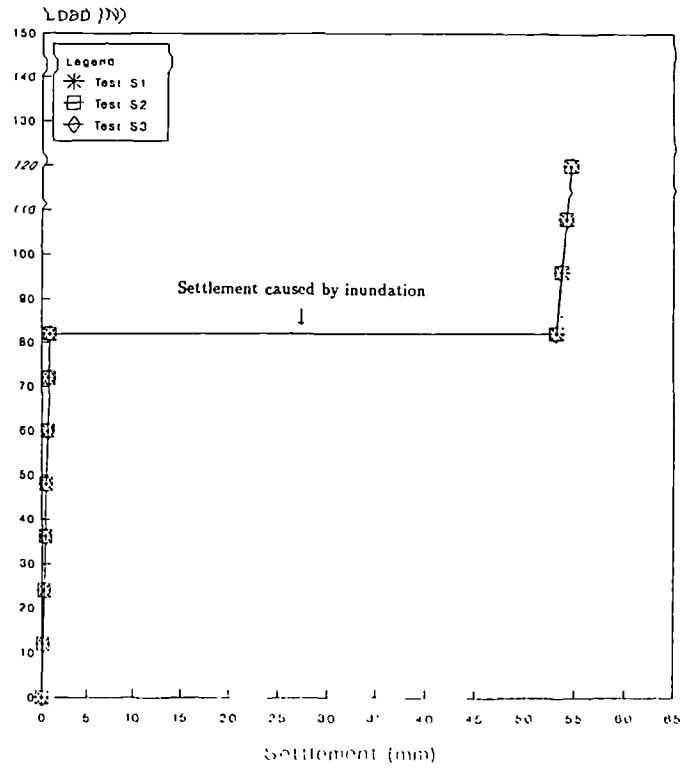

Fig. 7.3-b Test repeatability (II).

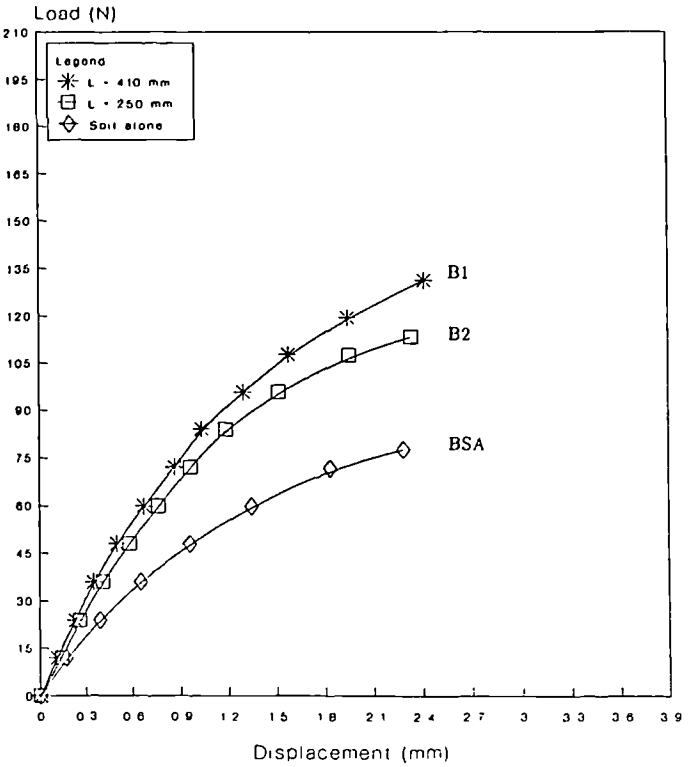

Fig. 7.4 **Load-displacement relationship for the collapsible soil and the stone columns as foundation supports.**

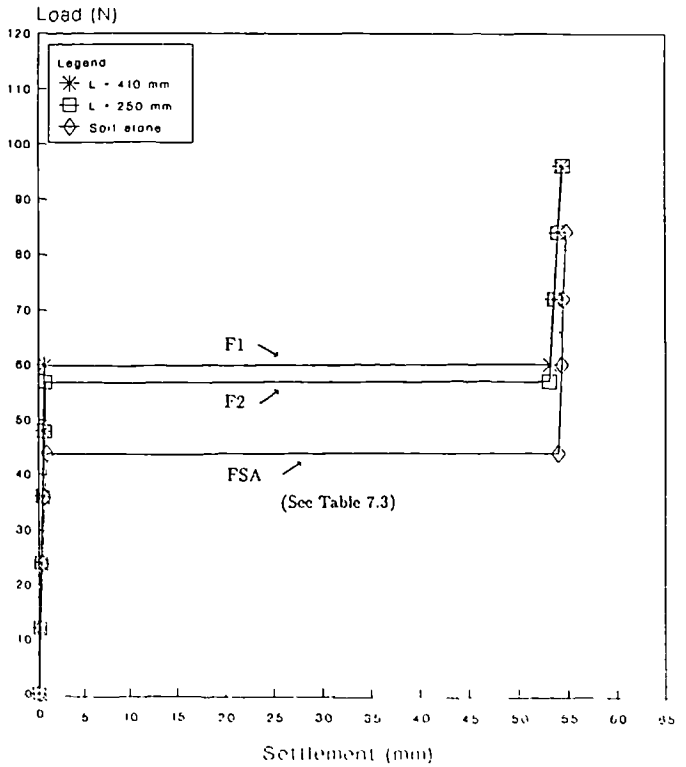

Fig. 7.5 **Settlement curves for the collapsible soil and the stone columns after full inundation under a working load = 30% P_u.**

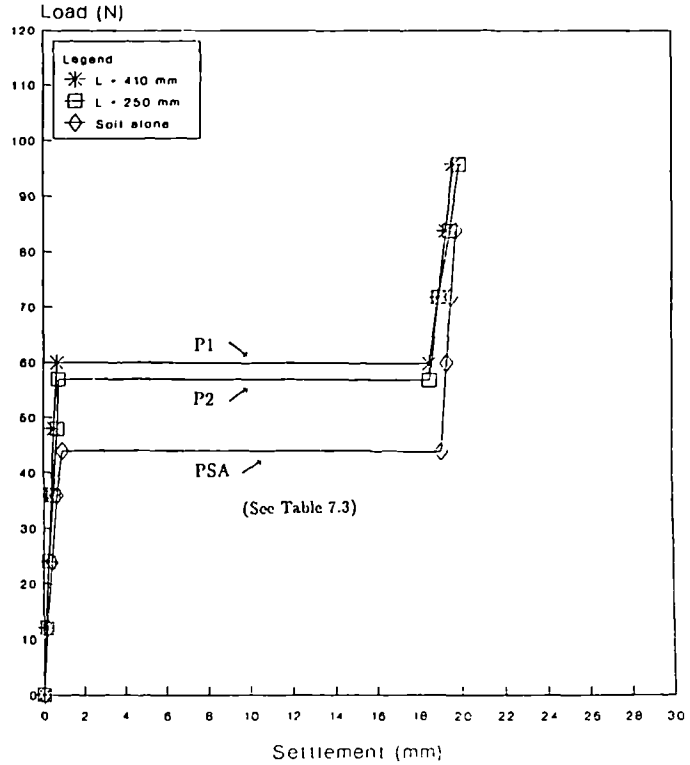

Fig 7.6 Settlement curves for the collapsible soil and the stone columns after partial inundation under a working load = 30% P_u.

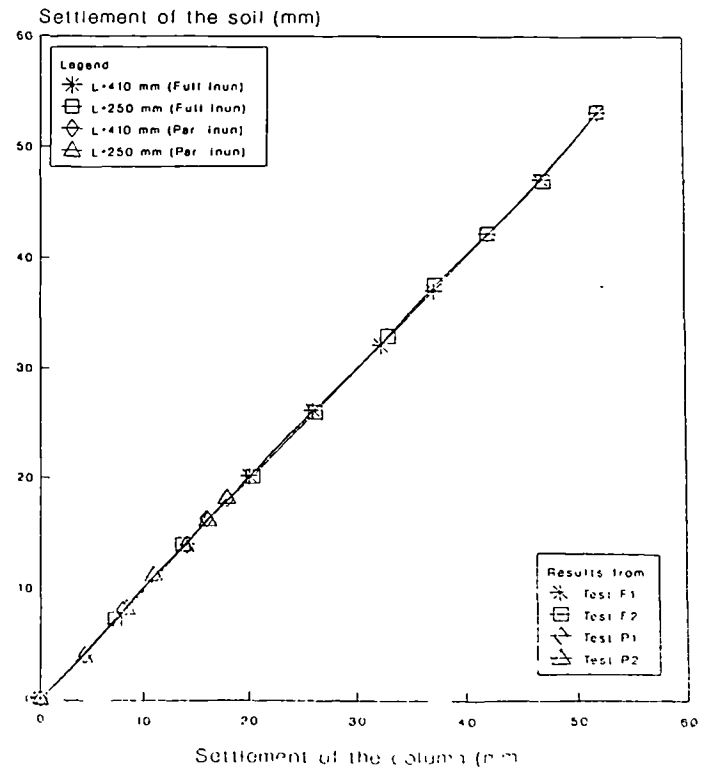

Fig. 7.7 Relationship between soil/column settlements.

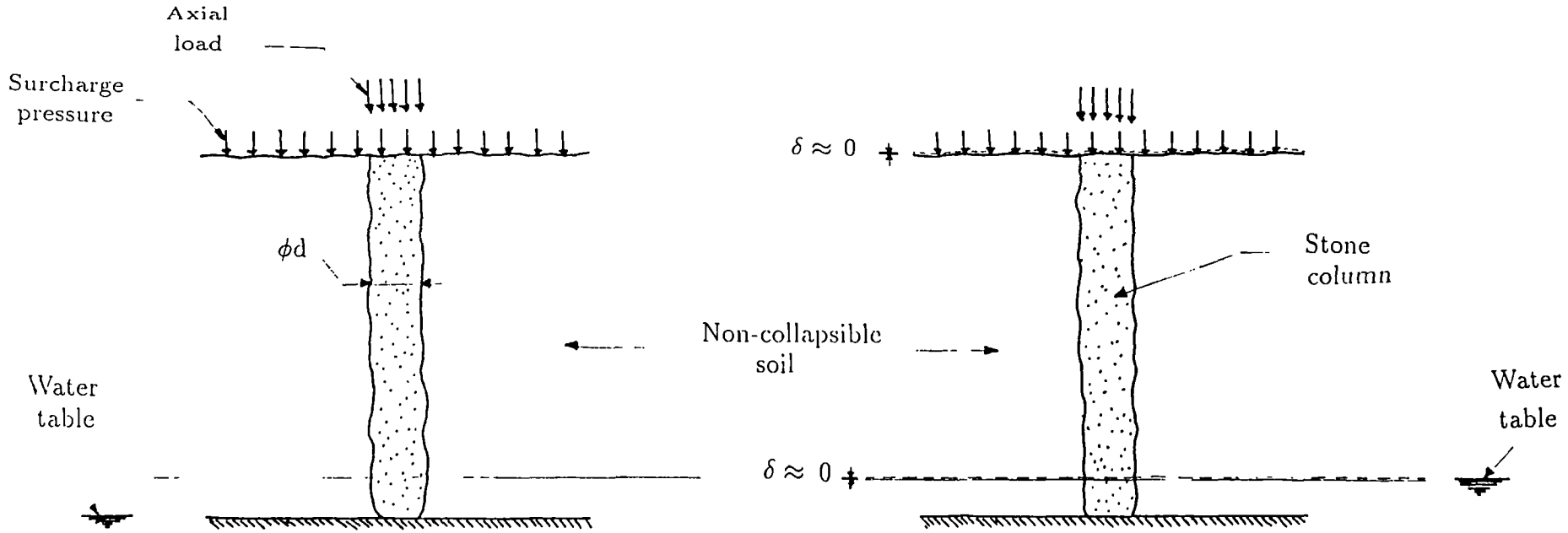

Fig. 7.8 Process of Settlement of a Non-Collapsible Fill, around a Stone Column, due to Inundation

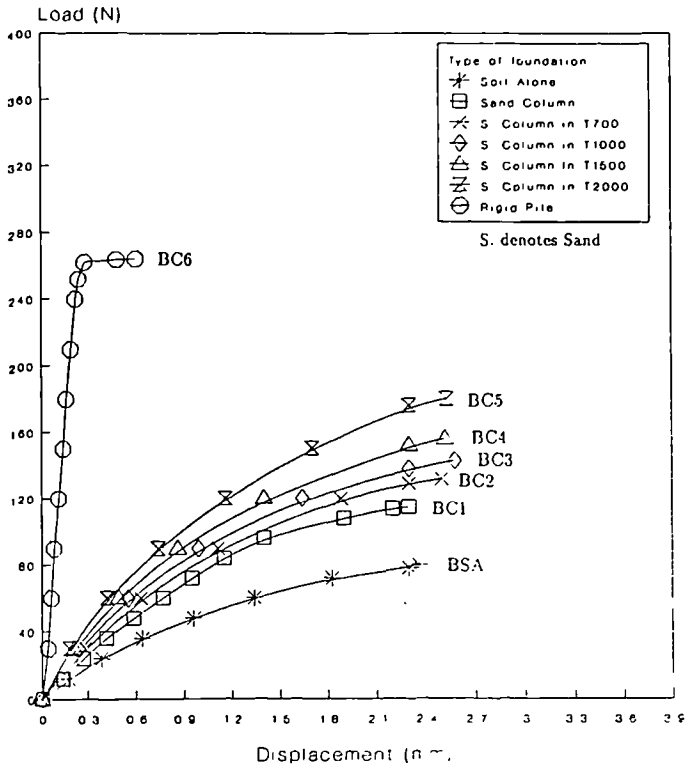

Fig. 7.9-a **Load-displacement relationship for sand columns encapsulated and not encapsulated in a geofabric and a rigid pile of length, L = 250 mm.**

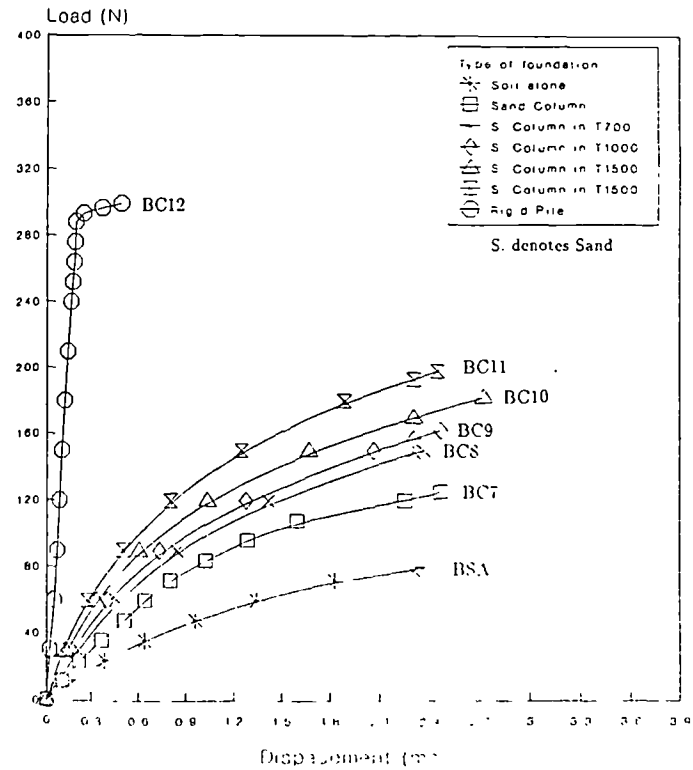

Fig. 7.9 b **Load-displacement relationship for stone columns encapsulated and not encapsulated in a geofabric and a rigid pile of length, L = 300 mm.**

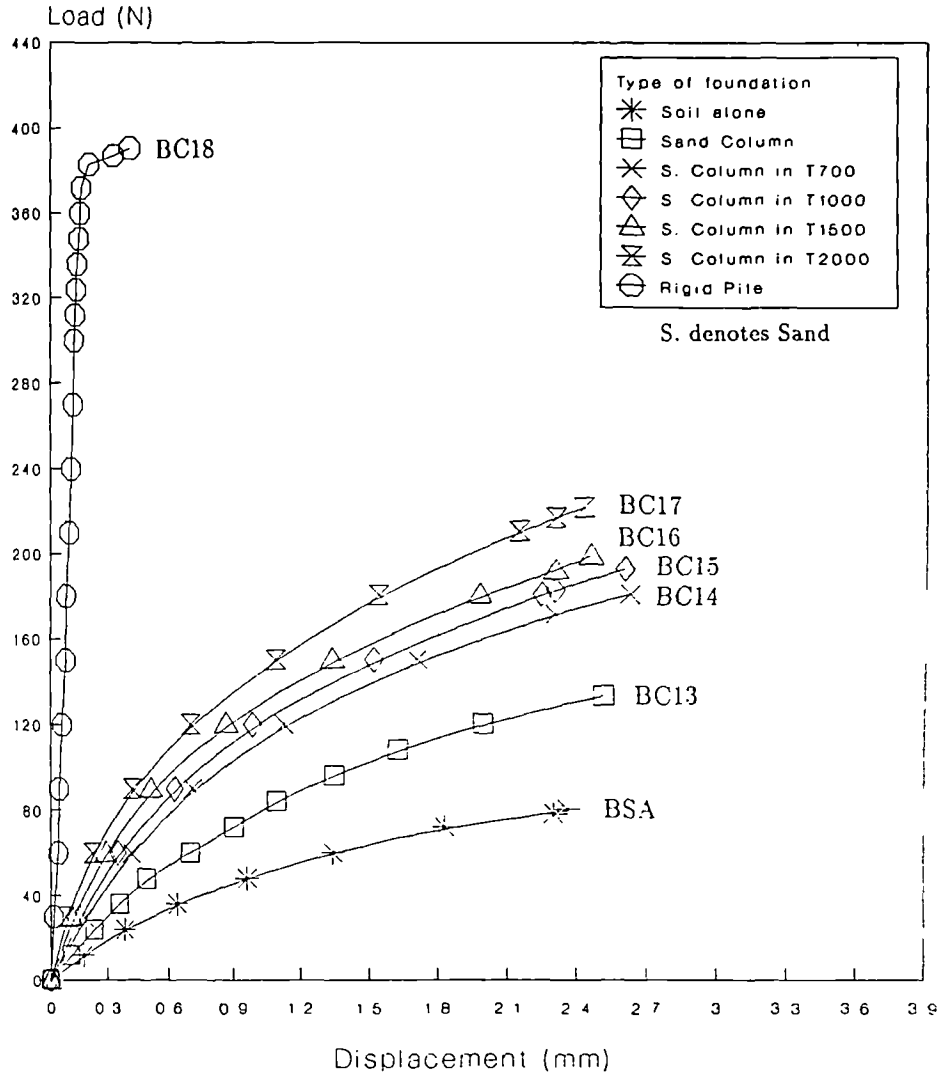

Fig. 7.9-c **Load-displacement relationship for sand columns encapsulated and not encapsulated in a geofabric and a rigid pile of length, L = 410 mm**

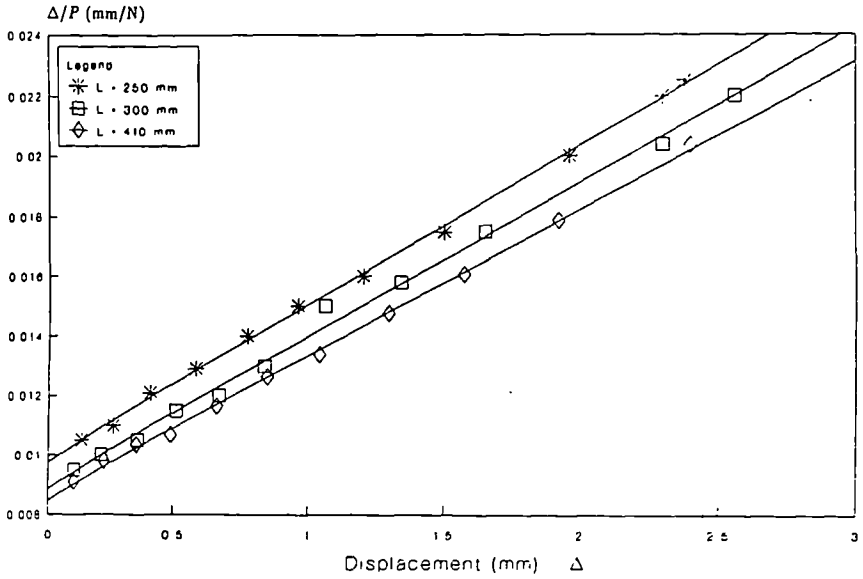

Fig. 7.10 Chin's plots for sand columns not encapsulated in a geofabric.

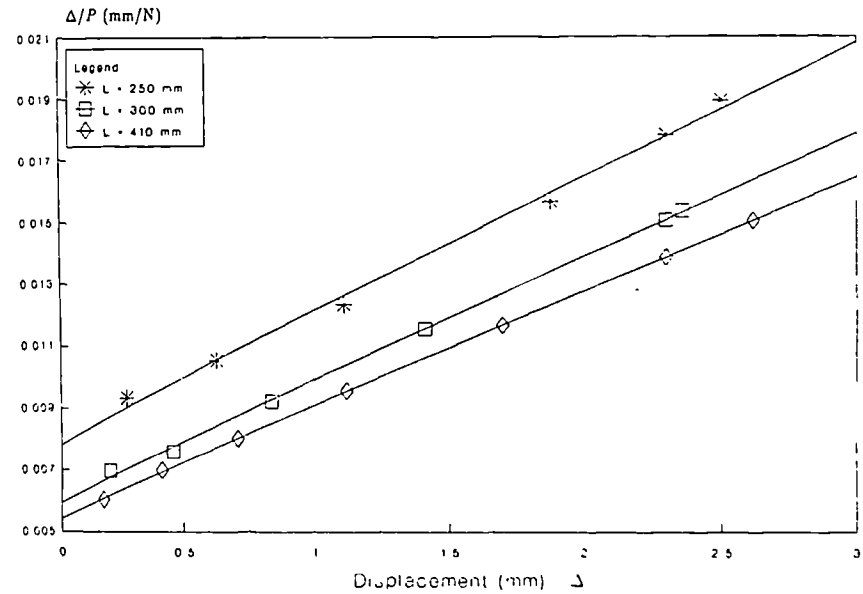

Fig. 7.11 Chin's plots for sand columns encapsulated in T700.

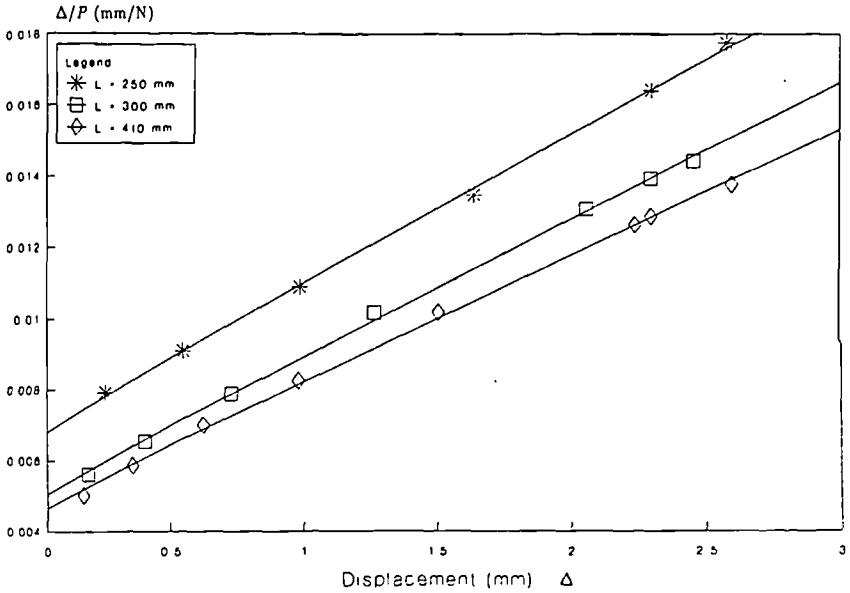

Fig. 7.12 Chin's plots for sand columns encapsulated in T1000.

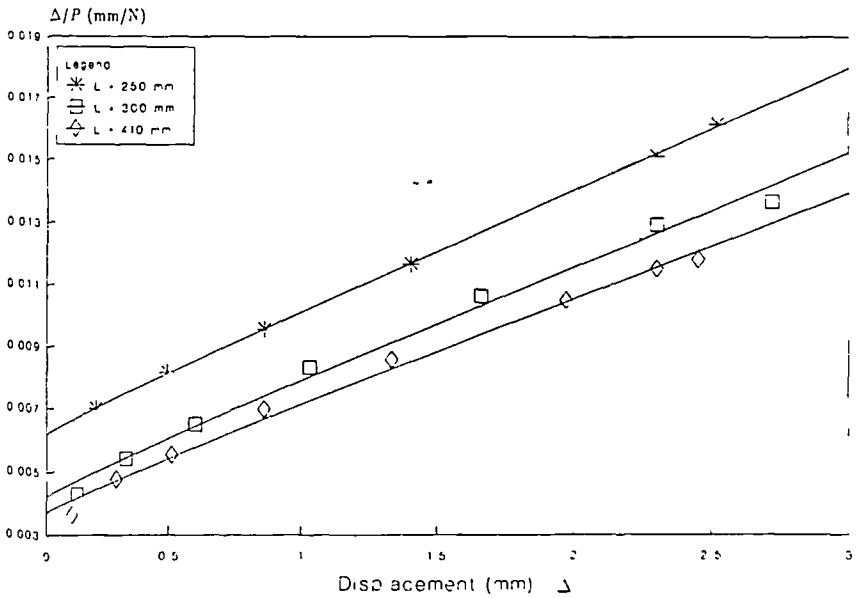

Fig. 7.13 Chin's plots for sand columns encapsulated in T1500.

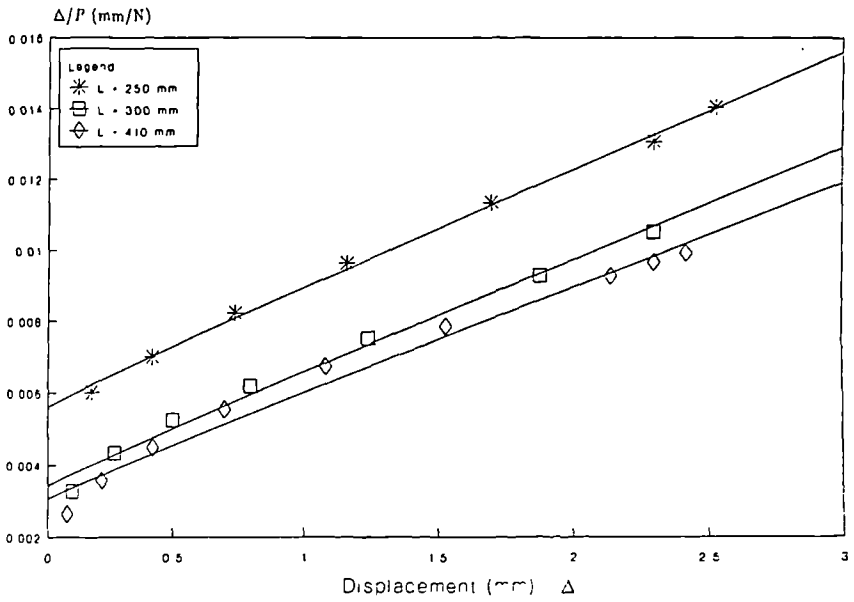

Fig. 7.14 Chin's plots for sand columns encapsulated in T2000.

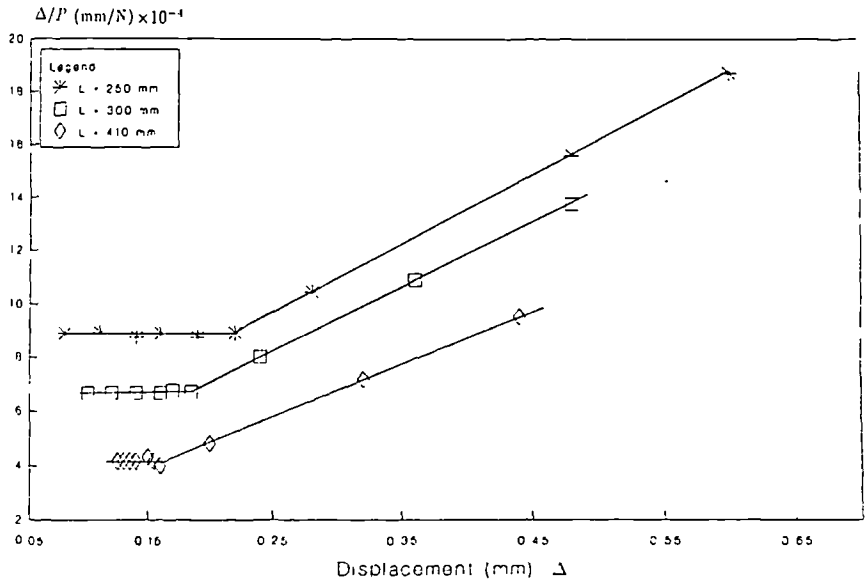

Fig. 7.15 Chin's plots for rigid piles.

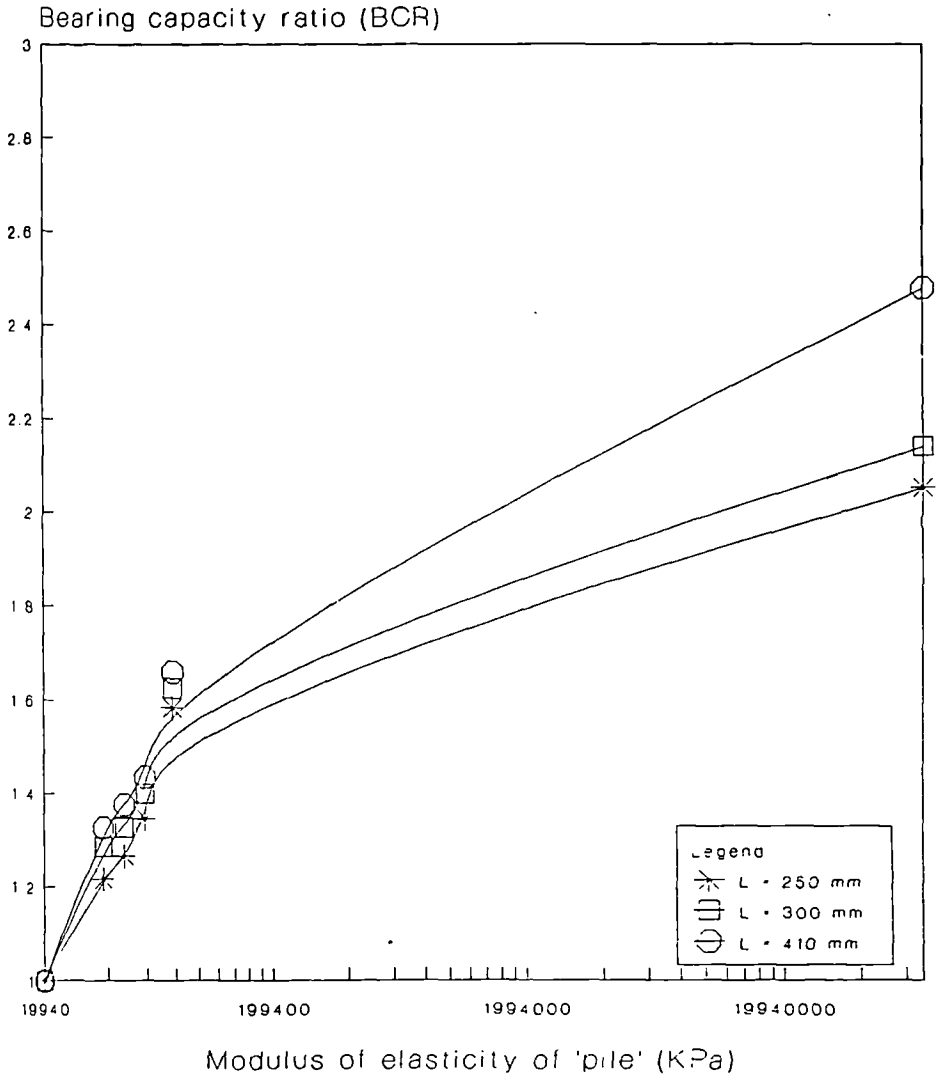

Fig. 7.16 Effect of 'pile'-stiffness on bearing capacity ratio.

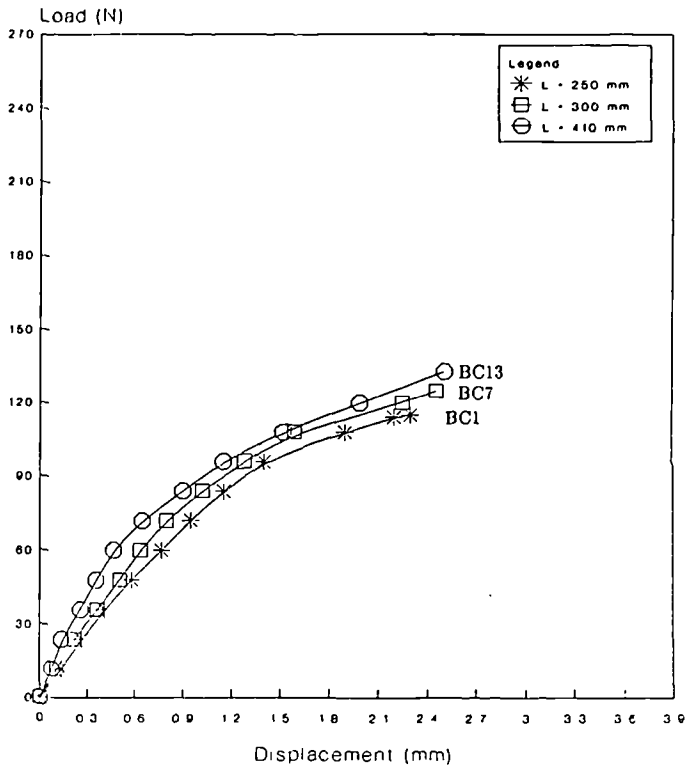

Fig. 7.17 Load-displacement relationship for sand columns not confined by a geofabric.

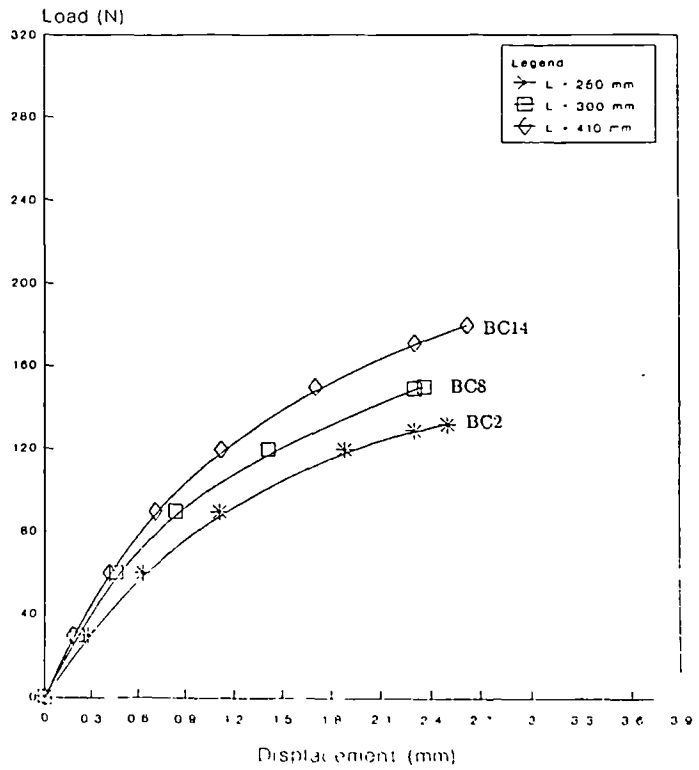

Fig. 7.18 Load-displacement relationship for sand columns confined by T700.

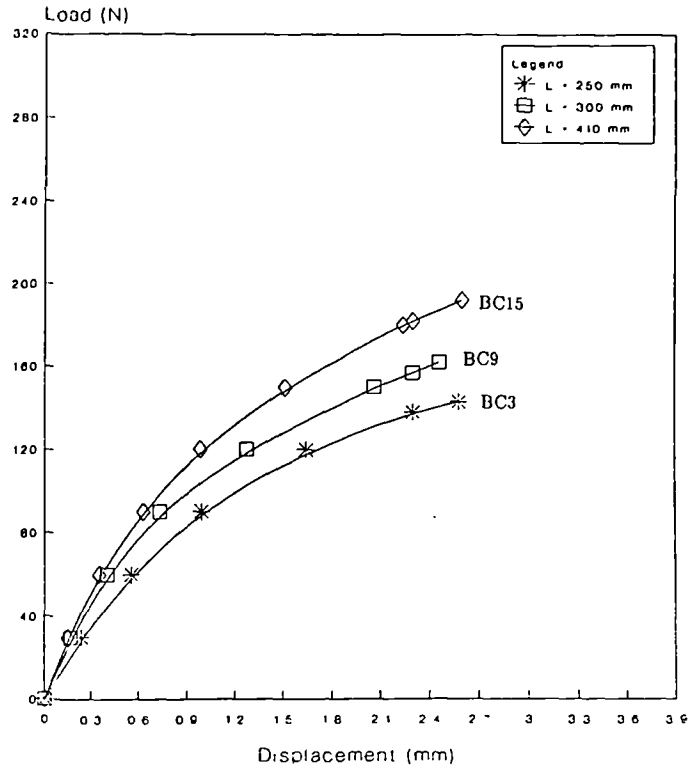

Fig. 7.19 **Load-displacement relationship for sand columns confined by T1000.**

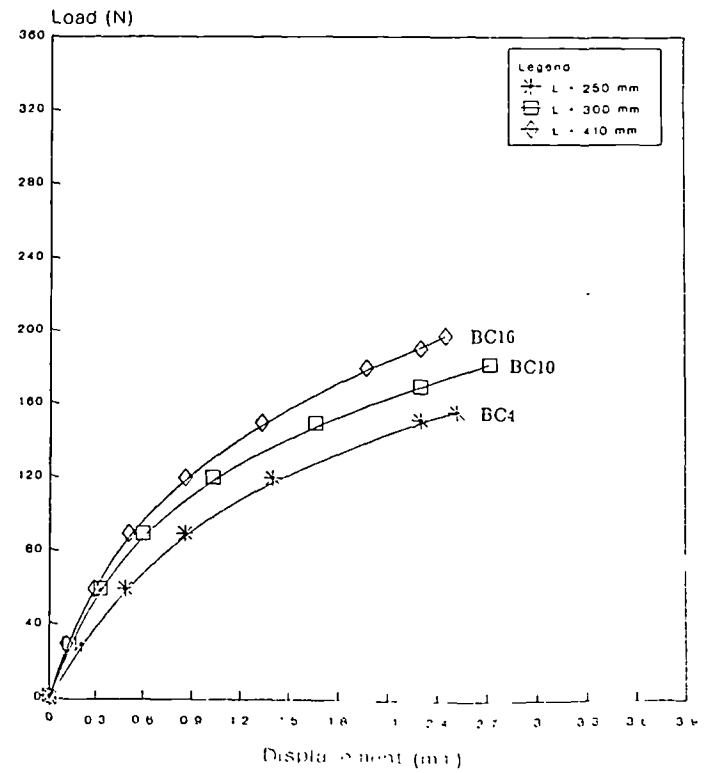

Fig. 7.20 **Load-displacement relationship for sand columns confined by T1500.**

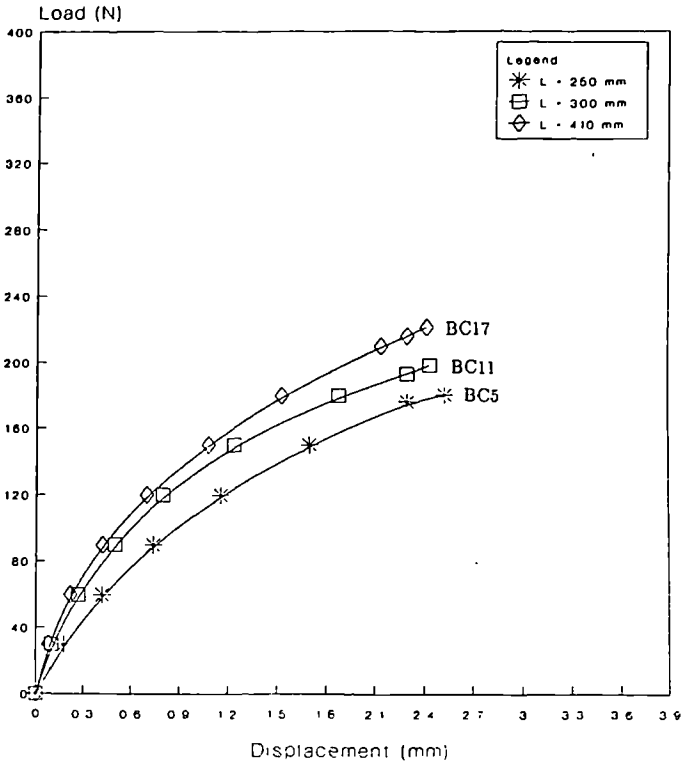

Fig. 7.21 Load-displacement relationship for sand columns confined by T2000.

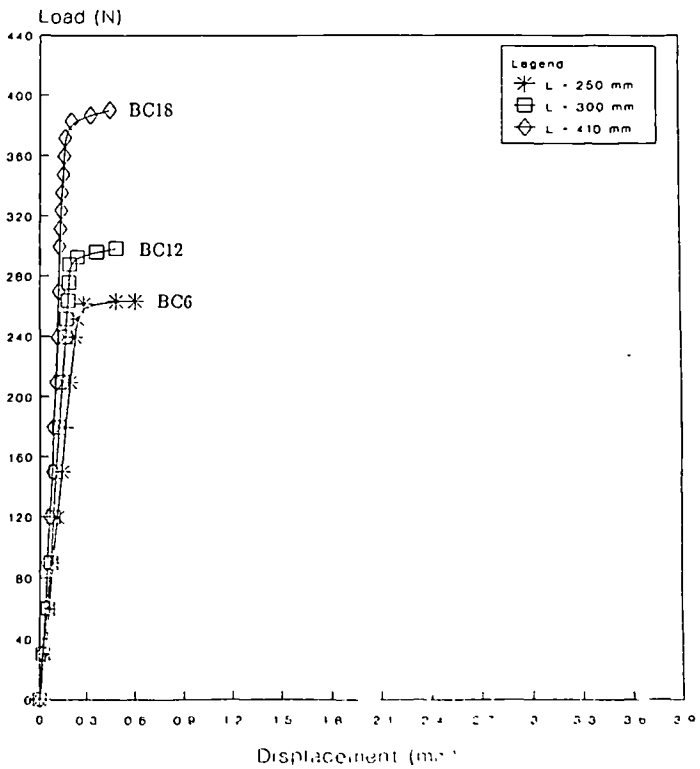

Fig 7.22 Load-displacement relationship for rigid piles.

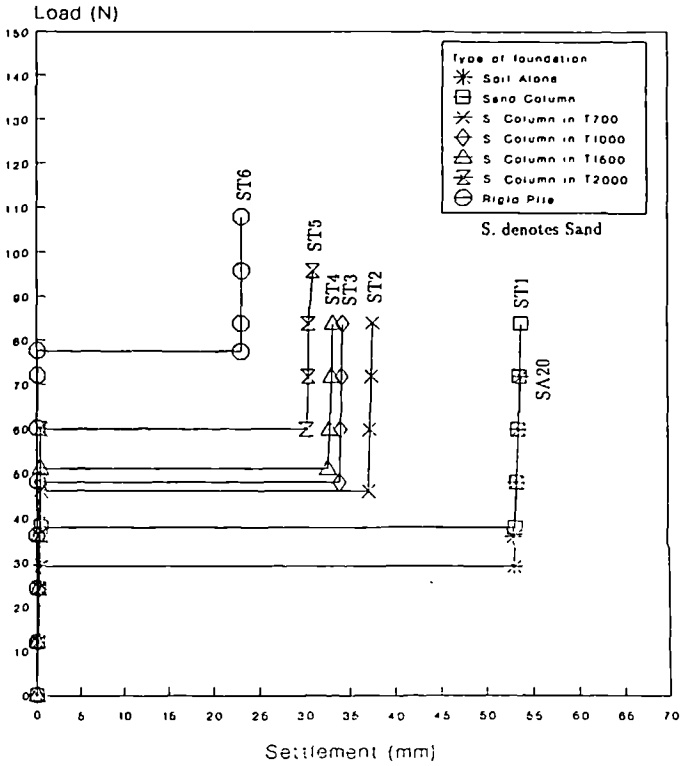

Fig 7.23-a Settlement curves for the different foundation supports, of length L = 250 mm, after full inundation under an applied load equal 20% P_u.

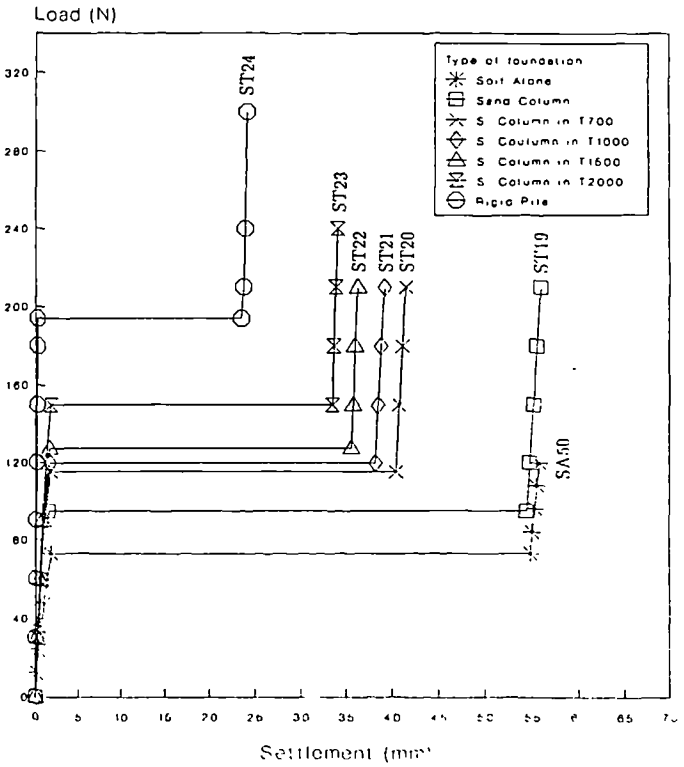

Fig 7.23-b Settlement curves for the different foundation supports, of length L = 250 mm, after full inundation under an applied load equal 50% P_u.

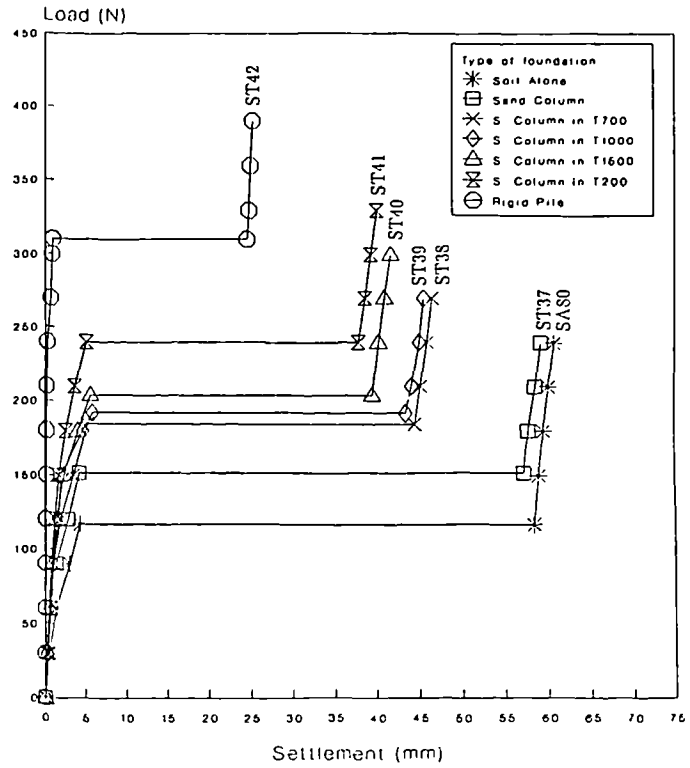

Fig. 7.23-c Settlement curves for the different foundation supports, of length L = 250 mm, after full inundation under an applied load equal 80% P_u.

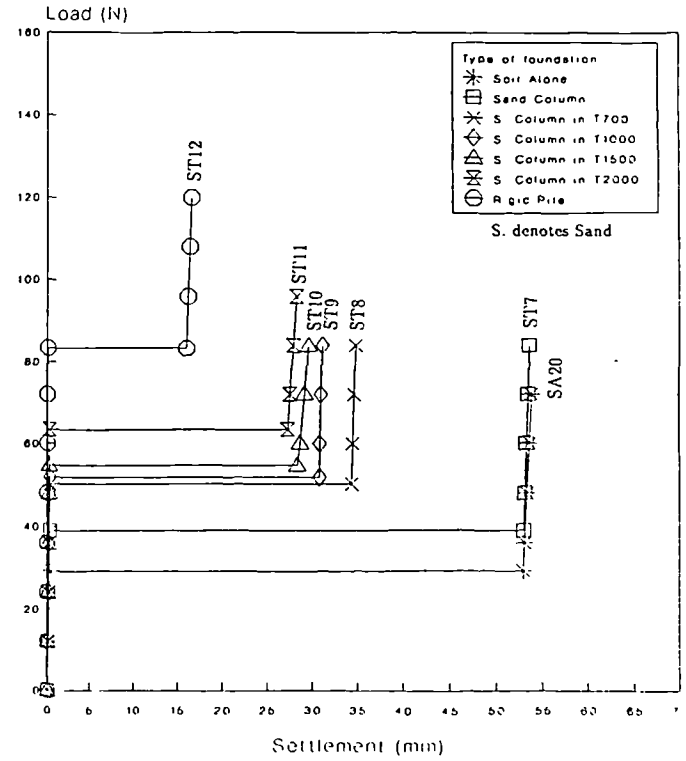

Fig. 7.24-a Settlement curves for the different foundation supports, of length L = 300 mm, after full inundation under an applied load equal 20% P_u.

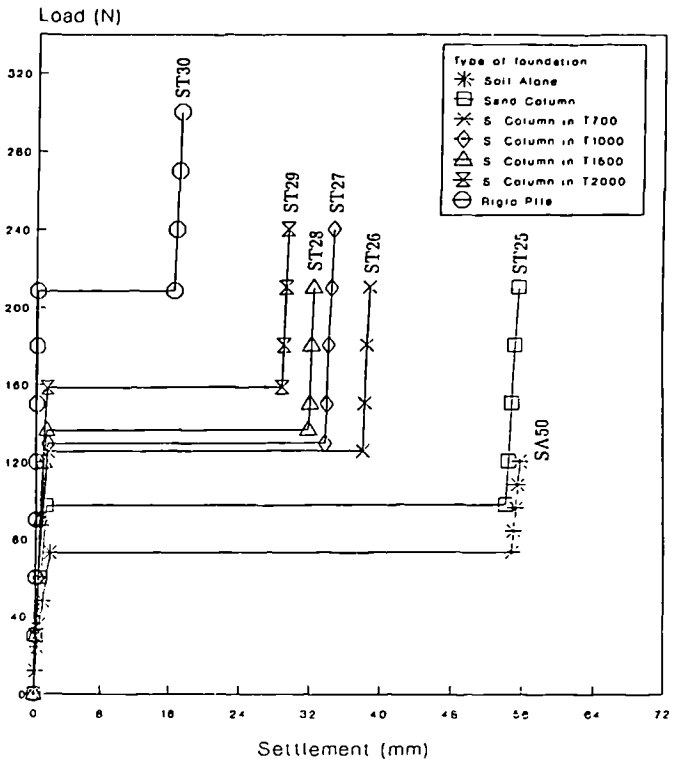

Fig. 7.24-b Settlement curves for the different foundation supports, of length L = 300 mm, after full inundation under an applied load equal 50% P_u.

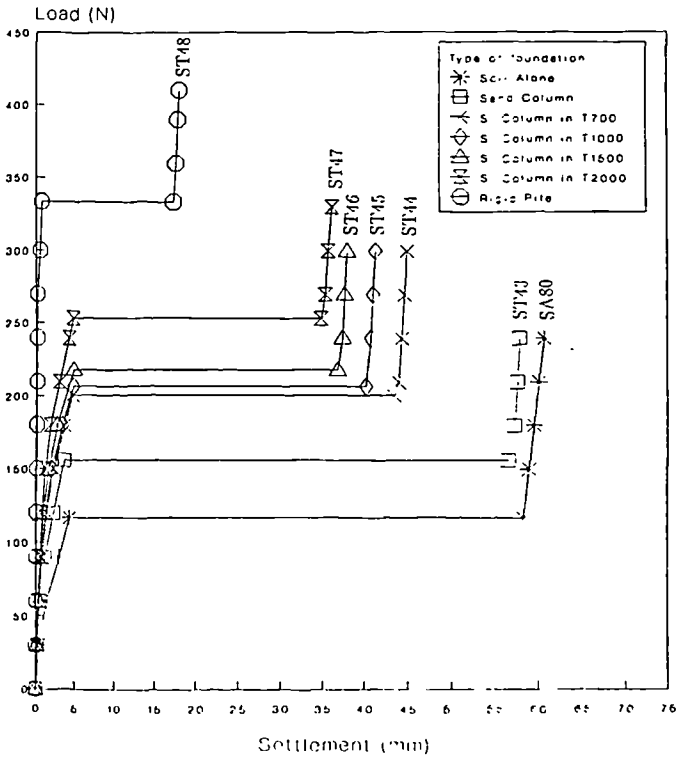

Fig. 7.24-c Settlement curves for the different foundation supports, of length L = 300 mm, after full inundation under an applied load equal 80% P_u.

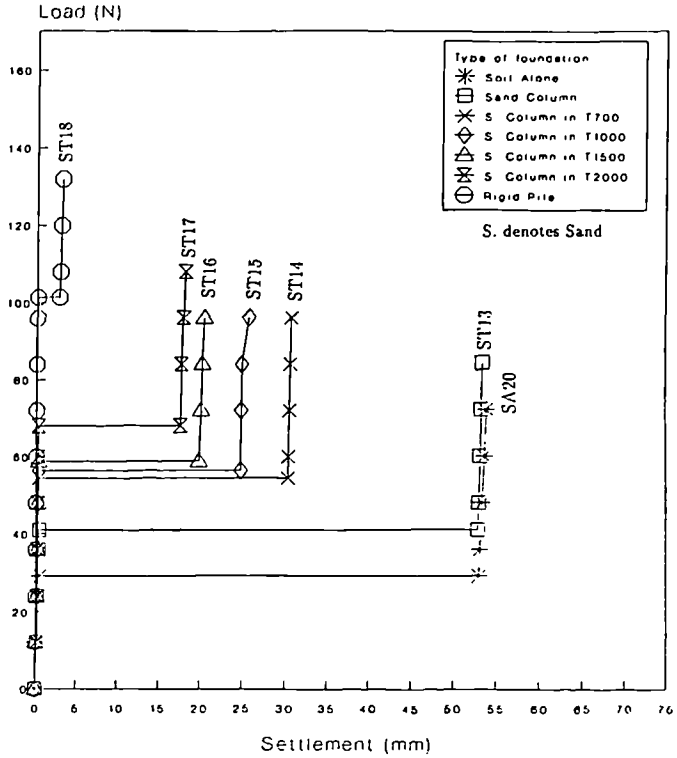

Fig. 7.25-a Settlement curves for the different foundation supports, of length L = 410 mm, after full inundation under an applied load equal 20% P_u.

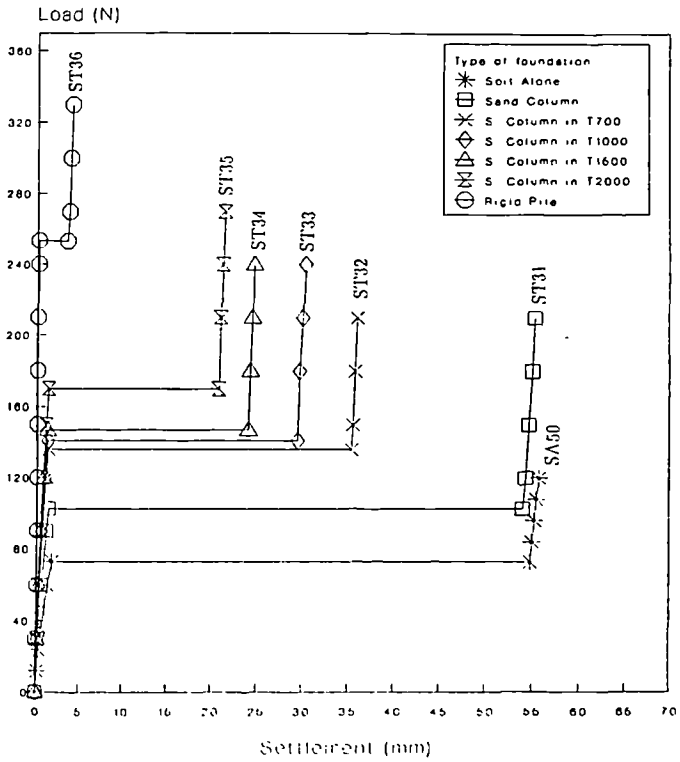

Fig. 7.25-b Settlement curves for the different foundation supports, of length L = 410 mm, after full inundation under an applied load equal 50% P_u.

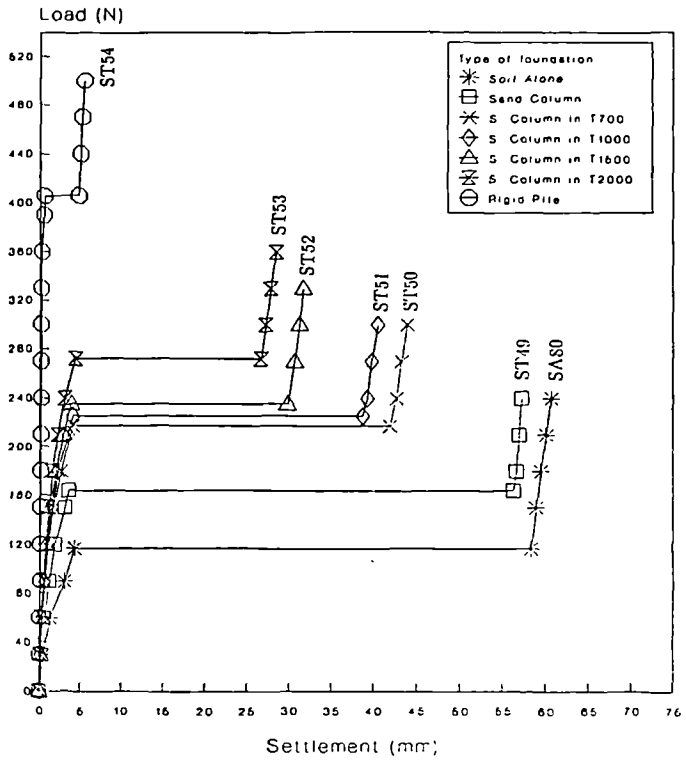

Fig. 7.25-c **Settlement curves for the different foundation supports, of length L = 410 mm, after full inundation under an applied load equal 80% P_u.**

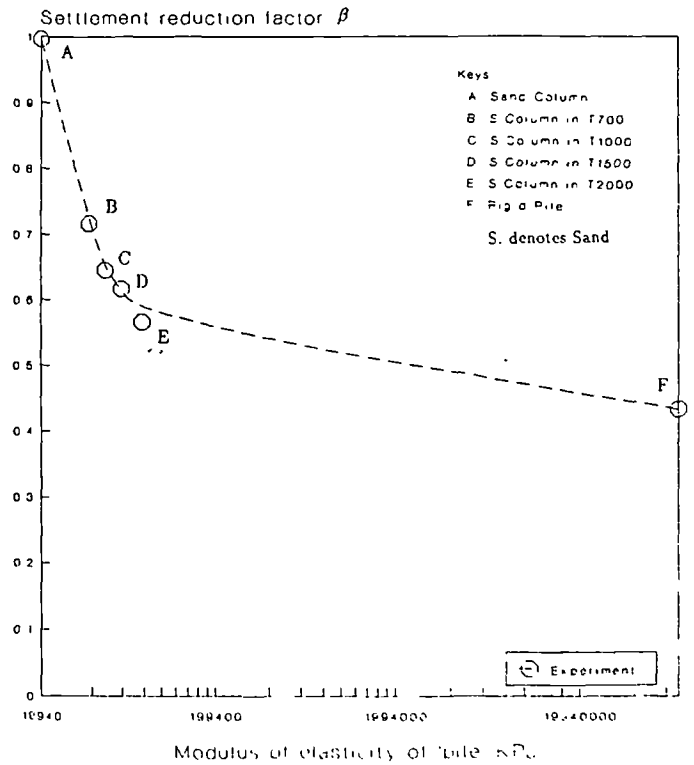

Fig 7.26-a **Reduction in vertical compression as a function of 'pile'-stiffness. (for L = 250 mm and an applied load = 20% P_u)**

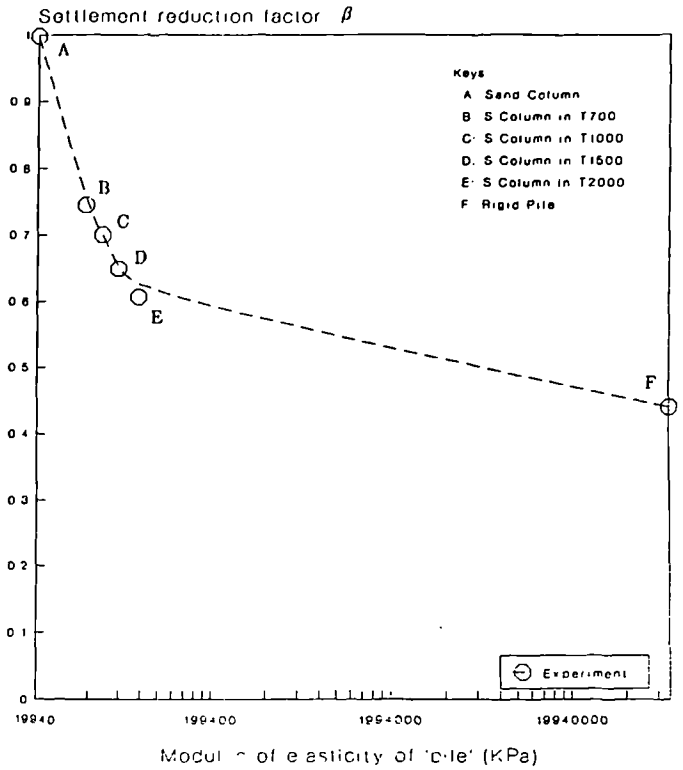

Fig 7.26-b Reduction in vertical compression as a function of 'pile'-stiffness. (for L = 250 mm and an applied load = 50% P_u)

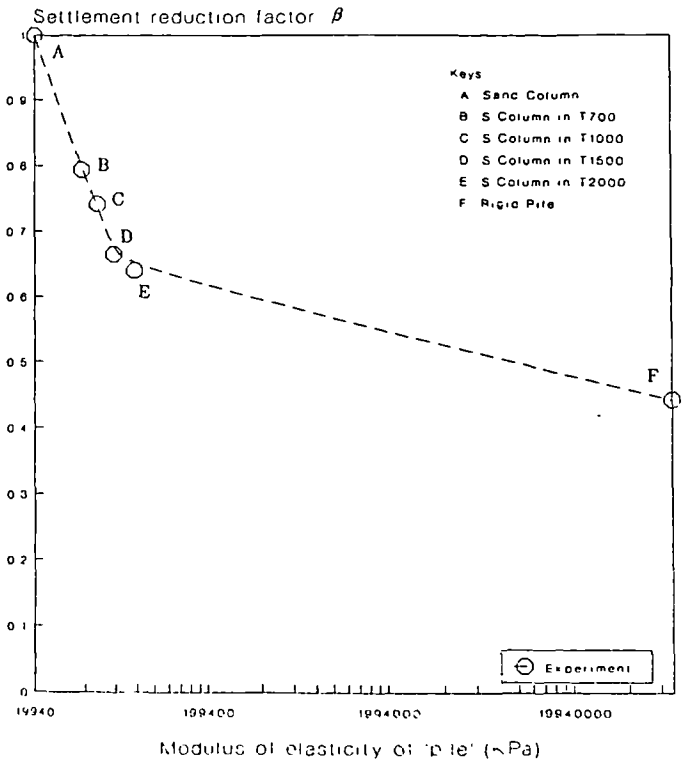

Fig. 7.26-c Reduction in vertical compression as a function of 'pile'-stiffness. (for L = 250 mm and an applied load = 80% P_u)

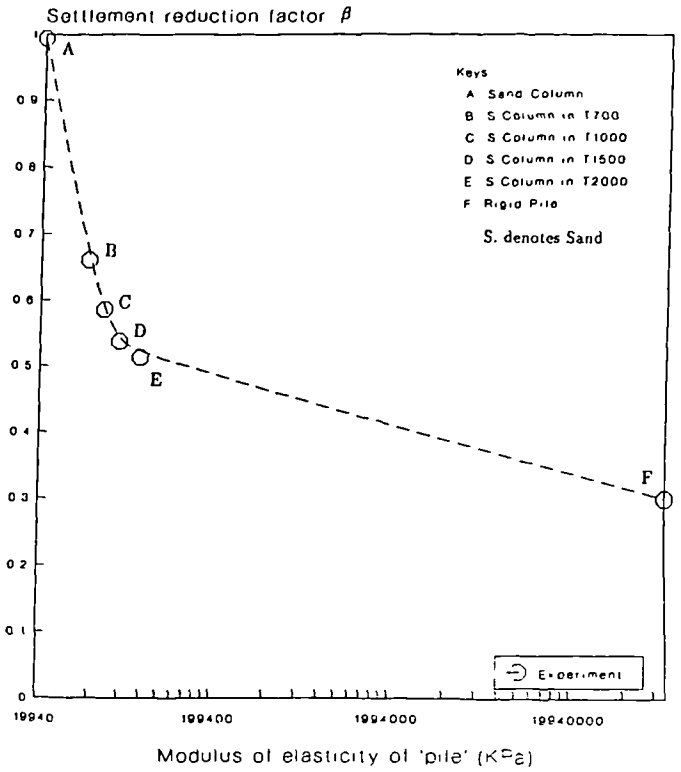

Fig. 7.27-a **Reduction in vertical compression as a function of 'pile'-stiffness. (for L = 300 mm and an applied load = 20% P_u)**

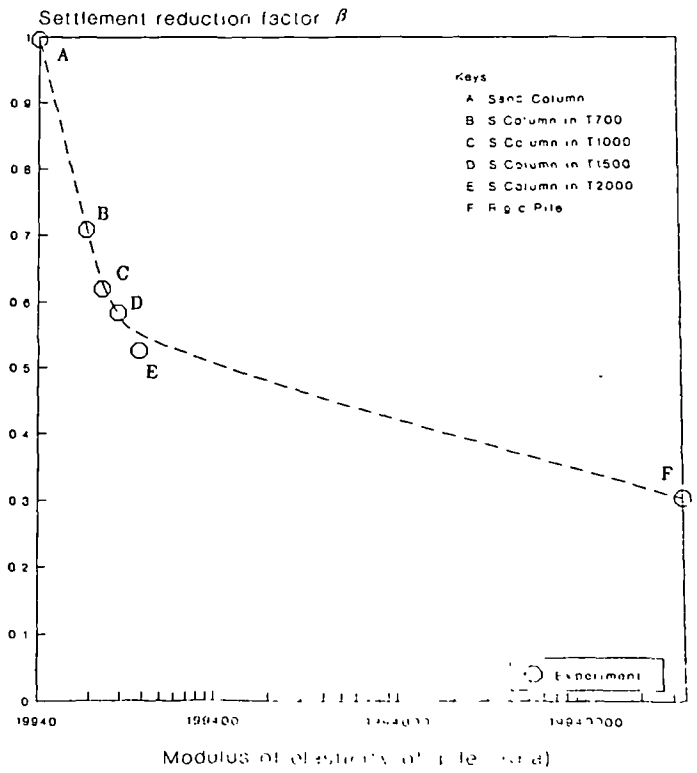

Fig. 7.27-b **Reduction in vertical compression as a function of 'pile'-stiffness. (for L = 300 mm and an applied load = 50% P_u)**

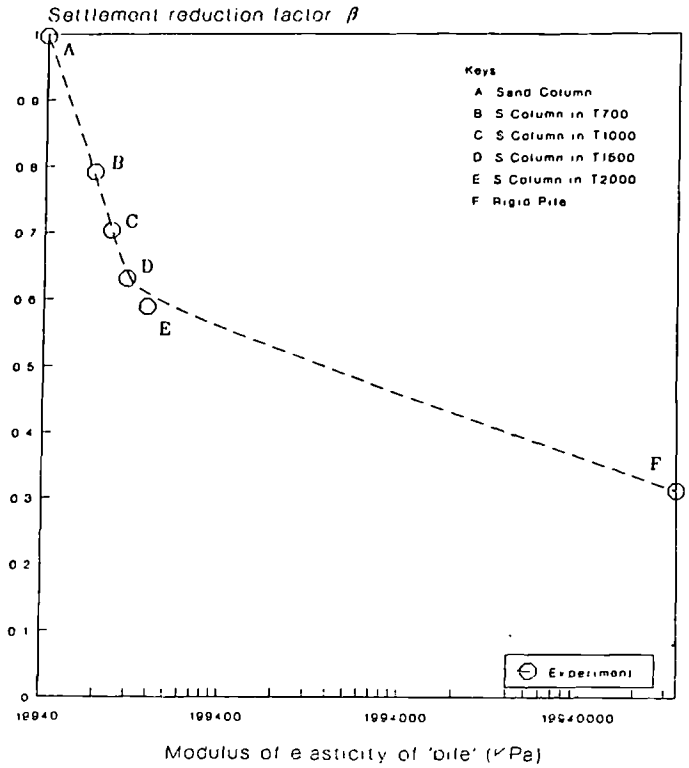

Fig. 7.27-c **Reduction in vertical compression as a function of 'pile'-stiffness. (for L = 300 mm and an applied load = 80% P_u)**

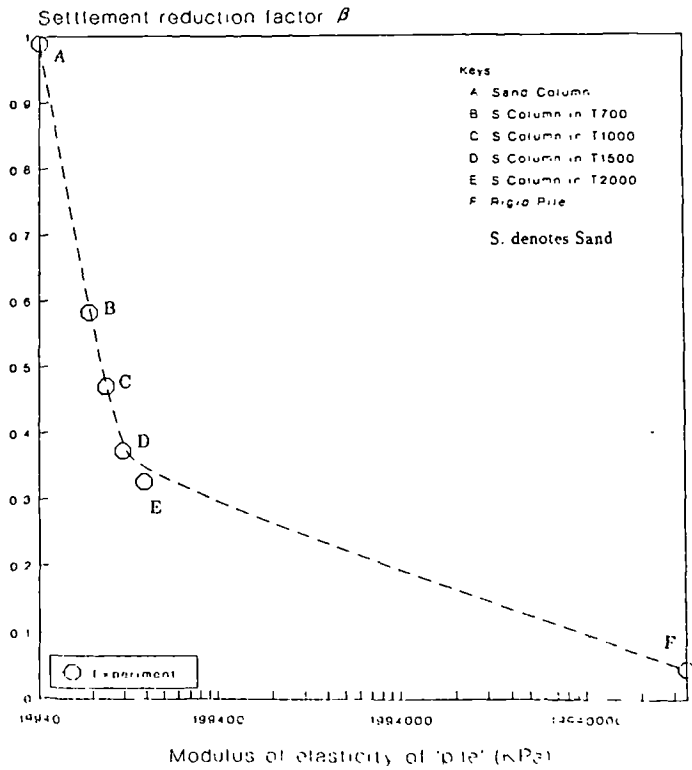

Fig. 7.28-a **Reduction in vertical compression as a function of 'pile'-stiffness. (for L = 410 mm and an applied load = 20% P_u)**

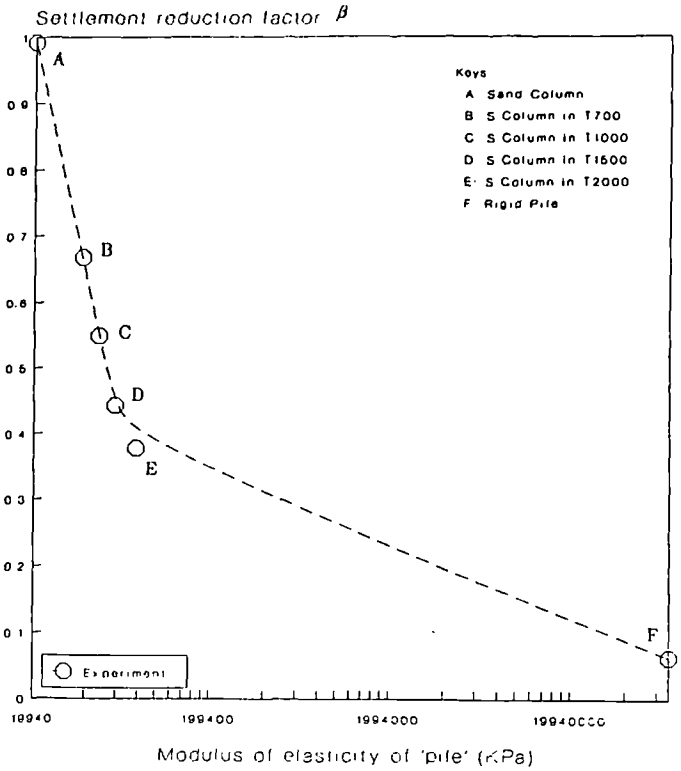

Fig. 7.28-b Reduction in vertical compression as a function of 'pile'-stiffness. (for L = 410 mm and an applied load = 50% P_u)

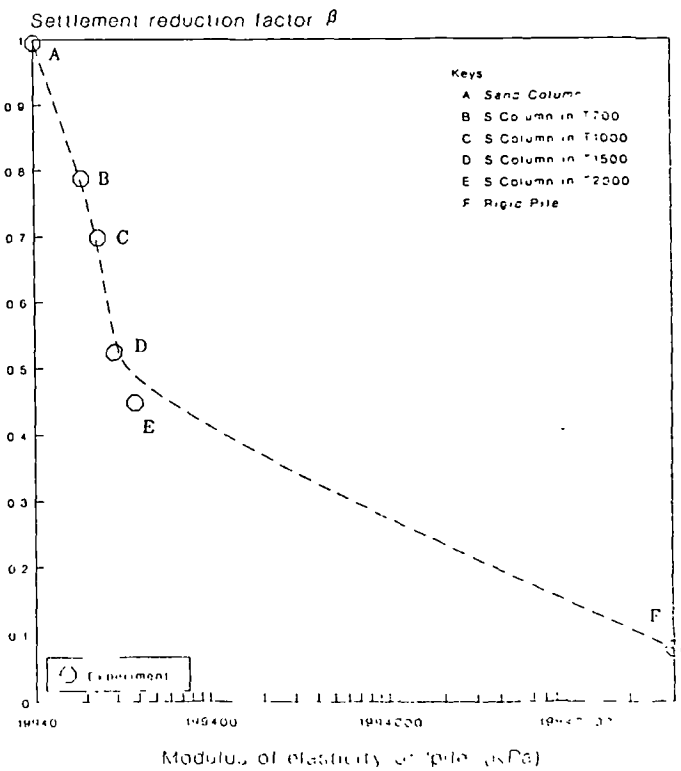

Fig. 7.28-c Reduction in vertical compression as a function of 'pile'-stiffness. (for L = 410 mm and an applied load = 80% P_u)

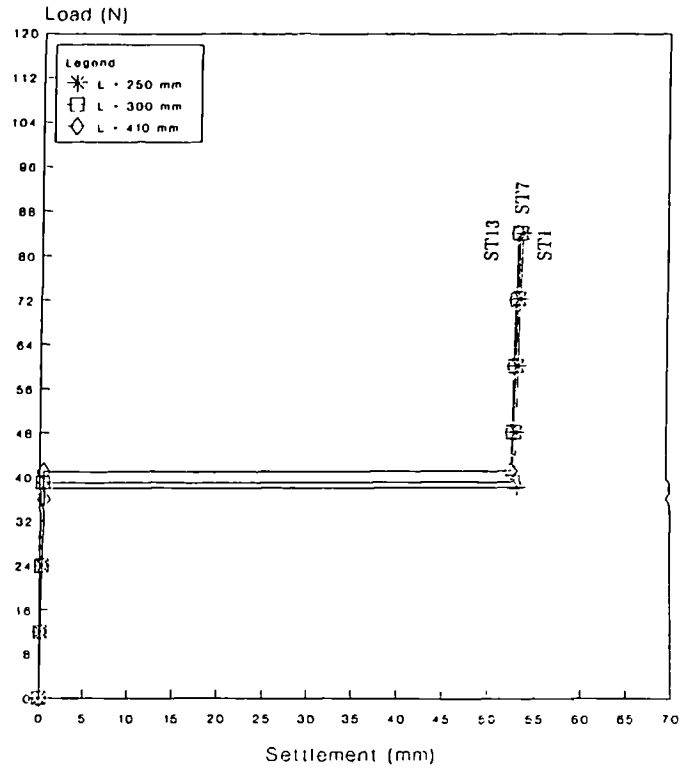

Fig. 7.29-a Settlement curves for sand columns not confined by a geofabric after full inundation under an applied load ≈ 20% P_u.

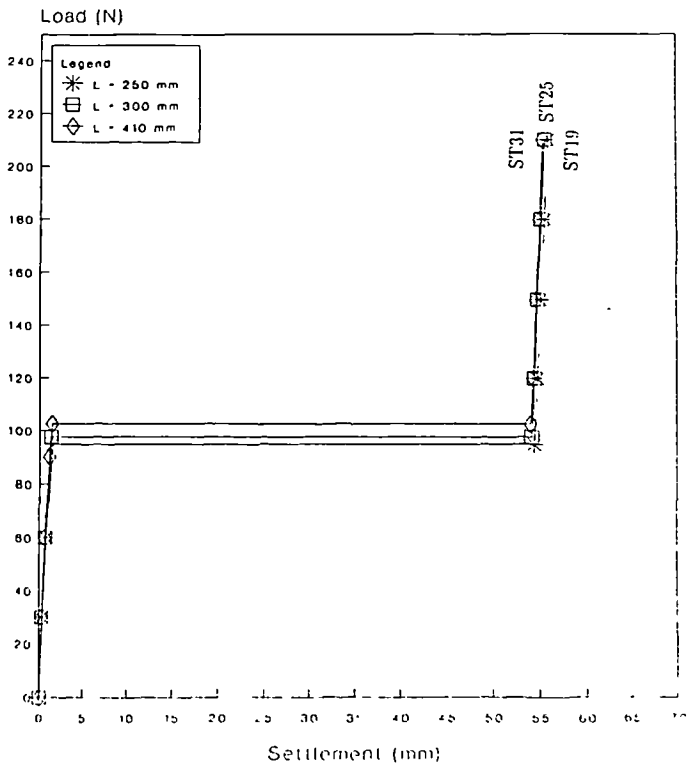

Fig. 7.29-b Settlement curves for sand columns not confined by a geofabric after full inundation under an applied load = 50% P_u.

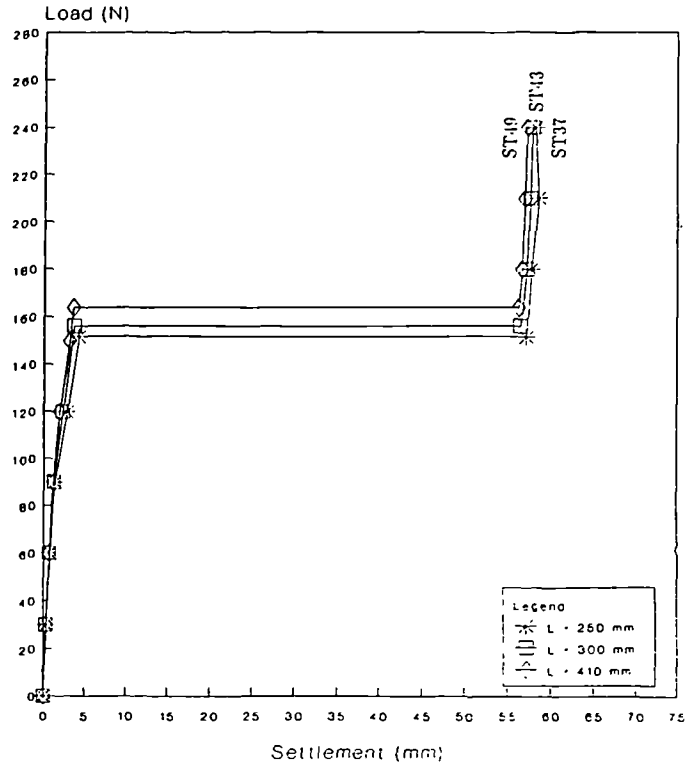

Fig. 7.29-c Settlement curves for sand columns not confined by a geofabric after full inundation under an applied load = 80% P_u.

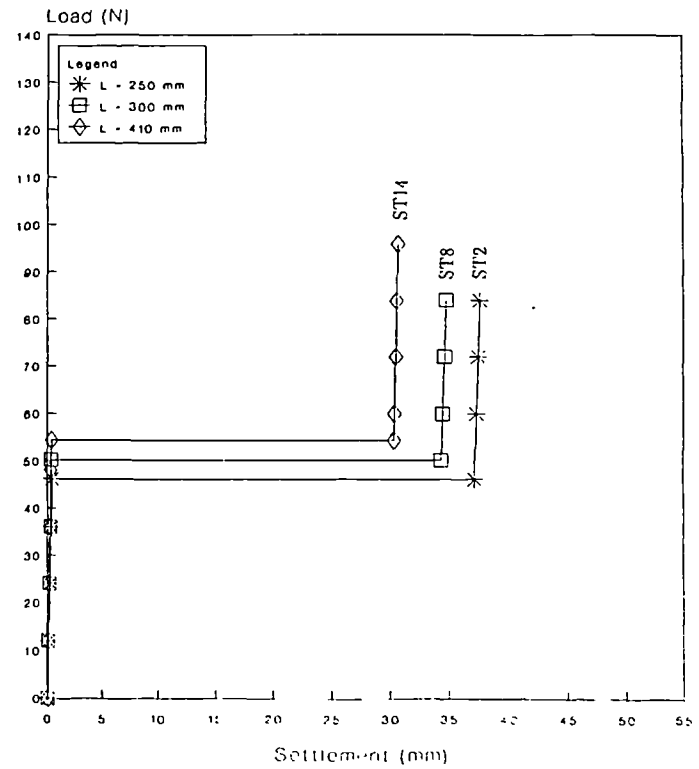

Fig. 7.30-a Settlement curves for sand columns confined by T700, after full inundation under an applied load = 20% P_u.

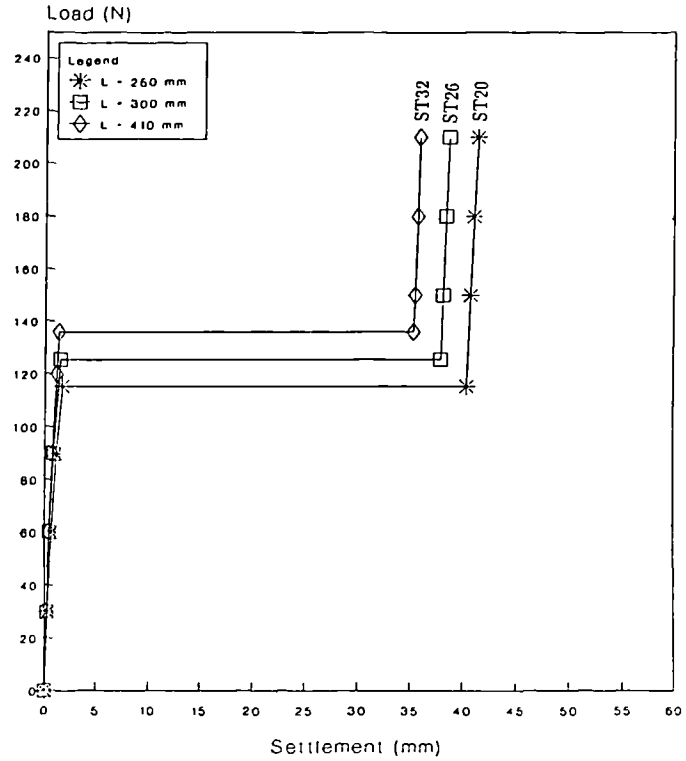

Fig. 7.30-b Settlement curves for sand columns confined by T700, after full inundation under an applied load = 50% P_u.

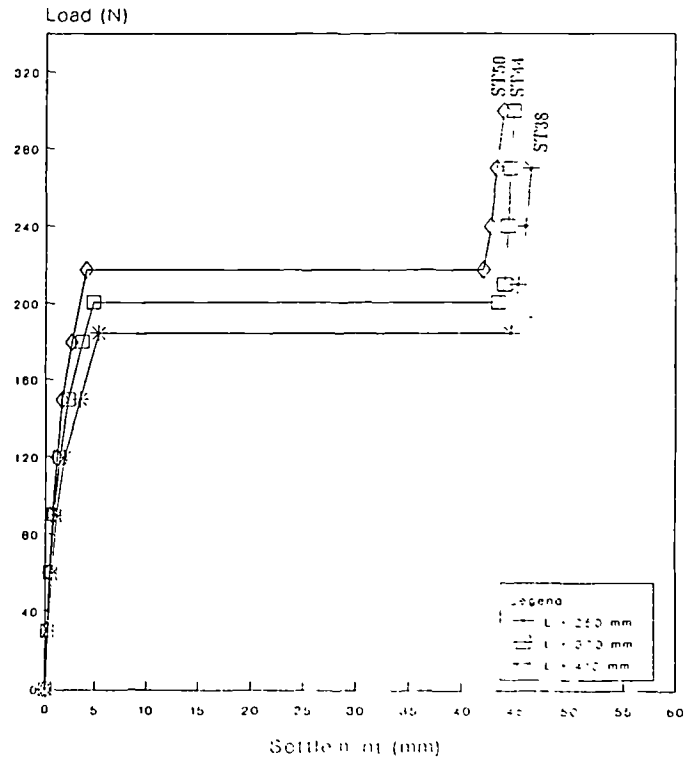

Fig. 7.30-c Settlement curves for sand columns confined by T700, after full inundation under an applied load = 80% P_u.

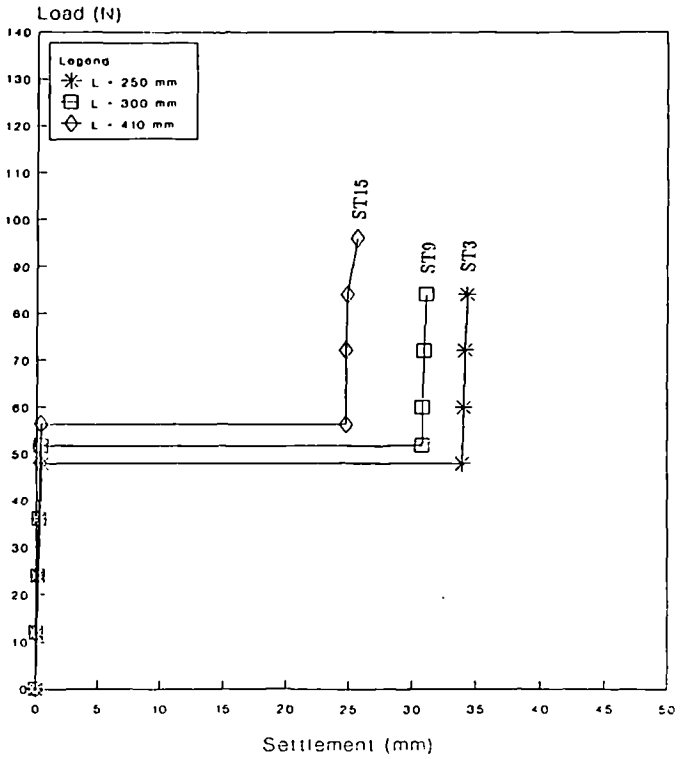

Fig. 7.31-a **Settlement curves for sand columns confined by T1000, after full inundation under an applied load = 20% P_u.**

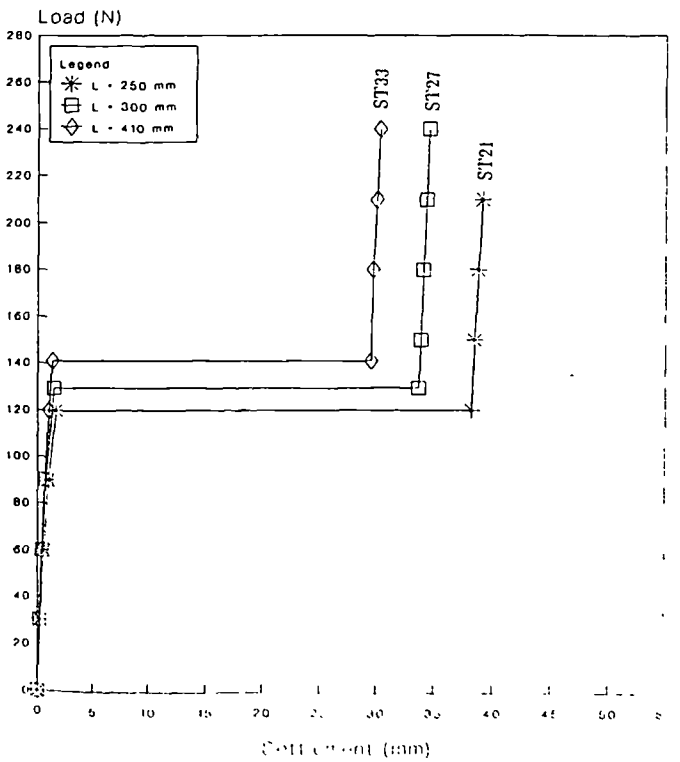

Fig. 7.31-b **Settlement curves for sand columns confined by T1000, after full inundation under an applied load = 50% P_u.**

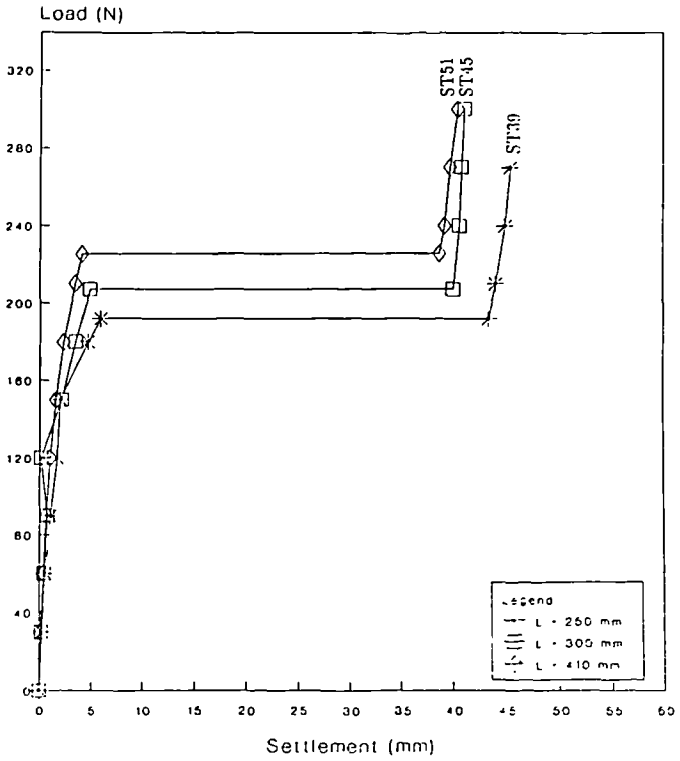

Fig. 7.31-c Settlement curves for sand columns confined by T1000, after full inundation under an applied load = 80% P_u.

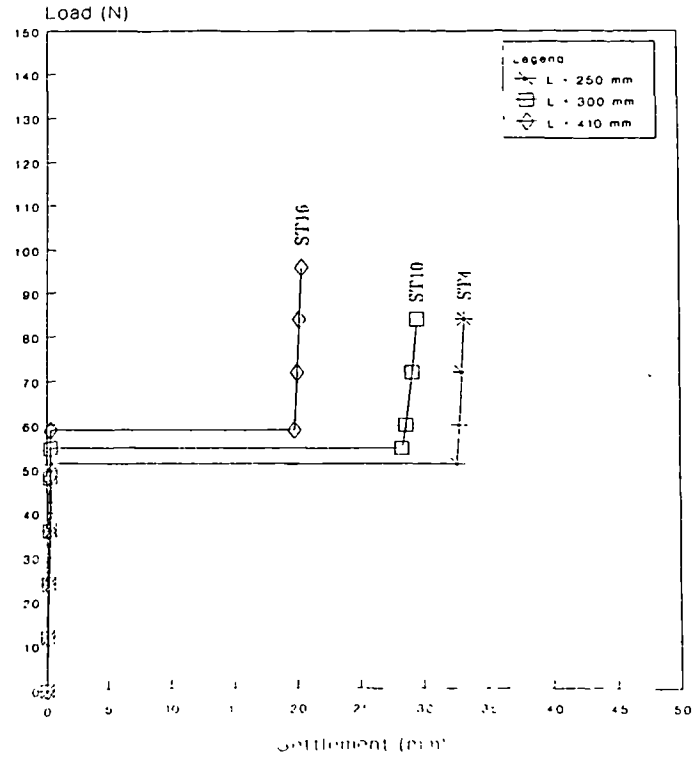

Fig. 7.32-a Settlement curves for sand columns confined by T1500, after full inundation under an applied load = 20% P_u.

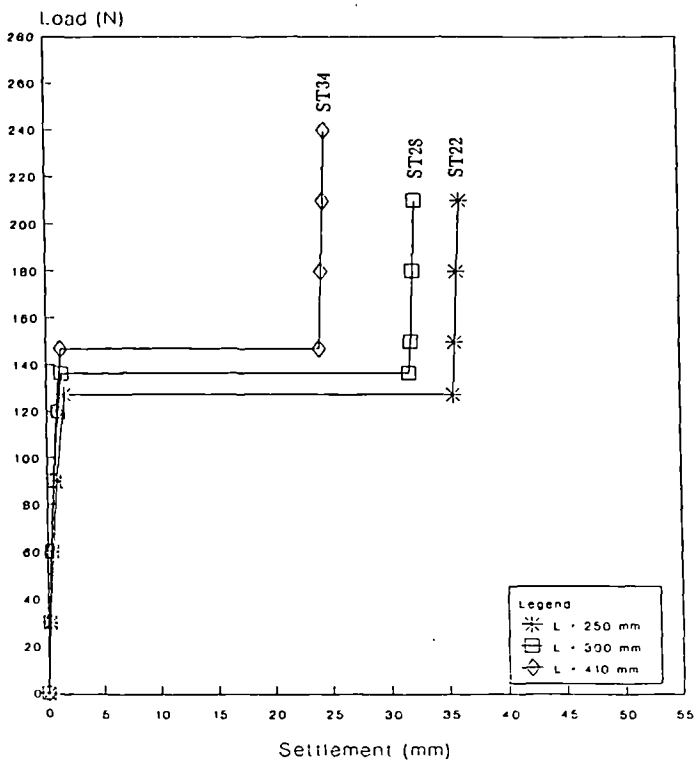

Fig. 7.32-b Settlement curves for sand columns confined by T1500, after full inundation under an applied load = 50% P_u.

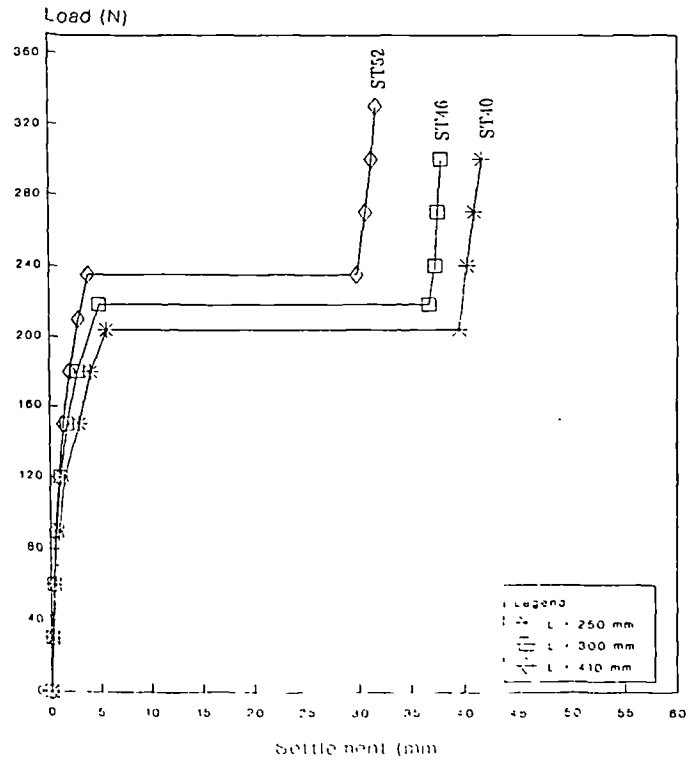

Fig. 7.32-c Settlement curves for sand columns confined by T1500, after full inundation under an applied load = 80% P_u.

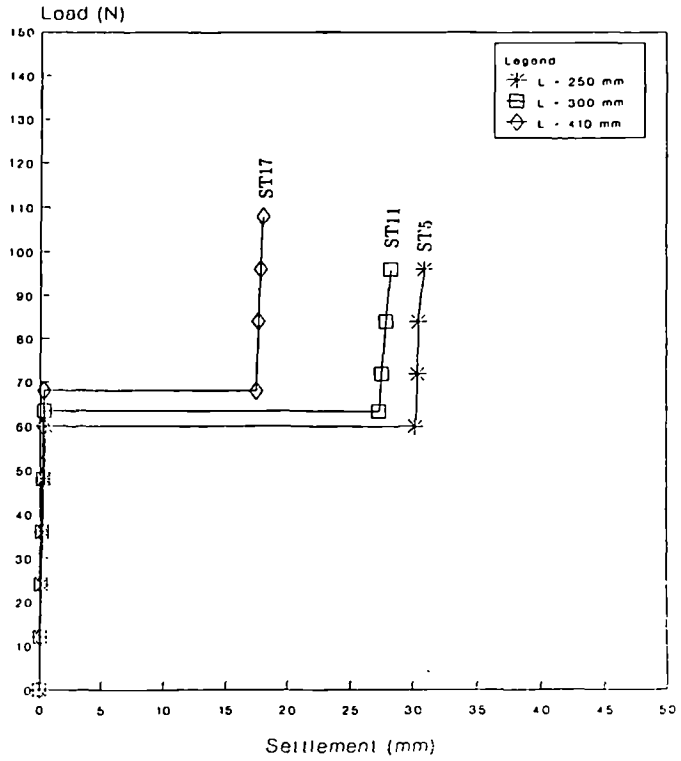

Fig. 7.33-a **Settlement curves for sand columns confined by T2000 after full inundation under an applied load = 20% P_u.**

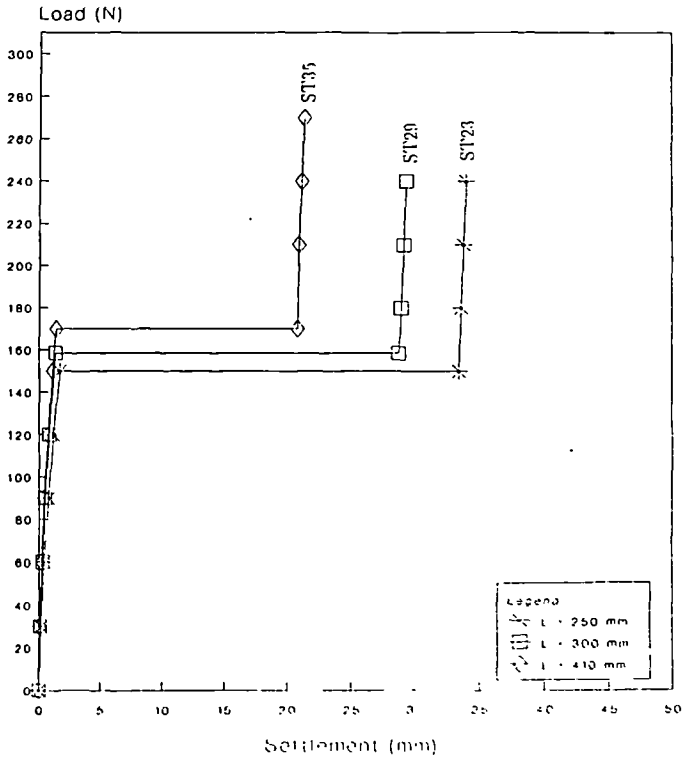

Fig. 7.33-b **Settlement curves for sand columns confined by T2000 after full inundation under an applied load = 50% P_u.**

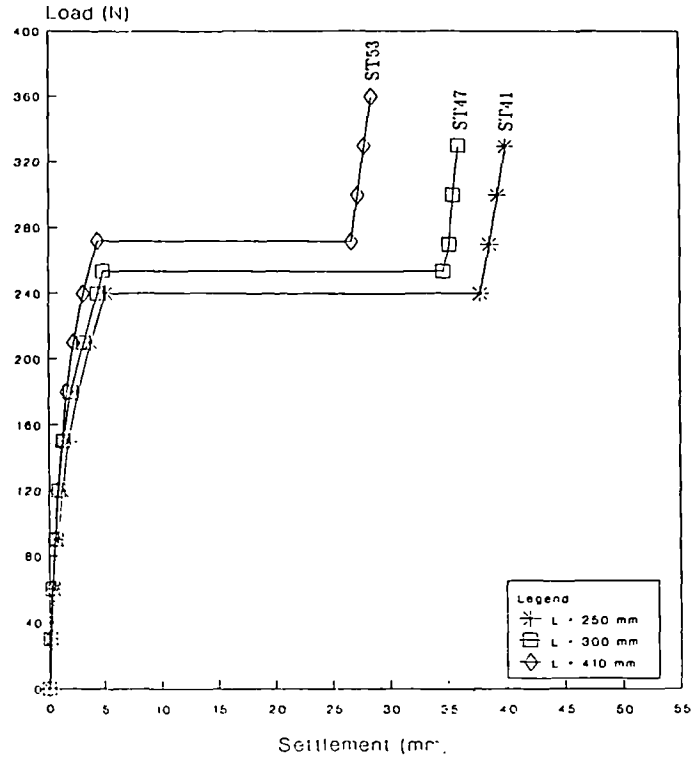

Fig. 7.33-c Settlement curves for sand columns confined by T2000 after full inundation under an applied load = 80% P_u.

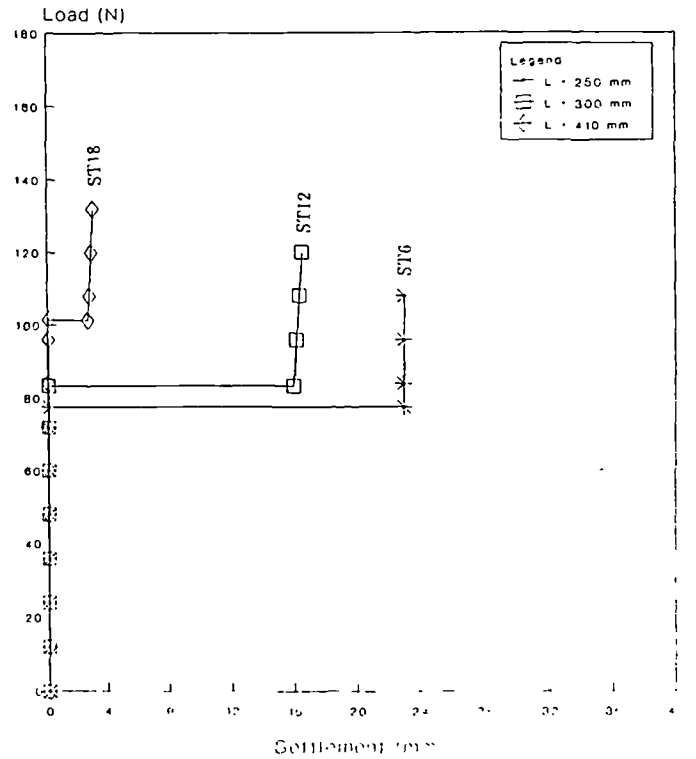

Fig. 7.34-a Settlement curves for rigid piles after full inundation under an applied load = 20% P_u.

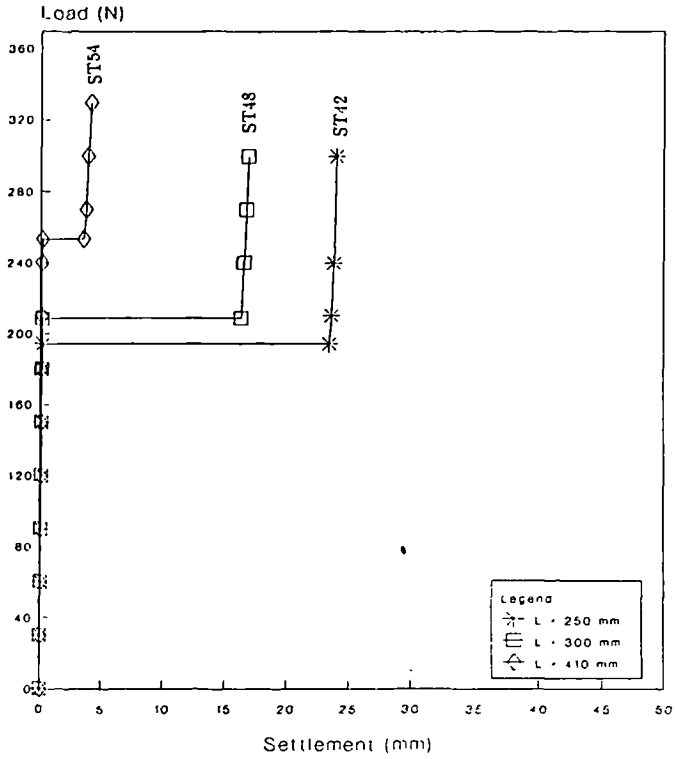

Fig. 7.34-b **Settlement curves for rigid piles after full inundation under an applied load = 50% P_u.**

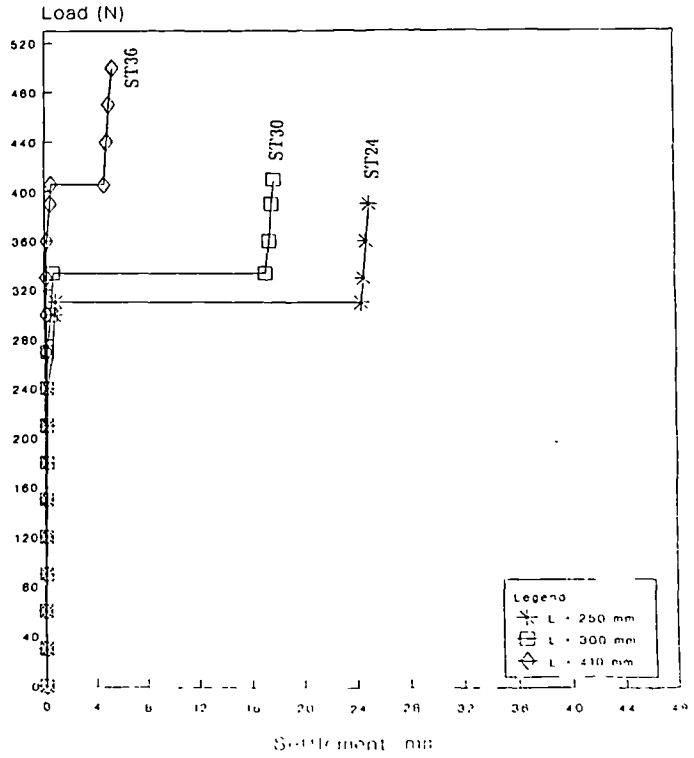

Fig. 7.34-c **Settlement curves for rigid piles after full inundation under an applied load = 80% P_u.**

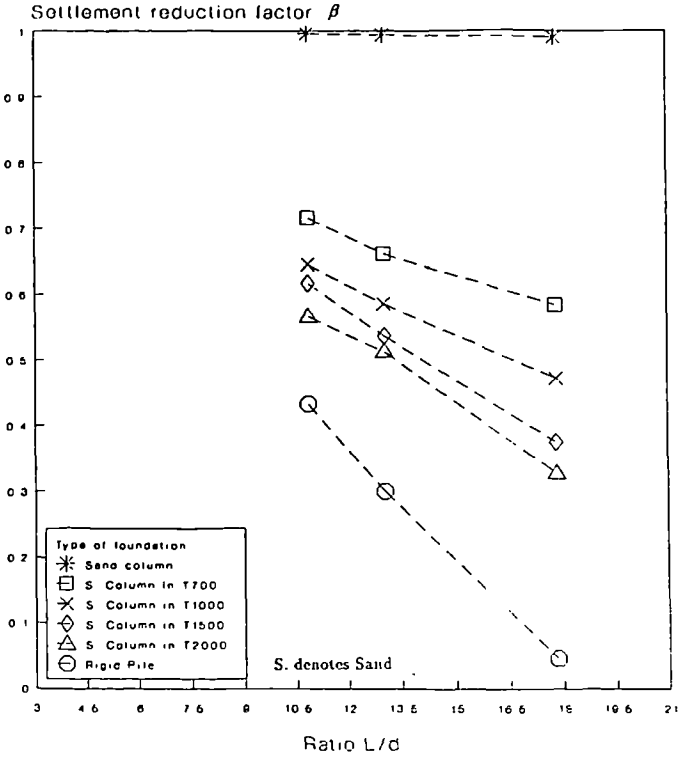

Fig. 7.35 **Reduction in vertical compression as a function of 'pile'-length for different types under an applied load = 20% P_u.**

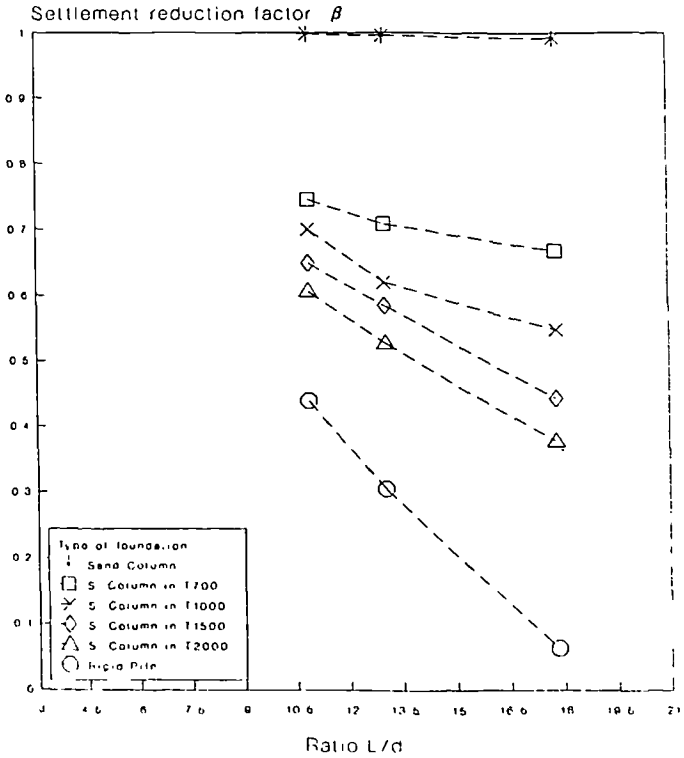

Fig. 7.36 **Reduction in vertical compression as a function of 'pile'-length for different types under an applied load = 50% P_u.**

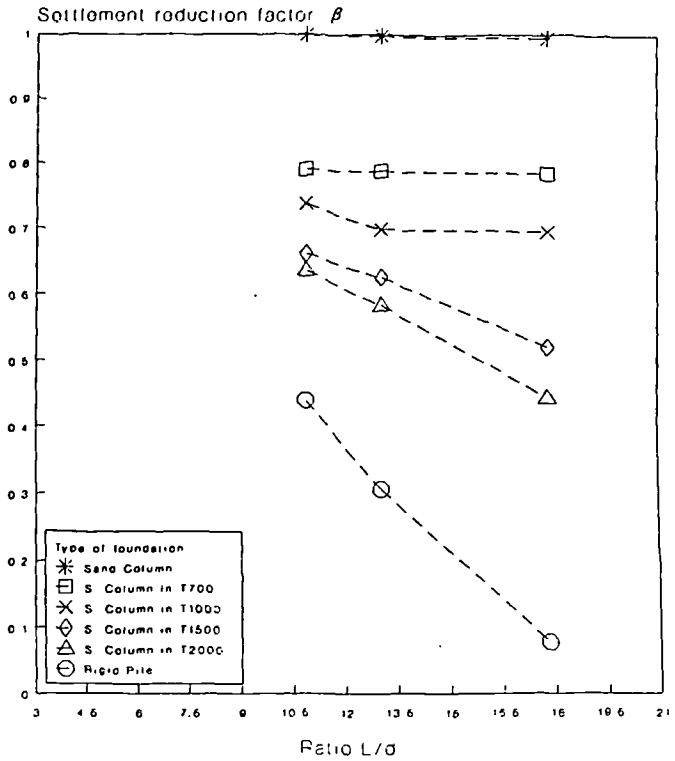

Fig. 7.37 **Reduction in vertical compression as a function of 'pile'-length for different types under an applied load = 80% P_u**

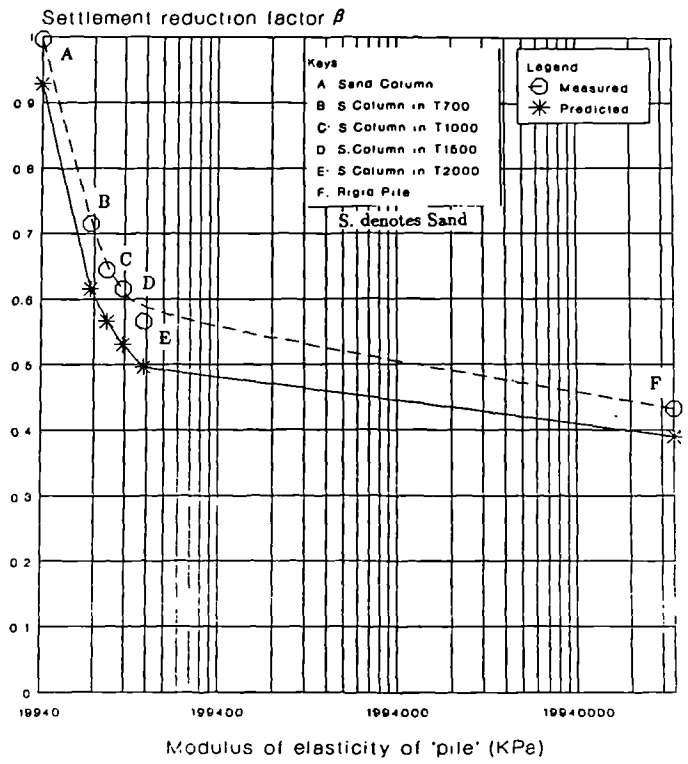

Fig. 7.38-a **Comparison of experimental and theoretical reduction in vertical compression curves as a function of 'pile'-stiffness (for L = 250 mm and an applied load = 20% P_u).**

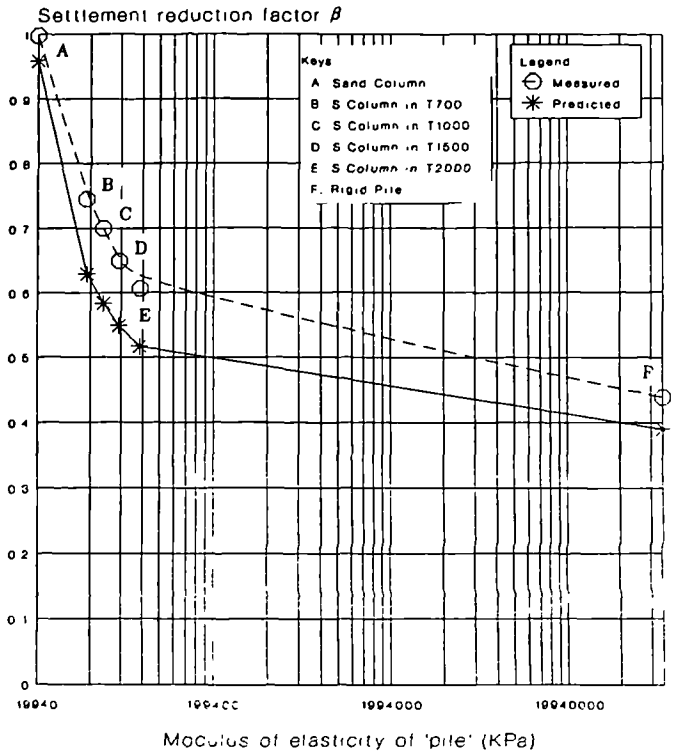

Fig. 7.38-b **Comparison of experimental and theoretical reduction in vertical compression curves as a function of 'pile'-stiffness (for L = 250 mm and an applied load = 50% P_u).**

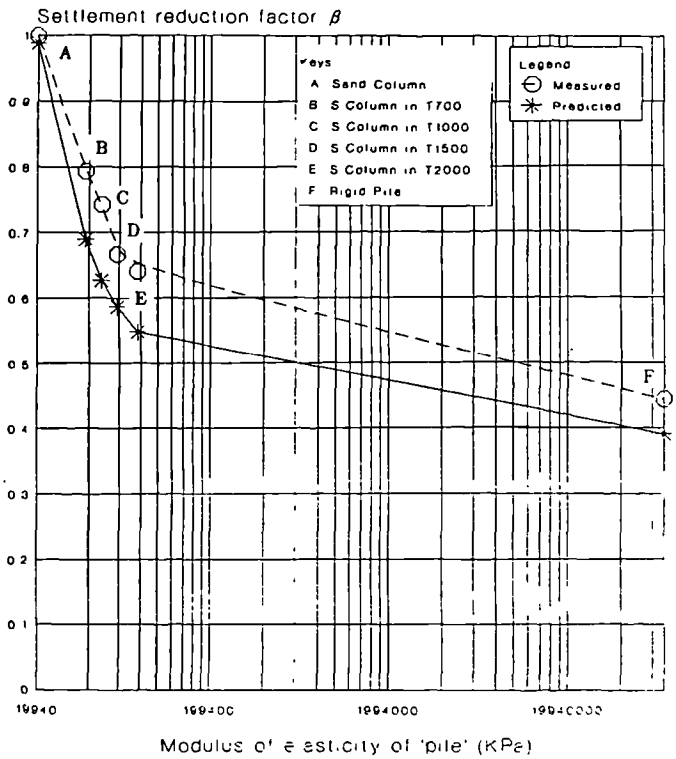

Fig. 7.38-c **Comparison of experimental and theoretical reduction in vertical compression curves as a function of 'pile'-stiffness (for L = 250 mm and an applied load = 80% P_u).**

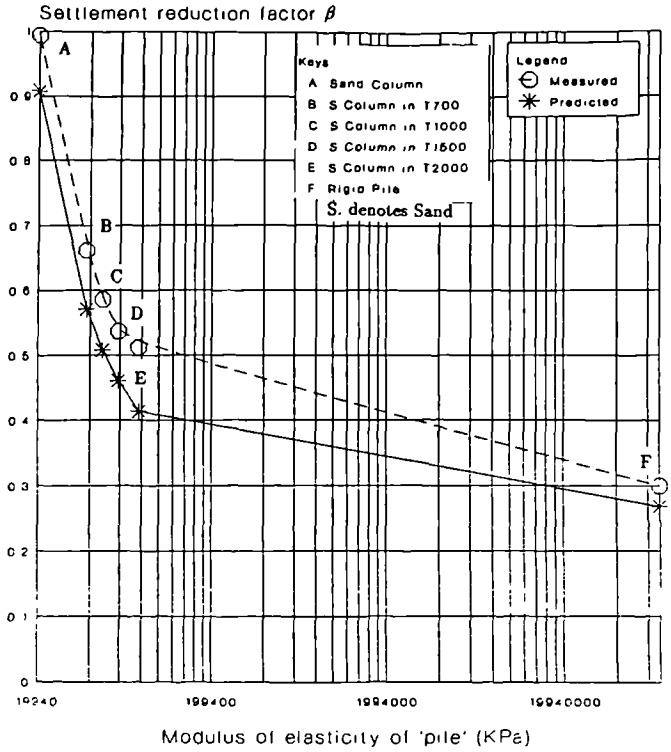

Fig. 7.39-a **Comparison of experimental and theoretical reduction in vertical compression curves as a function of 'pile'-stiffness (for L = 300 mm and an applied load = 20% P_u).**

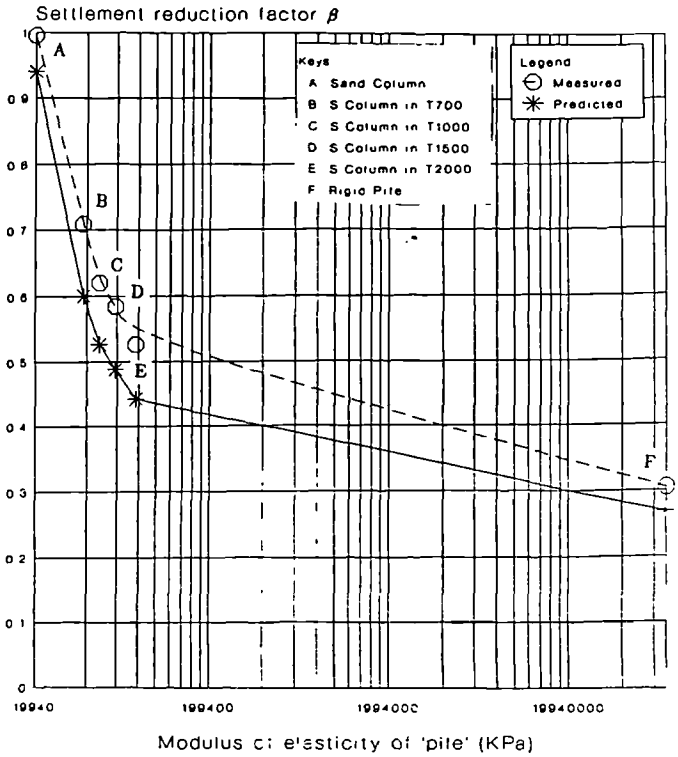

Fig. 7.39-b **Comparison of experimental and theoretical reduction in vertical compression curves as a function of 'pile'-stiffness (for L = 300 mm and an applied load = 50% P_u).**

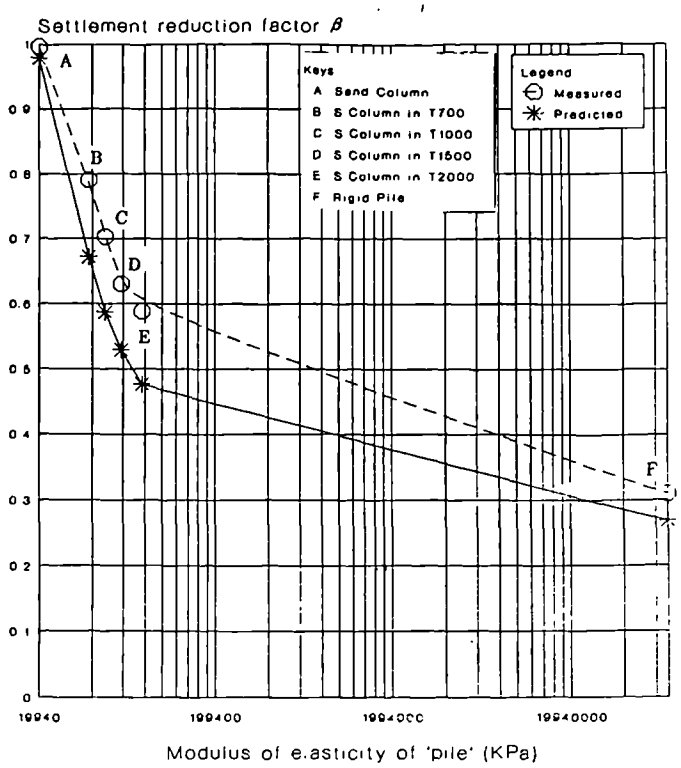

Fig. 7.39-c Comparison of experimental and theoretical reduction in vertical compression curves as a function of 'pile'-stiffness (for L = 300 mm and an applied load = 80% P_u).

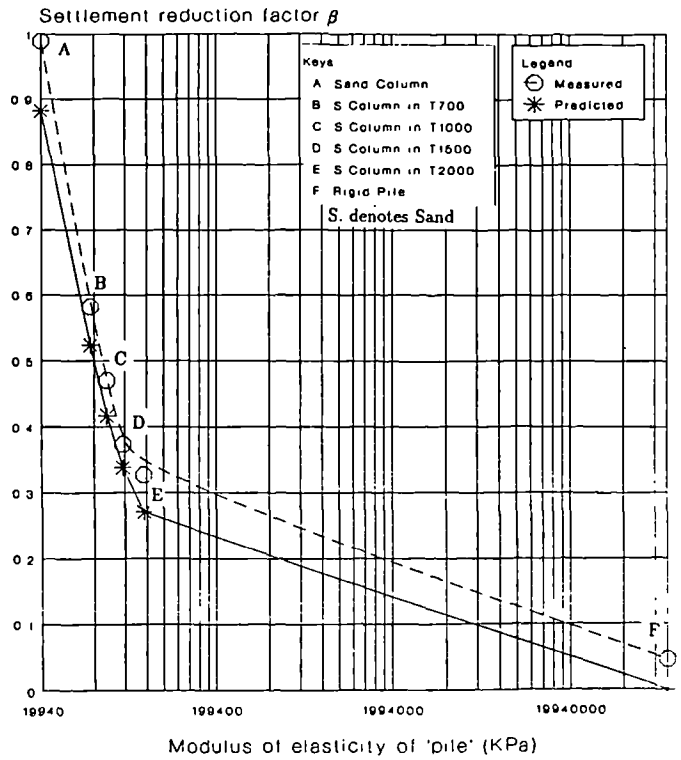

Fig. 7.40-a Comparison of experimental and theoretical reduction in vertical compression curves as a function of 'pile'-stiffness (for L = 410 mm and an applied load = 20% P_u).

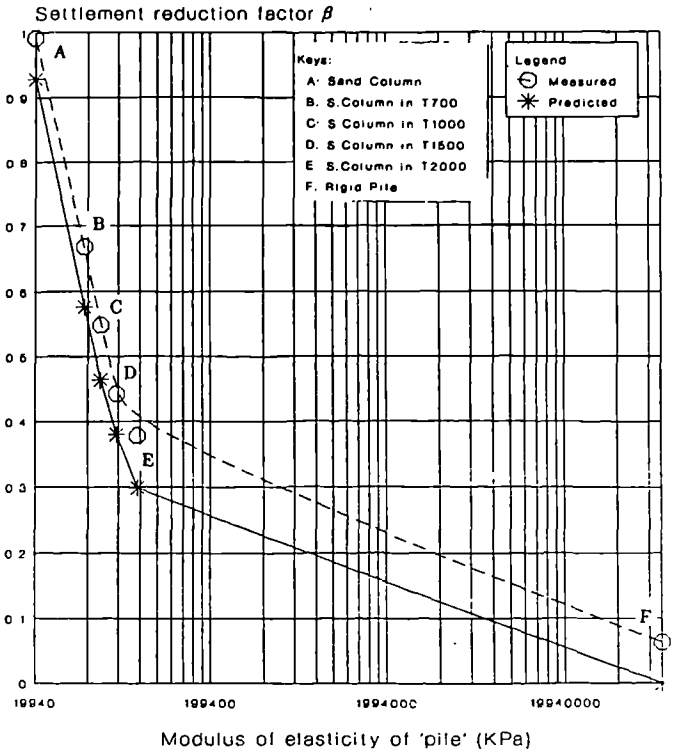

Fig. 7.40-b **Comparison of experimental and theoretical reduction in vertical compression curves as a function of 'pile'-stiffness (for L = 410 mmm and an applied load = 50% P_u).**

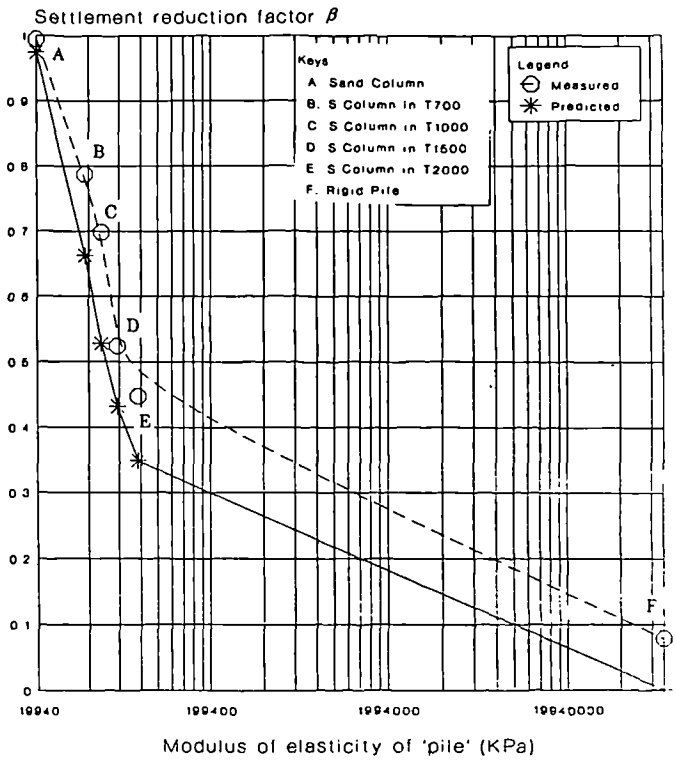

Fig. 7.40-c **Comparison of experimental and theoretical reduction in vertical compression curves as a function of 'pile'-stiffness (for L =410 mm and an applied load = 80% P_u).**

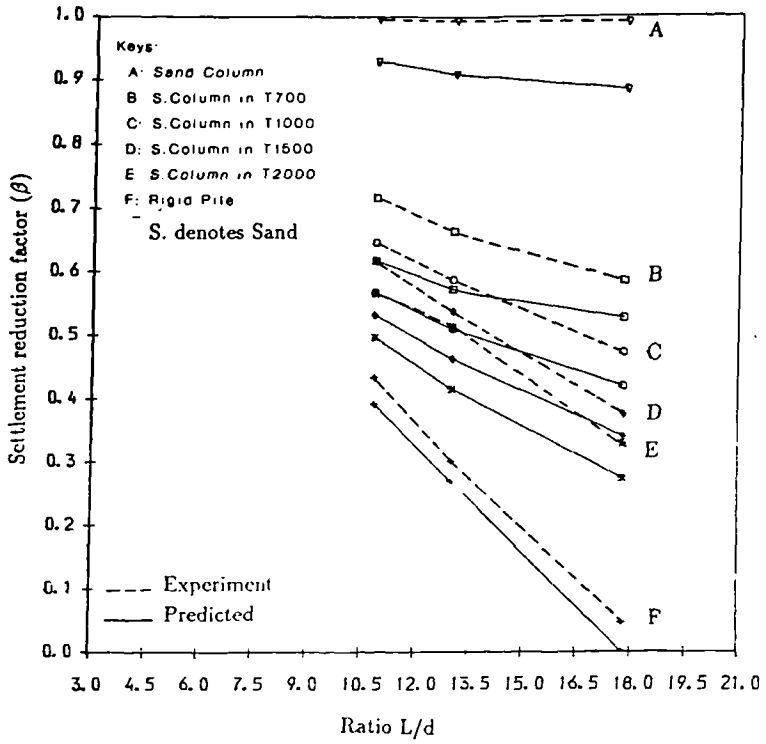

Fig. 7.41 Comparison of experimental and theoretical reduction in vertical compression curves as a function of 'pile'-length for the different types under an applied load = 20% P_u.

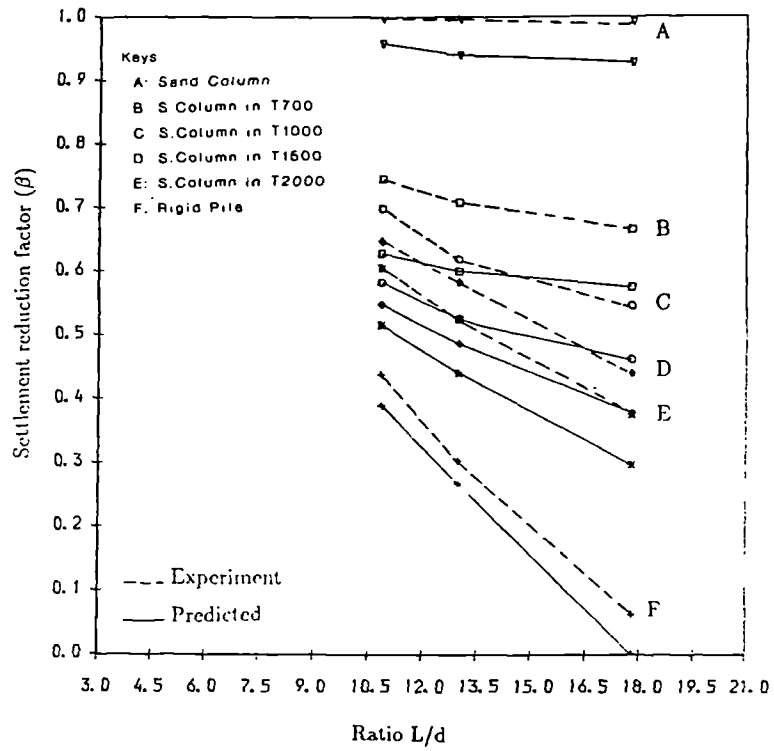

Fig. 7.42 Comparison of experimental and theoretical reduction in vertical compression curves as a function of 'pile'-length for the different types under an applied load = 50% P_u.

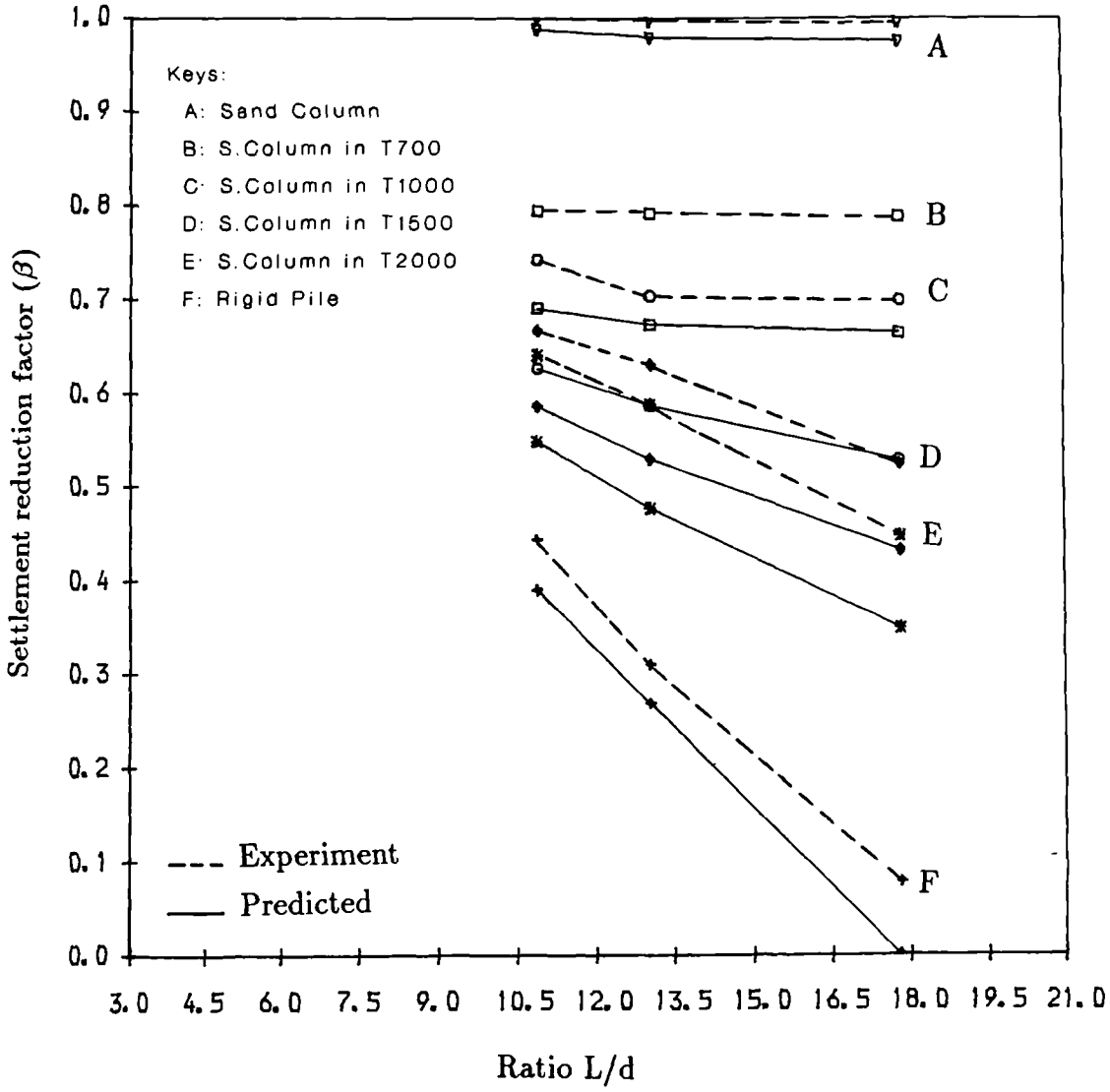

Fig. 7.43 **Comparison of experimental and theoretical reduction in vertical compression curves as a function of 'pile'-length for the different types under an applied load = 80% P_u.**

Chapter 8

Conclusions and Recommendations for Future Work

8.1 General:

In the previous chapter, all the results obtained from tests on sand columns confined or not confined by geotextiles and rigid piles have been presented and analysed in detail. It had been found that 'pile'-length and 'pile'-stiffness were the most critical parameters in governing the behaviour of the 'pile' acting as a foundation support in a collapsible soil subjected to inundation.

In this chapter, the main conclusions drawn from this work with suggestions for a further extention of this research are presented.

8.2 Main Conclusions:

The following conclusions can drawn for the experimental and analytical work carried out in this study.

1. Stone columns have failed in strengthening a loose fill which exhibits a collapse behaviour caused by inundation. The use of a stone column without confinement by a geotextile in a collapsible soil, which at some stage in its future could be subjected to inundation or partial inundation, is quite wrong.

2. Results of the ultimate carrying capacity tests on the different type of 'piles' show that,

   (a) The ultimate carrying capacity of these 'piles' increased with increase in their stiffnesses (for sand columns, the increase in stiffness was provided by the different strengths of the geotextile used).

   (b) The rate of increase of the bearing capacities between sand columns confined by T700, T1000 and T1500 was small compared to that recorded between sand columns not reinforced and sand columns encapsulated in T700 or between rigid piles and sand columns confined by T2000.

   (c) Following the same trend of the ultimate carrying capacities, the displacements at failure experienced by these 'piles' were also noticed to increase with increase in their stiffnesses.

   (d) For a given applied load the displacement of the 'pile' head of any of these types was found to decrease with increase in the 'pile' length.

3. Results of tests performed for the examination of settlement behaviour of the 'piles' under load and inundation show that,

   (a) The introduction of the geotextile reinforcement to the sand column has contributed to the reduction of settlement. This reduction was found to increase with increase in the 'pile' rigidity.

(b) The rate of increase of the settlement was found to be large between sand columns without confinement and sand columns encapsulated in T700 fabrics compared to changes observed for columns with different stiffnesses of fabric encapsulation.

(c) The total settlement of the 'pile' head due to an external load and inundation decreased by increasing the length of the 'pile'.

(d) Partial penetration represented the critical situation of all types of deep foundations in collapsible soils subjected to inundation. This can simply be explained by the existence of a collapsible layer beneath the tip of the partially penetrating foundation.

(e) It is practically more convenient to carry the foundation to a depth where the collapse is negligeable or doesn't exist. In practice it may not be possible to fulfil this ideal because of practical limitations in the depth capacity of the vibro machine.

(f) The use of sand columns encapsulated in a geofabric as deep foundations is more effective for light weights. For a fully penetrating sand column confined by T2000 fabric and under a working load of 20% P_u, it was found that the situation has changed from severe damage (for a foundation resting on the soil alone) to moderate damage.

(g) In general this method of reinforcing the sand columns is very promising and the use of other types of 'Terram' having a higher strength (e.g. T3000) will give a smaller settlement reduction factor.

4. Results from the analytical study of the settlement behaviour of the different types of foundation support under axial loads and inundation show that,

(a) The total and final settlement of a 'pile' in a collapsible soil, caused by inundation under an applied external load (P), can be computed by the following equation:

$$\Delta = \delta_1 + \delta_2 + \delta_3$$

where:

Δ: the total and final settlement caused by inundation under an external load (P),

δ_1: The elastic settlement due to load (P),

δ_2: The settlement caused by downdrag,

δ_3: The settlement due to lateral deformation in the column.

The general forms of the total settlement (Δ) are given in Sub-Section (3.4.2.3)

(b) For a given 'pile' the settlement predicted at any given working load using the elastic analysis is smaller than that computed by using the slip analysis.

(c) For relatively small values of 'pile'-stiffness, the reduction in settlement is large for small increases in E_p, but for larger values of E_p, the change in β (the settlement reduction factor) is small.

(d) The additional settlement of the soil layer situated beneath the tip of the 'pile' and caused by inundation is the predominant one in the settlement behaviour of partially penetrating 'piles'.

5. Comparing the measured and predicted results showed that,

(a) A remarkable degree of agreement between the shape of the experimental and theoretical curves of settlement reduction was found.

(b) The only point of disagreement is that the theory predicted a smaller settlement. The difference between the predicted and the measured settlement reductions increased by increasing the working load and decreased by increasing the 'pile'-length.

(c) To predict the settlement of the top of a 'pile' under an axial load in a collapsible soil subjected to inundation, the local yield or slip between the 'pile' and the soil must be taken into account.

(d) For estimating the total settlement of the top of a 'pile' in a collapsible soil it is recommended to use the modified Hughes method for the computation of the lateral deformation (δ_3).

(e) The agreement between measured and predicted results of the 'model' foundations is good. The lack of field data, for this type of foundation support, makes it difficult to confirm the practical applicability of the theory fully. However, the confirmation of the validity of the analytical solutions proposed by Poulos et al. and Hughes et al. for field predictions (Poulos et al., 1975; Hughes et al., 1975), suggests that it is reasonable to believe that the present theory should have validity when applied to full-scale vibro encapsulated columns.

8.3 Recommendation for Future Work:

In this study, a series of load-settlement tests have been carried out on sand columns encapsulated or not encapsulated in geotextiles and rigid piles embedded in a collapsible soil subjected to inundation to investigate the effects of 'pile'-length and 'pile'-stiffness on load-settlement behaviour. Analytical simulations of the experiments have also been performed by bringing together two different models,i.e. the Poulos-model and modified Hughes approach. Further work is still required to provide a better understanding of the load-settlement behaviour of the different types of foundation support. It is suggested that further work could include the following:

1. A better understanding of the mechanism of collapse of the sand columns during inundation by establishing the pattern of vertical displacements within the column and radial displacements at the edge of the column against depth.

2. Investigation of the distribution of settlement of sand columns encapsulated in geotextiles with depth by placing appropriate instrumentations on the 'pile'

body. One possible technique consists of placing thin rings of appropriate width and instrumented by strain gages on different positions of the 'pile' body.

3. The possibility of use of different forms of sand columns reinforcement e.g. internal as well as external reinforcement.

4. Modification of the analytical solution by considering the true form of the curve of the soil settlement distribution with depth during inundation, the compressibility of the bearing stratum, the linearity variation with depth of the soil and 'pile' modulii of elasticity and the estimation of the settlement, caused by lateral deformations, using the stress-strain behaviour of the fabric.

5. In the analytical simulations the soil and 'pile' parameters were derived from conventional triaxial tests. The suitability of the deformation parameters derived from these tests for settlement analysis should be further investigated.

6. Development of the analytical study to deal with the distribution of the settlement of the 'pile' with depth.

7. Investigating the effects of inundating the collapsing fill from the surface on the settlement behaviour of sand columns confined or not confined by a geofabric and rigid piles (e.g. simulating rainfall); then checking the suitability of the analytical solution adopted for this way of introducing inundation.

8. It would be useful to carry out full-scale tests on stone columns in collapsible soil to evaluate the suitability and the accuracy of the analytical solution adopted. Appendix E describes how stone columns might be constructed, in the field, with a fabric surround around them.

References

Abelev, Y.M. (1948) "The Essentials of Designing and Building on Micro-Porous Soils", Stroital Naya Promyshlemast, N^o.10.

Abelev, Y.M. (1975) "Compacting Loess Soils in the USSR", Geotechnique, 25, N^o.1, pp. 79-82.

Ali, M.M, Nowatzhi, E.A. and Myers, D.E. (1989) "Geostatistical Methods to Predict Collapsing Soils", Proc. of the 12^{th} Int. Conf. on SMFE, Rio de Janeiro, vol. 1, pp. 567-570.

Amirsoleymani, T. (1989) "Mathematical Approach to Evaluate the Behaviour of Collapsible Soils", Proc. of the 12th ICSMFE, Rio de Janeiro, vol. 1, pp. 575-582.

Arthur, J.R.F. and Phillips, A.B. (1975) "Homogeneous and Layered Sand in Triaxial Compression", Geotechnique, vol.25, N^o.4, pp. 799-815.

Atkinson, J.H., Evans, J.S. and Scott, C.R. (1985) "Developments in Microcomputer Controlled Stress Path Testing Equipment for Measurement of Soil Parameters", Ground Engineering, vol.18, N^o.1, pp. 15-22.

Balaam, N.P., Poulos, H.G. and Brown, P.T. (1977) "Settlement Analysis of Soft Clays Reinforced with Granular Pile", Proceedings of the 5th S.E. Asian conference on Soil Engineering, pp. 81-92, Bangkok, Thailand.

Balaam, N.P. and Booker, J.R. (1981) "Analysis of Rigid Rafts Supported by Granular Piles", Inter. J. Num. Meth. in Engng. 5, pp. 379-403.

Balaam, N.P. and Poulos, H.G. (1983) "The Behaviour of Foundations Supported by Clay Stabilised by Stone Columns", Proc. of the 8th European conf. on soil Mech. Found. Engng., Helsinki, pp. 199-204.

Balaam, N.P. and Booker, J.R. (1985) "Effect of Stone Columns Yield on Settlement of Rigid Foundations in Stabilized Clay", Int. Jnl Anal. Methods Geomech., 9(4), pp. 381-351.

Baldi, G. and Nova, R. (1984) "Membrane Penetration Effects in Triaxial Testing", ASCE, vol.110, N^o3, pp. 403-420.

Banerjee, P.K. (1969) Quoted by Banerjee (1971) Discussion on "Settlement and Construction Aspects", Behaviour of Piles, Proceedings of the Conference Organized by the Institution of Civil Engineering in London, September 1970, p.

207.

Bara, J.P (1976) "Collapsible Soils", Presented at the September 1976, ASCE Annual Convention and Exposition, held at Philadelphia.

Barden, L. (1974) "Consolidation of Clays Compacted 'Dry' and 'Wet' of optimum water content", Geotechnique, 24, 4, pp. 605-625.

Barden, L., Madedor, A.O. and Sides, G.R. (1969) "Volume Change Characteristics of Unsaturated Clay", Journal of SMFD, ASCE, vol.95, SM1, pp. 33-49.

Barden, L., McGown, A. and Collins, K. (1973) "The collapse Mechanism in Partly Saturated Soil", Engineering Geology, vol.7, pp. 49-60.

Barden, L. and Sides, G.R. (1970) "Engineering Behaviour and Structure of Compacted Clay", Journal of SMFD, ASCE, vol.96, SM4, pp. 1176-1200.

Barksdale, R.d and Bachus, R.C (1983) "Design and Construction of Stone Columns", Vol. *I*, U.S. Department of Transportation, Federal Highway Administration Report N^o. FHWA/RD-83/026, p. 210.

Beketove, A.K, Golovanov, A.M., Zelenskii, V.Yu. and Polyakov, V.L. (1967) "Imperial Technology in Silicatization of Loessial Soils", Soils Mechanics and Foundation Engineering, N^o.6.

Beles, A.A., Stanculescu, I.I. and Schally, V.R. (1969) "Prewetting of Loess-Soil Foundation for Hydraulic Structures", Proc. 7th. ICSMFE, vol.2, pp. 17-26.

Benites (1967) Quoted by Northey, R.D. (1969), Engineering Properties of Loess and Other Collapsible Soils", Proc. of the 7^{th} ICSMFE, Mexico, pp. 445-452.

Bhandari, R.K.M. (1983) "Behaviour of a Tank Founded on Soil Reinforced with Stone Columns", Proc. of the 8^{th} European Conf. SMFE, Helsinki, vol. 1, pp. 209-212.

Bieganousky, W.A. and Marcuson, W.F. (1976) "Uniform Placement of Sand", Journal of Geotech. Engng. Div. Proc. ASCE, 102, GT3, 229-233.

Bishop, A.W. (1960) "The Measurement of Pore Pressure in the Triaxial Test" Pore Pressure and Suction in Soils, Butterworths, London, pp. 38-46.

Bishop, A.W., Alpan, I., Blight, G.E. and Donald, I.B. (1960) "Factors Controlling the Strength of Partly Saturated Cohesive Soils", Proc. ASCE-Res. Conf. on Shear Strength of Cohesive Soils, Boulder, Colo., pp. 503-531.

Bishop, A.W. and Henkel, D.J. (1962) "The Measurement of Soil Properties in the Triaxial Test", Edward Arnold.

Bjerrum, L, Johannesson, I. and Eide, O (1969) "Reduction of Skin Friction on Steel Piles to Rock", Proc. of the 7^{th} ICSMFE, vol. 2, pp. 27-34.

Bjerrum, L., Simoms, N. and Torblaa, I. (1958) " The Effect of Time on The Shear Strength of Soft Marine Clay", Proc. Brussels Conference on Earth Pressure Problems, vol.1, pp. 148-158.

Black, D.K. and Lee, K.L. (1973) "Saturating Laboratory Samples by Back-Pressure", Journal of Geot.Engng Div., ASCE, vol.99, N^o.SM1, pp. 75-93.

Blight, G.E. (1961) "Strength and Consolidation Characteristics of Compacted Soils", Ph.D. Thesis, University of London.

Boghosian, H.H (1984) "Behaviour of Bent Piles in Sand" Ph.D. Thesis, Sheffield University.

Booth, A.R. (1975) "The Factors Influencing Collapse Settlement in Compacted Soils", Proc. 6th, Reg. Conf. for Africa on SMFE, Durban, South Africa, pp. 57-63.

Booth, A.R. (1977) "Collapse Settlement in Compacted Soils", CSIR Research Report 324, NITRR Bulletin 13, Pretoria, South Africa.

Bowles, J.E. (1978) "Engineering Properties of Soils and Their Measurements", McGraw-Hill Book Co., New York.

Bragg, R.A. and Andersland, O.B. (1980) "Strain Rate, Temperature and Sample Size Effects on Compression and Tensile Properties of Sand", Engineering Geology, Vol.18, pp. 35-46.

Brauns, J. (1978) "Die Anfangstraglast Von Schoettersaulen im Bindigen Untergrund", Die Bautechnik, 55, pp. 263-271.

Brink, A.B.A. and Kantey, B.A. (1961) "Collapsible Grain Structure in Residual Granite Soils in South Africa", Proc. 5^{th} Inter. Conf. SMFE, Paris, Vol. pp. 611-614.

British Standard Institution (1984) "Testing Aggregate- Part 101: Guide to Sampling and Testing Agregates" pp. 1-5.

Bromham, S.B. and Styles, J.R. (1971) "An Analysis of Pile Loading Tests in a Stiff Clay", Proc. 1^{th} Aust. -N.Z. Conf. Geomechs., Melbourne, vol.1, pp. 246-253.

Brown, S.F. and Snaith, M.S. (1974) "The Measurement of Recoverable and Irrecoverable Deformations in the Repeated Load Triaxial Test", Geotechnique, vol.24, N^o.2, pp. 255-259.

Brown, S.F., Austin, G. and Overy, R. (1980) "An Instrumented Triaxial Cell for Cyclic Loading of Clay", Geotechnical Testing Journal, vol.3, 4, pp.145-152.

Burland, J.B. (1965) "Some Aspects of the Mechanical Behaviour of Partly Saturated Soils", Moisture Equilibrium and Moisture Changes in Soils Beneath Covered Areas, Butterworths, Sydney, Australia, pp. 270-278.

Burland, J.B. and Symes, M. (1982) "A Simple Axial Displacement Gauge for Use in the Triaxial Apparatus" Geotechnique, 32, 1, pp. 62-65.

Butterfield, R. and Banergee, P.K. (1971) "The Elastic Analysis of Compressible Piles and Pile Groups" Geotechnique, 21, N^o1, pp. 43-60.

Carr, R.W. (1970) "An Experimental investigation of Plate Anchors in Sand", Ph.D. Thesis, University of Sheffield, England.

Castro, G. (1969) "Liquefaction of Sands", Ph.D. Thesis, Harvard University, Cambridge, Massachusetts.

Chan, S.F. (1976) "The Behaviour of Piles Subjected to Static and Repeated Loads", Ph.D. Thesis, University of Sheffield, England.

Charles, J.A. (1978) "Treatment and Subsequent Performance of Cohesive Fill Left by Open-Cast Ironstone Mining at Snatchill experimental Housing Site, Corby", Conference on Clays Fills, Institution of Civil Engineers, London, pp. 63-72.

Charles, J.A. and Watts, K.S. (1983) "Compressibility of Soft Clay Reinforced with Granular Columns", Proc. of the 8th. European Conference on SMFE, Helsinki, vol.1, pp. 347-352.

Chin, F.K. (1972) "The inverse Slope as a Prediction of Ultimate Bearing Capacity of Piles" Proc. 3rd Southeast Asian Conf. on Soil Engng, Hong Kong, pp. 83-91.

Chin, F.K. (1978) "Diagnosis of Pile Condition", Journal of Geotech. Engng. Asian Inst. Techn. 9, N^o.2, pp. 85-104.

Clemence, S.P. and Finbarr, A.O. (1981) "Design Considerations for Collapsible Soils", Journal of the Geot. Engng Div., ASCE, vol.107, GT3, pp.305-317.

Clememce, S.P. (1985) "Collapsible Soils: Identification, Treatment and Design Considerations", Current Practices in Geotechnical Engineering, vol.1, Geo-Environ Academia, Jodhpur.

Collins, K. and McGown, A. (1974) "The Form and Function of Microfabric Features in a Variety of Natural Soils", Geotechniques, 24, 2, pp. 223-254.

Costa-Filho, L.M. (1980) "A Laboratory Investigation os Small Strain Behaviour of London Clay" Ph.D. Thesis, University of London.

Cox, D.W. (1970) "Settlement Within Embankments" Ph.D. Thesis, University of Birmingham.

Coyle, H.M. and Reese, L.C. (1966) "Load Transfer for Axially Loaded Piles in Clay", Jnl of SMFD, ASCE, 92, N^o. SM2, pp. 1-26.

Cox, D.W. (1978) "Volume Change of Compacted Clay Fill", ICE conf. on Clay Fills, pp. 79-86.

D'Appolonia, E. and Romualdi, J.P. (1963) "Load Transfer in End-Bearing Steel H-Piles", Journal of SMFD, ASCE, vol.89, SM2, Proc. Paper 3450, pp. 1-25.

Daramola, O. (1978) " The influence of Stress History on the Deformation of Sand", Ph.D. Thesis, University of London.

Darwell, J.L. and Bruce, D. (1976) "Prediction of Metastable Soil Collapse", Publication N^o.121 of the Inter. Association of Hydrological Sciences, Proc.of the Anaheim Symposium, pp. 544-552.

Delage, P. (1989) "Effondrement d'un materiau de remblai compacte trop sec", 12th. ICSMFE, Rio de Janeiro, pp. 575-582.

Dullage, C.R. (1969) "An Investigation Into the Feasibility of Small-Scale Tests on Granular Piles in Clay", Ph.D. Thesis, University of Wales, Swansea.

Eid, M.M, (1978) "Expansion of Cylindrical Cavities in Clay", PhD thesis, Sheffield University.

El-Ruwayih, A.A. (1976) "Design, Manufacture and Performance of a Lateral Strain Device", Geotechnique, 26, 1, pp. 215-216.

Engelhardt, K. and Golding, H.C. (1975) "Field Testing to Evaluate Stone Column Performance in Seismic Area", Geotechnique, 25, 1, pp. 61-70.

Fargher, P.J., Woodburn, J.A. and Selby J. (eds) (1979) "Footings and Foundations for Small Buildings in Arid Climates", Institution of Engineering, Australia (South Australian Division).

Ferreira, R.C., Peres, J.E. and Monteiro, L.B. (1987) "Some Characteristics and Properties of Collapsible Brazilian Soils", Proceedings of the Int. Symposium on Geotechnical Eng. of Soft Soils, Mexico, pp. 39-44.

Ferreira, S.R.M. and Teixeira, D.C.L. (1989) "Collapsible Soil -A Practical Case in Construction (Pernambuco, Brasil)", 12th. ICSMFE, Rio de Janeiro, pp. 603-606.

Fredlund, D.G. (1979) "Second Canadian Geotechnical Colloquim: Appropriate Concepts and Technology for Unsaturated Soils", Canadian Geot. Journal, vol.16, pp. 121-139.

Ganeshan, V. (1982) "Strength and Collapse Characteristics of a Compacted Residual Soils", Thesis (M.E.), Asian Institute of Technology, Bangkok, Thailand.

Gibbs, H.J. and Bara, J.P. (1967) "Stability Problems of Collapsing Soil", Journal of Soil Mech. and Found. Eng., ASCE, vol.93, SM4, pp. 577-594.

Gibbs, H.J. and Bara, J.P. Quoted by Bara, J.P. (1976) "Collapsible Soils", Presented at the September ASCE Annual Convention and Exposition, Held at Philadelphia Pa.

Gol'Dshtein, M.N. (1969) "Principles of Building Design on Soils Prone to Slump-Type Settlement Owing to Wetting", Soil Mech. and Found. Engng, N^o.6, pp. 420-423.

Gorle, D. and Thijs, M. (1989) "Geosynthetic-reinforced Granular Materials", 12th. ICSMFE, Rio de Janiero, vol.1, pp. 715-718.

Goughnour, R.R. (1983) "Settlement of Vertically Loaded Stone Columns in Soft Ground", Proc. of the 8th. European Conference on Soil Mech. and Found.

Engng, Hilsinki, vol.1, pp. 235-240

Goughnour, R.R. and Bayuk, A.A. (1979) "Analysis of Stone Column-Soil Matrix Interaction Under Vertical Load", Intern. Conf. on Soil Reinforcement, Paris, pp. 271-277.

Gray, D.H., Athanasopoulos, G. and Ohashi, H. (1982) "Internal/External Fabric Reinforcement of Sand", Second Inter. Conf. on Geotextiles, Las Vegas, U.S.A, vol.III, pp. 611-616.

Gray, D.H and Ohashi, H. (1983) "Mechanics of Fiber Reinforcement in Sand", Jnl of Geotechnical Engn., ASCE, vol. 109, *N°*. 3, pp. 335-354.

Greenwood, D.A. (1970) "Mechanical Improvement of Soils Below Ground Surface", Proc. ICE, pp. 11-22.

Greenwood, D.A. and Kirsh, K (1984) "Specialist Ground Treatment by Vibratory and Dynamic Methods", Piling and Ground Treatment, Thomas Tedford Ltd, London, pp. 17-45.

Griogoryan, A.A. (1967) "Prediction of Deformation of Loess Soils Under Building and Structure Foundations", Proc. of the 3rd. Asian Reg. Conf. on Soil Mechanics and Found. Engng, pp. 9-12.

Griogoryan, A.A. and Griogoryan, R.G. (1975) " Experimental Investigation of 'Negative' Friction Forces in Lateral Surface of Pile with Collapse of the Soil Under the Dead Weight", Osn. Fundam. Mekh. Gruntov, *N°*.5, 10-12.

Gunawan, M. (1978) "The Liquefaction of Micaceous Sands", M.Eng. Dissertation, University of Sheffield.

Gupalenko, V.I. and Rudenko, A.A. (1976) "Investigation of Behaviour of Bored-Cast-In-Place Piles and Compacted Masses in the case of Collapse of the Soil Surrounding then under its Dead Weight", Osn. Fundam. Mekh. Gruntov, *N°*.2, pp. 22-24.

Hassani, A.W. and Goel, M.C. (1982) "An Evaluation of Problems in Collapsible Soils", Indian Journal of Power & River Valley Development, pp. 174-183.

Hassona, F.A. (1986) "Studies of the Liquefaction Behaviour of Cohesionless materials", Ph.D. Thesis, University of Sheffield, England.

Head, K.H. (1982) "Manual of Soil Laboratory Testing", vol.2, Pentech Press, Plymouth, London.

Hilf, J.W. (1948) "Estimating Construction Pore Pressure in Rolled Earth Dams", Proc. 2nd ICSMFE, vol.III, pp. 234-240.

Hilf, K.W. (1956) "An Investigation of Pore Water Pressures in Compacted Cohesive Soils", Bureau of Reclamation, Tech. Mem., p. 654.

Holtz, W.G. (1948) "The Determination of Limits for the Control of Placement Moisture in High Rolled Earth Dams", Proc. ASTM, Philadelphia, Pa., 1240-1248.

Holtz, W.G. and Hilf, J.W. (1961) "Settlement of Soil Foundations due to Saturation", Proc. 5th. ICSMFE, Paris, vol.1, pp. 673-679.

Houston, S.L., Houston, W.N., and Donald, J.S. (1988) "Prediction of Field Collapse of Soils due to Wetting", Jnl of Geot. Engineers, ASCE, N^o.1, pp. 40-58.

Hughes, J.M.O and Withers, N.J. (1974) "Reinforcing of Soft Cohesive Soils with Stone Columns", Ground Engineering, pp. 42-49.

Hughes, J.M.O., Withers, N.J. and Greenwood, D.A. (1975) "A Field Trial of the Reinforcing Effect of a Stone Column in Soil", Geotechnique, 25, 1, pp.31-44.

ICI (1977) "Designing with Terram" A Summary of Techniques and Physical Data Used in the Design of 'Terram'/Soil Structures. ICI fibres, Harrogate.

Jardine, R.J., Symes, M.J, and Burland, J.B. (1984) "The measurement of Soil Stiffness in the Triaxial Apparatus", Geotechnique, 34, 3, pp. 323-340.

Jennings, J.E. and Knight, K. (1975) "A Guide to Construction on or with Materials Exhibiting additional Settlement Due to 'Collapse' of Grain Structure", Proc. 6th. Regional Conf. For Africa on SMFE, Durban, South Africa.

Johnson, G.E. (1953) "The Stabilization of Soils By Silt Injection Method", Journal of the Soil Mech. and Found. Div., ASCE, vol.79, N^o. 323.

Juran ,I and Guermazi, A (1988) "Settlement Response of Soft Soils Reinforced by Compacted Stone Columns", ASCE, journal of geot. div., N^o.8, pp. 930-943.

Kane, H. (1973) "Confined Compression Of Loess", Proc. of the 8th. ICSMFE, vol.2, Section 4/19, pp. 115-122.

Karst, H., Legrand, J., Le Tirant, P., Sarda, J.P. and Weber, J. (1965) "Contribution a l'etude de la mecanique des milieux granulaires", Proc. 6th. ICSMFE, Canada, pp. 259-263.

Klepikov, S.N. and Saiko, B.A/ (1980) "Analysis of Bored-Cast-In-Place Pile Foundations in Soils of Type II Collapsibility", Osn. Fundam, Kiev, N^o.13, pp.13-19.

Knight, K. (1961) "The Collapse of Structure of Sandy Subsoil on Wetting", Ph.D. Thesis, University of the Witwatersrand, Johannesburg, South Africa.

Knight, K. (1963) "The Origin and Occurrence of Collapsing Soils", Proc. 3rd Regional Conf. for Africa on SMFE, vol.1, pp. 127-130.

Knodel, P.C. (1981) "Construction of Large Canal on Collapsing Soils", Journal of the Geot. Engng Div., ASCE, vol.107, Gt1, pp. 79-94.

Kolbuszewski, J. (1948) "An Experimental Study of Maximum and Minimum Porosities of Sands", Proc. 2nd. Int. Conf. on Soil Mech. and Found Engng, Rotterdam, 1, pp. 158-165.

Kondner, R.L. (1963) "Hyperbolic Stress-Strain Response: Cohesive Soils", J. Soil Mech. and Found. Div., Proc. ASCE, N^o.SM1, pp.115-141.

Kuwabara, F. and Poulos, H.G. (1989) "Downdrag Forces in Group of Piles", Jour. of Geot. Engng. Div., ASCE, vol.115, N^o.6, pp. 806-818.

Lade, P.V. and Harnandez, S.B. (1977) "Membrane Penetration Effect in Undrained Test", ASCE, vol.103, N^o.GT2, pp. 109-125.

Lambe, T.W (1962) "Pore Pressure in a Foundation Clay", Jnl of SMFD, ASCE, vol. 88, N^o. SM2, Proc. paper 3097, p. 19.

Lawton, E.C., Fragaszy, R.J. and James, H.H. (1989) "Collapse of Compacted Clayey Sand", Jour. of Geot. Engng Div., ASCE, vol.115, N^o.9, pp.1252-1267.

Lefebvre, G. and Ben Belfadhel, M. (1989) "Collapse at Permeation for a Compacted Non-Plastic Till", 12th. ICSMFE, Rio de Janeiro, pp. 619-622.

Leonards, G.A. and Altschaeffl, A.G. (1971) Discussion on "Review of Collapsing Soils", Jour. of the Soil Mech. and Found. Div., ASCE, vol.97, SM1, pp. 269-271.

Litvinov, I.M. (1969) "Conduction of Blasting Works For Deep Compaction of Slump-Prone Loess Soils in a Built-up Area", Soil Mech. and Found. Engng, N^o.4, pp.272-277.

Litvinov, I.M. (1971) "The Deep Compaction of Highly Compressible Loess", European Civil Engineering, N^o.1.

Lowe, J. and Johnson, T.C. (1960) "Use of Back Pressure to Increase Degree of Saturation of Triaxial Test Specimen", Presented at the 1960 ASCE research Conf. on Shear Strength of Cohesive Soils, Boulder, Col., pp. 819-836.

Luce, A.F. (1968) "The Strengthening in Depth of Weak Soils By Vibration at Tolka Quay", Jour. Inter. Instn Civ. Engns, pp. 3-12.

Lutenegger, A.J. and Saber, R.T. (1988) "Determination of Collapse Potential Of Soils", Geot. Testing Jnl, GTJODJ. vol. 11, N^o. 3, pp. 173-178.

Machado Filho, O.V.B. (1987) "Experimental Study of a Test Fill Founded on Stone Columns", Proc. of the Int. Symposium of Geot. Engng of Soft Soils, Mexico, vol.1, pp. 249-256.

Majorana, C., Mazzalai, P. and Odorizzi, S. (1983) "The Prediction Of the Settlement of Steel Petroleum Tanks Resting on Stone Columns Reinforced Soil", 8th. ICSMFE, Hilsinki, vol.1, pp. 271-274.

Makhlouf, A.M. and Stewart, J.J. (1965) "Factors Influencing the Modulus of Elasticity of Dry Sand", 6th. ICSMFE, Canada, pp. 298-302.

Markin, B.P. (1969) Discussion on "Standard Criteria of Sag in Loess Soils", Soil Mech. and Found. Engng, N^o.2, p. 137.

Maswoswe, J. (1985) "Stress-Paths for Compacted Soil During Collapse Due to Wetting",PhD Thesis, Imperial College of Sciences and Technology.

Mattes, N.S. (1969) "The Influence of Radial Displacement Compatability on Pile Settlement", Geotechnique, vol.19, pp. 157-159.

Mattes, N.S. (1972) "The Analysis of Settlement of Piles and Pile Groups in Clay Soils", Ph.D. Thesis, University of Sydney, Australia.

Mattes, N.S. and Poulos, H.G. (1969) "Settlement of Single Compressible Pile", J.S.M.F.D., ASCE, vol.95, SM1, pp. 189-207.

Mayer (1958) Quoted by Maswoswe (1985)

McGown, A. and Andrawes, K.Z. (1977) "The Influence of Non-Woven Fabric Inclusions on The Stress-Strain Behaviour of a Soil Mass", Proceedings Inter. Conf. on the Use of Fabrics in Geotechnics, Paris, vol.1, pp. 161-167.

McGown, A., Andrawes, K.Z. and Al-Hassani, M.M. (1978) "Effect of Inclusion Properties on The Behaviour of Sand", Geotechnique, vol.28, *N°*.3, pp. 327-346.

Mc Kenna, J.M., Eyre, W.A. and Wolstenholme, D.R. (1975) "Performance of an embankment supported by stone columns in soft ground", Geotechnique, 25, 1, pp. 51-60.

Mindlin, R.D. (1936) "Force at a Point in the Interior of a Semi-Infinite Solid", Physics 7: 195.

Mishu, L.P. (1963) "Collapse in One-Dimensional Compression of Compacted Clay on Wetting", MSc Thesis Presented to Purdue University, at West Lafayette.

Mitchell, J.K. and Huber, T.R. (1985) "Performance of a Stone Column Foundation", ASCE., Jnl of Geot. Div, vol.III, *N°*.2, Paper *N°*.19491.

Mitchell, J.K. and Katti, R.K.(1981) "Soil Improvement-State-of-the-Art Report" 10th. ICSMFE, Stockholm, pp. 261-317.

Molenkamp, F. and Luger, H.J. (1981) "Modelling and Minimization of Membrane Penetration Effects in Tests on Granular Soils", Geotechnique, vol.31, *N°*.4, pp. 471-486.

Moreau, Neil and Mary (1835) "Foundations-Emploi du Sable", Annales des Ponts et Chaussees, Memoires, *N°*. 224, pp. 171-214.

Morgenstern, N. and de Mattos, M.M. (1975) "Stability of Slopes in Residual Soils", Proc. 5th. Pan American Conf. on SMFE, Buenos Aires, Argentina, vol.3, pp. 367-383.

Morgenthaler, M, Cambou, B. and Sanglerat (1978) "Colonnes Ballastees, Essais de Chargement et de Calculs par la Methode des Elements Finis", Revue Francaise Geotechnique, 5.

Murayama, S. (1958) "Method to Install Sand Piles by Vibrating Casing Pipes", Japanese Patent, *N°*. 266080.

Northey, R.D. (1969) "Engineering Properties of Loess and Other Collapsible Soils", Proc. 7th. ICSMFE, Mexico, vol.3, pp. 445-452.

Ordermir, I and Ozkan, Y. (1985) "Compression of Alluvial Deposits Due to Wetting", Proc. of the 11^{th} ICSMFE, San Francisco, vol.4, pp. 2217-2221.

Poulos, H.G (1968) "Analysis of The Settlement of Pile Groups", Geotechnique, vol.18, N^o.4, pp. 449-471.

Poulos, H.G. (1982) "The Influence of Shaft Length on Pile Load Capacity in Clays", Geotechnique, vol.32, N^o.2, pp. 145-148.

Poulos, H.G. and Davis, E.R. (1968) "The Settlement Behaviour of Single Axially-Loaded Incompressible Piles and Piers", Geotechnique, vol.18, pp. 351-371.

Poulos, H.G. and Davis, E.R. (1975) "Prediction of Down-Drag Forces in End-Bearing Piles", Jnl. Geot. Engng. Div., ASCE, vol.101, GT2, pp. 189-204.

Poulos, H.G. and Davis, E.R. (1972) "The Development of Negative Friction with Time in End-Bearing Piles", Aust. Geomechs. Jnl., vol.G2, N^o.1, pp. 11-20.

Poulos, H.G. and Davis, E.R. (1980) "Pile Foundation Analysis and Design", Series in Geotechnical Engineering, John Wiley & Sons, Inc., New York.

Poulos, H.G. and Mattes, N.S. (1969) "The Analysis of Downdrag in End-Bearing Piles due to Negative Friction", Proc. of the 7th. ICSMFE, Mexico city, Mexico, vol.2, pp. 205-209.

Poteur, M. (1973) "Die Verbesserung der Tragfahigkeit Bindiger Boden Durch Reine Tauchruttelung", Baumaschine und Bautechnik, 10, pp. 385-393.

Potyondy, J.G.(1961) "Skin Friction Between Various Soils and Construction Materials", Geotechnique, vol. 11, pp. 339-353.

Priebe, H. (1976) "Abschatzunz des Setzungsverhattens Eines Durch Stopverdichtung Verbesserten Baugrundes", Die Bautechnik 53, pp. 160-162.

Prusza, A. and Choudry, T (1979) "Collapsibility of Residual Soils", Proc. 13th. Congres on Large Dams, New Delhi, India, Q.49, R.9, pp. 117-130.

Rad, N.S. Clough, G.W. (1984) "New Procedure for Saturating Sand Specimens", Jnl. of SMFD, ASCE, vol.110, N^o.9

Randolph, M.F. and Wroth, C.P. (1978) "Analysis of Deformation of Vertically Loaded Piles", Jnl of Geot. Engn. Div., ASCE, vol. 104, N^0. GT12: 1465-1488.

Rathgeb, E. and Kutzner, C. (1975) "Some Applications of the Vibro-Replacement Process" Geotechnique, 25, 1, pp.45-50.

Reginatto, A.R. and Ferrero, J.C. (1973) "Collapse Potential of Soils and Soil-Water Chemistry", Proc. 8th. ICSMFE, vol.2, pp. 177-183.

Rice, S.M.M (1975) "Field and Model Test on Anchors in Clay", PhD Thesis, Sheffield University.

Richardson, A.M. and Whitman, R. (1963) "Effect of Strain Rate upon Undrained Shear Resistance of a Saturated Remoulded Fat Clay", Geotechnique, vol.13, N^o.2, pp. 310-324.

Romana, M. (1983) "Settlement Control with Gravel Columns under Oil Tanks", 8th. ICSMFE, Hilsinki, vol.1, pp.301-306.

Ronan, S.R. (1980) "Heavy Structures Founded in Aeolian Soils", Proc. 3rd. ANZ Conf. on Geomechanics, Wellington, NZ Institute of Engineers.

Roscoe,K , Schofield, A.N. and Thurairajah, A. (1963) "An Evaluation of Test Data for Selecting a Yield Criterion for Soils", Proc. of the Symp. on Laboratory Shear Testing of Soils, STP 361, ASTM, Philadelphia, pp. 111-128.

Royce, J.R and Brown, S.F. (1976) "Measurement of Elastic Strain in Granular Material", Geotechnique, vol. 26, N^o. 4, pp. 637-640.

Rowe, P. and Barden, L. (1966) "A New Consolidation Cell", Geotechnique, vol.16, N^o.2, pp. 162-170.

Saber, R.T. (1987) Quoted by Lutenegger, A.J. and Saber, R.T. (1988) "Determination of Collapse Potential of Soils", Geotechnical Jnl., GTJODJ, vol.II, N^o.3, pp. 173-178.

Salameh, A.G. (1973) "A Study of Some Geotechnical Aspects of Collapsing Soils", M.Sc. Dissertation, Imperial College, London.

Salas, J.A.J. and Belzunce, J.A. (1965) "Resolution theorique de la distribution des forces dans les pieux", Proc. 6th. Int. Conf. SMFE, vol.2, pp. 309-313.

Schlosser, F. and Juran, Y (1979) "Parametres de Conception pour Sols Artificiellement Ameliores", Comptes Rendus du 7^{eme} Congres Europeen de Brighton, vol.5, pp. 227-252.

Rathgeb, E. and Kutzner, C. (1975) "Some Applications of the Vibro-Replacement Process" Geotechnique, 25, 1, pp.45-50.

Reginatto, A.R. and Ferrero, J.C. (1973) "Collapse Potential of Soils and Soil-Water Chemistry", Proc. 8th. ICSMFE, vol.2, pp. 177-183.

Rice, S.M.M (1975) "Field and Model Test on Anchors in Clay", PhD Thesis, Sheffield University.

Richardson, A.M. and Whitman, R. (1963) "Effect of Strain Rate upon Undrained Shear Resistance of a Saturated Remoulded Fat Clay", Geotechnique, vol.13, N^o.2, pp. 310-324.

Romana, M. (1983) "Settlement Control with Gravel Columns under Oil Tanks", 8th. ICSMFE, Hilsinki, vol.1, pp.301-306.

Ronan, S.R. (1980) "Heavy Structures Founded in Aeolian Soils", Proc. 3rd. ANZ Conf. on Geomechanics, Wellington, NZ Institute of Engineers.

Roscoe,K , Schofield, A.N. and Thurairajah, A. (1963) "An Evaluation of Test Data for Selecting a Yield Criterion for Soils", Proc. of the Symp. on Laboratory Shear Testing of Soils, STP 361, ASTM, Philadelphia, pp. 111-128.

Royce, J.R and Brown, S.F. (1976) "Measurement of Elastic Strain in Granular Material", Geotechnique, vol. 26, N^o. 4, pp. 637-640.

Rowe, P. and Barden, L. (1966) "A New Consolidation Cell", Geotechnique, vol.16, N^o.2, pp. 162-170.

Saber, R.T. (1987) Quoted by Lutenegger, A.J. and Saber, R.T. (1988) "Determination of Collapse Potential of Soils", Geotechnical Jnl., GTJODJ, vol.II, N^o.3, pp. 173-178.

Salameh, A.G. (1973) "A Study of Some Geotechnical Aspects of Collapsing Soils", M.Sc. Dissertation, Imperial College, London.

Salas, J.A.J. and Belzunce, J.A. (1965) "Resolution theorique de la distribution des forces dans les pieux", Proc. 6th. Int. Conf. SMFE, vol.2, pp. 309-313.

Schlosser, F. and Juran, Y (1979) "Parametres de Conception pour Sols Artificiellement Ameliores", Comptes Rendus du 7^{eme} Congres Europeen de Brighton, vol.5, pp. 227-252.

Seed, H.B. and Reese, L.C. (1955) "The action of Soft Clay Along Friction Piles", Proc. ASCE, 81, paper N^0. 842.

Selby, J. (1982) "Engineering Geology of Collapsing Soils in South Australia", Proc. of the 4th. Int. Congress, New-Delhi, vol.1, pp. 469-475.

Selig, E.T. and Grangaard, O.H.Jr. (1970) "A New Technique for Soil Strain Measurement", Materials Research and Standards, MTRSA, vol.10, N^o.10, pp. 19.

Simpson, B., Blower, T., Craig, R.N. and Wilkinson, W.B. (1989) "The engineering Implication of Rising Groundwater Levels in the Deep Aquifer Beneath London", CIRIA, Special Publication 69, pp. 59-69.

El-Sohby, M.A., Sherif, M.M., Elleboudy, A.M. and Saad, M.A. (1989) "Critical Evaluation of Collapsibility Measurement for Cemented Sand", 12th. ICSMFE, Rio de Janeiro, pp. 593-596.

Sokolovich, V.E. (1965) "Silicatization of Loess Soils", Soil Mech. and Found. Engng., N^o.1.

Sokolovich, V.E. (1971) "New Developments in the Chemical Strengthening of Ground", Soil Mech. and Found. Engng., N^o.2, pp. 114-118.

Steuerman, S. (1939) "A New Soil Compaction Device", Engineering News Record, July 20th.

Thorburn, S. (1975) "Building Structures Supported by Stabilised Ground", Geotechnique, 25, 1, pp. 83-94.

Thurman, A.G and D'Appolonia, E (1965) "Computed Movement of Friction and End-Bearing Piles Embedded in Uniform and Stratified Soils", Proc. 6^{th} Int. Conf. Soil Mech.,2 , pp. 323-327.

Tumay, M.T., Antonini, M. and Arman, A. (1979) "Metal Versus Non-Woven Fiber Fabric Earth Reinforcement in Dry Sands: A Comparative Statistical Analysis of Model Tests", Geotechnical Testing Journal, vol.2, N^o.1, pp. 44-56.

Van Impe, W. and de Beer, E. (1983) "Improvement of Settlement Behaviour of Soft Layers by Means of Stone Columns", Proc. 8th. European Conf. SMFE, Helsinki, pp. 309-312.

Vautrain, J. (1980) "Comportement et Dimensionnement des Colonnes Ballastees", Revue Francaise de Geotechnique, Paris, N^o.11, pp. 59-73.

Walker, L.K., and Darvall, P. and Le, P. (1973) "Dragdown on Coated and Uncoated Piles", Proc. of the 8^{th} ICSMFE, Moscow, Vol. 2, N^o.1, pp. 257-262.

Watt, A.J , De Boer, B.B and Greenwood, D.A. (1967) " Loading Tests on Structures Founded on Soft Cohesive Soils Strengthened by Compacted Granular Columns", Proc. of the 3^{rd} Asian Regional Conf. on SMFE, Haifa, pp. 248-251.

Wetson, D.J. (1980) "Compaction for Collapsing Sand Road Beds", Proc. of the 7^{th} Regional Conference for Africa on SMFE, Accra, vol.1, pp.341-354.

Whitaker, T (1957) "Experiments with Model Piles in Groups", Geotechnique, 7, 4, pp. 147-167.

Williams, J.D.G. (1969) "Small Scale Tests on Granular Piles in Soft Clay", B.Sc Thesis, University of Wales.

Williams (1971) Quoted by Maswoswe (1985).

Yoshimi, Y and Osterberg, J.O. (1963) "Compression of Partially Saturated Cohesive Soils", Jnl. of SMFD, ASCE, vol.89, SM4, pp. 1-24.

Yuen, C.M.K., Lo, K.Y., Palmer, J.H.L. and Leonards, G.A. (1978) "A New Apparatus for Measuring the Principal Strains in Anistropic Clays", Geot. Testing Jnl., vol. 1, N^o. 1, pp. 24-33.

Yung, P.C.Y. (1987) "The Measurement of the Deformation Properties of Cowden Till at Small Strains", Ph.D. thesis, University of Sheffield.

Zeevaert, L. (1972) "Foundation Engineering for Difficult Subsoil Conditions", Van Nostrand Reinhold Company, 652 pages.

Zur, A. and Wiseman, G. (1973) "A Study of Collapse Phenomena of an Undisturbed Loess", Proc. 8th. ICSMFE, vol.2, Section 4. pp. 265-269.

Abbreviations:

ASCE: American Society of Civil Engineers,
ICSMFE: International Conference of Soil Mechanics and Foundation Engineering,
SMFE: Soil Mechanics and Foundation Engineering
SMFD: Soil Mechanics and Foundation Division,
ASTM: American Society for Testing and Materials,
CIRIA: Construction Industry Research and Information Association.

Appendix A: Negative Skin Friction

Negative skin friction is a force developed through friction between the pile and the soil in a direction to increase the loading on the pile. Generally, the drag is downward because of a relative movement between the soil and pile. This may occur when a pile is driven through a compressible soil, which has recently, or will be, covered with a fill, so that the point is in firm material. As the soil consolidates, the earth fill moves downward. This movement develops friction forces on the perimeter of the pile which tends to carry the pile further into the ground. If the pile does not move , or if the pile does move, but not as much as the consolidation movement, the maximum friction strength of the fill soil is developed along the pile perimeter for the depth of the fill. This force may be large enough so that, in conjunction with the applied load, the pile will settle excessively. Alternatively, the stresses developed may be large enough to overstress the pile material.

The calculation of the total negative skin friction or 'dragdown' force on a pile is a matter of great complexity and the time factor is of importance. However, good agreement was found from empirical formulates based on the horizontal effective stresses developed during the process (Tomlinson, 1969; Zeevaert, 1972).

Appendix B: FORTRAN program

The computer program was written to determine the settlement reduction factor (β) of a sand column confined or not confined by a geofabric or a rigid pile embedded in a collapsible fill subjected to inundation. The input data are given in the (READ) statement which are:

1. The length of the 'pile' SL (m)
2. The Young's modulus of the 'pile' EP (kN/m^2)
3. The ultimate load of the 'pile' P (kN/m^2)
4. The Young's modulus of the geofabric ET (kN/m^2)
5. The thickness of the geofabric T (m)
6. The percentage X

DM, AP, Q, S0 refer to the 'pile' diameter, the 'pile' cross section, the surcharge pressure and the settlement of the collapsible layer beneath the tip of the 'pile' respectively.

I- Slip analysis using 'Poulos- modified Hughes' model:

```
PROGRAM SAPH
DIMENSION SL(100), EP(100), P(100), ET(100), T(100), X(100)
PRINT*, 'WHAT IS THE DATA1 FILENAME...MR. AYADAT'
READ(*,100)DATA1
PRINT*, 'WHAT IS THE DATA2 FILENAME...MR. AYADAT'
READ(*,100)DATA2
PRINT*, 'WHAT IS THE DATA3 FILENAME...MR. AYADAT'
READ(*,100)DATA3
PRINT*, 'WHAT IS THE DATA4 FILENAME...MR. AYADAT'
READ(*,100)DATA4
PRINT*, 'WHAT IS THE DATA5 FILENAME...MR. AYADAT'
READ(*,100)DATA5
PRINT*, 'WHAT IS THE DATA6 FILENAME...MR. AYADAT'
```

```
      READ(*,100)DATA6
      PRINT*, 'WHAT IS THE OUTPUT FILENAME...MR. AYADAT'
      READ(*,100)OUTPUT
100   FORMAT (A12)

C     Opening files:

      OPEN(2,FILE=DATA1)
      OPEN(3,FILE=DATA2)
      OPEN(4,FILE=DATA3)
      OPEN(5,FILE=DATA4)
      OPEN(6,FILE=DATA5)
      OPEN(7,FILE=DATA6)
      OPEN(8,FILE=OUTPUT)

C     Reading of the data:

      READ(2,*,END=8)(SL(I1), I1=1,100)
8     IMAX = I1
      READ(3,*,END=9)(EP(I2), I2=1,100)
9     JMAX = I2
      READ(4,*,END=10)(P(I3), I3=1,100)
10    KMAX = I3
      READ(5,*,END=11)(ET(I4), I4=1,100)
11    KNAX = I4
      READ(6,*,END=12)(T(I5), I5=1,100)
12    JNAX = I5
      READ(2,*,END=13)(X(I6), I6=1,100)
13    NMAX = I6

C     The constant parameters used in the calculation:

      Q = 100.0
      SP = Q*AP
      DM = 0.023
      AP = (3.14*(DM**2.0))/4.0
      CK0 = 0.43
      CA = 29.8
      TGKS = 0.298
      GAMA = 5.4
      S0 = 0.054
      SL0 = 0.41
      FITA = (3.14*41.0)/180.0
      QSK = (3.14*45.0)/180.0
      CKP = (TAN(QSK + (FITA/2.0)))**2.0
      RA = 1.0
```

```
      QR = 1.0
      QT = 1.0

C     Calculation stages:

      DO 15 J1=N1,N1
      DO 15 J2=M1,M1
      DO 15 J3=K1,K1
      DO 15 J4=M1,M1
      DO 15 J5=M1,M1
      DO 15 J6=1,3

C     Calculation of (δ1):

      PA1 = P(J3) * X(J6) + SP
      DELTA1 = (PA1 *SL(J1))/(EP(J2) * AP)

C     Calculation of (δ2):

      ROFS = ((2.0*Q*(SL(J1)**2.0)*RA)/(EP(J2)*DM))*((CA/Q + TGKS*
     ((GAMA*SL(J1))/(3.0*Q) + 1.0))
      DELTA2 = ROFS*QR*QT

C     Calculation of (δ3):

      PA2 = (P(J3) * X(J6) + SP)/AP
      RPA2 = PA2/CKP - CK0*(SP/AP)
      DELR = (RPA2*(DM/2.0))/(ET(J4)*T(J5))
      IF(J4.LE.5) THEN
      DELTA3 = 2.0*DELR*SL0
      ELSE
      DELTA3 = 0.0
      ENDIF

C     Settlement of the collapsible layer beneath the tip of the 'pile'(Sl):

      SI = S0 * ((SL0 - SL(J1))/SL0)

C     Calculation of the total settlement (Δ):

      DELTA = DELTA1 + DELTA2 + DELTA3 + SI

C     Calculation of the settlement reduction factor (β):

      BETA = DELTA/S0

C     Printing of the results:
```

```
      WRITE(8,*) BETA
15    PRINT*,BETA

C     Closing files:

      CLOSE (2)
      CLOSE (3)
      CLOSE (4)
      CLOSE (5)
      CLOSE (6)
      CLOSE (7)
      CLOSE (8)
      STOP
      END
```

II- Elastic analysis using 'Poulos-modified Hughes' model:

PROGRAM EAPH

The previous program is used with some modifications:

1- Add to DIMENSION an other vector called RF(100),

2- Open a new file,

```
      PRINT* 'WHAT IS THE DATA7 FILENAME...MR AYADAT'
      READ(*,100)DATA7
      OPEN(9,FILE=DATA7)
```

3- Read the new data:

```
      READ(8,*,END=14)(RF(I7), I7=1,100)
14    MNAX = I7
```

RF: is the settlement influence factor obtained from Fig. 3.10.

4- Add to calculation stage:

```
      DO 15 J7=K1,K1
```

5- Replace δ_2 by:

```
      ROFS = (Q * DM * RF(J7))/(EP(J2) * RA)
      DELTA2 = ROFS * QR * QT
```

6- Close the new file:

```
      CLOSE(9)
```

III- Elastic & Slip analyses using 'Poulos-Preibe' model:

PROGRAM EAPP & SAPP
The programs (I) or (II) can be used with the following modification:
The term DELR will be:

```
      DELR = RPA2*((1 + MU)/EP(J2))*((1 - 2.0*MU)*(1 - (R0/ER)
     **2.0))/(1 - 2.0*MU + (R0/ER)**2.0))
```

The new constant parameters have to be added in their corresponding section. They are:

```
      R0 = DM/2.0
      MU = 0.5
      ER = AP/A
C     A is the area of the unit cell
      A = (3.14* (0.39)**2.0)/4.0
C     D = 0.39 m is the diameter of the unit cell
```

Appendix C: Design example: calculation of the settlement reduction factor (β)

It is desired to determine the settlement reduction factor (β) for a sand column encapsulated in T2000 and fully penetrating in a collapsible fill subjected to full inundation. The working load on the 'pile' is 20% of its ultimate load (P_u).

Because the collapsible fill, in this case, is subjected to full inundation (saturated case) the following data will be required:

External loads on the 'pile':

Surcharge pressure: q = 100 kN/m^2

Axial load: P = 0.2 × P_u and (P_u = 340 N, Table 7.4)

The collapsible soil:

γ_d = 15.4 kN/m^3

ϕ' = 34.8°, c' = 0, k_0 = 0.43

The settlement of the untreated foundation: S_0= 54 mm

Stiffness: E_s= 2900 kN/m^2

The 'pile' (i.e. the sand column in T2000):

L = 410 mm, d = 23 mm

Stiffness of the composite: E_p = 79000 kN/m^2 (obtained from Fig. 4.22)

Friction angle of the sand (LBS): ϕ = 41°

Modulus of elasticity of the geofabric: E = 72000 kN/m^2 (obtained from Fig. 2.11)

Thickness of the geofabric: t = 1.0 mm

I- Slip analysis using 'Poulos-modified Hughes' model:

a) Calculation of the elastic settlement of the 'pile' due to the loads (δ_1):

$$\delta_1 = \frac{P_a L}{E_p A_p}$$

The axial force (P_a) in pile' at top of consolidating layer will arise from the applied axial load and the surcharge pressure:

$$P_a = 0.2P_u + qA_p$$

$$P_a = 0.2 \times 340 + 100 \times \frac{3.14 \times (0.023)^2}{4} = 109.5N$$

Therefore:

$$\delta_1 = \frac{109.5 \times 0.41}{79000 \times 10^3 \times 4.15 \times 10^{-4}} = 1.3 \times 10^{-3}m$$

b) Calculation of the settlement caused by downdrag (δ_2):

It will be assumed that, $k_s = k_0$ so $k_s\ tan\phi' = 0.43 \times tan34.8^o = 0.298$.

The equivalent 'pile'-soil adhesion, c_e' , is calculated from the equation:

$$c_e' = c' + p_0 k_s tan\phi'$$

Now:

p_0 = q = 100 kN/m^2

so:

$c_e' = 0 + 100 \times 0.298 = 29.8\ kN/m^2$,

$c_e'/q = 29.8/100 = 0.298$,

$(\gamma L)/q = ((15.4 - 10) \times 0.41)/100 = 0.022$.

By applying equation 3.6 :

$$\rho_{FS} = \frac{2qL^2R_A}{E_p d}\left[\frac{c_e'}{q} + k_s tan\phi'\left(\frac{\gamma L}{3q} + 1\right)\right]$$

Therefore:

$$\rho_{FS} = \frac{2 \times 100 \times (0.41)^2 \times 1}{79000 \times 0.023}[0.298 + 0.298\,(0.022/3 + 1)] = 11.07 \times 10^{-3}m$$

From Fig. 3.6-a and 3.6-b $Q_R = 1.0$ and from Fig. 3.7 $Q_T = 1.0$.

Now:

$$\delta_2 = \rho_{FS}\ Q_R\ Q_T = 11.07 \times 10^{-3} \times 1.0 \times 1.0 = 11.07 \times 10^{-3}m$$

c) Calculation of the settlement due to the lateral deformation (δ_3):

$$\Delta P = \frac{P_a}{A_p} \frac{1}{tan^2(45^o + \frac{\phi}{2})} - k_0 q$$

$$\Delta P = \frac{109.5 \times 10^{-3}}{4.15 \times 10^{-4}} \frac{1}{tan^2(45 + \frac{41}{2})} - 0.43 \times 100 \approx 17 kN/m^2$$

$$\delta_3 = 2\ \varepsilon_r\ L$$

where:

$$\varepsilon_r = \frac{\delta_r}{r} = \frac{\Delta P \frac{d}{2}}{Et}$$

$$\varepsilon_r = \frac{17 \times \frac{0.023}{2}}{72000 \times 0.001} \approx 2.7 \times 10^{-3} m$$

Therefore:

$$\delta_3 = 2 \times 2.7 \times 10^{-3} \times 0.41 \approx 2.2 \times 10^{-3} m$$

d) Calculation of the total settlement (Δ):

$$\Delta = \delta_1 + \delta_2 + \delta_3$$

$$\Delta = 1.3 \times 10^{-3} + 11.07 \times 10^{-3} + 2.2 \times 10^{-3} = 14.6 \times 10^{-3} m$$

So: $\Delta = 14.6$ mm

e) Calculation of the settlement reduction factor (β):

$$\beta = \frac{S_i}{S_0} = \frac{14.6}{54} \approx 0.27$$

II- Elastic analysis using 'Poulos-modified Hughes' model:

$$\delta_2 = \frac{q d I_\rho}{E_p R_A}$$

$I_\rho = 210$ obtained from Fig. 3.10 for:

K= $R_A(E_p/E_s) = 1 \times (79000/2900) \approx 27.3$ and L/d = $410/23 \approx 17.8$

Therefore:

$$\delta_2 = \frac{100 \times 0.023 \times 210}{79000 \times 1} \approx 6.11 \times 10^{-3} m = 6.11 mm$$

From the slip analysis:

$\delta_1 = 1.3$ mm and $\delta_3 = 2.2$ mm.

So:

$$\Delta = 1.3 + 6.11 + 2.2 = 9.6mm$$

$$\beta = \frac{9.6}{54} \approx 0.177$$

The determination of the settlement reduction factor β for the slip and the elastic analysis using 'Poulos-Preibe' model is similar.

Appendix D: Manufacture of Rubber Bellow

The rubber bellow used in the application of the surcharge pressure during the testing operation was manufactured in the laboratory. The bellow is similar to those used in the Rowe cell, but with a much larger diameter and height.

A former 0.35 m in diameter and 0.22 m high was constructed from wood with the shape shown in Fig. D1. The surface was coated with varnish to give a smooth surface. Dunlop latex was painted onto the former and air dried. When it was dry further coats of latex were added until the thickness of the rubber was approximately 4 mm. Care was taken to prevent air bubbles, which could turn into minute holes, forming on the surface of the wet latex. When the membrane was completely cured, the outside was dusted with French chalk and it was stripped off the former. The inside surface of the bellow was then coated with a layer of primer and then Devcon flexane. The flexane is a two parts mixture and cured in approximately 2 hours.

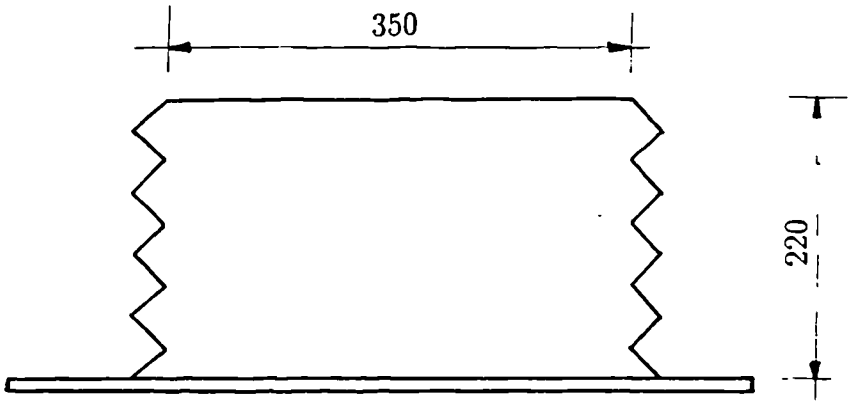

Fig. B1 Wooden Former for Manufacturing Rubber Bellow

Appendix E: Construction of stone columns, with a fabric surround around them, in the field

Several modern technique for the construction of compacted stone columns in soft soils and cohesionless fills were developed. Most of these methods can be used to install stone columns encapsulated in a geofabrics in a collapsible fill. Only two methods are described here:

E.1 Method 1: Vibro-displacement technique:

The machine penetrates both by vibratory impact and by its weight. There is no removal of soil which is displaced laterally involving local shearing like driven piling. Compressed air is used through the bottom jet during penetration.

On reaching the requisite depth it is necessary to extract the vibroflot from the bore to introduce the geofabric, in the form of a cylinder, and backfill. Backfill is tipped into the open bore and the machine lowered on top acting to displace the backfill laterally and downwards like a vibratory rammer. The procedure is repeated in approximately half metre lifts until the column is completed. In situations where the cylindrical probe has fins projecting from its edges, which may damage the geofabric during compaction, the backfill can be introduced through a separate pipe a head of the probe.

E.2 Method 2: Vibro-composer method:

This method was developed by Murayama in Japan in 1958 (Murayama, 1958). The apparatus and procedure used in the composer system are shown schematically in Fig. E 2.1.

A casing pipe is driven to the desired depth by a vibrator at the top. Provision is made for water jetting by pipes passing to the toe of the tube which is used if a plug of compacted soil inhibits progress. Jetting is continued whilst casings are pulled out.

On reaching the requisite depth the casing pipe is extracted and a cylindrical geofabric is introduced into the hole. The pipe is then lowered up to the bottom of the hole. A gravel charge is then introduced into the pipe, the pipe is withdrawn part way while compressed air is blown down inside the casing to hold the gravel in place. The pipe is vibrated down to compact the gravel column. The process is repeated until pipe reaches the ground surface.

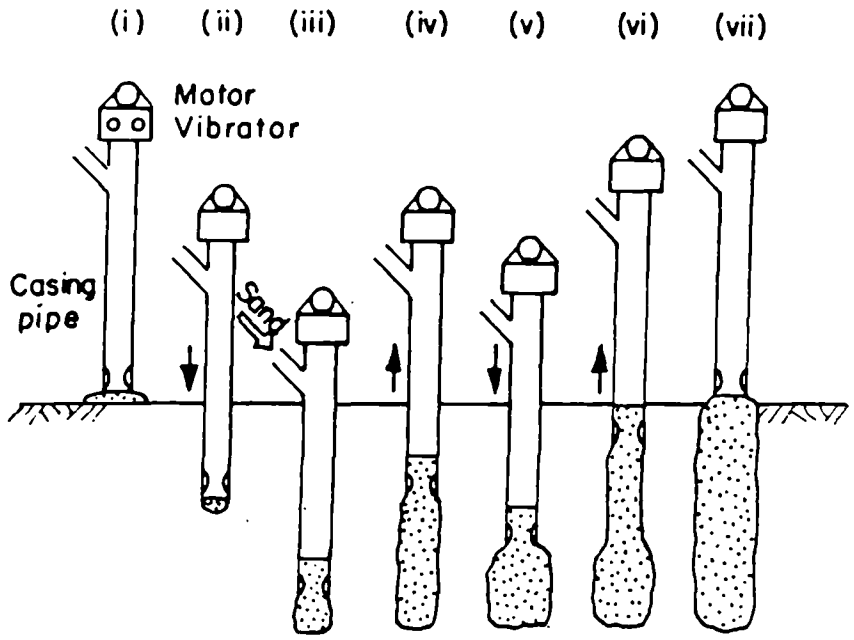

Fig. E2.1 Construction of Gravel Columns by the Composer System